

Nonperturbative aspects of Yang–Mills theory

Dissertation

zur Erlangung des Grades
eines Doktors der Naturwissenschaften

der Fakultät für Physik
der Eberhard-Karls-Universität zu Tübingen

vorgelegt von

WOLFGANG SCHLEIFENBAUM

aus Stuttgart

2008

Tag der mündlichen Prüfung : 28.05.2008
Dekan : Prof. Dr. N. Schopohl
Erster Berichtstatter : Prof. Dr. H. Reinhardt
Zweiter Berichtstatter : Prof. Dr. h.c. mult. A. Fäßler

Meinem Sohn Benjamin

Zusammenfassung

Das Thema dieser Dissertation ist die Starke Wechselwirkung zwischen Gluonen und Quarks mit Schwerpunkt auf den nicht störungstheoretischen Aspekten des Gluonensektors. Es werden hier Kontinuumsmethoden verwendet, um insbesondere das Phänomen des Farbeinschlusses zu untersuchen. Der Farbeinschluss, welcher die Detektion der elementaren Quarks und Gluonen als freie Teilchen verhindert, verlangt ein Verständnis der langreichweitigen Wechselwirkungen. In der Störungstheorie können nur kurzreichweitige Korrelationen verlässlich beschrieben werden. Ein nicht störungstheoretischer Zugang ist durch das Dyson–Schwinger–Integralgleichungssystem gegeben, das alle Greenfunktionen miteinander verknüpft. Eine Lösung für den Gluonpropagator wird im asymptotisch infraroten und ultravioletten Grenzwert erzielt.

In Kapitel 1 werden redundante Freiheitsgrade der Yang–Mills-Eichtheorie durch Fixierung der Weyl- und Coulombbeichung vor der Quantisierung entfernt. Die Quantisierung mit Zwangsbedingungen unter Verwendung von Dirac–Klammern wird explizit ausgeführt. Als Resultat erhält man den Yang–Mills–Hamiltonoperator.

Der asymptotische Infrarotlimes der Korrelationsfunktionen in Coulombbeichung wird in Kapitel 2 im Rahmen des Gribov–Zwanziger–Szenarios für den Farbeinschluss analytisch untersucht. Das Coulombpotential zwischen schweren Quarks als Teil des Yang–Mills–Hamiltonoperators wird in diesem Limes berechnet. Die Übertragung der Lösungen in Coulombbeichung auf den Infrarotlimes der Landaueichung wird diskutiert.

Der hergeleitete Hamiltonoperator ermöglicht die Bestimmung des Vakuumwellenfunktionals mithilfe des Variationsprinzips in Kapitel 3. Numerische Lösungen der Propagatoren in diesem Vakuumzustand werden besprochen, und es wird aufgezeigt, dass der vorhergesagte Infrarotlimes tatsächlich realisiert ist. Die Diskussion wird auf Vertexfunktionen erweitert. Des Weiteren wird der Einfluss der Näherungsmethoden auf die Lösungen untersucht.

Kapitel 4 ist vornehmlich dem Ultraviolettverhalten der Propagatoren gewidmet. Die Behandlung erfolgt sowohl in der Coulomb- als auch in der Landaueichung. Ein nicht störungstheoretischer laufender Kopplungsparameter wird definiert und berechnet. Der ultraviolette Teil der Variationslösungen aus Kapitel 3 wird mit den Forderungen der Störungstheorie verglichen.

In Kapitel 5 wird die Rückkopplung des Gluonensektors auf die Anwesenheit äußerer Ladungen (schwerer Quarks) behandelt. Zu diesem Zweck werden kohärente Gluonenanregungen vorgeschlagen, welche der Anwesenheit äußerer Ladungen Rechnung tragen. Weitere Alternativen zur Behandlung dieser Problemstellung werden besprochen.

Abstract

The subject of this thesis is the theory of strong interactions of quarks and gluons, with particular emphasis on nonperturbative aspects of the gluon sector. Continuum methods are used to investigate in particular the confinement phenomenon. Confinement—which states that the elementary quarks and gluons cannot be detected as free particles—requires an understanding of large-scale correlations. In perturbation theory, only short-range correlations can be reliably described. A nonperturbative approach is given by the set of integral Dyson–Schwinger equations involving all Green functions of the theory. A solution for the gluon propagator is obtained in the infrared and ultraviolet asymptotic limits.

In chapter 1, redundant degrees of freedom of the Yang–Mills gauge theory are removed by fixing the Weyl and Coulomb gauge prior to quantization. The constrained quantization in the Dirac bracket formalism is then performed explicitly to produce the quantized Yang–Mills Hamiltonian.

The asymptotic infrared limits of Coulomb gauge correlation functions are studied analytically in chapter 2 in the framework of the Gribov–Zwanziger confinement scenario. The Coulomb potential between heavy quarks as part of the Yang–Mills Hamiltonian is calculated in this limit. A connection between the infrared limits of Coulomb and Landau gauge is established.

The Hamiltonian derived paves the way in chapter 3 for finding the Coulomb gauge vacuum wave functional by means of the variational principle. Numerical solutions for the propagators in this vacuum state are discussed and seen to reproduce the anticipated infrared limit. The discussion is extended to the vertex functions. The effect of the approximations on the results is examined.

Chapter 4 is mainly devoted to the ultraviolet behavior of the propagators. The discussion is issued in both Coulomb and Landau gauge. A nonperturbative running coupling is defined and calculated. The ultraviolet tails of the variational solutions from chapter 3 are compared to the behavior demanded by perturbation theory.

In chapter 5, the back reaction of the gluon sector on the presence of external charges (heavy quarks) is explored. To this end, coherent excitations of gluonic modes are suggested to account for the presence of quarks. Further alternatives for the discussion of this issue are put forward.

Contents

1	Yang–Mills theory as a constrained dynamical system	11
1.1	Definition of Yang–Mills theory	11
1.2	Constrained dynamics	14
1.3	Quantum electrodynamics	19
1.4	Constrained quantization of Yang–Mills theory	23
2	Infrared ghost dominance	31
2.1	Gribov–Zwanziger scenario of confinement	32
2.2	Stochastic vacuum in Coulomb gauge	35
2.3	Dyson–Schwinger equations	36
2.4	Connection to Landau gauge	39
2.5	Ghost-gluon vertex	41
2.6	Analytical solution for propagators	44
2.7	Linear confining potential	51
2.8	On the uniqueness of the solution	53
3	Variational solution for the vacuum state	60
3.1	Gaussian types of wave functionals	61
3.2	Minimizing the energy density	64
3.3	Renormalization	66
3.4	Full numerical solutions	70
3.5	Vertices	75
3.6	Coulomb form factor	83
3.7	Subcritical solutions	87
4	Running coupling and ultraviolet behavior	89
4.1	Anti-screening of color charges	90
4.2	Nonperturbative running coupling	93
4.3	Ultraviolet behavior of Green functions	96
4.4	Infrared fixed point	101

5	Inclusion of external charges	106
5.1	Gluons in a quasi-particle representation	106
5.2	Coherent states	107
5.3	Energy of Yang–Mills theory in the coherent state	113
5.4	The gluon chain	123
5.5	Squeezed states	130
	Summary and outlook	133
A	Conventions and notation	136
A.1	Units, metric and group conventions	136
A.2	Notation	136
B	Two-point integrals	138
C	Infrared limit of the ghost-gluon vertex	143
D	Hamiltonian approach to ϕ^4 theory	146
E	Identities for Gaussian expectation values	149
	References	151
	Acknowledgments	163

1 Yang–Mills theory as a constrained dynamical system

In the development of quantum electrodynamics (QED) [1], local gauge invariance of the matter fields served as a guiding principle and it successfully led to a highly accurate description of electromagnetic forces [2]. The fundamental requirement of locality necessitates the existence of bosonic gauge fields which mediate the forces between the fermions. An impediment to the canonical quantization of such a dynamical system is the existence of redundant degrees of freedom. This obstacle can be overcome for the electromagnetic theory, thanks to the linear structure of its equations of motion. Quantum chromodynamics (QCD), on the other hand, bears non-linearities that make the treatment far more complicated. Since QCD is the non-abelian generalization of QED, the general structure of a gauge theory is inherited and along with it its difficulties. It will be shown in this chapter how the redundant degrees of freedom can be related to constraints in the classical phase space, and how quantization of such a dynamical system can be pursued. After a brief definition of Yang–Mills (YM) theories, amongst which QCD is the $SU(3)$ version, we first examine constrained systems in the context of classical mechanics to pave a way for the terminology. Second, constrained quantization is exhibited for electrodynamics as an illuminating example. Finally, we demonstrate how to systematically follow the steps of constrained quantization in the difficult case of Yang–Mills theory in Weyl and Coulomb gauge. The explicit form of the quantized Hamiltonian operator will thus be derived in a quantization approach that differs from the canonical method.

1.1 Definition of Yang–Mills theory

After a first sporadic attempt by Klein as early as 1939 to generalize the electromagnetic theory imposing non-abelian group structure [3], it took another 15 years until Yang and Mills were able to provide the full account of $SU(2)$ non-abelian gauge theory [4]. Its generalization to $SU(N_c)$ (with $N_c = 3$ realized in QCD) is straightforward, a clear introduction to the currently accepted definition of YM theory can be found, e.g., in Ref. [5]. There are some good text books on this topic, e.g. Ref. [6], yet the main elements of YM theory are outlined here to set up a notation for this thesis.

The basic idea, following electromagnetism as a guiding example, is to cancel the change of the Dirac Lagrangian

$$\mathcal{L}_D = \bar{\psi} (i\gamma^\mu \partial_\mu - m) \psi \tag{1.1}$$

under a local symmetry transformation of its fermion fields $\psi_a(x)$ in the intrinsic space¹

$$\psi_a(x) \rightarrow \psi_a^U(x) = U_{ab}(x)\psi_b(x) \tag{1.2}$$

¹The roman color indices are used as subscript or superscript interchangeably.

by the introduction of a gauge field $A_\mu^a(x)$. To achieve this, the derivative $\partial_\mu = \frac{\partial}{\partial x^\mu}$ in the Lagrangian (1.1) is replaced by

$$D_\mu := \partial_\mu + gA_\mu \quad (1.3)$$

which transforms homogeneously, $D_\mu \rightarrow UD_\mu U^\dagger$, whereas the matrix-valued gauge fields A_μ transform inhomogeneously, according to

$$A_\mu(x) \equiv A_\mu^a(x)T^a \rightarrow A_\mu^U(x) = U(x)A_\mu(x)U^\dagger(x) + \frac{1}{g}U(x)\partial_\mu U^\dagger(x). \quad (1.4)$$

The subsequent interaction of gauge and matter fields is controlled by the coupling constant g . Originally, this procedure coined the term “minimal substitution”. Nowadays, with a deeper understanding of the geometrical aspects which allow close analogies to general relativity [7], we call D_μ the “covariant derivative”, defined in Eq. (1.3) as acting on a field in the fundamental representation, such as the quark field $\psi^a(x)$.

The unitary group elements $U(x) \in SU(N_c)$,

$$U(x) = \exp(-\alpha^a(x)T^a), \quad \alpha \in \mathbb{R}, \quad (1.5)$$

are continuously generated by $N_c^2 - 1$ antihermitian matrices $T_a = -T_a^\dagger$ that obey the Lie algebra

$$[T^a, T^b] = f^{abc}T^c \quad (1.6)$$

with the structure constants f^{abc} . For the quarks to transform as $\mathbf{3}$ -vectors in the fundamental representation of $SU(3)$, one uses the well-known 3×3 Gell–Mann matrices for iT^a . The gauge fields A_μ , on the other hand, live in a $(N_c^2 - 1)$ -dimensional vector space spanned by the generators T^a with the additional operation of commutation (1.6). By an infinitesimal expansion of (1.4) in α using (1.6), one can see that A_μ^a must transform in the adjoint representation of $SU(N_c)$,

$$(A^U)_\mu^a = A_\mu^a + (\hat{T}^b)^{ac}A_\mu^b\alpha^c + \frac{1}{g}\partial_\mu\alpha^a + \mathcal{O}(\alpha^2), \quad (1.7)$$

where we defined

$$(\hat{T}^b)^{ac} := f^{abc}. \quad (1.8)$$

Any linear combination of the matrices \hat{T}^a with field operators shall be denoted by a caret, e.g. $\hat{A}_\mu \equiv A_\mu^a\hat{T}^a$, as opposed to the matrices A_μ introduced in Eq. (1.4). The covariant derivative \hat{D}_μ^{ab} acting on fields in the adjoint representation is defined by

$$\hat{D}_\mu^{ab} = \delta^{ab}\partial_\mu + g\hat{A}_\mu^{ab}. \quad (1.9)$$

Knowing the transformation properties of the gauge field (1.4), one may construct from the gauge covariant field strength tensor

$$F_{\mu\nu} := \frac{1}{g}[D_\mu, D_\nu] = \partial_\mu A_\nu - \partial_\nu A_\mu + g[A_\mu, A_\nu], \quad F_{\mu\nu} \rightarrow UF_{\mu\nu}U^\dagger \quad (1.10)$$

a gauge invariant contribution to the Lagrangian density that is purely gluonic. It is the first term in the *Yang–Mills Lagrangian*

$$\mathcal{L}_{YM} = \frac{1}{2} \text{tr} F_{\mu\nu}(x) F^{\mu\nu}(x) + g j_{\mu}^a(x) A_{\mu}^a(x), \quad (1.11)$$

whereas the second term represents the coupling to the quark Nöther current of the color symmetry,

$$j_{\mu}^a(x) = \bar{\psi}(x) \gamma_{\mu} i T^a \psi(x), \quad (1.12)$$

here treated as a classical external field. This thesis shall mainly be concerned with the dynamics of the Yang–Mills Lagrangian (1.11) and disregard the influence of dynamical quarks. It is hypothesized that unquenching has a small effect on the gauge field sector.² The color trace in Eq. (1.11) with the convention $\text{tr}(T^a T^b) = -\frac{1}{2} \delta^{ab}$ guarantees that the gluonic energy is positive definite, cf. (1.18).

With the action principle, the Lagrangian formalism provides a possibility to derive equations of motion where Lorentz invariance is manifest. Applying a functional derivative w.r.t. the gauge field to the Yang–Mills action

$$S = \int d^4x \mathcal{L}_{YM}(x) \quad (1.13)$$

one finds³

$$\hat{D}_{\mu}^{ab} F_b^{\mu\nu} = -g j_{\mu}^{\nu} \quad (1.14)$$

and, using the Bianchi identity $[D_{\mu}, F_{\nu\rho}] + \text{cycl.perm.} = 0$,

$$\frac{1}{2} \epsilon^{\mu\nu\rho\sigma} \hat{D}_{\mu}^{ab} F_{\rho\sigma}^a = 0. \quad (1.15)$$

In order to derive a Hamiltonian, one introduces conjugate momenta

$$\Pi_{\mu}^a(x) = \frac{\delta \mathcal{L}}{\delta \partial_0 A_{\mu}^a(x)} = F_{\mu 0}^a(x) \quad (1.16)$$

and readily notes that due to the antisymmetry of $F^{\mu\nu}$

$$\Pi_0^a(x) = 0. \quad (1.17)$$

²The nonperturbative confinement phenomenon is known to exist in the absence of flavors, $N_f = 0$, from lattice calculations [8]. In the perturbative regime, a small number of quark flavors ($N_f < 16$) will not remove the property of asymptotic freedom. Recent continuum studies [9] as well as lattice calculations [10] indicate that the effect of unquenching on hadronic observables is small.

³Note that F_{μ}^{ν} transforms in the adjoint representation, therefore it is natural that the covariant derivative \hat{D}_{μ} is found here.

Eq. (1.17) is understood as a constraint on the phase space variables and will be shown to complicate the quantization process. The Legendre transform gives the Hamiltonian H ,

$$\begin{aligned}
 H &= \int d^3x \left(\Pi_\mu^a \partial_0 A_a^\mu - \mathcal{L}_{YM} \right) \\
 &= \int d^3x \left(\Pi_a^k F_{0k}^a + \Pi_a^k \hat{D}_k^{ab} A_0^b + \frac{1}{2} F_{k0}^a F_a^{k0} + \frac{1}{4} F_{ij}^a F_a^{ij} - g j_\mu^a A_\mu^a \right) \\
 &= \int d^3x \left(-\frac{1}{2} \Pi_a^k \Pi_k^a + \frac{1}{4} F_{ij}^a F_a^{ij} - A_0^a \hat{D}_k^{ab} \Pi_b^k - g A_0^a \rho_{\text{ext}}^a - g A_k^a j_k^a \right) \\
 &= \frac{1}{2} \int d^3x \left(\mathbf{\Pi}_a^2 + \mathbf{B}_a^2 \right) - \int d^3x A_0^a \mathcal{G}^a + g \int d^3x \mathbf{A}^a \cdot \mathbf{j}^a, \tag{1.18}
 \end{aligned}$$

with the abbreviations for the external color charge density $\rho_{\text{ext}}^a = j_0^a$, the color magnetic field $B_k^a = -\frac{1}{2} \epsilon_{ijk} F_{ij}^a$ and

$$\mathcal{G}^a(x) = \hat{D}_k^{ab}(x) \Pi_b^k(x) + g \rho_{\text{ext}}^a(x). \tag{1.19}$$

In the Lagrangian equations of motion we recognize that the Gauss law can be written as $\mathcal{G}^a = 0$, see Eq. (1.14) for $\nu = 0$.⁴ However, in the Hamiltonian approach, the Gauss law cannot be found as an equation of motion but must be implemented as a constraint, as will be discussed below.

The quantization of a gauge theory is a delicate task, already in the abelian case. Since the gauge transformation indicates that the field variables $A_k^a(x)$ contain unphysical degrees of freedom, it is not clear a priori whether the canonical quantization leads to the correct results, i.e. whether it contains the classical theory in the limit $\hbar \rightarrow 0$. It is discussed in some detail in the following sections how a gauge theory can be understood as a constrained system and how to go about with its quantization.

Although in the Lagrangian formalism Lorentz invariance can be made manifest, it is sometimes favorable to use the Hamiltonian formalism instead. The path integral method provides an elegant way of quantizing a theory covariantly in the Lagrangian formalism. However, it is rather unsuitable to calculate, e.g., the Balmer formula for hydrogen, one of the first exercises in quantum mechanics [11]. The Hamiltonian approach to the quantum theory of electromagnetism and YM theory shall be the main focus of this work. Once the conjugate momenta are defined and one passes over to the Hamiltonian, Lorentz covariance is lost since a reference frame has been chosen. Nevertheless, Lorentz *invariance* is maintained. This can be understood, e.g., by explicit calculation in Coulomb gauge for electromagnetism [12] or by criteria for commutation relations in Coulomb gauge quantum Yang–Mills theory [13].

1.2 Constrained dynamics

In this section we shall discuss the importance of constraints of a dynamical system for its time evolution and for its quantization procedure. The basic idea was developed by Dirac [14, 15]

⁴In electrodynamics, one defines the electric field as $E^k = -\Pi^k$ and thus gains the familiar form of the Maxwell equation $\nabla \cdot \mathbf{E} = e\rho$.

and very pedagogically presented in his Yeshiva lectures [16]. Dirac and many of his successors tried to maintain a high level of generality in favor of the applicability to any given system, say electrodynamics or even general relativity [17]. However, it turned out that exceptions to the quite general claims can be found. Therefore, only the concepts relevant to Yang–Mills theory will be introduced here. For additional information, see e.g. [18, 19, 20].

Consider a classical mechanical system described by a Lagrangian $L(q_i, \dot{q}_j)$. The Legendre transformation to a Hamiltonian $H(q_i, p_j)$ with conjugate momenta p_k can be achieved if we can solve the equation

$$p_k := \frac{\partial L}{\partial \dot{q}_k} \quad (1.20)$$

for the velocities \dot{q}_k , which is locally guaranteed by a regular Hessian

$$\det \left(\frac{\partial^2 L}{\partial \dot{q}_i \partial \dot{q}_j} \right) \neq 0. \quad (1.21)$$

The phase space Γ is then defined as a set of independent elements $\{q_i, p_j\}$. In the case of a singular Lagrangian where Eq. (1.21) does not hold, some of the momenta p_k are dependent. Moreover, additional dependences among the q_k and p_k may arise from the Hamiltonian equations of motion. Generally, one may formulate all dependences as a number of constraints

$$\varphi_m(q, p) \approx 0. \quad (1.22)$$

by which the dimension of phase space is reduced. Below, the symbol ‘ \approx ’ is explained. The constraints (1.22) then hold in a subset $\Gamma_R \subset \Gamma$ of the original phase space. The Hamiltonian H can be supplemented by the constraints (1.22) with some arbitrary Lagrange multipliers v_m ,

$$H_T = H + v_m \varphi_m \quad (1.23)$$

We refer to H_T as the “total Hamiltonian”. The common variational calculus with constraints gives rise to Hamiltonian equations of motion in Γ_R ,

$$\dot{q}_k = \frac{\partial H}{\partial p_k} + v_m \frac{\partial \varphi_m}{\partial p_k} \approx \{q, H_T\} \quad (1.24a)$$

$$\dot{p}_k = -\frac{\partial H}{\partial q_k} - v_m \frac{\partial \varphi_m}{\partial q_k} \approx \{p, H_T\} \quad (1.24b)$$

Above, we have made use of the Poisson bracket for any functions $f(q, p)$ and $g(q, p)$,

$$\{f, g\} = \frac{\partial f}{\partial q_k} \frac{\partial g}{\partial p_k} - \frac{\partial f}{\partial p_k} \frac{\partial g}{\partial q_k} \quad (1.25)$$

Note that there is a ‘ \approx ’ symbol in Eq. (1.24), a notation due to Dirac which emphasizes that one is to first calculate the Poisson brackets and then set the constraints (1.22) to zero. These kinds of relations are termed “weak equations” and are specific to the use of Poisson brackets. It may be stressed here that the canonical quantization with such weak equations leads to the circumstance that some quantum constraints cannot be imposed as operator identities but only

as projections on states. Below, we shall introduce generalized Poisson brackets that make the usage of weak equations redundant.

The time evolution of any given phase space function $g(q, p)$ that does not explicitly depend on time is given by the Poisson bracket in a concise way:

$$\dot{g} \approx \{g, H_T\}. \quad (1.26)$$

The total Hamiltonian H_T obviously serves as the generator of time evolution. However, the multiplier functions v_m contained in it leave an arbitrariness. Given some initial conditions, say $g(0) = g_0$, $g(t)$ at some finite time t is not unique since we can choose the v_m to be one value or another. After an infinitesimally small time δt , the function g will yield

$$g(\delta t) \approx g_0 + \{g_0, H\}\delta t + v_m \{g_0, \varphi_m\}\delta t. \quad (1.27)$$

Imagine we take two different sets of multiplier functions v'_m and v''_m . Comparing these two arbitrary choices to calculate $g'(\delta t)$ and $g''(\delta t)$, using (1.27), leads to

$$g''(\delta t) \approx g'(\delta t) + \epsilon_m \{g_0, \varphi_m\} \quad (1.28)$$

with $\epsilon_m = (v''_m - v'_m)\delta t$. Evidently, the two physically equivalent values $g'(\delta t)$ and $g''(\delta t)$ are related by a term generated by the constraints φ_m . This suggests that the physical state remains unchanged under transformations of the kind

$$g(q, p) \rightarrow g^e(q, p) = g(q, p) + \epsilon_m \{g, \varphi_m\} \quad (1.29)$$

However, we have to be careful with the interpretation, as shown below.

The constraints (1.22) need to be checked for consistency, i.e. they should hold at all times. In view of Eq. (1.26) this requirement gives rise to the conditions

$$\dot{\varphi}_k = \{\varphi_k, H\} + \{\varphi_k, \varphi_m\}v_m \approx 0 \quad (1.30)$$

which can actually fix the multiplier functions v_m so long as the matrix

$$C_{km} := \{\varphi_k, \varphi_m\} \quad (1.31)$$

is invertible. We now distinguish *first-class* and *second-class* constraints [16]. By definition, a first-class constraint has vanishing Poisson brackets with all other constraints. With first-class constraints present, the matrix (C_{km}) in Eq. (1.31) becomes singular, $\det(C_{km}) \approx 0$. In the absence of first-class constraints, all constraints are termed second-class, and one can show [21] that

$$\det(C_{km}) \not\approx 0. \quad (1.32)$$

If Eq. (1.32) holds and only second-class constraints are present, we can fix the multiplier functions v_m using the consistency conditions (1.30) by

$$v_k = -C_{km}^{-1} \{\varphi_m, H\} \quad (1.33)$$

and derive that $g(t)$ with second-class constraints satisfies the equation of motion

$$\dot{g} = \{g, H\} - \{g, \varphi_k\} C_{km}^{-1} \{\varphi_m, H\} \equiv \{g, H\}_D . \quad (1.34)$$

Here, the *Dirac bracket* was introduced,

$$\{f, g\}_D := \{f, g\} - \{f, \varphi_k\} C_{km}^{-1} \{\varphi_m, g\} . \quad (1.35)$$

It is clear from Eq. (1.34) that the time evolution of the initial state g_0 is unique. The Dirac bracket provides a formalism that yields equations of motion with (second-class) constraints. Furthermore, the constraints (1.22) which are regarded as weak equations w.r.t. Poisson brackets, can be used as strong (ordinary) equations if one uses the Dirac bracket instead, since for any function f

$$\{\varphi_k, f\}_D = \{\varphi_k, f\} - \{\varphi_k, \varphi_j\} C_{jm}^{-1} \{\varphi_m, f\} = 0 . \quad (1.36)$$

These ideas led Dirac to propose a quantization technique for constrained dynamical systems, known as *constrained quantization*⁵, making use of the Dirac brackets in the fundamental commutation relations of operators \hat{q}_i and \hat{p}_i ,

$$i\hbar\{q_i, p_j\}_D \rightarrow [\hat{q}_i, \hat{p}_j] . \quad (1.37)$$

While the Dirac brackets has most of the features of the Poisson bracket—e.g. antisymmetry, linearity, Jacobi identity, product rule—the fundamental Dirac brackets are generally not as simple as the Poisson brackets, $\{q_i, p_j\}_D \neq \delta_{ij}$. In linear theories, such as QED (discussed in the next section) this does not pose a problem to the quantization prescription (1.37) since the fundamental Dirac brackets do not involve field variables. However, in the non-linear YM theory, constrained quantization is more difficult. This will be dealt with in section 1.4.

Let us come back to the claim that constraints generate transformations among physically equivalent states, see Eq. (1.29). For second-class constraints, this can certainly not be correct, since all multiplier functions are fixed, as we have seen in Eq. (1.33). To understand this caveat, note that the transformations (1.29) generated by second-class constraints kick the system out of the reduced phase space Γ_R since for $g = \varphi_k$

$$\varphi_k'' = \varphi_k' + \{\varphi_k, \varphi_m\} \epsilon_m \not\approx 0 . \quad (1.38)$$

That is, the transformations (1.29) generated by second-class constraints are not symmetries of the theory.

On the other hand, if we consider first-class constraints only, then the Poisson brackets all vanish, $\{\varphi_i, \varphi_j\} = 0$, and the transformations (1.29) are indeed such that the system remains in the reduced phase space Γ_R where the constraints are satisfied. They give rise to an equivalence class⁶

$$[(q, p)] = \{(q^\epsilon, p^\epsilon) \in \Gamma_R \mid (q, p) \sim (q^\epsilon, p^\epsilon), \epsilon \in \mathbb{R}\} \quad (1.39)$$

⁵It is also associated with the lengthy expression “reduced phase space quantization”.

⁶The equivalence relation \sim is here represented by the transformations infinitesimally defined in Eq. (1.29).

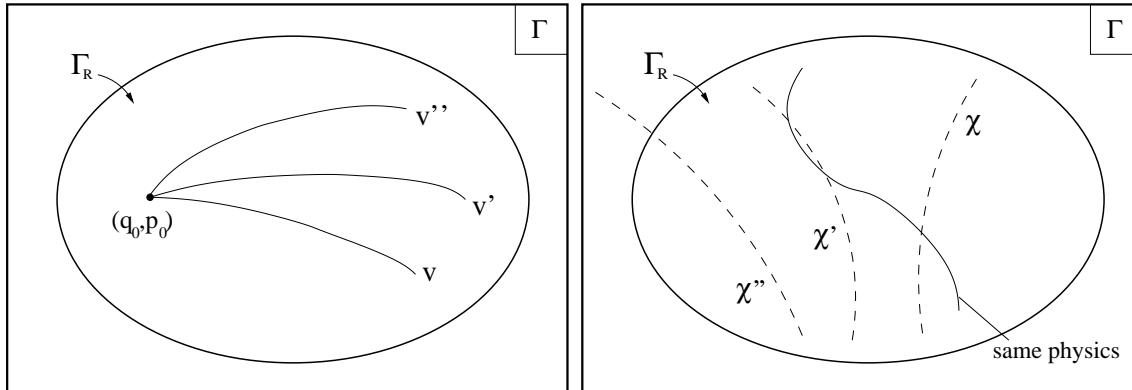


Figure 1.1: *Left: Ambiguity in time evolution of an initial point (q_0, p_0) in the reduced phase space Γ_R . Different choices (v, v', v'') of the arbitrary multiplier functions lead to different trajectories in Γ_R . Right: At a fixed time, the gauge orbit (solid line) represents physically equivalent states. The gauge fixing condition χ is admissible, whereas χ' fails to be unique and χ'' is not attainable by a gauge transformation.*

of phase space variables that all correspond to the same physical state. Any set of (q_i, p_j) uniquely determines the state but the reverse is not true, see Fig. 1.1. These considerations infer that the *first class constraints are the generators of symmetries of the theory*.

It should be noted here that the above statement, known as “Dirac’s conjecture” is not a rigorous theorem. Counter examples can be constructed [22], and it takes further classifications of constraints (“primary” and “secondary”) to identify the exact set of generators of symmetry transformations in general. However, all physical applications agree with Dirac’s conjecture and the issue is somewhat academic. In particular, the gauge transformations of QED and YM theory are generated by first-class constraints (see below). In this context, the equivalence class (1.39) is also referred to as the *gauge orbit*.

The quantization in the presence of first-class constraints is performed either in the path-integral formalism [23], or by a projection on the physical Hilbert subspace [5, 24]. Alternatively, one can fix the gauge on the classical level and then quantize with the Dirac prescription (1.37). When fixing the gauge, one effectively picks out a single representative from the equivalence class (1.39) generated by the first-class constraints. In practice, this is achieved by imposing supplementary constraints (“gauge conditions”)

$$\chi_n \approx 0 \tag{1.40}$$

that turn the first-class constraints φ_m into second-class ones and hence obey

$$\det(\{\chi_n, \varphi_m\}) \neq 0. \tag{1.41}$$

The constraints φ_m that formerly were first-class thus cease to cause an ambiguous time evolution of the system. With all constraints being second-class, all multiplier functions are fixed and one can use the Dirac bracket to proceed with the quantization.

In order to arrive at a “physical gauge” where all unphysical degrees of freedom are eliminated, the number of gauge conditions must equal the number of first-class constraints, hence the matrix that appears in Eq. (1.41) is quadratic. In principle, the gauge conditions (1.40) are quite arbitrary, except for the requirements of uniqueness and attainability. Uniqueness can be established locally as follows: Consider in Fig. 1.1 (right panel) the gauge orbit at a fixed time t_f and assume without loss of generality that the point (q^f, p^f) satisfies $\chi_n(q^f, p^f) = 0$. The transformation

$$\chi_n \rightarrow \chi_n^\epsilon = \chi_n + \epsilon_m \{\chi_n, \varphi_m\} \quad (1.42)$$

within the gauge orbit is not to yield any further solutions $\chi_n^\epsilon \approx 0$ unless it is the identity transformation, $\epsilon = 0$. Otherwise, the gauge fixing condition specifies (at least) two elements of the gauge orbit, see χ' in Fig. 1.1. With the condition (1.41) on the χ_n , one can see from Eq. (1.42) immediately that $\epsilon = 0$ is the only solution to $\chi_n^\epsilon \approx 0$ and therefore the point (q^f, p^f) is unique.⁷ Moreover, a sensible gauge condition has to be attainable by a gauge transformation. Otherwise, we would have the situation in which the gauge fixing condition does not intersect with the gauge orbit at all, see χ'' in Fig. 1.1.

In summary, the general procedure of quantizing classical mechanics in the presence of constraints has been discussed. It has not been shown how to find the entire set (1.22) of constraints starting from the Lagrangian. This can be achieved with the so-called Dirac-Bergmann algorithm [14, 15, 25]. It incorporates the stationarity of constraints that are found in the equation of motion or in the mere definition of conjugate momenta.

1.3 Quantum electrodynamics

An illuminating example of the formalism exhibited above is the quantization of electrodynamics in Weyl and Coulomb gauge. There are no difficulties in promoting the ideas from point mechanics to a field theory, the discrete indices of the generalized coordinates are merely replaced by the continuous spacetime dependence.

The electromagnetic theory is the abelian version of the general set of YM theories described in section 1.1, recovered by setting $f^{abc} = 0$ in the Lie algebra (1.6). In the absence of external charges, one finds from (1.11) the well-known Lagrangian density

$$\mathcal{L} = -\frac{1}{4}F_{\mu\nu}F^{\mu\nu}, \quad F_{\mu\nu} = \partial_\mu A_\nu - \partial_\nu A_\mu. \quad (1.43)$$

As quoted in Eq. (1.17), the conjugate momentum of the A_0 field vanishes and we can write down a first constraint φ_1 as⁸

$$\varphi_1(x) := \Pi_0(x) = \frac{\delta\mathcal{L}}{\delta\partial_0 A_0(x)} \approx 0. \quad (1.44)$$

⁷The global issues of uniqueness will be discussed below in the context of YM theory.

⁸In field theory, an infinite number of constraints is specified, one at each spacetime point.

The Hamiltonian function depending on the fields $A_0(x)$, $A_k(x)$ and the conjugate momenta $\Pi^k(x)$ reads

$$H = \frac{1}{2} \int d^3x (\mathbf{\Pi}^2(x) + \mathbf{B}^2(x)) - \int d^3x A_0(x) \partial_k \Pi^k(x). \quad (1.45)$$

From now on, we write $\Pi_k(x)$ for the components of the contravariant tensor $\Pi^k(x) = F^{k0}(x)$. This change in notation will become useful in the nonabelian case where the field operators also have a color index. The Hamiltonian (1.45) determines the time evolution via the Poisson brackets. The fundamental Poisson brackets are given by

$$\{A_\mu(\mathbf{x}, t), \Pi_\nu(\mathbf{y}, t)\} = \delta_{\mu\nu} \delta^3(\mathbf{x}, \mathbf{y}). \quad (1.46)$$

Since the constraint (1.44) is stationary,

$$\varphi_2(x) := \{\Pi_0(x), H_T\} = \{\Pi_0(x), H + \int d^3y v_1(y) \Pi_0(y)\} = \partial_k \Pi_k(x) \approx 0 \quad (1.47)$$

has to hold weakly where $v_1(x)$ is an arbitrary multiplier function. We recognize Eq. (1.47) as the Gauss law. Following the Dirac-Bergmann algorithm, we can check if further constraints arise from requiring that φ_2 is constant in time. One finds

$$\left\{ \varphi_2(x), H + \int d^3y (v_1(y) \Pi_0(y) + v_2(y) \partial_k \Pi_k(y)) \right\} = 0 \quad (1.48)$$

and thus the complete matrix of constraints C_{ij} , see Eq. (1.31), is given by φ_1 and φ_2 which are obviously first-class, $\{\varphi_1, \varphi_2\} = 0$.

As we have shown in the preceding section, the first-class constraints serve as generators of gauge transformations. Here, it can be explicitly verified that the transformations $A_\mu \rightarrow A_\mu + \delta A_\mu$ with

$$\delta_{\varphi_1} A_0(x) = \int d^3x' \{A_0(x), \varphi_1(x')\} \alpha_1(x') = \alpha_1(x), \quad \delta_{\varphi_1} A_k(x) = 0 \quad (1.49a)$$

$$\delta_{\varphi_2} A_k(x) = \int d^3x' \{A_k(x), \varphi_2(x')\} \alpha_2(x') = -\partial_k \alpha_2(x), \quad \delta_{\varphi_2} A_0(x) = 0 \quad (1.49b)$$

are symmetries of the Lagrangian (1.43). The general form (1.4) of gauge transformations in the Lagrangian formalism, with generator $T = i\mathbb{1}$ of the group $U(1)$ and gauge coupling $g = e$, reads

$$A_\mu(x) \rightarrow A_\mu^\alpha(x) = A_\mu(x) + \frac{1}{e} \partial_\mu \alpha(x). \quad (1.50)$$

If we wish to identify an $\alpha(x)$ in Eq. (1.50) that corresponds to the transformations (1.49), it is recognized that Eq. (1.49a) corresponds to spatially independent gauge transformations $\alpha(t)$ with $\alpha_1(t) = \partial_0 \alpha(t)/e$ whereas Eq. (1.49b) corresponds to time-independent gauge transformations with $\alpha(\mathbf{x}) = -\alpha_2(\mathbf{x})/e$.

In the quantization procedure, the problem arises that due to the gauge invariance (1.49) there are more variables than physical degrees of freedom. The constraints (1.44) and (1.47) then should be taken into account in the Dirac formalism. Before we do so, it is briefly sketched

here how the canonical quantization is usually pursued with Poisson brackets. With the choice of Weyl gauge, $A_0(x) = 0$, the first constraint, $\Pi_0(x) \approx 0$, does not cause any difficulties for the quantization of the time-components of the fields. The canonical Poisson brackets are used to promote the spatial classical fields to operator-valued fields that obey the equal-time commutation relations

$$[A_i(\mathbf{x}), \Pi_j(\mathbf{y})] = i\delta_{ij}\delta^3(\mathbf{x}, \mathbf{y}) . \quad (1.51)$$

Since the Gauss law (1.47) is an equation that holds only weakly on the classical level, it is not a surprise that it leads to a contradiction with the commutation relations,

$$0 = [A_k(\mathbf{x}), \partial_j^{\mathbf{y}}\Pi_j(\mathbf{y})] = \partial_j^{\mathbf{y}}[A_k(\mathbf{x}), \Pi_j(\mathbf{y})] = i\partial_k^{\mathbf{y}}\delta^3(\mathbf{x}, \mathbf{y}) \neq 0 . \quad (1.52)$$

The requirement that the Gauss law holds as an operator identity is therefore abandoned and one usually restricts the Hilbert space to the kernel of the Gauss law operator \mathcal{G} ,

$$\partial_k^{\mathbf{y}}\Pi_k(\mathbf{y}) |\Psi\rangle = 0 , \quad (1.53)$$

Let us mention here that the quantum theory is described in the Schrödinger picture where the field operators are independent of time.

Constrained quantization has the generic feature that the constraints can be imposed as strong equations once the Poisson brackets are replaced by the Dirac brackets. In the so quantized theory, the constraints hold as operator identities and can be used to eliminate unphysical degrees of freedom. Before the Dirac brackets can be introduced, all first-class constraints have to be degraded to second class by imposing gauge fixing conditions. We now choose Weyl and Coulomb gauge to render the constraints (1.44) and (1.47) second class,

$$\chi_1(x) = A_0(x) \approx 0 \quad (1.54a)$$

$$\chi_2(x) = \partial_k A_k(x) \approx 0 \quad (1.54b)$$

The Weyl or “temporal” gauge condition (1.54a) fixes the gauge transformations (1.49a) generated by the first-class constraint $\Pi_0 \approx 0$, whereas the Coulomb gauge condition (1.54b) fixes the gauge transformations (1.49b) generated by the first-class constraint $\partial_k \Pi_k(x) \approx 0$ which is the Gauss law. Thus, the gauge is fixed completely⁹ on the classical level and we will refer to the joint conditions (1.54a) and (1.54b) as the *temporal Coulomb gauge*.

All (second-class) constraints are now collected in a vector $\phi = (\varphi_1, \varphi_2, \chi_1, \chi_2)$, and we redefine the matrix (1.31) by $C_{ij}(\mathbf{x}, \mathbf{y}) = \{\phi_i(\mathbf{x}), \phi_j(\mathbf{y})\}$ which can be evaluated for a fixed time t using the fundamental Poisson brackets (1.46) to yield

$$(C_{ij})(\mathbf{x}, \mathbf{y}) = \begin{pmatrix} 0 & 0 & -\delta^3(\mathbf{x}, \mathbf{y}) & 0 \\ 0 & 0 & 0 & \partial^2\delta^3(\mathbf{x}, \mathbf{y}) \\ \delta^3(\mathbf{x}, \mathbf{y}) & 0 & 0 & 0 \\ 0 & -\partial^2\delta^3(\mathbf{x}, \mathbf{y}) & 0 & 0 \end{pmatrix} , \quad (1.55)$$

⁹ Up to global gauge transformations.

Since C_{ij} is regular by construction, we can also write down its inverse,

$$(C_{ij}^{-1})(\mathbf{x}, \mathbf{y}) = \begin{pmatrix} 0 & 0 & +\delta^3(\mathbf{x}, \mathbf{y}) & 0 \\ 0 & 0 & 0 & \frac{1}{4\pi|\mathbf{x}-\mathbf{y}|} \\ -\delta^3(\mathbf{x}, \mathbf{y}) & 0 & 0 & 0 \\ 0 & -\frac{1}{4\pi|\mathbf{x}-\mathbf{y}|} & 0 & 0 \end{pmatrix}. \quad (1.56)$$

The fundamental Dirac brackets can be calculated straightforwardly from the definition (1.35),

$$\begin{aligned} \{A_i(\mathbf{x}), \Pi_j(\mathbf{y})\}_D &= \{A_i(\mathbf{x}), \Pi_j(\mathbf{y})\} \\ &\quad - \int d^3x' d^3y' \{A_i(\mathbf{x}), \phi_m(\mathbf{x}')\} C_{mn}^{-1}(\mathbf{x}', \mathbf{y}') \{\phi_n(\mathbf{y}'), \Pi_j(\mathbf{y})\} \\ &= \delta_{ij} \delta^3(\mathbf{x}, \mathbf{y}) - \int d^3x' d^3y' \partial_i^{\mathbf{x}'} \delta(\mathbf{x}, \mathbf{x}') \frac{1}{4\pi|\mathbf{x}'-\mathbf{y}'|} \partial_j^{\mathbf{y}'} \delta(\mathbf{y}', \mathbf{y}) \\ &= \delta_{ij} \delta^3(\mathbf{x}, \mathbf{y}) - \partial_i^{\mathbf{x}} \partial_j^{\mathbf{y}} \frac{1}{4\pi|\mathbf{x}-\mathbf{y}|} =: t_{ij}(\mathbf{x}) \delta^3(\mathbf{x}, \mathbf{y}) =: t_{ij}(\mathbf{x}, \mathbf{y}) \end{aligned} \quad (1.57)$$

where the last line defines the transverse projector $t_{ij}(\mathbf{x})$. The definition of the matrix-valued distribution $t_{ij}(\mathbf{x}, \mathbf{y})$ will be useful as well.

Quantization is achieved by the prescription¹⁰

$$\{A_i(\mathbf{x}), \Pi_j(\mathbf{y})\}_D = t_{ij}(\mathbf{x}, \mathbf{y}) \quad \rightarrow \quad [A_i(\mathbf{x}), \Pi_j(\mathbf{y})] = it_{ij}(\mathbf{x}, \mathbf{y}) \quad (1.58)$$

which provides information on how the momentum operator $\Pi_k(\mathbf{x})$ acts on the wave functional $\langle A | \Psi \rangle = \Psi[A]$ in the coordinate representation. Yet, not all components of $\Pi_k(\mathbf{x})$ are determined by Eq. (1.58) since the transverse projector has zero modes, $\partial_{\mathbf{x}}^i t_{ij}(\mathbf{x}, \mathbf{y}) = \partial_{\mathbf{y}}^j t_{ij}(\mathbf{x}, \mathbf{y}) = 0$. To be specific, the longitudinal components of the field operators are left unconstrained by Eq. (1.58). We split the field operators into longitudinal and transversal components, $A_i = A_i^\perp + A_i^\parallel$ with $A_i^\perp(\mathbf{x}) = t_{ij}(\mathbf{x}) A_j(\mathbf{x})$ (and for Π accordingly), and find from Eq. (1.58) that

$$[A_i^\perp(\mathbf{x}), \Pi_j^\perp(\mathbf{y})] = it_{ij}(\mathbf{x}, \mathbf{y}). \quad (1.59)$$

The additional information needed for A_k^\parallel and Π_k^\parallel comes from the constraints themselves, Eqs. (1.47) and (1.54b), that now hold as operator identities. The longitudinal projections by $\ell_{ij} := \delta_{ij} - t_{ij}$ of both field operators are identically zero,

$$A_i^\parallel(\mathbf{x}) \equiv \ell_{ij}(\mathbf{x}) A_j(\mathbf{x}) = 0 \quad (1.60)$$

$$\Pi_i^\parallel(\mathbf{x}) \equiv \ell_{ij}(\mathbf{x}) \Pi_j(\mathbf{x}) = 0 \quad (1.61)$$

Here, no contradiction to the commutation relations (1.58) arises,

$$0 = [A_k(\mathbf{x}), \partial_j^{\mathbf{y}} \Pi_j(\mathbf{y})] = \partial_j^{\mathbf{y}} [A_k(\mathbf{x}), \Pi_j(\mathbf{y})] = i \partial_j^{\mathbf{y}} t_{kj}(\mathbf{x}, \mathbf{y}) = 0, \quad (1.62)$$

¹⁰The field operators are denoted by the same symbols as their classical counterparts. It should be clear from the context which objects the symbols refer to.

unlike in the quantization procedure with Poisson brackets, cf. Eq. (1.52). The transverse components of the momentum operator is found in view of Eq. (1.59) to be

$$\Pi_k^\perp(\mathbf{x}) = t_{kj}(\mathbf{x}) \frac{\delta}{i\delta A_j^\perp(\mathbf{x})}. \quad (1.63)$$

Quantization is thus complete and one may find from (1.45) the gauge-fixed quantum Hamiltonian

$$H[A^\perp, \Pi^\perp] = \frac{1}{2} \int d^3x \left(\mathbf{\Pi}^{\perp 2} + \mathbf{B}^2[A^\perp] \right). \quad (1.64)$$

After all, we have arrived at a Hamiltonian expressed in terms of gauge-invariant variables. Note that A_k^\perp is left unchanged by gauge transformations (1.50) and $\Pi_k = F_{k0}$ transforms homogeneously in view of (1.10) and hence transforms trivially in the abelian theory.

1.4 Constrained quantization of Yang–Mills theory

The transfer of the techniques used in the previous section to non-abelian theories is aggravated by non-linearities in the equations of motions. Nevertheless, constrained quantization of YM theory in the temporal Coulomb gauge is feasible. This section is devoted to presenting the steps of calculation that lead to the gauge-fixed Hamiltonian operator of YM theory with static external quark fields.

Usually, the canonical quantization is performed in the Weyl gauge where the spatial components of the gauge field can be treated as a set of Cartesian coordinates, and after quantization a coordinate transformation to curvilinear coordinates in the Coulomb gauge is undertaken [24, 26, 27, 28]. This corresponds to an incomplete gauge fixing before quantization and is known to bring about a number of difficulties [29]. For instance, if only the Weyl gauge, $A_0^a = 0$, is enforced, the Gauss law cannot be used as an operator equation and has to be imposed as a projection onto a physical Hilbert space [30, 5], see also [31]. The physical states are not normalizable as an artefact of the residual gauge invariance [32]. Moreover, the commutator $[\mathcal{G}^a, \mathcal{G}^b]$ may be anomalously broken which obscures the projection on states [33, 34]. Another difficulty in fixing only the Weyl gauge is that the perturbative gauge field propagator is plagued by unphysical poles [35].

In the present thesis, the gauge shall be completely fixed¹¹ already at the classical level by imposing the temporal Coulomb gauge conditions

$$A_0^a(x) \approx 0 \quad (1.65a)$$

$$\hat{D}_k^{ab}(x) A_k^b(x) = \partial_k A_k^a(x) \approx 0 \quad (1.65b)$$

and only afterwards, the quantization will be issued with the Dirac brackets. This choice was also discussed in [36, 37]. Complete gauge fixing, such as the temporal Coulomb gauge (1.65),

¹¹See footnote 9.

has the advantage that it can be chosen such as to remove all unphysical degrees of freedom. The Gauss law then holds as an operator identity. In exchange, the algebra of the quantization procedure is slightly more involved.

Analogously to electrodynamics, the first constraint to momentum phase-space is given by the time component of the momentum operator

$$\varphi_1^a(x) := \Pi_0^a(x) = \frac{\delta \mathcal{L}_{YM}}{\delta \partial_0 A_0^a(x)} \approx 0. \quad (1.66)$$

The Hamiltonian (1.18) with $\mathbf{j}^a = 0$ for simplicity,

$$H = \frac{1}{2} \int d^3x (\Pi_k^a \Pi_k^a + B_k^a B_k^a) - \int d^3x A_0^a \mathcal{G}^a \quad (1.67)$$

serves as the generator of time translations.¹² The stationarity of the constraint (1.66) gives a further constraint,

$$\varphi_2^a(x) := \{\varphi_1^a(x), H_T\} = \mathcal{G}^a(x) = \hat{D}_k^{ab}(x) \Pi_k^b(x) + g \rho_{\text{ext}}^a(x) \approx 0, \quad (1.68)$$

where the equal-time fundamental Poisson brackets were employed,

$$\left\{ A_\mu^a(\mathbf{x}, t), \Pi_\nu^b(\mathbf{y}, t) \right\} = \delta_{\mu\nu} \delta^{ab} \delta^3(\mathbf{x}, \mathbf{y}). \quad (1.69)$$

The constraint φ_2 is found to be stationary using the well-known identity [34]

$$\{\mathcal{G}^a(\mathbf{x}, t), \mathcal{G}^b(\mathbf{y}, t)\} = g f^{abc} \mathcal{G}^c(\mathbf{x}, t) \delta^3(\mathbf{x}, \mathbf{y}) \approx 0. \quad (1.70)$$

The above quantity weakly vanishes¹³ in view of Eq. (1.68) and therefore the constraints φ_1 and φ_2 in Eqs. (1.66) and (1.68) form the complete set of constraints. The latter are first-class and are turned into second-class by the gauge fixing condition (1.65).

Before proceeding to the calculation of the Dirac brackets, let us introduce a convenient shorthand notation. The coordinate dependence is absorbed into the color index which is thus understood as a collective index. Vectors in Lorentz space keep their Lorentz indices to avoid an over-estranged notation. All fields are considered at a fixed time. Repeated indices are summed over, i.e. for the color indices this implies an integration over the implicit coordinate dependence.

For instance,

$$A_k^a(\mathbf{x}) \equiv A_k^a, \quad \Pi_k^a(\mathbf{x}) \equiv \Pi_k^a. \quad (1.71)$$

In addition, derivatives are written as matrices in coordinate and color space,

$$\partial_k^{\mathbf{x}} \delta^3(\mathbf{x}, \mathbf{y}) \delta^{ab} \equiv \partial_k^{ab}, \quad \hat{D}_k^{ab}(\mathbf{x}) \delta^3(\mathbf{x}, \mathbf{y}) \equiv \hat{D}_k^{ab}. \quad (1.72)$$

¹²In the same way as in the previous section, we write $\Pi_k^a(x)$, meaning $\Pi^{ka}(x)$.

¹³A theorem due to Dirac [14] ensures that a Poisson bracket of two first-class constraints is again first-class.

Note that these matrices are antisymmetric under the exchange of the collective indices,

$$\partial_k^{ab} = -\partial_k^{ba}, \quad \hat{D}_k^{ab} = -\hat{D}_k^{ba}. \quad (1.73)$$

Also note the symmetric matrices

$$\delta^{ab}\delta^3(\mathbf{x}, \mathbf{y}) \equiv \delta^{ab}, \quad \delta^{ab}t_{ij}(\mathbf{x}, \mathbf{y}) \equiv t_{ij}^{ab}, \quad \delta^{ab}\ell_{ij}(\mathbf{x}, \mathbf{y}) \equiv \ell_{ij}^{ab}. \quad (1.74)$$

The constraints along with the gauge-fixing conditions are collected in a vector ϕ with elements

$$\phi_1^a = \varphi_1^a = \Pi_0^a \approx 0 \quad (1.75a)$$

$$\phi_2^a = \varphi_2^a = \mathcal{G}^a \approx 0 \quad (1.75b)$$

$$\phi_3^a = \chi_1^a = A_0^a \approx 0 \quad (1.75c)$$

$$\phi_4^a = \chi_2^a = \partial_k^{ab} A_k^b \approx 0 \quad (1.75d)$$

to give a regular constraint matrix $C^{ab} = (\{\phi_m^a, \phi_n^b\})$. The relevant Poisson brackets for its calculation yield

$$\{A_0^a, \Pi_0^b\} = \delta^{ab} \quad (1.76a)$$

$$\{A_i^a, \Pi_j^b\} = \delta_{ij}\delta^{ab} \quad (1.76b)$$

$$\{A_k^a, \phi_2^b\} = \hat{D}_j^{bc}\{A_k^a, \Pi_j^c\} = -\hat{D}_k^{ab} \quad (1.76c)$$

$$\{\phi_4^a, \Pi_k^b\} = \partial_j^{ac}\{A_j^c, \Pi_k^b\} = \partial_k^{ab} \quad (1.76d)$$

$$\{\phi_2^a, \phi_4^b\} = \hat{D}_i^{ac}\partial_j^{bd}\{\Pi_i^c, A_j^d\} = \hat{D}_i^{ac}\partial_i^{cb} =: -[G^{-1}]^{ab} \quad (1.76e)$$

In the last line we have defined the non-local matrix G^{-1} which is symmetric in view of the antisymmetric matrices in Eq. (1.73). Furthermore, due to the Coulomb gauge condition (1.65b), it obeys the relation

$$[G^{-1}]^{ab} = -\hat{D}_k^{ac}\partial_k^{cb} = -\partial_k^{ac}\hat{D}_k^{cb} \quad (1.77)$$

and its inverse G is defined by

$$G^{ac}[G^{-1}]^{cb} = [G^{-1}]^{ac}G^{cb} = \delta^{ab}. \quad (1.78)$$

All (weakly) non-zero matrix elements $(C^{ab})_{mn}$ are now given by Eqs. (1.76a) and (1.76e) so that the constraint matrix reads

$$C^{ab} \approx \begin{pmatrix} 0 & 0 & -\delta^{ab} & 0 \\ 0 & 0 & 0 & -[G^{-1}]^{ab} \\ \delta^{ab} & 0 & 0 & 0 \\ 0 & [G^{-1}]^{ab} & 0 & 0 \end{pmatrix} \quad (1.79)$$

and its inverse is given by

$$[C^{-1}]^{ab} \approx \begin{pmatrix} 0 & 0 & \delta^{ab} & 0 \\ 0 & 0 & 0 & G^{ab} \\ -\delta^{ab} & 0 & 0 & 0 \\ 0 & -G^{ab} & 0 & 0 \end{pmatrix}. \quad (1.80)$$

At this point, let us emphasize that the matrix G , which will be the classical counterpart of the ghost operator, can only be made explicit by an infinite series expansion in the coupling constant g .¹⁴ This has led some authors to refrain from the constrained quantization with such a constraint matrix, see Refs. [19, 38, 39]. In Refs. [40, 41], a Hamiltonian operator is obtained but one is left with operator ordering ambiguities. In other gauges, where $A_0 \neq 0$, the expression for C^{ab} becomes even more complicated [20]. Our approach aims at a comparison to the Christ-Lee Hamiltonian [24] in the temporal Coulomb gauge. Therefore, let us press on with the formal expression for G defined by (1.78) and with the inverse constraint matrix (1.80).

The fundamental Dirac brackets are defined by

$$\{A_\mu^a, \Pi_\nu^b\}_D = \{A_\mu^a, \Pi_\nu^b\} - \{A_\mu^a, \phi_m^{a'}\}([C^{-1}]^{a'b'})_{mn}\{\phi_n^{b'}, \Pi_\nu^b\} \quad (1.81)$$

and, using Eq. (1.76), are calculated to yield

$$\{A_0^a, \Pi_k^b\}_D = \{A_0^a, \Pi_0^b\}_D = \{A_k^a, \Pi_0^b\}_D = 0 \quad (1.82)$$

$$\{A_i^a, \Pi_j^b\}_D = \delta_{ij}\delta^{ab} - (-\hat{D}_i^{ac})G^{cd}\partial_j^{db} = \delta_{ij}\delta^{ab} + \hat{D}_i^{ac}G^{cd}\partial_j^{db} =: T_{ij}^{ab} \quad (1.83)$$

It is clear that the Dirac brackets (1.82) must vanish since, by construction, the Dirac bracket of a constraint with any phase space function vanishes, recall Eq. (1.36). In particular, the Gauss law functional $\mathcal{G}^a = \phi_2^a$ has vanishing Dirac bracket with any function $\mathcal{O}[A, \Pi]$,

$$\{\mathcal{G}^a, \mathcal{O}^b\}_D = 0, \quad (1.84)$$

as one may easily convince oneself, cf. Eq. (1.36). All second-class constraints equations hold strongly. The non-symmetric matrix T_{ij}^{ab} occurring in Eq. (1.83) can be understood in some sense as a non-abelian generalization of the transverse projector t_{ij} .¹⁵ It obviously has the projector property $T^2 = T$, and the projector orthogonal to it is given by $L := \mathbb{1} - T$. We thus have

$$L_{ij}^{ab} = -\hat{D}_i^{ac}G^{cd}\partial_j^{db}, \quad T_{ij}^{ab} = \delta_{ij}^{ab} + \hat{D}_i^{ac}G^{cd}\partial_j^{db}, \quad TL = LT = 0. \quad (1.85)$$

Just like for t_{ij} , it is important to note that T_{ij}^{ab} has zero modes,

$$\partial_i^{ab}T_{ij}^{bc} = T_{ij}^{ab}\hat{D}_j^{bc} = 0. \quad (1.86)$$

We are now ready to pass to the quantum theory with the prescription

$$i\{A_\mu^a, \Pi_\nu^b\}_D \rightarrow [A_\mu^a, \Pi_\nu^b]. \quad (1.87)$$

It is understood that all fields are operators henceforth. The second-class constraints (1.75) now hold strongly and can be imposed as operator identities,

$$A_0^a = \Pi_0^a = \mathcal{G}^a = A_k^{\parallel a} = 0. \quad (1.88)$$

¹⁴On top of that, zero modes of the matrix G^{-1} infer that G exists only in subspace of Γ_R . This will be discussed in chapter 2.

¹⁵Letting $\hat{D} \rightarrow \partial$, one regains the familiar expression (1.57). Note the sign in $G = -(\hat{D}\partial)^{-1}$.

In order to arrive at a representation for the momentum operator Π_k^a that is to obey

$$[A_i^{\perp a}, \Pi_j^b] = iT_{ij}^{ab}, \quad (1.89)$$

it is helpful to split it into the orthogonal projections (from the right side) of T and L ,

$$\Pi_k^a = \Pi_k^{Ta} + \Pi_k^{La}, \quad \Pi_k^{Ta} = \Pi_j^b T_{jk}^{ba}, \quad \Pi_k^{La} = \Pi_j^b L_{jk}^{ba}. \quad (1.90)$$

The commutation relations (1.89) are thus decomposed into two separate ones,

$$[A_i^{\perp a}, \Pi_j^{Lb}] = 0 \quad (1.91)$$

$$[A_i^{\perp a}, \Pi_j^{Tb}] = iT_{ij}^{ab} \quad (1.92)$$

and a situation similar to the abelian case, cf. section 1.3, occurs. Recall that the longitudinal component Π^{\parallel} obeyed a trivial commutation relation equivalent to Π^L in (1.91) and had to be determined by the (strong) Gauss law (1.61). The transverse component Π^{\perp} obeyed $[A_i^{\perp}, \Pi_j^{\perp}] = t_{ij}$ which has the easily found solution (1.63). Here, the “non-abelian projector” T (1.85) in $[A^{\perp}, \Pi^T] = iT$ contains field operators A^{\perp} . Nevertheless, a representation of Π_k^{Ta} can be found to be

$$\Pi_k^{Ta} = T_{jk}^{ba} \frac{\delta}{i\delta A_j^{\perp b}} = T_{jk}^{ba} \Pi_j^{\perp b}, \quad (1.93)$$

as verified by plugging Eq. (1.93) into Eq. (1.92). Note here that T is not symmetric.

The component Π^L is determined by the Gauss law (1.68) which yields

$$\hat{D}_k^{ab} \Pi_k^b = \hat{D}_k^{ab} T_{jk}^{cb} \Pi_j^{\perp c} + \hat{D}_k^{ab} \Pi_j^c L_{jk}^{cb} = \hat{D}_k^{ab} \Pi_k^{Lb} = -g\rho_{\text{ext}}^a. \quad (1.94)$$

where the contribution of Π^T vanishes in view of Eq. (1.86). To solve Eq. (1.94) for Π^L , one may use the Helmholtz theorem to write Π^L as the gradient field of some field operator Φ since

$$(\partial \times \Pi^L)_k^a = \epsilon_{ijk} \partial_i^{ab} \Pi_j^{Lb} = -\epsilon_{ijk} \partial_i^{ab} \Pi_n^e \hat{D}_n^{ed} G^{dc} \partial_j^{cb} = 0. \quad (1.95)$$

We can then write $\Pi_k^{La} = -\partial_k^{ab} \Phi^b$ and solve the Gauss law (1.94) by $\Phi^a = -gG^{ab} \rho_{\text{ext}}^b$. The operator Π^L then is explicitly given as a functional of field operators A^{\perp} ,

$$\Pi_k^{La} [A^{\perp}] = g\partial_k^{ab} G^{bc} [A^{\perp}] \rho_{\text{ext}}^c. \quad (1.96)$$

One may subsequently verify the commutation relation (1.91).

Before we go on to derive the Hamiltonian operator from the classical one (1.67) by promoting the fields A_k^a and Π_k^a to their operator-valued counterparts, operator ordering is briefly discussed, cf. Ref. [24]. Gauge fixing gives rise to non-trivial factors in the Hamiltonian, as can be seen in the path integral formalism. Using the the Faddeev–Popov trick [42], the kinetic

energy E_k yields¹⁶

$$\begin{aligned}
 E_k &= \langle \Psi | \Psi \rangle^{-1} \frac{1}{2} \langle \Psi | \Pi_k^a \Pi_k^a | \Psi \rangle \\
 &= \langle \Psi | \Psi \rangle^{-1} \frac{1}{2} \int \mathcal{D}A \Psi^*[A] \Pi_k^a \Pi_k^a \Psi[A] \\
 &= \langle \Psi | \Psi \rangle^{-1} \frac{1}{2} \int \mathcal{D}A (\Pi_k^a \Psi)^*[A] (\Pi_k^a \Psi)[A] \\
 &= \frac{1}{2} \int \mathcal{D}A^\perp \mathcal{J}[A^\perp] ((\Pi_k^{Ta} + \Pi_k^{La})\Psi)^*[A^\perp] ((\Pi_k^{Ta} + \Pi_k^{La})\Psi)[A^\perp] \\
 &= \frac{1}{2} \int \mathcal{D}A^\perp \mathcal{J}[A^\perp] \Psi^*[A^\perp] \left(\frac{1}{\mathcal{J}[A^\perp]} (\Pi_k^{Ta\dagger} + \Pi_k^{La\dagger}) \mathcal{J}[A^\perp] (\Pi_k^{Ta} + \Pi_k^{La}) \right) \Psi[A^\perp],
 \end{aligned} \tag{1.98}$$

where the state norm $\langle \Psi | \Psi \rangle$ was chosen such as to cancel the group volume, and

$$\mathcal{J}[A^\perp] = \text{Det}(G^{-1})[A^\perp] \tag{1.99}$$

is the Faddeev–Popov determinant. The last line in Eq. (1.98) is obtained by taking the hermitian adjoint of the product $\mathcal{J}(\Pi^T + \Pi^L)$ with respect to the inner product in functional space when bringing the Ψ^* to the left. One can read off from Eq. (1.98) the form of the kinetic part of the Hamiltonian operator

$$H_k[A^\perp, \Pi^T, \Pi^L] = \frac{1}{2} \mathcal{J}^{-1}[A^\perp] \left(\Pi_k^{Ta\dagger} + \Pi_k^{La\dagger} \right) \mathcal{J}[A^\perp] (\Pi_k^{Ta} + \Pi_k^{La}). \tag{1.100}$$

The decomposition of the momentum operator $\Pi = \Pi^T + \Pi^L$ with the expressions (1.93) and (1.96) can now be inserted into (1.100), giving rise to four terms. Let us consider these separately. One term reads

$$\begin{aligned}
 H_k^{LL} &= \frac{1}{2} \mathcal{J}^{-1} \Pi_k^{La\dagger} \mathcal{J} \Pi_k^{La} \\
 &= \frac{1}{2} \mathcal{J}^{-1} \left(g \partial_k^{ab} G^{bc} \rho_{\text{ext}}^c \right) \mathcal{J} \left(g \partial_k^{ad} G^{de} \rho_{\text{ext}}^e \right) \\
 &= \frac{g^2}{2} \rho_{\text{ext}}^c G^{cb} \left(-\partial_k^{ba} \partial_k^{ad} \right) G^{de} \rho_{\text{ext}}^e \\
 &= \frac{g^2}{2} \rho_{\text{ext}}^c F^{ce} \rho_{\text{ext}}^e
 \end{aligned} \tag{1.101}$$

and is recognized as the Coulomb interaction of external charges via the Coulomb Green function $F := G(-\partial^2)G$. Using the relation $t_{ij}^{ab} T_{jk}^{bc} \partial_k^{cd} = -t_{ij}^{ab} L_{jk}^{bc} \partial_k^{cd}$ as well as the identification

¹⁶The result is reminiscent of the Laplace–Beltrami operator Δ with a non-trivial metric $g_{\mu\nu}$ and its determinant $g = \det(g_{\mu\nu})$, see Ref. [43],

$$\Delta = -\frac{1}{\sqrt{g}} \partial_\mu \sqrt{g} g^{\mu\nu} \partial_\nu, \tag{1.97}$$

as pointed out in Refs. [24, 44]. The Weyl gauge operators are then in Cartesian coordinates, whereas the Coulomb gauge operators correspond to curvilinear ones. In contrast to Ref. [24], we here have no Cartesian coordinates to start with, since the temporal Coulomb gauge was already fixed on the classical level.

of the dynamical gluonic charge ρ_{dyn} in¹⁷

$$\hat{D}_k^{ab} \Pi_k^{\perp b} = \Pi_k^{\perp b} \hat{D}_k^{ab} = g \hat{A}_k^{\perp ab} \Pi_k^{\perp b} =: g \rho_{\text{dyn}}^a \quad (1.102)$$

we further find

$$\begin{aligned} H_k^{LT} &= \frac{1}{2} \frac{1}{\mathcal{J}} \Pi_k^{La\dagger} \mathcal{J} \Pi_k^{Ta} \\ &= \frac{1}{2} g \partial_k^{ab} G^{bc} \rho_{\text{ext}}^c T_{mk}^{da} \Pi_m^{\perp d} \\ &= \frac{g}{2} \rho_{\text{ext}}^c G^{cb} \left(-\partial_k^{ba} \right) \hat{D}_m^{dd'} G^{d'a'} \partial_k^{a'a} \Pi_m^{\perp d} \\ &= \frac{g}{2} \rho_{\text{ext}}^c G^{cb} \left(-\partial_k^{ba} \partial_k^{aa'} \right) G^{a'd'} \hat{D}_m^{d'd} \Pi_m^{\perp d} \\ &= \frac{g^2}{2} \rho_{\text{ext}}^c F^{cd'} \rho_{\text{dyn}}^{d'} \end{aligned} \quad (1.103)$$

and

$$\begin{aligned} H_k^{TL} &= \frac{1}{2} \frac{1}{\mathcal{J}} \Pi_k^{Ta\dagger} \mathcal{J} \Pi_k^{La} \\ &= \frac{1}{2} \frac{1}{\mathcal{J}} \Pi_m^{\perp b} T_{mk}^{ba} \mathcal{J} g \partial_k^{ac} G^{cd} \rho_{\text{ext}}^d \\ &= \frac{g}{2} \frac{1}{\mathcal{J}} \Pi_m^{\perp b} \hat{D}_m^{bb'} \mathcal{J} G^{b'a'} \partial_k^{a'a} \partial_k^{ac} G^{cd} \rho_{\text{ext}}^d \\ &= \frac{g^2}{2} \frac{1}{\mathcal{J}} \rho_{\text{dyn}}^{b'} \mathcal{J} F^{b'd} \rho_{\text{ext}}^d, \end{aligned} \quad (1.104)$$

two contributions that account for the Coulomb interaction of dynamical and external charges. Using the identity $t_{m'm}^{b'b} T_{mk}^{ba} T_{nk}^{ca} t_{nn'}^{cc'} = t_{m'n'}^{b'c'} + t_{m'm}^{b'b} L_{mk}^{ba} L_{nk}^{ca} t_{nn'}^{cc'}$ we get two further contributions to H_k ,

$$\begin{aligned} H_k^{TT} &= \frac{1}{2} \frac{1}{\mathcal{J}} \Pi_k^{Ta\dagger} \mathcal{J} \Pi_k^{Ta} \\ &= \frac{1}{2} \frac{1}{\mathcal{J}} \Pi_m^{\perp b} T_{mk}^{ba} \mathcal{J} T_{nk}^{ca} \Pi_n^{\perp c} \\ &= \frac{1}{2} \frac{1}{\mathcal{J}} \Pi_k^{\perp a} \mathcal{J} \Pi_k^{\perp a} + \frac{1}{2} \frac{1}{\mathcal{J}} \Pi_m^{\perp b} \hat{D}_m^{bb'} G^{b'a'} \partial_k^{a'a} \mathcal{J} \hat{D}_n^{cc'} G^{c'a''} \partial_k^{a''a} \Pi_n^{\perp c} \\ &= \frac{1}{2} \frac{1}{\mathcal{J}} \Pi_k^{\perp a} \mathcal{J} \Pi_k^{\perp a} + \frac{g^2}{2} \frac{1}{\mathcal{J}} \rho_{\text{dyn}}^{b'} \mathcal{J} G^{b'a} \left(-\partial_k^{a'a} \partial_k^{aa''} \right) G^{a''c'} \rho_{\text{dyn}}^{c'} \\ &= \frac{1}{2} \frac{1}{\mathcal{J}} \Pi_k^{\perp a} \mathcal{J} \Pi_k^{\perp a} + \frac{g^2}{2} \frac{1}{\mathcal{J}} \rho_{\text{dyn}}^{b'} \mathcal{J} F^{b'c'} \rho_{\text{dyn}}^{c'}, \end{aligned} \quad (1.105)$$

namely the kinetic energy of transverse gluons as well as the Coulomb interaction of dynamical charges. The magnetic potential operator H_p can be obtained straightforwardly from its classical counterpart in Eq. (1.67) since it only comprises the coordinates A_k^a . It simply yields

$$H_p = \frac{1}{2} B_k^a [A^\perp] B_k^a [A^\perp]. \quad (1.106)$$

¹⁷With the conventions used here, $\rho_{\text{dyn}}^a = \hat{A}_k^{\perp ab} \Pi_k^{\perp b} = -\hat{\mathbf{A}}^{\perp ab} \cdot \mathbf{\Pi}^b$. Thus, one arrives at $\partial_k \Pi_k^a = -g(\rho_{\text{ext}}^a + \rho_{\text{dyn}}^a)$.

Adding the contributions (1.101), (1.103), (1.104), (1.105) and (1.106), we finally arrive at the Hamiltonian operator in temporal Coulomb gauge. In explicit notation, it reads

$$\boxed{
 \begin{aligned}
 H[A^\perp, \Pi^\perp] &= \frac{1}{2} \int d^3x \frac{1}{\mathcal{J}} \Pi_k^{\perp a}(\mathbf{x}) \mathcal{J} \Pi_k^{\perp a}(\mathbf{x}) + \frac{1}{2} \int d^3x B_k^{\perp a}(\mathbf{x}) B_k^{\perp a}(\mathbf{x}) \\
 &\quad + \frac{g^2}{2} \int d^3x d^3y \frac{1}{\mathcal{J}} \rho^a(\mathbf{x}) \mathcal{J} F^{ab}(\mathbf{x}, \mathbf{y}) \rho^b(\mathbf{y}) .
 \end{aligned}
 } \tag{1.107}$$

Here, we have defined the total charge density

$$\rho^a(\mathbf{x}) := \rho_{\text{dyn}}^a(\mathbf{x}) + \rho_{\text{ext}}^a(\mathbf{x}) = \hat{A}_k^{ab}(\mathbf{x}) \Pi_k^b(\mathbf{x}) + \psi^\dagger(\mathbf{x}) i T^a \psi(\mathbf{x}) . \tag{1.108}$$

For future reference, let us write down the explicit form of the Coulomb operator F ,

$$F^{ab}(\mathbf{x}, \mathbf{y}) = \int d^3x' G^{ac}(\mathbf{x}, \mathbf{x}') (-\partial^2) G^{cb}(\mathbf{x}', \mathbf{y}) \tag{1.109}$$

and of the inverse ghost operator

$$[G^{-1}]^{ab}(\mathbf{x}, \mathbf{y}) = -\delta^{ab} \partial^2 \delta^3(\mathbf{x}, \mathbf{y}) - g \hat{A}_k^{ab}(\mathbf{x}) \partial_k^{\mathbf{x}} \delta^3(\mathbf{x}, \mathbf{y}) . \tag{1.110}$$

Christ and Lee [24] derived the same result as in Eq. (1.107) using a different approach. They quantized the Cartesian coordinates in Weyl gauge and only subsequently transformed into the Coulomb gauge, keeping the Gauss law as a constraint on the wave functional. Here, we were able to reinforce the Gauss law as a operator identity, having used Dirac's concept of constrained quantization. It is reassuring to see that the two methods produce the same result for the Yang–Mills energy spectrum, keeping in mind that in general such an equivalence cannot be established [44, 45, 46, 47, 48].

2 Infrared ghost dominance

The complex structure of the Yang–Mills Hamiltonian (1.107) derived in the previous section does not allow for a rigorous calculation of the energy spectrum or the Green functions. Perturbation theory in the gauge coupling g provides a possibility to describe interactions with high momentum transfer in QCD where asymptotic freedom guarantees that g can be treated as a small parameter. The infrared sector, however, is not accessible by perturbative methods since we know from the renormalization group that g increases as we go to lower energies. An understanding of long-range interactions of quarks and gluons thus calls for nonperturbative methods. *Color confinement*, the experimental evidence that quarks and gluons have never been detected as asymptotic states and must be confined into color singlets, is to date one of the most challenging topics in theoretical physics.

By means of lattice calculations, it has been possible to penetrate the infrared nonperturbative sector of QCD and uncover a confining potential between (static) quarks [49, 8]. At present, however, available lattice sizes do not suffice to describe the Green functions in the deep infrared [50, 51]. Despite the ever-growing computational power, a numerical simulation of confinement on the lattice will always fall short of proving it. Nevertheless, the achievements of the lattice community with calculations that are particularly reliable in the intermediate momentum regime, are indispensable for the mutual dialogue with the continuum approach. A joint theoretical investigation of QCD phenomena is a promising project for progressive research.

The continuum approach has the intriguing feature that the asymptotic infrared limit can be studied analytically. In the last decade, a new understanding of infrared QCD has arisen from studying continuum Yang–Mills (YM) theory via Dyson–Schwinger equations. The Landau gauge has the advantage of being covariant, allowing for straightforward perturbative calculations, and it therefore encouraged many to intensive investigation of the infrared properties of YM theory [52, 53, 54]. In Coulomb gauge, non-covariance brings about severe technical difficulties which are only recently on the verge of being overcome [55, 56, 57]. Nevertheless, the Coulomb gauge might be the more efficient choice to identify the nonabelian degrees of freedom. It is well-known that screening and anti-screening contributions to the interquark potential are neatly separated in Coulomb gauge perturbation theory [58]. As for the infrared domain, the Gribov–Zwanziger scenario serves as a transparent confinement mechanism [59, 60].

In this chapter, the Gribov–Zwanziger scenario shall be introduced and analyzed in the temporal Coulomb gauge. It will be thus possible to provide information on the asymptotic infrared behavior of the Green functions and recover a linearly rising potential between static color charges, i.e. heavy quark confinement. A full numerical calculation in chapter 3 will be seen to reproduce the infrared asymptotics given here analytically. Moreover, the infrared asymptotics of Landau gauge can be retrieved from a generalization of the results in the temporal Coulomb gauge.

2.1 Gribov–Zwanziger scenario of confinement

Having outlined the issues of redundant degrees of freedom in section 1.2, a discussion of gauge fixing in the context of Yang–Mills theory may follow naturally. In particular, we have touched upon the issue of uniqueness of a gauge fixing condition

$$\chi^a[A] = 0. \quad (2.1)$$

Uniqueness was shown to be locally guaranteed by the criterion (1.41) which reads for the classical YM theory

$$\text{Det} \left(\{\chi^a, \mathcal{G}^b\} \right) \not\approx 0. \quad (2.2)$$

Locally means here that only a small neighborhood of the point \mathcal{A} in configuration space that satisfies (2.1) is considered. An infinitesimal gauge transformation according to Eq. (1.29),

$$\chi^a[\mathcal{A}] \rightarrow \chi^a[\mathcal{A}] + \{\chi^a, \mathcal{G}^b\} \Big|_{\mathcal{A}=\mathcal{A}} \epsilon^b, \quad (2.3)$$

shows that \mathcal{A} is the unique solution to (2.1) only if Eq. (2.2) holds. Let us now turn to the quantum theory in the Schrödinger picture. Gribov [59] discovered that if the Coulomb gauge condition $\chi^a(\mathbf{x}) = \partial_k A_k^a(\mathbf{x}) = 0$ is chosen, uniqueness of its solution \mathcal{A} is lost if the matrix G^{-1} with components

$$[G^{-1}]^{ab}(\mathbf{x}, \mathbf{y}) = \left(-\partial^2 \delta^{ab} - g \hat{A}_k^{ab} \partial_k^{\mathbf{x}} \right) \delta^3(\mathbf{x}, \mathbf{y}) \quad (2.4)$$

develops zero modes. From the explicit form of G^{-1} this is seen to happen for large magnitudes of gA , i.e. in the nonperturbative domain. The field configuration \mathcal{A} can then be shown to be connected by a gauge transformation to one or more \mathcal{A}^U , called *Gribov copies*, that also obey the Coulomb gauge condition. Gribov copies lead to incorrect results in the calculation of expectation values due to over-counting of physically equivalent field configurations. The criterion for avoiding Gribov copies is the quantum analogue of Eq. (2.2), noting that $G^{-1} = \{\partial_k A_k, \mathcal{G}\}$, and reads

$$\mathcal{J}[A] = \text{Det} (G^{-1}) \neq 0. \quad (2.5)$$

It is illuminating to see how the above uniqueness condition follows from a direct calculation. Consider a gauge transformation \mathcal{A}^U where $U(\mathbf{x}) = e^{-\alpha(\mathbf{x})} \approx 1 - \alpha(\mathbf{x})$ is very close to unity. The field \mathcal{A}^U is a Gribov copy of \mathcal{A} if

$$\begin{aligned} 0 &= \partial_k \mathcal{A}_k^U = \partial_k U \mathcal{A}_k U^\dagger + \frac{1}{g} \partial_k U \partial_k U^\dagger \\ &= U \left(-(\partial_k \alpha) \mathcal{A}_k + \mathcal{A}_k (\partial_k \alpha) - \frac{1}{g} (\partial_k \alpha) (\partial_k \alpha) + \frac{1}{g} (\partial^2 \alpha) + \frac{1}{g} (\partial_k \alpha) (\partial_k \alpha) \right) U^\dagger \\ &= \frac{1}{g} U \left((\partial^2 \alpha) + g [\mathcal{A}_k, (\partial_k \alpha)] \right) U^\dagger \\ &= \frac{1}{g} U T^a \left(\left(\delta^{ab} \partial^2 + g \hat{A}_k^{ab} \partial_k \right) \alpha^b \right) U^\dagger. \end{aligned} \quad (2.6)$$

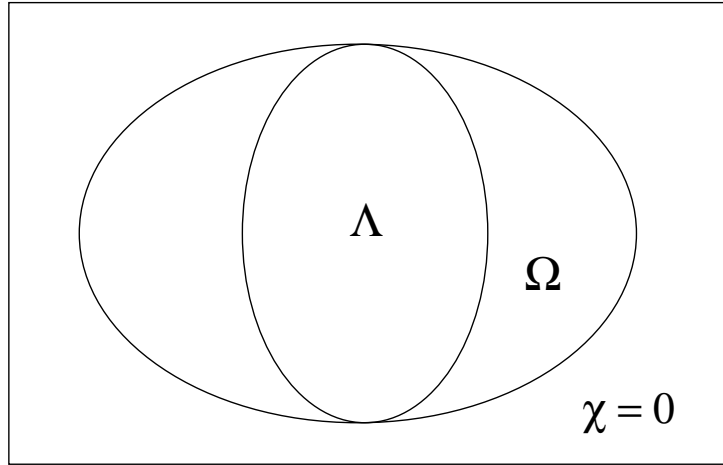


Figure 2.1: Configuration space and its restriction to the gauge fixing condition $\chi = 0$, the (first) Gribov region Ω and the fundamental modular region Λ .

Since the matrices U are regular and T^a are linearly independent, Eq. (2.6) can be written as

$$\int d^3y [G^{-1}]^{ab}(\mathbf{x}, \mathbf{y}) \alpha^b(\mathbf{y}) = 0. \quad (2.7)$$

Thus, if the condition (2.5) is fulfilled, then $\alpha^a(\mathbf{x}) = 0$ and $\mathcal{A}^U = \mathcal{A}$, and the solution \mathcal{A} of the gauge fixing condition (2.1) is unique.

The configuration space is therefore decomposed into the so-called *Gribov regions*, alternating in sign of the Faddeev–Popov determinant \mathcal{J} . By definition, the first Gribov region Ω contains the perturbative vacuum, $gA = 0$, and has a positive definite Faddeev–Popov determinant,

$$\Omega = \{A \mid \partial_k A_k = 0, \mathcal{J}[A] > 0\}. \quad (2.8)$$

In order to avoid Gribov copies, it is necessary to restrict the configuration space to the first Gribov region Ω , bounded by the Gribov horizon $\partial\Omega$, see Fig. 2.1. Practically, it is not straightforward to implement this restriction. One might naturally ask whether a gauge fixing condition exists, different from the Coulomb gauge, for which the Faddeev–Popov determinant is manifestly positive and the Gribov problem does not arise. However, a theorem due to Singer [61] states that (on a three- or four-dimensional compact manifold) there exists no gauge fixing condition that does not have the Gribov problem.

A restriction to Ω can be realized by an action principle, as noted by Polyakov¹. It requires that the L^2 norm of the gauge field $A_k(\mathbf{x})$ be minimal along its orbit, parametrised by the

¹See footnote in Ref. [62].

gauge transformations $U(\mathbf{x}) = e^{-\alpha(\mathbf{x})}$,

$$\begin{aligned} F_A[U] &:= \int d^3x \operatorname{tr} (A_k^U(\mathbf{x}))^2 \\ &= F_A[1] - \frac{2}{g} \int d^3x \operatorname{tr} (\alpha(\mathbf{x}) \partial_k A_k(\mathbf{x})) + \\ &\quad \frac{1}{g^2} \int d^3x d^3y \operatorname{tr} (\alpha^\dagger(\mathbf{x}) G^{-1}[A](\mathbf{x}, \mathbf{y}) \alpha(\mathbf{y})) . \end{aligned} \quad (2.9)$$

The stationarity condition sets $A = \mathcal{A}$ and the minimum condition yields $\mathcal{J}[\mathcal{A}] > 0$. Action principles are a common technique to implement gauge fixing on the lattice [63].

However, the restriction to Ω is not sufficient to exclude gauge copies. Various examples [64, 65] indicate that there are Gribov copies inside Ω . A proof of existence was given by Ref. [66], see also Ref. [67]. These remnant Gribov copies show that the minima of $F_A[U]$ in Eq. (2.9) are degenerate. Lattice calculations confirm that there are indeed Gribov copies inside Ω [68, 69, 70]. A further restriction of configuration space is needed to completely exclude Gribov copies. The *fundamental modular region* Λ is defined to be the set of unique² absolute minima of the functional (2.9) among gauge orbits,

$$\Lambda := \{A : F_A[1] \leq F_A[U] \quad \forall U\} . \quad (2.10)$$

It was shown that the interior of Λ is indeed free of Gribov copies whereas the boundary $\partial\Lambda$ still contains Gribov copies [71]. The gauge condition specified by Eq. (2.10) is also termed “minimal Coulomb gauge” [72]. Although conceptually vital, the fundamental modular region as yet lacks the utility for explicit calculations. Little is known about the boundary $\partial\Lambda$. Fortunately, it was shown in Ref. [73] by means of stochastic quantization that despite the Gribov copies inside Ω , expectation values are computed correctly if the integration domain is Ω instead of Λ . This is due to the finding [74] that the dominant field configurations lie on $\partial\Omega \cap \partial\Lambda$, the common boundary of Ω and Λ .³ We shall therefore restrict the configuration space to Ω in the following. Gauge fields A are always transverse and the superscript \perp is abandoned for brevity.

The restriction to a compact region in configuration space, be it Ω or Λ , has important consequences for the infrared sector of the theory. Due to asymptotic freedom, the ultraviolet is not affected by the horizon since when the coupling becomes small, all relevant configurations are in the vicinity of $gA = 0$. It was shown that this point always has a finite distance from the horizon [77]. The nonperturbative infrared sector, on the other hand, can in principle be governed by any region within Ω . From statistical mechanics, we know that in a compact sphere with radius r of high dimension N , the probability distribution is concentrated at the boundary, due to the “entropy factor” $r^{N-1} dr$. If Yang–Mills theory is regularized on the lattice,

²Up to global gauge transformations.

³In this context, let us mention that the field configurations on $\partial\Omega \cap \partial\Lambda$ can be identified as center vortices. These field configurations were found to drive the confining mechanism on the lattice in Coulomb gauge [75] as well as in Landau gauge [76].

Zwanziger argued [60] that the situation is comparable to the latter example, the dimensionality N even diverges in the continuum limit. In the asymptotic infrared, the momentum space ghost propagator

$$D_G(k) := \frac{1}{N_c^2 - 1} \delta^{ab} \int d^3x \langle G[A] \rangle^{ab}(\mathbf{x}, \mathbf{y}) e^{-i\mathbf{k} \cdot (\mathbf{x} - \mathbf{y})}, \quad k = |\mathbf{k}| \quad (2.11)$$

is therefore expected to diverge strongly,

$$\lim_{k \rightarrow 0} [k^2 D_G(k)]^{-1} = 0, \quad (2.12)$$

due to divergent eigenvalues of the operator G on the Gribov horizon. Eq. (2.12) is known as the *horizon condition*. Gribov discussed perturbatively in Ref. [59] that only for $k = 0$ the ghost propagator $D_G(k)$ can have a pole. Zwanziger's horizon condition (2.12), on the other hand, is a nonperturbative statement. Since the Coulomb potential $V_C(k)$ between external color charges is proportional to

$$\int d^3x \langle G(-\partial^2)G \rangle^{ab}(\mathbf{x}, \mathbf{y}) e^{-i\mathbf{k} \cdot (\mathbf{x} - \mathbf{y})}, \quad (2.13)$$

the infrared enhancement of $D_G(k)$ from effects on the Gribov horizon might be the driving mechanism for $V_C(k)$ to diverge as k^{-4} and for a linear confining potential between heavy quarks to emerge. This notion is known as the *Gribov–Zwanziger scenario* of confinement in the Coulomb gauge.

2.2 Stochastic vacuum in Coulomb gauge

Vacuum expectation values that are solely dominated by entropy in configuration space are intriguingly simple. According to the Gribov–Zwanziger scenario, infrared correlation functions of Coulomb gauge YM theory fall under this category and hence can asymptotically be described by a vacuum wave functional $\Psi_0[A]$ stochastically distributed in configuration space. Whilst the full structure of a vacuum expectation value, in particular the perturbative regime, is sensitive to a non-trivial probability distribution $|\Psi[A]|^2$, the infrared limit is fully determined by the geometry in phase space, and one may write $\Psi_0[A] = 1$ to find correct results [78]. This choice of the wave functional is here referred to as the *stochastic vacuum* and suggests the following schematic prescription for the asymptotic evaluation of Coulomb gauge expectation values of any operator $\mathcal{O}(k)$, depending on momentum k ,

$$\langle \Psi | \mathcal{O}(k) | \Psi \rangle = \int_{\Omega} \mathcal{D}A \mathcal{J} \Psi^* \mathcal{O}(k) \Psi \xrightarrow{k \rightarrow 0} \frac{1}{\text{Vol}(\Omega)} \int_{\Omega} \mathcal{D}A \mathcal{J} \mathcal{O} = \langle \Psi_0 | \mathcal{O} | \Psi_0 \rangle. \quad (2.14)$$

We introduced a factor $\text{Vol}(\Omega) = \int_{\Omega} \mathcal{D}A \mathcal{J}[A]$ to normalize the wave functional, $\langle \Psi_0 | \Psi_0 \rangle = 1$, which is possible in the compact region Ω . A legitimate question to ask is whether the factor of the Faddeev–Popov determinant \mathcal{J} does not spoil the argument that the probability distribution is strongly enhanced at the Gribov horizon. Recall that the Gribov horizon $\partial\Omega$

was defined as the boundary of Ω where the Faddeev–Popov matrix G^{-1} picks up vanishing eigenvalues. Hence, the factor $\mathcal{J} = \text{Det } G^{-1}$ will *suppress* the probability distribution on $\partial\Omega$. Nevertheless, it is not clear a priori whether this suppression is strong enough to spoil the enhancement of entropy and we shall put forth as a working hypothesis that it does not.⁴ On the lattice, the density of eigenmodes of the Faddeev–Popov operator is under current investigation [80].

Although the prescription (2.14) for infrared correlations can be motivated from the Gribov–Zwanziger scenario, it cannot be taken for granted that the solutions thus obtained are mathematically unique on the one hand, or physical on the other. To further contemplate Eq. (2.14), note that $\Psi_0[A] = 1$ is the correct wave functional in 1 + 1 dimensional Yang–Mills theory [81, 82]. However, the entropy argument is lacking in 1 + 1 dimensions where the gauge field becomes a compact quantum mechanical variable. In 3 + 1 dimensions, the dynamics might be substantially different. After all, we will try to find the vacuum wave functional in 3 + 1 dimensions that describes not only the infrared limit but also ultraviolet correlations. In the Hamiltonian formalism, the Ritz–Rayleigh variational method gives the possibility to introduce a variational parameter into the wave functional and determine it by minimizing the energy. This method will be discussed in chapter 3 to discuss the full momentum dependence of the Green functions. It will turn out that the full solutions agree with the solution in the stochastic vacuum for asymptotically small momenta [83, 84, 85, 86]. Turning the argument around, these findings support the Gribov–Zwanziger scenario and the notion of a stochastically distributed probability distribution $|\Psi[A]|^2$ in the infrared. The investigation of the stochastic vacuum pursued in this chapter is quite different from a variational approach in that it lacks equations of motion arising from minimizing the energy. However, we may extract information from the geometry in configuration space. In the following section, it will be shown how the boundary conditions of the Gribov region give rise to Dyson–Schwinger integral equations that determine the properties of the Green functions.

2.3 Dyson–Schwinger equations

A convenient tool for the evaluation of expectation values are generating functionals. In particular, the Dyson–Schwinger equations that intercorrelate all Green functions can be straightforwardly derived from the path integral representation of a generating functional. The classification of Green functions into *full*, *connected* and *proper* Green functions is common and the same applies for generating functionals [6]. Full Green functions corresponding to the stochastic vacuum Ψ_0 can be found by

$$\langle \mathcal{O}[A] \rangle \equiv \langle \Psi_0 | \mathcal{O}[A] | \Psi_0 \rangle = \frac{1}{Z[j]} \mathcal{O} \left[\frac{\delta}{\delta j} \right] Z[j] \Big|_{j=0} \quad (2.15)$$

⁴As a simple example [79], consider a d -dimensional sphere with $0 < r < 1$ and let the probability distribution $p(r)$ be damped at the boundary by a factor $(1 - r)^n$ with order $n(d)$. The entropy factor from the integral measure, $dr r^{d-1}$, enhances the probability at the boundary. For large dimensions d , $p(r) = r^{d-1}(1 - r)^n$ is then sharply peaked at $r = 1 - \frac{n}{d}$, provided $\frac{n}{d} \ll 1$, despite the damping factor.

if we define the generating functional $Z[j]$ of full Green functions by

$$Z[j] = \int \mathcal{D}A \mathcal{J}[A] e^{j \cdot A}, \quad j \cdot A \equiv \int d^3x A_i^a(\mathbf{x}) t_{ik}(\mathbf{x}) j_k^a(\mathbf{x}). \quad (2.16)$$

It is easily verified that Eq. (2.15) indeed reproduces the expectation values in the stochastic vacuum, see Eq. (2.14). Dyson–Schwinger equations follow from a quite simple statement, namely that the (path) integral of a total derivative can be expressed by boundary terms. This idea is applied to the path integration in configuration space, bounded by the Gribov horizon. The gauge-fixing procedure endowed us the Faddeev–Popov determinant \mathcal{J} in the path integral, see Eq. (2.4). One is thus led to the identity

$$0 = \int \mathcal{D}A \frac{\delta}{\delta A_j^b(\mathbf{y})} \mathcal{J}[A] e^{j \cdot A} = \int \mathcal{D}A \mathcal{J}[A] \left(\frac{\delta \ln \mathcal{J}[A]}{\delta A_j^b(\mathbf{y})} + t_{jm}(\mathbf{y}) j_m^b(\mathbf{y}) \right) e^{j \cdot A} \quad (2.17)$$

since at the Gribov horizon the Faddeev–Popov determinant vanishes by definition, $\mathcal{J}[A]|_{\partial\Omega} = 0$. Applying to Eq. (2.17) a functional derivative $\delta/\delta j_i^a(\mathbf{x})$, dividing by $Z[j]$ and setting sources to zero, $j = 0$, gives

$$t_{ij}^{ab}(\mathbf{x}, \mathbf{y}) = - \left\langle A_i^a(\mathbf{x}) \frac{\delta \ln \mathcal{J}[A]}{\delta A_j^b(\mathbf{y})} \right\rangle. \quad (2.18)$$

In order to make sense of the above expression, first note that⁵ [83]

$$\frac{\delta \ln \mathcal{J}[A]}{\delta A_i^a(\mathbf{x})} = \text{Tr} \frac{\delta \ln G^{-1}[A]}{\delta A_i^a(\mathbf{x})} = - \text{Tr} \left(G[A] \Gamma_i^{0,a}(\mathbf{x}) \right), \quad (2.19)$$

where $\Gamma_i^{0,a}(\mathbf{x})$ is the tree-level ghost-gluon vertex, here matrix-valued with components

$$\left(\Gamma_i^{0,a}(\mathbf{x}) \right)^{bc}(\mathbf{y}, \mathbf{z}) = - \frac{\delta [G^{-1}]^{bc}(\mathbf{y}, \mathbf{z})}{\delta A_i^a(\mathbf{x})} = g(\hat{T}^a)^{bc} t_{ik}(\mathbf{x}) \delta^3(\mathbf{x}, \mathbf{y}) \partial_k^{\mathbf{y}} \delta^3(\mathbf{y}, \mathbf{z}). \quad (2.20)$$

Second, plugging (2.19) into (2.18), the object $\langle AG \rangle$ can be identified as the dressed connected ghost-gluon vertex that may be decomposed by⁶

$$\begin{aligned} \langle A_i^a(\mathbf{x}) G[A] \rangle &= \int d^3y \langle A_i^a(\mathbf{x}) A_j^b(\mathbf{y}) \rangle \left\langle \frac{\delta G[A]}{\delta A_j^b(\mathbf{y})} \right\rangle \\ &= \int d^3y \langle A_i^a(\mathbf{x}) A_j^b(\mathbf{y}) \rangle \langle G[A] \Gamma_j^{0,b}(\mathbf{y}) G[A] \rangle \\ &= \int d^3y D_{ij}^{ab}(\mathbf{x}, \mathbf{y}) D_G \Gamma_j^b(\mathbf{y}) D_G \end{aligned} \quad (2.21)$$

into the proper ghost-gluon vertex Γ_k^a with propagators attached, namely the gluon propagator

$$D_{ij}^{ab}(\mathbf{x}, \mathbf{y}) := \langle A_i^a(\mathbf{x}) A_j^b(\mathbf{y}) \rangle, \quad (2.22)$$

⁵It is convenient to denote by \mathcal{O} a matrix with elements $\mathcal{O}^{ab}(\mathbf{x}, \mathbf{y}) = \langle \mathbf{x}, a | \mathcal{O} | \mathbf{y}, b \rangle$ in color and (continuous) coordinate space. The trace “Tr” sums up diagonal elements in both the latter spaces. For notation, see also appendix A.

⁶If the generating functional is Gaussian, Wick’s theorem infers the factorization in the first line of Eq. (2.21). Without the use of Wick’s theorem, as for the stochastic vacuum, one may use functional methods [73].

and the (here matrix-valued) ghost propagator D_G , with matrix elements

$$D_G^{ab}(\mathbf{x}, \mathbf{y}) = \langle G[A]^{ab}(\mathbf{x}, \mathbf{y}) \rangle . \quad (2.23)$$

The present calculations circumvent the common introduction of ghost fields by interpreting $\mathcal{J}[A]$ as a Gaussian integral over Grassmann variables. In fact, the introduction of Grassmann fields and their sources spoils the argument that boundary terms from the Gribov horizon vanish [73]. It is therefore advisory to stick to the functional determinant $\mathcal{J}[A]$ and not to introduce ghost sources. Nevertheless, we refer to D_G as the “ghost” propagator and Γ_k as the “ghost-gluon” vertex.

With the above definitions, the Dyson–Schwinger equation (2.18) becomes

$$\begin{aligned} t_{ij}^{ab}(\mathbf{x}, \mathbf{y}) &= \text{Tr} \left(\langle A_i^a(\mathbf{x}) G[A] \rangle \Gamma_j^{0,b}(\mathbf{y}) \right) \\ &= \int d^3 z D_{ik}^{ac}(\mathbf{x}, \mathbf{z}) \text{Tr} \left(D_G \Gamma_k^c(\mathbf{z}) D_G \Gamma_j^{0,b}(\mathbf{y}) \right) . \end{aligned} \quad (2.24)$$

It would be pleasant to invert the gluon propagator in Eq. (2.24), but the transverse projector t_{ij} is singular. Yet, without loss of generality, we can define the matrix D_A by $D_{ij}^{ab}(\mathbf{x}, \mathbf{y}) = t_{ij}(\mathbf{x}) D_A^{ab}(\mathbf{x}, \mathbf{y})$ and its inverse, $D_A^{-1} D_A = \mathbb{1}$. The translationally invariant function

$$[D_{ij}^{-1}]^{ab}(\mathbf{x}, \mathbf{y}) := t_{ij}(\mathbf{x}) [D_A^{-1}]^{ab}(\mathbf{x}, \mathbf{y}) \quad (2.25)$$

is referred to as the inverse gluon propagator.⁷ One can now deduce from Eq. (2.24) the coordinate space gluon DSE in its most useful form,

$$[D_{ij}^{-1}]^{ab}(\mathbf{x}, \mathbf{y}) = \text{Tr} \left(D_G \Gamma_i^a(\mathbf{x}) D_G \Gamma_j^{0,b}(\mathbf{y}) \right) . \quad (2.27)$$

In Fig. 2.2, the gluon DSE (2.27) is interpreted diagrammatically. By the loop diagram on the r.h.s., the so-called *ghost loop*, the gluon propagator D_{ij} is correlated with the ghost propagator D_G . The latter needs to be determined by its own DSE. To derive it [83], first note that

$$G^{-1} = G_0^{-1} - \int d^3 x A_k^a(\mathbf{x}) \Gamma_k^{0,a}(\mathbf{x}) . \quad (2.28)$$

Multiplying the above equation with G_0 from the left and G from the right gives

$$G = G_0 + G_0 \int d^3 x A_k^a(\mathbf{x}) \Gamma_k^{0,a}(\mathbf{x}) G . \quad (2.29)$$

Taking the expectation value of (2.29) and using the identity (2.21) for the connected ghost-gluon vertex yields

$$D_G = G_0 + G_0 \Sigma D_G \quad (2.30)$$

⁷Note that D_{ij}^{-1} is inverse to D_{ij} only in the transverse subspace of the full Lorentz space,

$$\int d^3 z [D_{ik}^{-1}]^{ac}(\mathbf{x}, \mathbf{z}) [D_{kj}]^{cb}(\mathbf{z}, \mathbf{y}) = t_{ij}^{ab}(\mathbf{x}, \mathbf{y}) . \quad (2.26)$$

$$\begin{aligned}
 D_G^{-1} &= \text{---}^{-1} = \text{.....}^{-1} - \text{---} \text{---} \text{---} \\
 D_{ij}^{-1} &= \text{---}^{-1} = \text{---} \text{---} \text{---}
 \end{aligned}$$

Figure 2.2: The set of Dyson–Schwinger equations in the stochastic vacuum. Dashed lines represent interacting connected ghost propagators whereas the dotted line is the tree-level ghost propagator. Curly lines represent the gluon propagator. Empty blobs stand for proper ghost-gluon vertices and dots represent tree-level ghost-gluon vertices.

with the ghost self energy

$$\Sigma^{ab}(\mathbf{x}, \mathbf{y}) = \int d^3[x'y'uv] [\Gamma_i^{0,c}(\mathbf{u})]^{aa'}(\mathbf{x}, \mathbf{x}') D_{ij}^{cd}(\mathbf{u}, \mathbf{v}) D_G^{a'b'}(\mathbf{x}', \mathbf{y}') [\Gamma_j^d(\mathbf{v})]^{b'b}(\mathbf{y}', \mathbf{y}). \quad (2.31)$$

A multiplication with G_0^{-1} from the left and D_G^{-1} from the right gives the final form of the ghost DSE in coordinate space,

$$[D_G^{-1}]^{ab}(\mathbf{x}, \mathbf{y}) = [G_0^{-1}]^{ab}(\mathbf{x}, \mathbf{y}) - \Sigma^{ab}(\mathbf{x}, \mathbf{y}), \quad (2.32)$$

shown in Fig. 2.2. Let us emphasize that Eq. (2.32) was not derived from the path integral, in contrast to the gluon DSE (2.27). The “operator method” using Eq. (2.29) offers an alternative to the conventional path integral method, without the introduction of ghost sources. Restriction to the Gribov region Ω is ensured by cutting off the path integral at $\partial\Omega$, the operator method formally also accounts for this restriction since the operator G in Eq. (2.29) is not defined on $\partial\Omega$.

Having at hand the gluon DSE (2.27) and the ghost DSE (2.32) shown in Fig. 2.2, one may now try and solve for the two-point Green functions (“propagators”) D_G and D_{ij} . However, the proper ghost-gluon vertex that appears in both DSEs couples the propagators to higher n -point functions, thus giving rise to the typical infinite tower of coupled integral equations. After establishing a connection to the Landau gauge, an approximation for the ghost-gluon vertex will be motivated in section 2.5 which makes a solution for D_G and D_{ij} feasible.

2.4 Connection to Landau gauge

Linear covariant gauges are a natural choice for perturbative calculations in the Lagrangian formalism. With Lorentz invariance being manifest and after Wick rotation to Euclidean space, perturbative loop integrals can be computed with standard methods [87]. However, this is at the cost of losing a positive definite metric in Hilbert space. One cannot simultaneously

maintain locality, positivity and manifest Lorentz invariance [88]. A Hamiltonian approach is thus obscured and the potential between static quarks as it occurs in the Coulomb gauge Hamiltonian is not accessible in the Landau gauge. The confinement problem must therefore be studied by alternative means, e.g. the Kugo–Ojima confinement criterion [89, 90].

Usually, the class of linear covariant gauge conditions $\chi^a(x) = \partial^\mu A_\mu^a(x) - B^a(x) \approx 0$, is implemented in the path integral by means of the Faddeev–Popov method. The arbitrary function $B^a(x)$ is integrated out with a Gaussian weighting of width ξ , which effectively smears of the Lorenz gauge condition,

$$\delta(\partial^\mu A_\mu^a) \rightarrow e^{-\frac{1}{2\xi}(\partial^\mu A_\mu^a)^2} \quad (2.33)$$

controlled by an arbitrary parameter ξ . Apart from the Faddeev–Popov determinant $\mathcal{J} = \text{Det } \mathcal{M}$, with

$$\mathcal{M}^{ab}(x, y) = \frac{\delta(\partial^\mu A_\mu^a(x))}{\delta\alpha^b(y)}, \quad (2.34)$$

the YM Lagrangian is thus supplemented by a gauge fixing term $\mathcal{L}_{gf} = -\frac{1}{2\xi}(\partial^\mu A_\mu^a)^2$. The Landau gauge is then obtained in the limit $\xi \rightarrow 0$. From gauge invariance, a Slavnov–Taylor identity can be derived [91] that states that the longitudinal part of the gluon propagator remains unchanged by radiative corrections,

$$\ell^{\mu\nu}(k)D_{\mu\nu}(k) = \xi. \quad (2.35)$$

It is important to realize that during calculations, ξ is kept non-zero, so that the gluon propagator has an inverse. The fields $A_\mu^a(x)$ are therefore not transverse, only the Landau gauge correlation functions are. In particular, the ghost-gluon vertex in Landau gauge does not have a transverse projector attached to its gluon leg, since the transversality is imposed “off-shell”. This is in contrast to the constrained quantization in temporal Coulomb gauge, where the transversality condition is enforced “on-shell” and the operators $A_i^a(\mathbf{x})$ are manifestly transverse.⁸

The Gribov problem affects the configuration space in Landau gauge just like it does for Coulomb gauge. In fact, the Faddeev–Popov gauge fixing procedure in Landau gauge gives rise to the Faddeev–Popov determinant

$$\mathcal{J}[A] = \text{Det} \left(-\delta^{ab}\partial_\mu\partial^\mu - g\hat{A}_\mu^{ab}\partial^\mu \right) \quad (2.36)$$

and one cannot miss to acknowledge the similarity to the one in Coulomb gauge. It was pointed out by Gribov in his seminal paper [62] that if Wick rotation is employed, the Landau gauge condition becomes equivalent to the Coulomb gauge condition. The dimension $D = 3 + 1$ of Minkowski spacetime infers that $d = 4$ after Wick rotation, as opposed to $d = 3$ in the temporal Coulomb gauge.

⁸The terminology using “on-shell” and “off-shell” to describe the gauge-fixing technique is encountered, e.g., in Ref. [73].

Recall the Gribov–Zwanziger scenario in the Coulomb gauge. The entropy argument for infrared dominant field configurations at the Gribov horizon along with the horizon condition (2.12) for the ghost propagator applies to the Landau gauge in Euclidean space just the same [74]. One may therefore expect that the infrared limit in Landau gauge yields the same set of integral equations as for the Coulomb gauge, with the dimension shifted to $d = 4$. To see how it comes about, consider the expression for a Landau gauge-fixed expectation value,

$$\langle \mathcal{O}[A] \rangle = \int \mathcal{D}A \mathcal{J}[A] e^{-\int d^4x_E \mathcal{L}_{YM}(x_E)} \quad (2.37)$$

where the weight of field configurations is determined by the Euclidean Yang–Mills action. Shifting the field variable by $A \rightarrow gA$, the weight acquires the form

$$e^{-\int d^4x_E \mathcal{L}_{YM}(x_E)} \rightarrow e^{-\frac{1}{g^2} \int d^4x_E \mathcal{L}_{YM}(x_E)} \quad (2.38)$$

and one recognizes that to zeroth order of the *strong coupling expansion* in $\frac{1}{g^2} \ll 1$, the evaluation of expectation values depends only on the Faddeev–Popov determinant [73] and is therefore equivalent to the stochastic vacuum (2.14), with the difference that the Faddeev–Popov determinant in (2.36) is to be computed in $d = 4$ dimensional Euclidean Lorentz space.

The full structure of Landau gauge Dyson–Schwinger equations was studied intensively in the past decade [92, 54]. It turned out that the infrared sector of the solutions is asymptotically determined by the set of equations shown in Fig. 2.2. Apparently, the strong coupling expansion in the Landau gauge Lagrangian formalism accounts for the correct infrared physics, while in the Coulomb gauge Hamiltonian formalism the stochastic vacuum is a simple but sufficient state to describe infrared correlations. The approximation needed to arrive at a solution to the coupled Dyson–Schwinger equations shown in Fig. 2.2 concerns the ghost-gluon vertex. This will be the topic of the next section.

2.5 Ghost-gluon vertex

In gauges where the gluon propagation is transverse, such as Coulomb and Landau gauge, the ghost-gluon vertex has the feature of nonrenormalization. In this context, one can motivate that the vertex is approximately tree-level for all momentum configurations. The solutions to all Green functions will qualitatively depend on the simple structure of the ghost-gluon vertex and therefore this section is devoted to assess the tree-level approximation.

As far as renormalization is concerned, the ghost-gluon vertex in Coulomb or Landau gauge is quite an unusual Green function. Whereas one usually encounters ultraviolet divergences in a perturbative expansion of a Green function, the ghost-gluon vertex appears to be a finite function, to all orders of perturbation theory. This can be understood by considering a Dyson–Schwinger equation for this vertex. In the Landau gauge, the ghost-gluon vertex Dyson–Schwinger equation was derived in Ref. [93] and can be represented in momentum space as shown in Fig. 2.3. The proper ghost-gluon vertex $\Gamma_\mu(k; q, p)$ is related to its tree-level

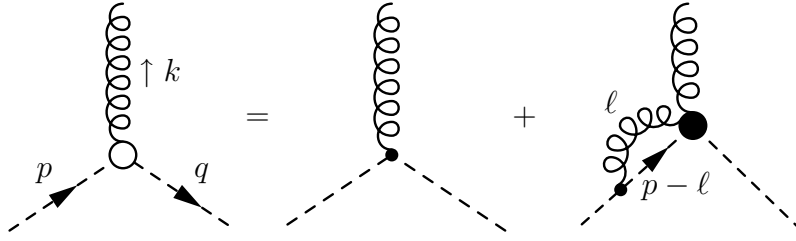


Figure 2.3: *Dyson–Schwinger equation for the ghost-gluon vertex. The l.h.s. represents the proper ghost-gluon vertex, with definitions of the momenta k , q and $p = q + k$. The filled blob on the r.h.s. corresponds to a four-point function, see text.*

counterpart $\Gamma_\mu^0(q)$ and a connected four-point function $\Gamma_{\mu\nu}(k, \ell; q, p)$ that will be explicitly defined in section 3.5. Here, it shall suffice to recognize the generic structure of the loop diagram,

$$\Gamma_\mu(k; q, p) = \Gamma_\mu^0(q) + \int d^4\ell \Gamma_\rho^0(p - \ell) D_{\rho\nu}(\ell) D_G(\ell - p) \Gamma_{\nu\mu}(k, -\ell; \ell - p, q). \quad (2.39)$$

Taylor anticipated in Ref. [94] the structure of the Dyson–Schwinger equation (2.39) and perceived that the contribution of $\Gamma_\mu^0(p - \ell)$ to the loop integration can be factored out due to the transversality of the gluon propagator. In momentum space, with the color structure suppressed, the contraction of the gluon propagator $D_{\mu\nu}$ with the tree-level ghost-gluon vertex, $\Gamma_\mu^0(q) = igq_\mu$, yields

$$\Gamma_\rho^0(p - \ell) D_{\rho\mu}(\ell) = \Gamma_\rho^0(p) D_{\rho\mu}(\ell). \quad (2.40)$$

Hence, the degree of divergence of the ℓ -integration is diminished. Landau gauge perturbation theory explicitly confirms that the divergent part of the g^3 contribution to the vertex is proportional to ξ , i.e. it vanishes in the Landau gauge limit, see e.g. [95]. Taylor further argued that if the loop diagram does not develop any poles in the infrared, one can take the infrared limit of the incoming ghost momentum $p \rightarrow 0$ and find from Eq. (2.39)

$$\lim_{p \rightarrow 0} \Gamma_\mu(k; q, p) = \Gamma_\mu^0(q). \quad (2.41)$$

For the labelling of momenta, see Fig. 2.3. Since one particular momentum configuration, given by Eq. (2.41), is found where the ghost-gluon vertex is finite, its multiplicative renormalization constant \tilde{Z}_1 , being momentum independent, has to be finite, $\tilde{Z}_1 < \infty$. In an appropriate renormalization scheme, \tilde{Z}_1 can be defined to be trivial, $\tilde{Z}_1 = 1$. Multiplicative renormalization of the bare ghost-gluon vertex Γ_B , understood here as a vector, is defined by

$$\Gamma_B(k, q, p; \Lambda) = \tilde{Z}_1(\mu, g, \xi, \Lambda) \Gamma(k, q, p; \mu) \quad (2.42)$$

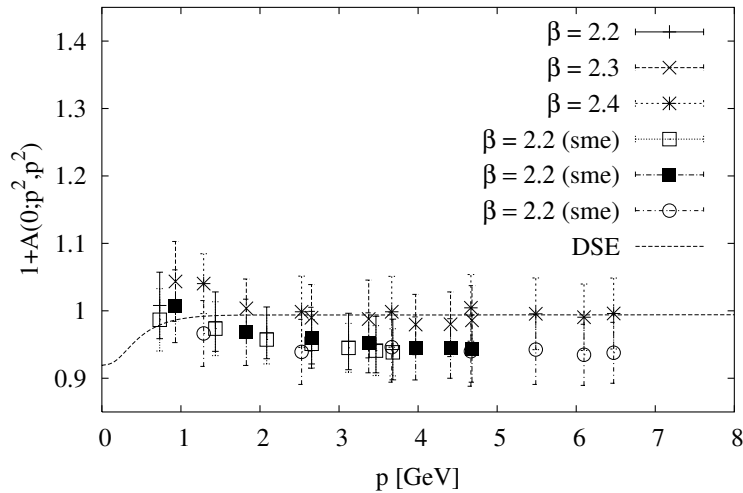


Figure 2.4: *Projection of the ghost-gluon vertex in 3 + 1 dimensional Landau gauge as a function of one momentum, taken from Ref. [93] (for details, see there). Both the DSE result and the lattice data show that the ghost-gluon vertex is basically at tree-level.*

and relates Γ_B to the renormalized vertex Γ . Since in the Landau gauge limit, $\xi \rightarrow 0$, one has $\tilde{Z}_1 < \infty$, we can drop all dependences on the regulator Λ . The dependence of \tilde{Z}_1 on the dimensionful renormalization scale μ must drop out since g and \tilde{Z}_1 are both dimensionless. The number \tilde{Z}_1 is then defined by a renormalization prescription, i.e. a certain momentum configuration $P := \{k_r^2, q_r^2, p_r^2\}$ is chosen for which $\Gamma(k_r, q_r, p_r) = \Gamma^0(\mu)$. In order to avoid cuts in the complex plane, P is usually chosen in the perturbative regime. Nevertheless, the renormalization prescription with $P = \{\mu^2, \mu^2, 0\}$ is a convenient one since Eq. (2.41) then infers that $\tilde{Z}_1 = 1$. Marciano and Pagels [96] pointed out that for the symmetric point $P = \{\mu^2, \mu^2, \mu^2\}$ with $\mu^2 \neq 0$, one generally has $\tilde{Z}_1 \neq 1$ (cf. [97]). The symmetric point with $\mu^2 = 0$, however, does not necessarily give $\tilde{Z}_1 = 1$ since the infrared limits of momenta are not interchangeable, as argued below in section 3.5. In Ref. [98], the choice $P = \{0, \mu^2, \mu^2\}$ was advocated. In the following, we will set $\tilde{Z}_1 = 1$, but come back to it in chapter 4.

Due to the nonrenormalization of the ghost-gluon vertex and the related property (2.41), recent Landau gauge DSE studies used a tree-level ghost-gluon vertex for all momentum configurations [92, 54]. Of course, this approximation needs to be assessed further. It was discussed in Ref. [93] that with the tree-level vertex as a starting point, the iteration of the vertex DSE (2.39) will not lead too far away from the tree-level value. The changes stay in the range of 10% – 20%. Furthermore, lattice calculations [98, 99, 100] confirmed that the vertex is basically tree-level. In Fig. 2.4, the DSE results along with the lattice results for the vertex are shown. Thus, strong support is available that the perturbative arguments of Taylor, stated above, hold in the nonperturbative regime.

In Coulomb gauge, the argumentation for a tree-level ghost-gluon vertex is similar. Although

the perturbative calculations in Coulomb gauge are far from trivial [55, 56, 57], the DSE for the ghost-gluon vertex can be shown to reproduce the Landau gauge structure depicted in Fig. 2.3 [55]. The gluon propagator is transverse as well and therefore Taylor’s reasoning for nonrenormalization can also be applied to the Coulomb gauge. Within a set of interpolating gauges, the nonrenormalization of the ghost-gluon vertex can be established as well, considering the Coulomb gauge limit [101]. The Landau gauge calculations shown in Fig. 2.4 were also carried out in $d = 3$ spatial dimensions and the results were qualitatively the same [93]. Therefore, it seems to be an appropriate approximation to the Coulomb gauge DSEs to use a tree-level vertex instead of a proper vertex, analogously to the Landau gauge,

$$\Gamma_k(\mathbf{x}) \approx \Gamma_k^0(\mathbf{x}) . \quad (2.43)$$

2.6 Analytical solution for propagators

The approximation scheme (2.43) exhibited in the previous section enables us to find a solution to the coupled set of Dyson–Schwinger equations. With the Coulomb and Landau gauge differing in the number d of spatial dimensions only, it is convenient to keep d as an unspecified parameter. The gluon DSE (2.27) can be transformed into momentum space defining the scalar gluon propagator $D_A(k)$ by⁹

$$\delta^d(k-p)\delta^{ab}D_A(k) = \int d^d[xy]D_A^{ab}(x,y)e^{-ik\cdot x+ip\cdot y} . \quad (2.44)$$

Translational invariance allows us to write $D_A(k)$ as a function of one variable which makes momentum space calculations convenient. The color structure of propagators is chosen to be diagonal, i.e. $D_G^{ab}(x,y) = D_G(x,y)\delta^{ab}$. In the approximation scheme with a tree-level ghost-gluon vertex, it is verified straightforwardly in a perturbative expansion to all orders (“rainbow expansion”) that color-diagonal propagators solve the set of integral equations. Using Eq. (2.11) for the definition of the momentum space ghost propagator $D_G(k)$, Fourier transformation of the gluon DSE (2.27) expressed in terms of $D_{ij}^{-1}(k) := t_{ij}(k)D_A^{-1}(k)$ yields

$$D_{ij}^{-1}(k) = -N_c \int d^d\ell \Gamma_i^0(k,\ell)\Gamma_j^0(k,\ell-k)D_G(\ell)D_G(\ell-k) . \quad (2.45)$$

Here, the tree-level ghost-gluon vertex in momentum space is derived by Fourier transform from Eq. (2.20),

$$\begin{aligned} \int d^d[xyz](\Gamma_k^{0,a}(x))^{bc}(y,z)e^{-ik\cdot x-iq\cdot y+ip\cdot z} &= (\hat{T}^a)^{bc}\delta^d(p-q-k)\Gamma_k^0(k,q) \\ &\Rightarrow \Gamma_k^0(k,q) = igt_{kj}(k)q_j . \end{aligned} \quad (2.46)$$

The color trace in (2.45) was computed using $\text{tr}(\hat{T}^a\hat{T}^b) = -N_c\delta^{ab}$, see appendix A. Eq. (2.45) is seen to be manifestly transverse. This follows from the fact that in the derivation of the

⁹Note that in momentum space, the matrix notation of coordinate space is no longer used. Moreover, we simplify the notation henceforth by abandoning the bold-face typesetting for spatial vectors. Latin Lorentz indices now range from 1 to d .

DSEs in section 2.3 the Coulomb gauge condition was imposed “on-shell”. We shall see in section 2.8 that the “off-shell” gauge condition leads to a (slightly) different gluon DSE. In Eq. (2.45), we can take the trace in Lorentz space to find, using $t_{ii}(k) = d - 1$ and Eq. (2.46) and writing $\hat{k} = k/|k|$,

$$D_A^{-1}(k) = g^2 N_c \frac{1}{(d-1)} \int \bar{d}^d \ell \ell^2 \left(1 - (\hat{\ell} \cdot \hat{k})^2\right) D_G(\ell) D_G(\ell - k). \quad (2.47)$$

The ghost DSE (2.32) can be Fourier transformed in the same manner. With a tree-level ghost-gluon vertex, it reads in momentum space

$$D_G^{-1}(k) = k^2 - g^2 N_c k^2 \int \bar{d}^d \ell \left(1 - (\hat{\ell} \cdot \hat{k})^2\right) D_A(\ell) D_G(\ell - k). \quad (2.48)$$

Eq. (2.48) can be put in a form that explicitly satisfies the horizon condition (2.12) by subtracting $k^{-2} D_G^{-1}(k)$ at zero momentum. This subtraction does not introduce an extra parameter since by the horizon condition (2.12), $(k^2 D_G(k))^{-1}|_{k=0} = 0$, and we get

$$(k^2 D_G(k))^{-1} = g^2 N_c \int \bar{d}^d \ell D_A(\ell) \left(1 - (\hat{\ell} \cdot \hat{k})^2\right) (D_G(\ell) - D_G(\ell - k)) \quad (2.49)$$

for the ghost DSE with an integral that converges more strongly in the ultraviolet than the one in Eq. (2.48). In the ultraviolet sector, the horizon condition can be used to remove ultraviolet divergences in the ghost DSE.

The set of equations (2.47) and (2.49) was first solved without approximations in Refs. [97, 102] by a power law ansatz. The derivation and the solution is reviewed here, and some subtleties are pointed out.

With power law ansätze for the propagators,

$$D_A(k) = \frac{A}{(k^2)^{1+\alpha_A}}, \quad D_G(k) = \frac{B}{(k^2)^{1+\alpha_G}} \quad (2.50)$$

the integrals in (2.47) and (2.49) turn into linear combinations of a particularly simple kind of integrals we refer to as *two-point integrals*,

$$\Xi_m(\alpha, \beta) := \int \bar{d}^d \ell \frac{(\ell \cdot k)^m}{(\ell^2)^\alpha ((\ell - k)^2)^\beta}, \quad \alpha, \beta \in \mathbb{R}, \quad m \in \mathbb{N}. \quad (2.51)$$

In appendix B, explicit solutions for the two-point integrals (2.51) are given and their convergence properties are discussed. The gluon DSE (2.47) may be rewritten in terms of two-point integrals as

$$(k^2)^{1+\alpha_A} = \frac{g^2 N_c A B^2}{d-1} \left(\Xi_0(\alpha_G, 1 + \alpha_G) - \frac{1}{k^2} \Xi_2(1 + \alpha_G, 1 + \alpha_G) \right) \quad (2.52)$$

and it converges in the ultraviolet (as $\ell \rightarrow \infty$) for $1 + 2\alpha_G > \frac{d}{2}$. Infrared divergences are absent so long as $\alpha_G < \frac{d}{2}$.

In the ghost DSE (2.49), the horizon condition allowed for a subtraction which in turn improves the UV convergence. The two-point integral occurring in the “unrenormalized” DSE (2.48) is

divergent, but it can be unambiguously split into a momentum-independent divergent part and a regular part, see appendix B. The divergent part is subtracted using the horizon condition in (2.49) and the formulae (B.6) for $\Xi_m(\alpha, \beta)$ yield the correct values for the regular part. Thus,

$$(k^2)^{\alpha_G} = -g^2 N_c A B^2 \left(\Xi_0(1 + \alpha_Z, 1 + \alpha_G) - \frac{1}{k^2} \Xi_2(2 + \alpha_Z, 1 + \alpha_G) \right)_{reg.} \quad (2.53)$$

where the remark “reg.” indicates that the regular part of $\Xi_m(\alpha, \beta)$ is taken. The integrals in (2.53) are then UV-convergent if $\alpha_G < 1$. In the infrared, poles are avoided for $-\frac{1}{2} < \alpha_G < \frac{d}{2}$. Only values for α_A and α_G are considered for which the integrals converge.

Solving a well-defined (convergent) set of integral equations, we can rescale the integration variable in (2.51) by $\ell \rightarrow \lambda \ell$, and readily find that $\Xi_m(\alpha, \beta) = I_m(\alpha, \beta)(k^2)^{d/2+m-\alpha-\beta}$ with some dimensionless functions $I_m(\alpha, \beta)$. These power law solutions can be plugged into the DSEs (2.47) and (2.49) and a relation between the exponents α_A and α_G is gained,

$$\alpha_A + 2\alpha_G = \frac{d-4}{2}. \quad (2.54)$$

Eq. (2.54) is referred to as the “*sum rule* (for power law exponents)”.

Let us emphasize that the sum rule (2.54) can be directly traced back to the nonrenormalization of the ghost-gluon vertex [103]. Following Ref. [104], a quite general ansatz for the proper ghost-gluon vertex is

$$\Gamma_k(k; q, p) = i g t_{kj}(k) q_j \sum_a C_a \left(\frac{k}{\sigma}\right)^{l_a} \left(\frac{q}{\sigma}\right)^{m_a} \left(\frac{p}{\sigma}\right)^{n_a}, \quad (2.55)$$

where the constraint $l_i + m_i + n_i = 0, \forall i$, guarantees the independence of the renormalization scale σ , i.e. nonrenormalization of the vertex. It is readily shown that the sum rule (2.54) is not affected by a dressing of the ghost-gluon vertex such as (2.55), since it turns into

$$\alpha_A + 2\alpha_G = \frac{d-4}{2} + \sum_i (l_i + m_i + n_i). \quad (2.56)$$

Any consequence of the sum rule is therefore understood as due to the nonrenormalization of the ghost-gluon vertex.

By virtue of the sum rule (2.54), one of the exponents α_A and α_G can be eliminated. We choose to define

$$\kappa := \alpha_G \quad (2.57)$$

and express α_A in terms of κ .

The integrals in (2.47) and (2.49) can now be written down concisely, using the formulae in (B.6),

$$(k^2)^{d/2-1-2\kappa} = g^2 N_c A B^2 I_A(\kappa) (k^2)^{d/2-1-2\kappa} \quad (2.58a)$$

$$(k^2)^\kappa = g^2 N_c A B^2 I_G(\kappa) (k^2)^\kappa \quad (2.58b)$$

where the dimensionless functions I_A and I_G were introduced,

$$I_A(\kappa) = \frac{1}{2(4\pi)^{d/2}} \frac{\Gamma(\frac{d}{2} - \kappa)^2 \Gamma(1 - \frac{d}{2} + 2\kappa)}{\Gamma(d - 2\kappa) \Gamma(1 + \kappa)^2}, \quad (2.59a)$$

$$I_G(\kappa) = -\frac{4^\kappa (d-1)}{(4\pi)^{d/2+1/2}} \frac{\Gamma(\frac{d}{2} - \kappa) \Gamma(-\kappa) \Gamma(\frac{1}{2} + \kappa)}{\Gamma(\frac{d}{2} - 2\kappa) \Gamma(1 + \frac{d}{2} + \kappa)}. \quad (2.59b)$$

Eq. (2.58) requires that

$$g^2 N_c AB^2 I_A = 1 = g^2 N_c AB^2 I_G. \quad (2.60)$$

The infrared exponent $\kappa(d)$ is therefore implicitly defined by

$$I_{id} := \frac{I_G(\kappa)}{I_A(\kappa)} \stackrel{!}{=} 1. \quad (2.61)$$

Above, convergence of the integrals in the DSEs was discussed. In terms of the exponent κ , the conditions for convergence can be re-expressed. However, recall that the ultraviolet behavior of $D_A(k)$ and $D_G(k)$ is not governed by the stochastic vacuum but by perturbation theory. The power law behavior (2.50) is just regarded as a possible infrared limit that will actually be realized (see chapter 3). Hence, the restriction on the infrared exponents by analyzing the UV convergence is spurious. Discarding UV criteria for both $I_A(k)$ and $I_G(k)$, we find from the condition that no divergences appear in the infrared integration domain the relation $-\frac{1}{2} < \kappa < \frac{d}{2}$. Moreover, the horizon condition demands $\kappa > 0$. Altogether, we have

$$0 < \kappa < \frac{d}{2} \quad (2.62)$$

and in this range solutions to (2.61) are investigated.¹⁰ Manipulating the gamma functions in (2.59), one finds the compact expression

$$I_{id}(d, \kappa) = \frac{\sin(\frac{\pi}{2}(d - 4\kappa))}{\sin(\pi\kappa)} \frac{(d-1)\Gamma(1+2\kappa)\Gamma(d-2\kappa)}{\Gamma(1+\kappa+d/2)\Gamma(d/2-\kappa)} \stackrel{!}{=} 1 \quad (2.63)$$

for finding $\kappa(d)$. The solutions are shown in Fig. 2.5. These are exhaustive for κ in the range (2.62) and complete a recent calculation [105]. For a given Euclidean dimension d , several solutions for κ are available. One of them can be found by algebraic manipulations,

$$\kappa_a(d) = \frac{d}{2} - 1, \quad (2.64)$$

as verified by plugging $\kappa_a(d)$ into Eq. (2.63). The other (irrational) solutions $\kappa_b(d)$ and $\kappa_c(d)$ were determined numerically.

There are some exceptional points in the (d, κ) diagram that are only solutions to Eq. (2.63) if approached in a certain direction. One of them is the point $(\frac{d=4}{\kappa=1})$ that solves Eq. (2.63) if

¹⁰According to the principle of locality, the Green functions should be tempered distributions which restricts κ further. We do not focus on this aspect here.

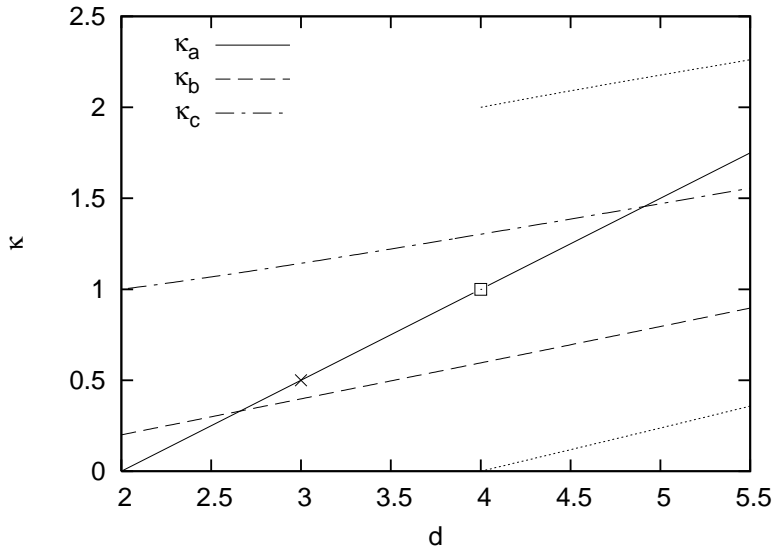


Figure 2.5: Solutions for $\kappa(d)$. The box indicates an exceptional point, see text. The cross marks the solution favorable for reasons given below. The dotted lines are extra solutions that occur for $d > 4$. Note that κ is restricted to the range (2.62).

approached along the line (2.64). This peculiarity appears for *even* dimensions d and *integer* values for κ . Setting

$$d = 2m - 2\lambda\epsilon \quad (2.65)$$

$$\kappa = n + \epsilon \quad (2.66)$$

with $m, n \in \mathbb{N}$, we approach in the limit $\epsilon \rightarrow 0$ the values for even d and integer κ . The parameter $\lambda \in \mathbb{R}$ controls the slope $-\frac{1}{2\lambda}$ of the line on which the point $\binom{2m}{n}$ is approached in a (d, κ) -diagram. Choosing $n < m$ guarantees the integrability of infrared poles in the ghost loop integral, see Eq. (2.62). Treating the $\frac{0}{0}$ expressions that occur in (2.63) carefully, we find

$$\lim_{\epsilon \rightarrow 0} I_{id}(2m - 2\lambda\epsilon, n + \epsilon) = (-1)^{1+m+n} (m-n)_{m-n} \frac{(2m-1)(2n)!}{(m+n)!} (2 + \lambda) \quad (2.67)$$

where $(a)_n = a(a+1)\dots(a+n-1)$ is the Pochhammer symbol. Setting $\lambda = 0$ corresponds to keeping a fixed dimension throughout the calculation. From Eq. (2.67) it can be deduced that for no values of m, n the equation $I_{id} = 1$ (2.63) is solved if $\lambda = 0$. Hence the failure of trying to find the point $\binom{d=4}{\kappa=1}$ as a Landau gauge solution [106], with arguments in Refs. [107, 102] that this solution should exist. For the set of points with $n = m - 1$, i.e.

$$\binom{d}{\kappa} \in \left\{ \binom{2}{0}, \binom{4}{1}, \binom{6}{2}, \dots \right\}, \quad (2.68)$$

we find from (2.67) the simple result

$$\lim_{\epsilon \rightarrow 0} I_{id}(2m - 2\lambda\epsilon, m - 1 + \epsilon) = 2 + \lambda. \quad (2.69)$$

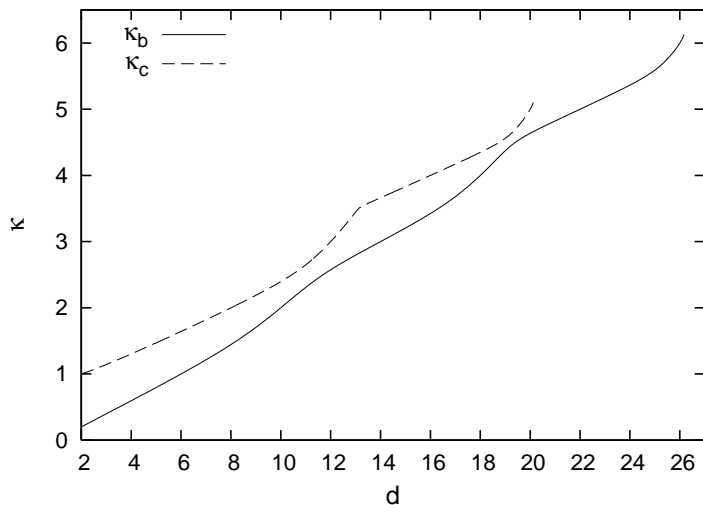


Figure 2.6: Two solution branches of $\kappa(d)$ and their behavior for large dimensions d . The upper solution becomes complex at $d \approx 20.15$, the lower one at $d \approx 26.18$.

Tuning $\lambda = -1$, the points (2.68) are solutions to (2.63), at least in principle. One may adopt the point of view that the dimension d is fixed and the points in Fig. 2.5 can only be approached along vertical lines. In fact, rendering d a variable is here not understood in the context of dimensional regularization where divergences are thus regularized. Rather, d is here a fixed parameter for which (2.63) needs to be solved. The exceptional points (2.68) are therefore discarded.

As seen in Fig. 2.5, there are several solutions for κ as a function of d . How many solutions are found for a given dimension? For even dimensions d , Eq. (2.63) can be turned into a polynomial equation in κ of degree $d+1$ which has the $\frac{d}{2}+1$ integer solutions $\kappa \in \{0, 0, 1, 2, \dots, \frac{d}{2}-1\}$ for λ given by Eq. (2.67). The double root at $\kappa = 0$ is excluded by the horizon condition. Thus, these integer solutions lie below (or on) the branch (2.64) looking somewhat odd in Fig. 2.5. There are further non-integer solutions for even dimensions, $\frac{d}{2}$ at the most being real.

Apart from the branch $\kappa_a(d)$ in Eq. (2.64), there are two other solutions $\kappa_b(d)$ and $\kappa_c(d)$ in the range in $d \in (2, 4]$, see Fig. 2.5. Let us investigate the continuity of these three solution branches as functions of d , cf. [78]. Here, we do not consider the limit $d \rightarrow 1$ since the $1+1$ dimensional theory does not have any degrees of freedom and power law solutions might not be appropriate. Instead, we discuss the high- d range. The Gribov–Zwanziger scenario should work particularly well for higher-dimensional YM theory where entropy is even more enhanced at the boundary of configuration space. First of all, the solution $\kappa_a(d)$ holds for all d . The two other solutions in $\kappa_b(d)$ and $\kappa_c(d)$ in the interval $2 < d \leq 4$ connect to the curves shown in Fig. 2.6 or higher d . The upper solution approximately yields $\kappa_c = \frac{d}{6} + \frac{2}{3}$ for $2 < d \leq 8$ and oscillates around $\kappa = \frac{d}{4}$ for $8 \leq d \leq 20$. It ceases to be real for $d \approx 20.15$. The lower solution matches $\kappa_b = \frac{d}{5} - \frac{1}{5}$ for $2 < d \leq 6$, in agreement with Ref. [78], but oscillates around $\kappa = \frac{d}{4} - \frac{1}{2}$

d	κ	D_G	D_A
2	$\frac{1}{5}$	$\sim \frac{1}{k^{2.400}}$	$\sim k^{0.800}$
3	0.398	$\sim \frac{1}{k^{2.795}}$	$\sim k^{0.590}$
3	$\frac{1}{2}$	$\sim \frac{1}{k^3}$	$\sim k$
3	1.143	$\sim \frac{1}{k^{4.285}}$	$\sim k^{3.570}$
4	0.595	$\sim \frac{1}{k^{3.191}}$	$\sim k^{0.381}$
4	1.303	$\sim \frac{1}{k^{4.605}}$	$\sim k^{3.210}$

Table 2.1: Power law solutions for propagators in the stochastic vacuum.

for $6 \leq d \leq 26$ and becomes complex at $d \approx 26.18$. The continuity of the solutions for κ as functions of d is therefore strongest for the solution $\kappa_a(d)$ which holds for all d .

A restriction on the set of solutions in Fig. 2.5 comes from dealing with only power laws for the propagators, due to the ansatz (2.50). The two-point integrals in (2.51) cease to be power laws if $\frac{d}{2} + m - \alpha - \beta = 0$. Actually, they cease to exist, due to a logarithmic ultraviolet divergence. We have argued that these ultraviolet divergences are subtracted by some renormalization scheme in the perturbative sector. One might therefore suggest to consider instead the integrals $\Xi_m(\alpha, \beta)$ subtracted at μ and then approach $\frac{d}{2} + m - \alpha - \beta = 0$. For instance, if $m = 0$, then

$$\begin{aligned}
 \lim_{\alpha \rightarrow \frac{d}{2} - \beta} \left(\Xi_0(\alpha, \beta) - \Xi_0(\alpha, \beta)|_{q=\mu} \right) &= \frac{1}{(4\pi)^{\frac{d}{2}}} \frac{1}{\Gamma(\frac{d}{2})} \lim_{\epsilon \rightarrow 0} \Gamma(\epsilon) [(k^2)^{-\epsilon} - (\mu^2)^{-\epsilon}] \\
 &= \frac{1}{(4\pi)^{\frac{d}{2}}} \frac{1}{\Gamma(\frac{d}{2})} \ln \frac{\mu^2}{k^2}.
 \end{aligned} \tag{2.70}$$

Evidently, after subtraction of the ultraviolet divergence, the solution of the two-point integral (with exponent zero) is a logarithm. These functions call for a separate treatment. The allowed values of κ (2.62) are therefore further restricted by

$$\kappa \neq \frac{d}{4} - \frac{1}{2} \tag{2.71}$$

to avoid a ghost loop that gives a logarithm. The lower solution branch $\kappa_b(d)$ in Fig. 2.6 oscillates around the forbidden values (2.71) for high d , exactly yielding (2.71) for $d = 6, 10, 14, 18, \dots$. A discussion on a possible extension to solutions with logarithms will follow in section 2.8.

To summarize this section, we solved the momentum space Dyson–Schwinger equations of the stochastic vacuum with a tree-level ghost-gluon vertex by power law ansätze and thoroughly discussed the validity of the solutions. For the propagators in the temporal Coulomb and the Landau gauge, with $d = 3$ and $d = 4$, resp., the solutions are shown in Table 2.1. In $2 + 1$ dimensional YM theory, the temporal Coulomb gauge corresponds to $d = 2$ and the Landau gauge to $d = 3$.

2.7 Linear confining potential

The Hamiltonian approach in the temporal Coulomb gauge allows for a direct calculation of the potential energy between two static quarks. Let the external charge density be given by two point charges, separated by the distance r ,

$$\rho_{\text{ext}}^a(x) = \delta^{a3} \left(\delta^{(3)}(x - r/2) - \delta^{(3)}(x + r/2) \right). \quad (2.72)$$

The color vector $\rho_{\text{ext}}(x)$ was here chosen in the 3-direction of $SU(2)$, for convenience. From the Hamiltonian (1.107) the $|x - y| = r$ dependent color Coulomb potential $V_C(r)$ can be identified by

$$V_C(r) = \frac{g^2}{2} \int d^3[xy] \rho_{\text{ext}}^a(x) \langle F^{ab}(x, y) \rangle \rho_{\text{ext}}^b(y). \quad (2.73)$$

With Eq. (2.72), the Coulomb potential $V_C(r)$ can be written as

$$V_C(r) = g^2 \langle F^{33}(0) - F^{33}(r) \rangle, \quad (2.74)$$

with the self-energy of the quarks, $\langle F^{33}(0) \rangle \equiv \langle F^{33}(x, x) \rangle$.

An approximation is needed to express $V_C(r)$ in terms of the known Green function $D_G(k)$. In arriving at the solutions for the propagators in the previous section, the ghost-gluon vertex was approximated to be at tree-level. An approximation for writing $V_C(r)$ in terms of D_G that is equivalent to the vertex approximation would be desirable. Let us recall that factorizing the expectation value $\langle G\Gamma^0 G \rangle \approx \langle G \rangle \Gamma^0 \langle G \rangle$ implies $\Gamma \approx \Gamma^0$, see Eq. (2.21). In the same manner, we factorize

$$\begin{aligned} \langle F^{ab}(x, y) \rangle &= \int d^3 z \langle G^{ad}(x, z) (-\partial^2) G^{db}(z, y) \rangle \\ &\approx \int d^3 z \langle G^{ad}(x, z) \rangle (-\partial^2) \langle G^{db}(z, y) \rangle. \end{aligned} \quad (2.75)$$

Checking the validity of this approximation is an issue dealt with in section 3.6. The expression (2.74) thus turns into

$$V_C(r) = g^2 \int d^3 k k^2 D_G^2(k) \left(1 - e^{ik \cdot r} \right). \quad (2.76)$$

Plugging in $D_G(k) = B/(k^2)^{1+\kappa}$ from (2.50) permits an explicit evaluation of $V_C(r)$,¹¹

$$\begin{aligned} V_C(r) &= \frac{g^2 B^2}{2\pi^2} \int_0^\infty dk k^{-4\kappa} \left(1 - \frac{\sin(kr)}{kr} \right) \\ &= \frac{g^2 B^2}{2\pi^2} r^{4\kappa-1} \left\{ \left(\frac{1}{4\kappa-1} - \frac{1}{4\kappa} - \frac{1}{4\kappa(4\kappa-1)} \right) \frac{1}{\epsilon^{4\kappa-1}} + \frac{1}{4\kappa(4\kappa-1)} \int_0^\infty dx \frac{\sin x}{x^{4\kappa-1}} \right\} \\ &= \frac{g^2 B^2}{2\pi^2} \Gamma(-4\kappa) \sin(2\kappa\pi) r^{4\kappa-1} \end{aligned} \quad (2.77)$$

¹¹In the first line, the pole at $k = 0$ is regularized by integrating only from $0 < \epsilon \ll 1$ to ∞ and letting $\epsilon \rightarrow 0$ at the end. In the second line, partial integration is used repeatedly, and in the last line an integral representation of the gamma function in Ref. [108], formula 3.761.4 was used.

for values $\frac{1}{4} < \kappa < \frac{3}{4}$ where this integral exists. In the latter interval, two solutions of the DSEs exist, see Table 2.1. One of them, found on the branch $\kappa_a(d)$ in Fig. 2.5, yields $\kappa_a = \frac{1}{2}$ and thus a heavy quark potential $V_C(r)$ that rises linearly. From Eq. (2.77) one gets for $\kappa = \kappa_a$

$$V_C^{lin}(r) = \frac{g^2 B^2}{8\pi} r. \quad (2.78)$$

By the above linear potential, heavy quarks are held together by a constant force given by the *Coulomb string tension* $\sigma_C = g^2 \frac{B^2}{8\pi}$. Thus, heavy quarks are confined.

Let us reflect on how we obtained such a heavy quark potential. It is known that $V_C(r)$ cannot rise stronger than linearly [109, 110], but it could saturate for large r (see further discussions in the chapters below). The linearity of the potential agrees exactly with lattice calculations (see e.g. Ref. [8]). Hence, support is given for the validity of the result (2.78). It is enlightening to survey the origin of this outcome. The Gribov–Zwanziger scenario was exhibited in section 2.1. Gribov copies necessitate the restriction of configuration space and Zwanziger’s entropy arguments demand the horizon condition. The simplest possible state, the stochastic vacuum, is deemed sufficient to describe the infrared properties of the theory. Dyson–Schwinger equations comprise the information on the Green functions and with a few approximations, we thus arrived at the linear potential (2.78). One might be astonished by the simplicity of these ideas. In particular, discarding the entire Yang–Mills action S_{YM} (setting $\Psi[A] = 1$) and still producing sensible results seems puzzling. The only physical content in the generating functional

$$Z[j] = \frac{1}{Vol(\Omega)} \int_{\Omega} \mathcal{D}A \mathcal{J}[A] e^{j \cdot A} \quad (2.79)$$

that drives the (infrared) dynamics comes from the gauge fixing procedure.¹² This notion goes by the name *infrared ghost dominance*. Merely the Faddeev–Popov kernel \mathcal{M} (2.34) and its boundary conditions on the Gribov horizon $\partial\Omega$ are sufficient to give rise to a linear confinement potential. The crucial infrared properties are thus governed by entropy in configuration space.

A caveat in the above reasoning for quark confinement in the Coulomb gauge is that the Coulomb potential $V_C(r)$ is only an upper bound to the gauge-invariant potential $V_W(r)$ defined by the Wilson loop [111]. The Coulomb string tension is therefore larger or equal to the string tension from the Wilson loop, $\sigma_C \geq \sigma_W$. Hence, it cannot serve as an order parameter for the deconfinement transition. The mechanism that lowers the Coulomb string tension to its physical value is expected to be due to constituent gluons along the color flux tube. So far, the vacuum Green functions are unaware of the presence of external charges. It will be the subject of chapter 5 to investigate the effect of the back reaction of the external color charges onto the gauge field sector.

Some further critical remarks are at order.

- *Perturbative sector.* If the solutions in the stochastic vacuum are independent of S_{YM} , how do they connect to the ultraviolet regime?

¹²Note that the Faddeev–Popov determinant is gauge invariant.

- *Approximations.* How can we estimate the effect of the approximations made in deriving the Green functions?
- *Uniqueness.* Are the power law solutions found unique? Which one of them is realized in physics?

In the following it will be attempted to give answers to the questions listed above. The latter item is dedicated to the next section.

2.8 On the uniqueness of the solution

Whether the solutions for the propagators found in section 2.6 can be regarded as unique solutions to the infrared sector of YM theory is an important issue addressed in this section. A thorough discussion of uniqueness would probably have to begin with the perturbative sector and any approximations should be avoided. Here, we shall turn to a much simpler task. In view of the approximated DSEs (2.47) and (2.49), it is investigated if any of the solutions listed in Table 2.1 can be considered unique.

A free parameter

First of all, let us start with a generalization of the DSEs. In the context of renormalization in the perturbative regime, a local action is indispensable and the transversality condition on the gauge field, be it Coulomb gauge or Landau gauge, needs to be taken “off-shell”. A crucial difference to the “on-shell” formulation is that the tree-level Green functions are slightly different. In particular, the ghost-gluon vertex does not come with a transversal projector attached to its gluon leg. Instead of $\Gamma_k^0(k, q)$, the local formulation yields $\Gamma_k^0(q)$ with

$$\Gamma_k^0(q) = igq_k \quad \Leftrightarrow \quad \Gamma_k^0(k, q) = igt_{kj}(k)q_j . \quad (2.80)$$

Consequently, in the local formulation not all Feynman graphs are transverse in the gluon momenta. For instance, the $\mathcal{O}(g^2)$ gluon propagator in Landau gauge is known to be comprised by a gluon loop, a ghost loop and a tadpole term. Only the sum of these diagrams yields a transverse gluon propagator. This subtlety slightly alters the DSEs derived in section 2.6. We do not repeat the derivation here, but simply state the results,

$$D_{ij}^{-1}(k) = -N_c \int \bar{d}^d \ell \Gamma_i^0(\ell) \Gamma_j^0(\ell - k) D_G(\ell) D_G(\ell - k) \quad (2.81a)$$

$$D_G^{-1}(k) = k^2 - g^2 N_c k^2 \int \bar{d}^d \ell \left(1 - (\hat{\ell} \cdot \hat{k})^2 \right) D_A(\ell) D_G(\ell - k) , \quad (2.81b)$$

as opposed to Eqs. (2.45) and (2.48). Here, the proper ghost-gluon vertices were again replaced by the tree-level ones. The ghost DSE stays the same. In the gluon DSE (2.81a), on the other hand, note the tiny difference that the ghost-gluon vertices $\Gamma_k^0(q)$ are the ones defined in

Eq. (2.80). Although the nonperturbative ghost loop on the r.h.s. of Eq. (2.81a) should be transverse with a proper ghost-gluon vertex,¹³ it is generally not transverse with the tree-level ghost-gluon vertices (2.80). Transversality is lost due to the approximation of the vertex. To control the longitudinal contributions, contract Eq. (2.81a) with the tensor

$$R_{ij}^{\zeta}(k) := \delta_{ij} - \zeta \ell_{ij}(k). \quad (2.82)$$

The factor $\zeta \ell_{ij}(k)$ would give no contribution if both left and right hand side of (2.81a) were transverse. The sensitivity of the solution with respect to ζ thus measures the violation of transversality and the quality of the approximation used.

Before we use the tensor R_{ij}^{ζ} , let us calculate the inverse gluon propagator in Eq. (2.81a) explicitly with the ansatz (2.50) for the ghost propagator $D_G(k)$,¹⁴

$$\begin{aligned} B^{-2} D_{ij}^{-1}(k) &= g^2 N_c \int \bar{d}^d \ell \frac{\ell_i(\ell - k)_j}{(\ell^2)^{1+\kappa} ((\ell - k)^2)^{1+\kappa}} \\ &= g^2 N_c \frac{1}{(4\pi)^{d/2}} (k^2)^{d/2-1-2\kappa} \left\{ \frac{\Gamma(d/2 - \kappa)^2 \Gamma(2\kappa + 1 - d/2)}{2\Gamma(1 + \kappa)^2 \Gamma(d - 2\kappa)} \delta_{ij} \right. \\ &\quad - \frac{\Gamma(d/2 - \kappa) \Gamma(d/2 - 1 - \kappa) \Gamma(2\kappa - d/2 + 2)}{\Gamma(1 + \kappa)^2 \Gamma(d - 1 - 2\kappa)} \ell_{ij}(k) \\ &\quad \left. + \frac{\Gamma(d/2 + 1 - \kappa) \Gamma(d/2 - 1 - \kappa) \Gamma(2\kappa - d/2 + 2)}{\Gamma(1 + \kappa)^2 \Gamma(d - 2\kappa)} \ell_{ij}(k) \right\} \\ &= I_A [\delta_{ij} - (4\kappa - d + 2) \ell_{ij}(k)] (k^2)^{d/2-1-2\kappa}, \end{aligned} \quad (2.83)$$

with the function I_A given by Eq. (2.59a). The Lorentz structure of $D_{ij}^{-1}(k)$ is most easily recognized by the last line in (2.83). It reproduces a familiar result from perturbation theory ($\kappa = 0$): the ghost loop has longitudinal components. Furthermore, one can see that quite generally the ghost loop is not transverse. Transversality is maintained if and only if the infrared exponent κ satisfies

$$\kappa = \frac{d-1}{4}, \quad (2.84)$$

as seen directly in Eq. (2.83). For other values of κ , projections of the gluon DSE (2.81a) with the tensor $R_{ij}^{\zeta}(k)$ in Eq. (2.82) will depend on the value of ζ . In this case, the computation of the DSEs can be repeated to give a condition $I_{id}(\kappa, \zeta) = 1$, analogously to Eq. (2.61). The latter condition yields a solution $\kappa(d, \zeta)$ that is not unique in the sense that it depends on ζ . This dependence is due to the approximation of the ghost-gluon vertex and must be spurious. In principle, ζ can be regarded as a free parameter. A good approximation will give a weak ζ -dependence.

We now focus on $d = 3$ where one can derive that [113]

$$I_{id}(\kappa, \zeta) = \frac{32(\kappa - 1)\kappa \cos(2\pi\kappa)}{(1 + 2\kappa)(3 + 2\kappa)(2(1 - \kappa) - \zeta(1 - 2\kappa)) \sin(\pi\kappa)^2} = 1 \quad (2.85)$$

¹³If the ghost loop dominates in the infrared, it must itself be transverse.

¹⁴The tensor integral may be expanded into scalar integrals by means of the Passarino–Veltman algorithm [112].

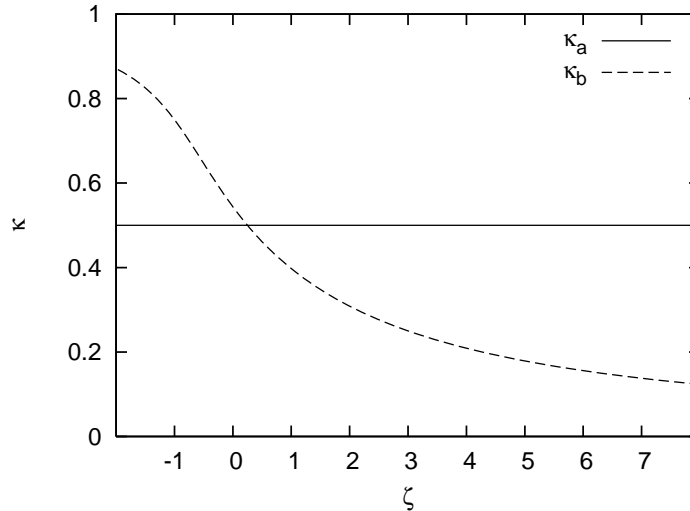


Figure 2.7: The function $\kappa(d = 3, \zeta)$. Due to the approximation of the ghost-gluon vertex, the infrared exponent κ depends on the parameter ζ , except for $\kappa_a = 1/2$.

determines the value of κ , spuriously dependent on ζ . For $\zeta = 1$, the two solutions $\kappa_a = \frac{1}{2}$ and $\kappa_b = 0.398$ from Table 2.1 are recovered. In Fig. 2.7, it is shown that other solutions for κ can be found if $\zeta \neq 1$. The important feature to notice here is that while κ_b depends on ζ , κ_a is ζ -independent. This can be seen immediately from (2.84) by noting that $\kappa_a = \frac{1}{2}$ yields a transverse ghost loop. Although favored in Refs. [113, 105] for 3-dimensional Landau gauge, the solution κ_b is quite sensitive to approximations in the off-shell formulations, and hence might be unphysical. For the solution $\kappa_a = \frac{1}{2}$, the approximations made are more trustworthy and it allows any value of ζ . Further arguments in favor of κ_a will be given in section 3.5, in the context of well-defined infrared limits of the ghost-gluon vertex. Here, let us finish the discussion by noting that it is κ_a that naturally yields a linearly confining potential in the Coulomb gauge.

In the Landau gauge ($d = 4$), the solutions listed in Table 2.1 are all sensitive to the value of ζ and none of the solutions is characteristic in this respect. The accepted value for the infrared exponent, is $\kappa = 0.595$, as reviewed in Ref. [54].

Logarithmic degeneracy

The infrared power law ansätze made so far yielded integrals that can be generically represented by

$$I(\alpha; p^2) := \int d^d \ell (\ell^2)^\alpha \phi(\ell - p) = I(\alpha) (p^2)^{\alpha + \varphi}, \quad p \rightarrow 0 \quad (2.86)$$

for some suitable function $\phi(\ell^2)$. The solutions to the integral in Eq. (2.86) with $\phi(\ell^2)$ being a power law were discussed, and it is clear how to find the exponent φ that depends on the

dimension d of the integral and the function ϕ . The dimensionless numbers $I(\alpha)$ can be computed with the methods given in Ref. [103]. Each of the DSEs are of the form

$$(p^2)^\beta = I(\alpha; p^2). \quad (2.87)$$

Matching both sides of Eq. (2.87), we get the sum rule $\beta = \alpha + \varphi$ on the one hand and the condition $I(\alpha) = 1$ on the other hand. This determines α as well as β .

In order to incorporate logarithms into the infrared ansätze such as $(\ell^2)^\alpha \ln^n(\ell^2)$ we note that simple powers can serve as generating functions of the logarithm to some power $n \in \mathbb{Z}$, that is,

$$(p^2)^\alpha \ln^n p^2 = \begin{cases} \frac{\partial^n}{\partial \alpha^n} (p^2)^\alpha & n > 0 \\ \underbrace{\int \dots \int}_{|n|} d\alpha (p^2)^\alpha & n < 0 \end{cases}. \quad (2.88)$$

As long as the generators of the logarithm, i.e. the derivatives or the α -integrals, may be interchanged with the loop integration of $d^d \ell$ we can compute

$$J(\alpha, n; p^2) := \int d^d \ell (\ell^2)^\alpha \ln^n \ell^2 \phi(\ell - p), \quad p \rightarrow 0 \quad (2.89)$$

by applying these generators to Eq. (2.86). E.g., for $n = 1$ we simply have to write

$$\begin{aligned} J(\alpha, 1; p^2) &= \int d^d \ell (\ell^2)^\alpha \ln \ell^2 \phi(\ell - p) = \int d^d \ell \frac{\partial}{\partial \alpha} (\ell^2)^\alpha \phi(\ell - p) \\ &= \frac{\partial}{\partial \alpha} I(\alpha; p^2) = \left(\frac{\partial I(\alpha)}{\partial \alpha} + I(\alpha) \ln p^2 \right) (p^2)^{\alpha+\varphi} \\ &\xrightarrow{p \rightarrow 0} \ln p^2 I(\alpha; p^2) \end{aligned} \quad (2.90)$$

In the limit $p \rightarrow 0$, the logarithm dominates any constant and thus only the above term remains. For any $n \in \mathbb{N}$, the result yields

$$J(\alpha, n; p^2) = (p^2)^{\alpha+\varphi} \sum_{k=0}^n \binom{n}{k} \frac{\partial^k I(\alpha)}{\partial \alpha^k} \ln^{n-k} p^2 \quad (2.91)$$

Equivalently to the case $n = 1$, one gets the infrared limit

$$\lim_{p \rightarrow 0} J(\alpha, n; p^2) = \ln^n p^2 I(\alpha; p^2), \quad n \in \mathbb{N}. \quad (2.92)$$

Let us turn to $n < 0$. From the prescription (2.88) one can derive the formula for J by repeated partial integration. To prove the result thus obtained, it is easier to turn the integral form of Eq. (2.88) into a differential equation,

$$I(\alpha; p^2) = \frac{\partial^{|n|}}{\partial \alpha^{|n|}} J(\alpha, n; p^2), \quad n < 0. \quad (2.93)$$

For $n = -1$, we get

$$J(\alpha, -1; p^2) = \frac{(p^2)^{\alpha+\varphi}}{\ln p^2} \sum_{k=0}^{\infty} \frac{\partial^k I(\alpha)}{\partial \alpha^k} \frac{(-1)^k}{\ln^k p^2} + C(p^2) \quad (2.94)$$

with a constant $C(p^2)$ that does not depend on α .

Proof:

$$\begin{aligned} \frac{\partial}{\partial \alpha} J(\alpha, -1; p^2) &= \frac{(p^2)^{\alpha+\varphi}}{\ln p^2} \sum_{k=0}^{\infty} \left(\frac{\partial^k I(\alpha)}{\partial \alpha^k} \frac{(-1)^k}{\ln^{k-1} p^2} + \frac{\partial^{k+1} I(\alpha)}{\partial \alpha^{k+1}} \frac{(-1)^k}{\ln^k p^2} \right) \\ &= (p^2)^{\alpha+\varphi} \sum_{k=0}^{\infty} \left(\frac{\partial^k I(\alpha)}{\partial \alpha^k} \frac{(-1)^k}{\ln^k p^2} - \frac{\partial^{k+1} I(\alpha)}{\partial \alpha^{k+1}} \frac{(-1)^{k+1}}{\ln^{k+1} p^2} \right) \\ &= (p^2)^{\alpha+\varphi} I(\alpha) = I(\alpha; p^2). \end{aligned} \quad (2.95)$$

Note in Eq. (2.94) that for $p \rightarrow 0$ only the term with $k = 0$ is relevant. The arbitrary integration constants $C(p^2)$ can always be chosen such that they are subleading in the infrared. The result (2.94) can now be generalized to any $n < 0$. By induction, one can show that

$$J(\alpha, n; p^2) = \frac{(p^2)^{\alpha+\varphi}}{\ln^{|n|} p^2} \prod_{j=1}^{|n|} \sum_{k_j=0}^{\infty} \frac{\partial^{\sum_i |n| k_i} I(\alpha)}{\partial \alpha^{\sum_i |n| k_i}} \frac{(-1)^{\sum_i |n| k_i}}{\ln^{\sum_i |n| k_i} p^2} + \mathcal{O}(\alpha^{|n-1|}) \quad , \quad n < 0 \quad (2.96)$$

satisfies the differential equation (2.93). The infrared limit yields

$$\lim_{p \rightarrow 0} J(\alpha, n; p^2) = \frac{I(\alpha; p^2)}{\ln^{|n|} p^2}, \quad n \in \mathbb{Z}^-. \quad (2.97)$$

In summary, we have shown that in the infrared limit for any $n \in \mathbb{Z}$ the logarithms in the integrals $J(\alpha, n; p^2)$ in Eq. (2.89) can be removed from under the integral and placed in front of the integral, evaluated at the external momentum p^2 , i.e.

$$\lim_{p \rightarrow 0} J(\alpha, n; p^2) = \ln^n p^2 I(\alpha; p^2), \quad n \in \mathbb{Z}. \quad (2.98)$$

Therefore, if an integral equation of the DSE type, as given in Eq. (2.87), is solved by plain power laws in the infrared, an ansatz of the kind $(\ell^2)^\alpha \ln^n(\ell^2)$ with $n \in \mathbb{Z}$ will also be a solution. To see that, note that the logarithm will appear on both sides of Eq. (2.87) and the determining equation $I(\alpha) = 1$ for the infrared exponent α is left unchanged. In this sense, there is a degeneracy in the infrared power law solutions that are insensitive to logarithms.

However, it is not clear how to rigorously generalize these results to $n \in \mathbb{R}$. There are methods to define fractional derivatives and fractional integration [114] and a careful treatment might recover the result (2.98) for arbitrary $n \in \mathbb{R}$. This is something that would be worth looking into. We conjecture here that in the infrared limit,

$$\lim_{k \rightarrow 0} \int \bar{d}^d q \frac{\ln^m q^2 \ln^n(q-k)^2}{(q^2)^\alpha ((q-k)^2)^\beta} = \ln^{m+n} k^2 \Xi_0(\alpha, \beta) \quad (2.99)$$

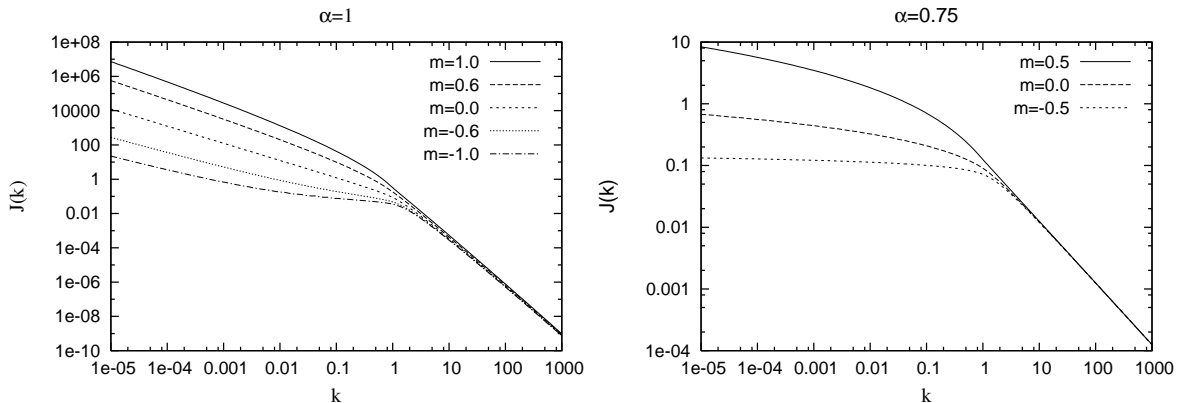


Figure 2.8: Left: *Logarithmic dressings of a power law with $\alpha = 1$ in the infrared. The curves confirm that in the infrared limit, the logarithm simply factors out, according to Eq. (2.99).* Right: *Here, $\alpha = 0.75$. The upper curve with $m = 0.5$ yields $\ln^2 k^2$, the middle curve with $m = 0$ yields $\ln k^2$ and the lower curve with $m = -0.5$ gives $\ln \ln k^2$ in the infrared.*

where $\Xi_0(\alpha, \beta)$ are the functions defined in (2.51), basically the l.h.s. of (2.99) without the logarithms. Hence, Eq. (2.99) states that in the infrared limit the logarithms factor out. For the time being, it shall suffice to corroborate this conjecture by a few modest numerical investigations. In Fig. 2.8, we have implemented the integrals

$$J(k) := \int \bar{d}^3 q \phi(q) \phi(q - k) \rightarrow \ln^{2m} k^2 \frac{I(\alpha)}{k^{4\alpha-3}} \quad (2.100)$$

with the simple functions

$$\phi(k) = \begin{cases} \frac{\ln^m k^2}{(k^2)^\alpha} & \text{for } k < 1 \\ \frac{1}{k^3} & \text{for } k > 1 \end{cases} \quad (2.101)$$

for several values of α and m . In the left panel of Fig. 2.8, the infrared limit indicated in Eq. (2.100) with $I(\alpha) = \Gamma^2(3/2 - \alpha) \Gamma(2\alpha - 3/2) / (8\pi^{3/2} \Gamma^2(\alpha) \Gamma(3 - 2\alpha))$ following from Eq. (B.6a) is found exactly. This supports the hypothesis (2.99).

In Ref. [115], the possibility of logarithmic corrections to the power law solutions was discussed using the angular approximation. It is easily verified that the angular approximation is unable to reproduce reliable results for the class of two-point integrals we are dealing with. Moreover, the hypothesis (2.99) needs a more refined treatment than the angular approximation can provide. The denial of logarithmic corrections in Ref. [115] is therefore likely to be due to the angular approximation.

A further point is made in the right panel of Fig. 2.8. If the power law exponent α in the integrand of Eq. (2.100) is such that the integral is dimensionless, i.e. $\alpha = \frac{3}{4}$ with $m = 0$, the results will be a logarithm, rather than $k^0 = \text{const.}$ If furthermore $m \neq 0$, the result

is $\ln^{1+2m} k^2$. This can be seen in the two upper curves of the plot. The lower curve with the choice $m = -\frac{1}{2}$ renders the exponent of the logarithm zero. The asymptotic result found numerically is the function $\ln \ln k^2$. With zero exponents of power laws incrementing the logarithm power, and with zero logarithm power incrementing the $\ln \ln k^2$ power, it is intuitive to expect this logic to continue to $\ln \ln \ln k^2$, $\ln \ln \ln \ln k^2$ and so on. Let us have these general ideas be followed up with a specific example. Consider an iteration of the DSEs in $d = 3$ with $\kappa = \frac{1}{4}$ as a starting point, i.e. $D_G^{(0)}(k) \sim 1/(k^2)^{5/4}$. The ghost loop then produces, after UV subtraction, a logarithm in the IR, cf. Eq. (2.70). Consequently, the IR gluon propagator yields $D_A^{(1)}(k) \sim 1/(\ln k^2)$. Plugged into the ghost DSE, the log sum rule (2.99) yields that $D_G^{(1)}(k) \sim (\ln k^2)/(k^2)^{5/4}$. Every iteration increments the logarithm power of the ghost propagator, so after the n th iteration, $D_G^{(n)}(k) \sim (\ln^n k^2)/(k^2)^{5/4}$. The choice $\kappa = \frac{1}{4}$ must therefore be excluded, see Eq. (2.71).

However, as long as such subtleties are avoided, the solutions for the ghost and gluon propagators can be appended by

$$\begin{aligned} D_A(k) &= \frac{A}{(k^2)^{1+\alpha_A} \ln^\gamma(k^2/\mu^2)} \\ D_G(k) &= \frac{B}{(k^2)^{1+\alpha_G} \ln^\delta(k^2/\mu^2)} \end{aligned} \quad (2.102)$$

with the conditions (2.54) and (2.61) from the power law analysis and the log sum rule

$$\gamma + 2\delta = 0 \quad (2.103)$$

from Eq. (2.99). Due to the factoring out of the logarithms in the infrared limit, no changes are expected for the value of $\kappa = \alpha_G$. Neither are any qualitative changes expected if logarithms are present in the infrared, for they are always subdominant to power laws.

To summarize this section, the power solutions found in sections 2.6 are not necessarily unique. First of all, a free parameter can be dialled in the off-shell formulation to yield different values of the infrared exponents. Only the one solution, $\kappa_a = \frac{1}{2}$ for $d = 3$ (see Fig. 2.5), is insensitive to this parameter. Secondly, the amendment of logarithms to the power law solutions give one possibility to generalize the solutions. Logarithms will be of particular interest in the discussion of the ultraviolet behavior of the Green functions. That will be the topic of chapter 4.

3 Variational solution for the vacuum state

While in the previous chapter the stochastic vacuum state was investigated to derive the infrared properties of the theory, this chapter is devoted to determine the vacuum wave functional in the temporal Coulomb gauge by variational methods. A Gaussian type of ansatz wave functional is put forward to calculate the energy and minimize it with respect to the parameters of the ansatz. The solutions for the Green functions thus obtained turn out to approach the power law solutions for $d = 3$ of the previous chapter in the infrared. In the ultraviolet, the propagators are those of free particles, up to logarithmic corrections.

By virtue of the (time-independent) Yang–Mills Schrödinger equation, additional information is available from the spectral properties of the Hamiltonian, as opposed to the exclusive consideration of Dyson–Schwinger equations. In this respect, the Hamiltonian approach is superior to the Lagrangian approach, utilizing the principle of minimal energy. In quantum field theory, variational methods have enjoyed considerable attention [116, 117]. However, critical remarks were issued by Feynman. In the 1987 Wangerooge conference, Feynman claimed that variational methods were “no damn good at all” in quantum field theory [117], essentially for the following reason. The only wave functionals that can be used reasonably, are Gaussians. Any corrections to the Gaussians can only be calculated numerically, involving intolerable errors. The inaccuracies in the ultraviolet sector spoil the reliability of infrared quantities, especially in non-linear theories such as QCD where the UV and IR modes mix. Therefore, if Gaussian wave functionals are not good enough, there is no chance in finding reasonable results with the variational method, according to Feynman. The calculations presented in this chapter are, of course, overshadowed by the latter remarks. Nevertheless, on a qualitative level, the results turn out immune to the criticism. First of all, a generalization of Gaussian wave functionals is feasible and will be exhibited in the following section. Secondly, the Gribov–Zwanziger scenario infers that the gauge-fixed configuration space itself governs the infrared, regardless of the ultraviolet accuracy of the wave functional. The crucial infrared properties do not follow from the variational minimization of the vacuum energy, but can be extracted directly from the path integration inside the Gribov horizon, along with the horizon condition. We are therefore confident that the infrared power laws do not suffer from any other approximations than those discussed in the previous chapter.

It is well-known from nuclear physics that the ground state energy is quite insensitive to errors in the wave function. The accuracy of the wave function is tested by the calculation of transition amplitudes, not by the vacuum state itself. In the same sense, one may expect that the Yang–Mills vacuum energy density is not too far off using the crude approximation of a Gaussian vacuum wave functional. Other quantities, such as the vertices, may be more sensitive to changes in the wave functional. These assertions will be discussed in the course of this chapter.

3.1 Gaussian types of wave functionals

Gaussian types of Coulomb gauge wave functionals are put forward in this section. They were first proposed in Refs. [85, 83],

$$\Psi_\lambda[A] = \mathcal{N} \mathcal{J}^{-\lambda}[A] \exp \left[-\frac{1}{2} \int d^3[xy] A_i^a(x) \omega(x, y) A_i^a(y) \right], \quad (3.1)$$

where $\omega(x, y)$ is a variational kernel and \mathcal{N} normalizes the wave functional, $\langle \Psi | \Psi \rangle = 1$. [Note that henceforth, we refrain from using bold-faced symbols for 3-vectors, unless necessary for clarity.] The factor of the Faddeev–Popov determinant with the real exponent λ allows for a further enhancement (if $\lambda > 0$) of the probability density near the Gribov horizon. One specific choice, $\lambda = \frac{1}{2}$, resembles the usage of a “radial wave function”, familiar from the calculation of the hydrogen atom. In this case, the evaluation of expectation values becomes straightforward because the generating functional of full Green functions,

$$\begin{aligned} Z_\lambda[j] &= \langle \Psi | \exp \left[\int d^3 x j_k^a(x) A_k^a(x) \right] | \Psi \rangle \\ &= \mathcal{N}^2 \int \mathcal{D}A \mathcal{J}^{1-2\lambda}[A] \exp \left[- \int d^3[xy] A_k^a(x) \omega(x, y) A_k^a(y) + \int d^3 x j_k^a(x) A_k^a(x) \right], \end{aligned} \quad (3.2)$$

is actually a Gaussian path integral for $\lambda = \frac{1}{2}$. Before we write down the result, let us try to understand the meaning of the parameter λ .

A Dyson–Schwinger equation (DSE) for the gluon propagator can be written down for the path integral in Eq. (3.2) in order to relate ω and λ to the gluon propagator D_{ij} ,

$$\begin{aligned} 0 &= \mathcal{N}^2 \int \mathcal{D}A \frac{\delta}{\delta A_i^a(x)} \mathcal{J}^{1-2\lambda} \\ &\quad \exp \left[- \int d^3[x'y'] A_k^c(x') \omega(x', y') A_k^c(y') + \int d^3 x' j_k^c(x') A_k^c(x') \right] \\ &= \mathcal{N}^2 \int \mathcal{D}A \mathcal{J}^{1-2\lambda} \left((1-2\lambda) \frac{\delta \ln \mathcal{J}}{\delta A_i^a(x)} - 2 \int d^3 z \omega(x, z) A_i^a(z) + t_{im}(x) j_m(x) \right) \\ &\quad \exp \left[- \int d^3[x'y'] A_k^c(x') \omega(x', y') A_k^c(y') + \int d^3 x' j_k^c(x') A_k^c(x') \right]. \end{aligned} \quad (3.3)$$

Taking a derivative w.r.t. $j_j^b(y)$ and setting sources to zero yields

$$0 = (1-2\lambda) \left\langle \frac{\delta \ln \mathcal{J}}{\delta A_i^a(x)} A_j^b(y) \right\rangle_\lambda - 2 \int d^3 z \omega(x, z) \left\langle A_i^a(z) A_j^b(y) \right\rangle_\lambda + t_{ij}^{ab}(x, y). \quad (3.4)$$

Setting $\lambda = \frac{1}{2}$ in the above equation, the gluon propagator is seen to be determined by the variational kernel $\omega(x, y)$,

$$\left\langle A_i^a(x) A_j^b(y) \right\rangle_{\frac{1}{2}} = \frac{1}{2} \delta^{ab} t_{ij}(x) \omega^{-1}(x, y). \quad (3.5)$$

For $\lambda \neq \frac{1}{2}$, we rewrite the first term in Eq. (3.4) by partial integration,

$$\begin{aligned}
 & \left\langle \frac{\delta \ln \mathcal{J}}{\delta A_i^a(x)} A_j^b(y) \right\rangle_\lambda \\
 &= \mathcal{N}^2 \int \mathcal{D}A \mathcal{J}^{1-2\lambda} \frac{\delta \ln \mathcal{J}}{\delta A_i^a(x)} \left(-\frac{1}{2} \int d^3z \omega^{-1}(y, z) \frac{\delta}{\delta A_j^b(z)} \right) \\
 & \quad \exp \left[- \int d^3[x'y'] A_k^c(x') \omega(x', y') A_k^c(y') \right] \\
 &= \int d^3z \left(\left\langle \frac{\delta^2 \ln \mathcal{J}}{\delta A_i^a(x) \delta A_j^b(z)} \right\rangle_\lambda + (1-2\lambda) \left\langle \frac{\delta \ln \mathcal{J}}{\delta A_i^a(x)} \frac{\delta \ln \mathcal{J}}{\delta A_j^b(z)} \right\rangle_\lambda \right) \frac{1}{2} \omega^{-1}(z, y). \quad (3.6)
 \end{aligned}$$

We now introduce an approximation for the evaluation of Green functions, referred to as the *loop expansion*. Whereas its common definition concerns an expansion in \hbar , we here use the term *loop expansion* for ordering diagrams by the number of loops, integrating nonperturbative ghost or gluon propagators. Applied to Eq. (3.6), it can be realized that the first term comprises one loop, and the second term comprises two loops.¹ In the one-loop expansion, we may write Eq. (3.4) as

$$\begin{aligned}
 0 &= (1-2\lambda) \int d^3z \left\langle \frac{\delta^2 \ln \mathcal{J}}{\delta A_i^a(x) \delta A_j^b(z)} \right\rangle_\lambda \frac{1}{2} \omega^{-1}(z, y) \\
 & \quad - 2 \int d^3z \omega(x, z) \left\langle A_k^a(z) A_j^b(y) \right\rangle_\lambda + t_{ij}^{ab}(x, y). \quad (3.7)
 \end{aligned}$$

We recognize in Eq. (3.7) the ghost loop, here denoted by χ_{ij} with

$$\chi_{ij}^{ab}(x, y) = -\frac{1}{2} \left\langle \frac{\delta^2 \ln \mathcal{J}}{\delta A_i^a(x) \delta A_j^b(y)} \right\rangle_\lambda. \quad (3.8)$$

Since by the quantity χ_{ij} the non-trivial metric of the gauge-fixed variables is expressed, the momentum space quantity

$$\chi(k) = \frac{1}{(d-1)(N_c^2-1)} t_{ij}(x) \delta^{ab} \int d^3x \chi_{ij}^{ab}(x, y) e^{-ik \cdot (x-y)} \quad (3.9)$$

is also referred to as the *curvature* [83], with the spatial dimension $d=3$. Introducing for the gluon propagator the function $\Omega(x, y)$ by

$$\left\langle A_i^a(x) A_j^b(y) \right\rangle_\lambda = \frac{1}{2} t_{ij}(x) \Omega^{-1}(x, y), \quad (3.10)$$

and employing the one-loop approximation, Eq. (3.7) can be found to yield

$$\Omega(x, y) = \omega(x, y) + (1-2\lambda) \chi(x, y). \quad (3.11)$$

Recall from the last chapter that the DSEs, following directly from the boundary conditions on the path integration within the Gribov horizon, fully determine the Green functions of the

¹Each functional trace “Tr”, as found in $\ln \mathcal{J} = \text{Tr} \ln G^{-1}$, gives rise to a loop.

theory. In the variational approach, on the other hand, the Green functions have a parametric dependence on the kernel ω and on the parameter λ . The DSE (3.11) merely tells us how the gluon propagator is related to the variational kernel ω . The equation that actually determines ω is the Schrödinger equation, $H |\Psi\rangle = E |\Psi\rangle$, that yields for the vacuum state a variational equation of the Rayleigh-Ritz type,

$$\langle H \rangle \rightarrow \min . \quad (3.12)$$

The Schrödinger equation is not strictly a DSE, regarding its origin. Nevertheless, we will often refer to the Schrödinger equation as a DSE since, after all, it has the same form of a non-linear integral equation.

One infers from Eq. (3.11) that for the evaluation of the gluon propagator to one-loop order, the Faddeev–Popov determinant in (3.2) can be replaced by a Gaussian,

$$J = \exp \left[- \int d^3[xy] A_i^a(x) \chi_{ij}^{ab}(x, y) A_j^b(y) \right] , \quad (3.13)$$

and it suffices to use the following generating functional

$$\begin{aligned} Z_\lambda[j] &= \int \mathcal{D}A \exp \left[- \int d^3[xy] A_k^a(x) \Omega(x, y) A_k^a(y) + \int d^3 x j_k^a(x) A_k^a(x) \right] \\ &= \exp \left[\frac{1}{4} \int d^3[xy] j_m^a(x) t_{mn}(x) \Omega(x, y) j_n^a(y) \right] . \end{aligned} \quad (3.14)$$

From the relation

$$\langle \mathcal{O}[A] \rangle_\lambda = \mathcal{O} \left[\frac{\delta}{\delta j} \right] Z_\lambda[j] \quad (3.15)$$

one can verify that the gluon propagator yields Eq. (3.11).

It was shown in Ref. [85] that for the calculation of expectation values in the Schrödinger equation to one-loop order, the Faddeev–Popov determinant can be replaced according to Eq. (3.13). Thus, the “Gaussian type” of wave functionals (3.1) are indeed Gaussian to the level of approximation. The functional form of Wick’s theorem [118] thus becomes applicable and results in the concise prescription (3.15) to evaluate expectation values. With ω replaced by Ω in Eq. (3.14), the Schrödinger equation minimizes the energy with respect to the gluon propagator (3.10) and the value of λ is therefore irrelevant [85]. We will make the choice $\lambda = \frac{1}{2}$ to solve the Schrödinger equation following Ref. [83]. Let us point out here that the restriction to the Gribov region is abandoned in the evaluation of the Gaussian path integrals, see Eq. (3.14). It is therefore of particular interest to compare the results to lattice calculations.

With a Gaussian wave functional at hand, the gauge fields can be transformed into the particle representation and interpreted as particles with energy modes $\omega(k)$. Since the function $\omega(k)$ turns out to be a non-trivial dispersion relation, gluons are interpreted as quasi-particles. This will be further discussed in chapter 5.

3.2 Minimizing the energy density

The vacuum energy density of Yang–Mills theory with vanishing external charges, $\rho_{\text{ext}}^a(x) = 0$, was calculated in the state (3.1) with $\lambda = \frac{1}{2}$ to two-loop order (in the energy) in Ref. [83]. Subsequently, the Yang–Mills Schrödinger equation was used to determine the vacuum state by minimizing the energy density w.r.t. the kernel $\omega(k)$. This leads to the equation²

$$\frac{\delta}{\delta\omega} \langle H \rangle = 0 \quad (3.16)$$

which is basically the only equation that follows from minimizing the energy. Since it gives rise to a dispersion relation with a mass gap, we refer to Eq. (3.16) as the *gap equation*. The gap equation has quite a complex structure, involving the ghost propagator in particular, and we have to resort to auxiliary equations in order to calculate the expectation values. One of these equations is the ghost DSE derived in chapter 2 and another one accounts for the factorization of the Coulomb potential, see below. The entire calculation of Ref. [83] shall not be repeated here, but only the essential steps are outlined and some subtleties are pointed out.

For the expectation value $E = \langle H[A, \Pi] \rangle$ with the Yang–Mills Hamiltonian $H[A, \Pi]$ given by Eq. (1.107), to be calculable by the prescription (3.15), the momentum operators Π are eliminated by action on the wave functional $\Psi[A] = \langle \Psi | A \rangle$. We introduce by

$$\begin{aligned} \sqrt{\mathcal{J}} \Pi_k^a(x) \frac{1}{\sqrt{\mathcal{J}}} \left(\sqrt{\mathcal{J}} \Psi[A] \right) &= \left(\frac{\delta}{i \delta A_k^a(x)} - \frac{1}{2i} \frac{\delta \ln \mathcal{J}}{\delta A_k^a(x)} \right) \mathcal{N} e^{-\frac{1}{2} \int A \omega A} \\ &= i Q_k^a(x) \left(\sqrt{\mathcal{J}} \Psi[A] \right) \end{aligned} \quad (3.17)$$

the quantity

$$Q_k^a(x) = \int d^3 y \omega(x, y) A_k^a(y) - \frac{1}{2} t_{kj}(x) \text{Tr} \left(G \Gamma_k^{0,a}(x) \right). \quad (3.18)$$

One can then show that for the given wave functional $\Psi_{\frac{1}{2}}[A]$,

$$E = \langle H[A, \Pi] \rangle = \langle H[A, Q[A]] \rangle \quad (3.19)$$

and Wick's theorem (3.15) becomes applicable. The vacuum energy $E = E_k + E_p + E_C$ can be computed [83] and it yields the kinetic energy

$$E_k = \frac{N_c^2 - 1}{2} (2\pi)^3 \delta^3(0) \int \bar{d}^3 k \frac{[\omega(k) - \chi(k)]^2}{\omega(k)}, \quad (3.20)$$

the magnetic potential

$$\begin{aligned} E_p &= \frac{N_c^2 - 1}{2} (2\pi)^3 \delta^3(0) \int \bar{d}^3 k \frac{k^2}{\omega(k)} \\ &\quad + \frac{N_c (N_c^2 - 1)}{16} g^2 (2\pi)^3 \delta^3(0) \int \bar{d}^3 k \bar{d}^3 k' \frac{1}{\omega(k)\omega(k')} \left(3 - (\hat{k} \cdot \hat{k}')^2 \right), \end{aligned} \quad (3.21)$$

²In this section, all expectation values are taken in the vacuum state (3.1) with $\lambda = \frac{1}{2}$.

and the Coulomb potential

$$E_C = g^2 \frac{N_c(N_c^2 - 1)}{8} (2\pi)^3 \delta^3(0) \int \bar{d}^3 k \bar{d}^3 k' \left(1 + (\hat{k} \cdot \hat{k}')^2\right) \frac{d(k - k')^2 f(k - k')}{(k - k')^2} \frac{([\omega(k) - \chi(k)] - [\omega(k') - \chi(k')])^2}{\omega(k)\omega(k')} . \quad (3.22)$$

These terms arise from the kinetic, magnetic, and Coulomb parts of the Hamiltonian, listed in that order in Eq. (1.107). The overall volume factor of $(2\pi)^3 \delta^3(0)$ is due to the translational invariance in the absence of localized external charge distributions. In the above expressions, two form factors were introduced. The ghost form factor $d(k)$ measures the deviation of the ghost propagator $D_G(k)$ from tree-level,³

$$D_G(k) = \frac{d(k)}{k^2} , \quad (3.23)$$

and the Coulomb form factor $f(k)$ measures the deviation from the factorization in the expectation value of the Coulomb operator F (cf. Eq. (2.75)),

$$\langle F(k) \rangle = \frac{d^2(k) f(k)}{k^2} . \quad (3.24)$$

From the definition (3.9), the curvature $\chi(k)$ is found to define the following integral,

$$\chi(k) = g^2 \frac{N_c}{4} \int \bar{d}^3 \ell \left(1 - (\hat{\ell} \cdot \hat{k})^2\right) \frac{d(\ell) d(\ell - k)}{(\ell - k)^2} . \quad (3.25)$$

The gap equation can be derived from Eq. (3.16) using

$$\frac{\delta E}{\delta \omega(k)} = \frac{N_C^2 - 1}{2} \delta^3(0) \frac{1}{\omega^2(k)} \left[-k^2 + \omega^2(k) - \chi^2(k) - I_\omega^0 - I_\omega(k)\right] , \quad (3.26)$$

to yield in momentum space [83]

$$\omega^2(k) = k^2 + \chi^2(k) + I_\omega(k) + I_\omega^0 \quad (3.27)$$

with the abbreviations

$$I_\omega^0 = g^2 \frac{N_C}{4} \int \bar{d}^3 \ell \left(3 - (\hat{k} \cdot \hat{\ell})^2\right) \frac{1}{\omega(\ell)} \quad (3.28a)$$

$$I_\omega(k) = g^2 \frac{N_C}{4} \int \bar{d}^3 \ell \left(1 + (\hat{k} \cdot \hat{\ell})^2\right) \frac{d(k - \ell)^2 f(k - \ell)}{(k - \ell)^2} \frac{[\omega(\ell) - \chi(\ell) + \chi(k)]^2 - \omega(k)^2}{\omega(\ell)} \quad (3.28b)$$

In addition, the ghost form factor $d(k)$ obeys the ghost DSE (2.48),

$$\frac{1}{d(k)} = 1 - g^2 \frac{N_c}{2} \int \bar{d}^3 \ell \left(1 - (\hat{\ell} \cdot \hat{k})^2\right) \frac{d(\ell - k)}{(\ell - k)^2 \omega(\ell)} \quad (3.29)$$

³Note that this definition is different from Ref. [83]. Here, at tree-level $d(k) = 1$.

and the Coulomb form factor obeys another integral equation that will be discussed further in section 3.6,

$$f(k) = 1 + g^2 \frac{N_c}{2} \int \bar{d}^3 \ell \left(1 - (\hat{\ell} \cdot \hat{k})^2 \right) \frac{d^2(\ell - k) f(\ell - k)}{(\ell - k)^2 \omega(\ell)} \quad (3.30)$$

The equations (3.27), (3.29) and (3.30) are here collectively called the Dyson–Schwinger equations (DSEs) of our approach to Coulomb gauge Yang–Mills theory. The approximations used in deriving the DSEs include the tree-level approximation for the ghost-gluon vertex and the one-loop expansion in the gap equation.

3.3 Renormalization

Each one of the Dyson–Schwinger equations, the one for the ghost form factor $d(k)$, the Coulomb form factor DSE for $f(k)$, the gap equation for $\omega(k)$ and also the curvature integral $\chi(k)$ require subtraction of the UV divergences. This can be seen by plugging in the ultraviolet behavior of the form factors known from perturbation theory. As discussed in more detail in chapter 4, the ultraviolet asymptotic propagators should attain tree-level up to logarithmic corrections. The tree-level values for the ghost form factor as well as the Coulomb form factor are simply unity. Whereas the latter are genuinely instantaneous in our approach, the gluon propagator may be regarded as the equal-time part of the tree-level propagator in Euclidean spacetime,

$$D_{ij}^0(\mathbf{k}, \Delta t = 0) = \int_{-\infty}^{\infty} \bar{d}k_0 \frac{t_{ij}(\mathbf{k})}{k_0^2 + \mathbf{k}^2} = \frac{t_{ij}(\mathbf{k})}{2|\mathbf{k}|} \quad (3.31)$$

and a first guess⁴ for $\omega(k)$ in the UV therefore is $\omega(k \rightarrow \infty) = k$, yielding the dispersion relation of a free massless particle. By simple power counting in the ultraviolet, the integrals in (3.29) and (3.30) are found to be logarithmically divergent. The gap equation (3.27) and the curvature integral (3.25), on the other hand, contain power divergences.

Renormalization, the concept of redefining the parameters of a theory such that expectation values are free of infinities, can be introduced multiplicatively in perturbation theory [119]. That is, the local field operators are multiplied by renormalization constants such as to remove the divergences occurring in the perturbative expansion. In the Lagrangian language, multiplicative renormalization may be described by appropriate counter terms in the Lagrangian that respect its symmetries. The arbitrariness in defining the finite part of a divergent quantity can be controlled by the renormalization group. Nonperturbatively, a systematic concept of removing divergences is lacking. This also applies to the present nonperturbative approach to Coulomb gauge YM theory. In Ref. [120], counter terms to the Hamiltonian were introduced which are seen—a posteriori—to remove the divergences in the DSEs. Below, we will follow

⁴Recall that $D_{ij}(k) = \frac{1}{2} t_{ij}(k) \omega^{-1}(k)$.

the renormalization procedure given in Ref. [120]. Thus, some additional parameters are introduced into the theory. It will be seen that, at least for the asymptotic IR and UV behavior, the solutions are independent of these parameters.

Renormalization of the Faddeev–Popov determinant

The curvature integral (3.25) is linearly divergent. From the identity $\mathcal{J} = \exp(-\int A\chi A)$, see Eq. (3.13), valid to one-loop order, it is evident that the divergences in $\chi(k)$ can be traced back to the Faddeev–Popov determinant. Eq. (3.13) suggests that the counter terms required to renormalize the Faddeev–Popov determinant, or more precisely its logarithm, have to be of the form $\sim \int AA$. Since the log of the Faddeev–Popov determinant can be regarded as part of the “action”, we renormalize the Faddeev–Popov determinant as

$$J \rightarrow J \cdot \Delta J = \exp \left[\text{Tr} \ln G^{-1} + C_\chi(\Lambda) \int d^3x A_k^a(x) A_k^a(x) \right] \quad (3.32)$$

or by using the representation Eq. (3.13), we obtain

$$J \cdot \Delta J = \exp \left[- \int A (\chi - C_\chi(\Lambda)) A \right]. \quad (3.33)$$

Obviously, the counter term $C_\chi(\Lambda)$ has to be chosen to eliminate the ultraviolet divergent part of the curvature $\chi(k)$. Thus the renormalization condition reads in momentum space

$$\chi(k) - C_\chi(\Lambda) = \text{finite}. \quad (3.34)$$

As usual, there is some freedom in choosing the finite constants of the right hand side of Eq. (3.34). In principle, we could just eliminate the ultraviolet divergent part of $\chi(k)$ by appropriately choosing the counter term $C_\chi(\Lambda)$. However, it is more convenient to choose $C_\chi(\Lambda)$ to be the curvature at some renormalization scale μ , resulting in the renormalization condition

$$C_\chi(\Lambda) = \chi(\mu) \quad (3.35)$$

and in the finite renormalized curvature

$$\bar{\chi}(k) = \chi(k) - \chi(\mu). \quad (3.36)$$

It is easy to check that this quantity is indeed ultraviolet finite and obviously it satisfies the condition

$$\bar{\chi}(k = \mu) = 0. \quad (3.37)$$

By adopting the renormalization condition Eq. (3.35), the renormalized quantity $\bar{\chi}(k)$ in Eq. (3.36) depends on the so far arbitrary scale μ . By choosing the renormalization condition Eq. (3.37) this renormalization scale becomes a parameter of our “model”, since it defines the infrared content of the curvature $\chi(k)$ kept in the renormalization process. For instance,

choosing $\mu = 0$, the whole infrared divergent part of the curvature is chopped off. The numerical calculations below use a finite $\mu > 0$.

In Ref. [121], a different renormalization condition was chosen, keeping from the ultraviolet divergent quantity $\chi(\mu)$ the finite part $\chi'(\mu)$. This amounts to setting

$$C_\chi(\Lambda) = \chi(\mu) - \chi'(\mu), \quad (3.38)$$

which results in the renormalized curvature

$$\chi(k) = \bar{\chi}(k) + \chi'(\mu). \quad (3.39)$$

Only the divergent part of the curvature is subtracted, keeping fully its finite part. Here, we have an extra parameter $\chi'(\mu)$ of the theory and the renormalization scale μ is not related to the zero of the renormalized quantity $\chi(k)$ in Eq. (3.39). The latter method of removing divergences may be looked upon as an alternative, the former (3.36) will be used below. Both methods can be accounted for by the specific choice of the counter term $\Delta\mathcal{J}$ to the Faddeev–Popov determinant.

Counter terms to the Hamiltonian

In order to eliminate the divergences in the gap equation, it turns out the counter terms

$$\Delta H = C_0(\Lambda) \int d^3x A_k^a(x) A_k^a(x) + iC_1(\Lambda) \int d^3x A_k^a(x) \Pi_k^a(x) \quad (3.40)$$

should be added to the Hamiltonian. Here the coefficients $C_0(\Lambda)$ and $C_1(\Lambda)$ depend on the momentum cutoff Λ and have to be adjusted so that the UV singularities in the gap equation disappear. Note that these coefficients multiply ultralocal operators which are singular in quantum field theory. For the wave functional at hand, the expectation value of the counter term Eq. (3.40) is given by

$$\Delta E = C_0(\Lambda) \frac{1}{2} t_{ii} \delta^{aa} \int d^3x \omega^{-1}(x, x) - C_1(\Lambda) \int d^3x \langle A_k^a(x) Q_k^a(x) \rangle. \quad (3.41)$$

With the identity

$$\langle A_k^a(x) Q_k^a(x) \rangle = \int d^3x' \omega^{-1}(x, x') (\omega(x', x) - \chi(x', x)) \delta^{aa} \quad (3.42)$$

shown in Ref. [83], Eq. (3.41) can be written in momentum space as

$$\Delta E = (N_C^2 - 1) (2\pi)^3 \delta^3(0) \left[C_0(\Lambda) \int d^3k \frac{1}{\omega(k)} - C_1(\Lambda) \int d^3k \frac{\omega(k) - \chi(k)}{\omega(k)} \right]. \quad (3.43)$$

Taking the variation of this expression with respect to $\omega(k)$, we obtain

$$\frac{\delta \Delta E}{\delta \omega(k)} = (N_C^2 - 1) \delta^3(0) \left[-C_0(\Lambda) \frac{1}{\omega^2(k)} - C_1(\Lambda) \frac{\chi(k)}{\omega^2(k)} \right]. \quad (3.44)$$

Note that $\chi(k)$ depends only on the ghost propagator but not on the gluon energy ω , at least as long as $\chi(k)$ is not yet the self-consistent solution. Adding the counter terms from Eq. (3.43) to the energy in the gap equation (3.26), one finds

$$\omega^2(k) = k^2 + \chi^2(k) + I_\omega^0 + I_\omega(k) - 2C_0(\Lambda) - 2C_1(\Lambda)\chi(k). \quad (3.45)$$

Renormalization of the gap equation

We now turn to the renormalization of the gap equation (3.45) which already includes the counter terms. After the renormalization of the Faddeev–Popov determinant, the curvature $\chi(k)$ can be replaced by the renormalized one $\bar{\chi}(k)$, Eq. (3.36). Note that the Coulomb integral $I_\omega(k)$ does not depend on any constant part of the curvature, see Eq. (3.28b), so that $\chi(k)$ could have been replaced right away by the finite quantity $\bar{\chi}(k)$. Replacing $\chi(k)$ by $\bar{\chi}(k)$ and using the relation

$$I_\omega(k) = I_\omega^{(2)}(k) + 2\bar{\chi}(k)I_\omega^{(1)}(k), \quad (3.46)$$

the gap equation in Eq. (3.45) becomes

$$\omega^2(k) - \bar{\chi}^2(k) = k^2 + I_\omega^0 + I_\omega^{(2)}(k) - 2C_0(\Lambda) + 2\bar{\chi}(k) \left(I_\omega^{(1)}(k) - C_1(\Lambda) \right). \quad (3.47)$$

The integrals $I_\omega^{(n=1,2)}(k)$ are the linearly ($n = 1$) and quadratically ($n = 2$) UV divergent parts of $I_\omega(k)$ in Eq. (3.28b), see also Ref. [83]. The integral I_ω^0 in Eq. (3.28a) is also quadratically divergent but independent of the external momentum. We can therefore eliminate all UV-divergences by choosing $C_0(\Lambda) \sim \Lambda^2$ and $C_1(\Lambda) \sim \Lambda$. In principle, the coefficients of the counter terms $C_0(\Lambda)$ and $C_1(\Lambda)$ have to be chosen to eliminate the UV divergent parts of the quantities appearing in the gap equation. This means that we should choose these infinite coefficients as

$$\left(I_\omega^0 + I_\omega^{(2)}(k) \right)_{\text{UV divergent part}} - 2C_0(\Lambda) = 0 \quad (3.48)$$

$$I_\omega^{(1)}(k) \Big|_{\text{UV-divergent part}} - C_1(\Lambda) = 0 \quad (3.49)$$

Note that the UV divergent parts of $I_\omega^{(n=1,2)}(k)$ are by dimensional arguments independent of the external momentum k . Technically it is more convenient to choose the following alternative renormalization conditions. As usual we have the freedom in choosing the renormalization conditions up to finite constants. Given the fact that I_ω^0 is independent of the external momentum and the differences

$$\Delta I_\omega^{(n)}(k, \nu) = I_\omega^{(n)}(k) - I_\omega^{(n)}(\nu) \quad (3.50)$$

are UV-finite, we can eliminate all UV-divergences by choosing the renormalization conditions

$$I_\omega^0 + I_\omega^{(2)}(k = \nu) - 2C_0(\Lambda) = 0 \quad (3.51a)$$

$$I_\omega^{(1)}(k = \nu) - C_1(\Lambda) = 0, \quad (3.51b)$$

where ν is an arbitrary renormalization scale, which could be chosen to be the same scale μ of the renormalization of the curvature, but given the fact that with the renormalization prescription (3.35), the scale μ becomes a physical parameter, the two renormalization parameters ν and μ need not necessarily be the same. With the renormalization conditions (3.51) the renormalized (finite!) gap equation reads

$$\omega^2(k) - \bar{\chi}^2(k) = k^2 + \Delta I_\omega^{(2)}(k, \nu) + 2\bar{\chi}(k)\Delta I_\omega^{(1)}(k, \nu). \quad (3.52)$$

Assuming that the integrals $I_\omega^{(n=1,2)}(k)$ are infrared finite and furthermore that the renormalized curvature $\bar{\chi}(k)$ is infrared divergent, the infrared limit of the renormalized gap equation is given by

$$\lim_{k \rightarrow 0} (\omega(k) - \bar{\chi}(k)) = \Delta I_\omega^{(1)}(k=0, \nu) . \quad (3.53)$$

The 't Hooft loop, which yields a perimeter law in the confinement phase, can be explicitly calculated using its representation found in Ref. [122]. In the Gaussian vacuum, it is sensitive to the quantity (3.53) and it is shown in Refs. [123, 121] that only the choice $\nu = 0$ gives the perimeter law. With this choice the renormalized gap equation becomes

$$\omega^2(k) - \bar{\chi}^2(k) = k^2 + \Delta I_\omega^{(2)}(k, 0) + 2\bar{\chi}(k)\Delta I_\omega^{(1)}(k, 0) . \quad (3.54)$$

Renormalization of the ghost and Coulomb form factor

The Dyson–Schwinger equation for the ghost propagator is given by Eq. (3.29) and bears a logarithmic divergence in the ultraviolet part of the integral. By a simple subtraction at μ_d , this divergence is removed. Hence,

$$\frac{1}{d(k)} = \frac{1}{d(\mu_d)} - \left[g^2 \frac{N_c}{2} \int \bar{d}^3 \ell \left(1 - (\hat{\ell} \cdot \hat{k})^2 \right) \frac{d(\ell - k)}{(\ell - k)^2 \omega(\ell)} - (k \leftrightarrow \mu_d) \right] \quad (3.55)$$

is a finite equation. In principle, one can choose μ_d different from μ . In view of the horizon condition, it is convenient to set $\mu_d = 0$ while keeping a finite μ (in particular for the sake of the curvature).

The DSE for the Coulomb form factor is given by Eq. (3.30) and can be subtracted at μ_f to yield the finite expression

$$f(k) = f(\mu_f) + \left[\frac{g^2 N_c}{2} \int \bar{d}^3 \ell \left(1 - (\hat{\ell} \cdot \hat{k})^2 \right) \frac{d^2(\ell - k)f(\ell - k)}{(\ell - k)^2 \omega(\ell)} - (k \leftrightarrow \mu_f) \right] . \quad (3.56)$$

We choose here $\mu_f = \mu$. The coupled DSEs then contain the following undetermined parameters: the renormalization scale μ of the renormalization of the curvature and the renormalization constant $f(\mu)$ of the Coulomb form factor. The parameter $d(\mu_d)$ may (or may not) be taken care of by implementing the horizon condition.

3.4 Full numerical solutions

The renormalized and thus finite DSEs (3.54, 3.55, 3.56) are cast in a form tractable for a numerical study. Solving such a coupled set of integral equations is pursued by iteration. An educated guess for initial form factors is plugged into the integrals and the results are recorded by the Chebychev approximation to be processed further. For asymptotic values of momentum, it is instructive for the numerics to make use of the analytical results, cf. the

methods used in Refs. [124, 125, 106, 126]. The set of nodes cover a finite momentum region. In order to extrapolate this to the whole infinite momentum range, the general algebraic forms obtained analytically serve as ansätze. However, contrary to what has been previously done in Dyson–Schwinger studies, the parameters of these asymptotic forms are still determined numerically. E.g., in the infrared it was shown analytically that power laws provide a solution. The numerics will have the asymptotic form of the power laws (2.50) as an input but determine the various exponents and coefficients as parameters by nonlinear least-squares fitting. Thus, this numerical method provides a check on the analytical results of Table 2.1 rather than imposing the latter.

Previously, a numerical solution of the Coulomb gauge DSEs was found in Ref. [83]. The infrared behavior agreed approximately with the exponent $\kappa = 0.398$ of Table 2.1. A heavy quark potential was obtained that confines but does not rise linearly, as compared to the Wilson loop on the lattice. Therefore, a string tension cannot be extracted from these results. After analytical investigations of the infrared behavior of the Coulomb gauge Green functions in Ref. [103], it became clear that yet another solution, with $\kappa = \frac{1}{2}$ should exist. Eventually, improved numerical methods were able to indeed confirm $\kappa = \frac{1}{2}$ and reveal a strictly linearly rising potential in Ref. [86]. These results will be exhibited in this section.

The technical details of the numerical calculation are described in Ref. [86]. It shall suffice here to mention the essence of the set-up. For convenience, the gauge coupling g is set to unity. The functions⁵ $\omega(k)$ and $\chi(k)$ are both described in the far infrared by a power law A/k^α where A and α are extracted by fitting the solution. It is possible to gain more information on the intermediate momentum regime by setting up an infrared expansion of the function

$$\omega(k) - \chi(k) = c + c_1 k^\gamma, \quad k \rightarrow 0, \gamma > 0. \quad (3.57)$$

and again determining its parameters by fitting. While both $\omega(k)$ and $\chi(k)$ are infrared enhanced, we have $c < \infty$. Recalling that the 't Hooft loop requires for confinement $\nu = 0$ in Eq. (3.53), we realize that $c = 0$.

In the ultraviolet, we use the asymptotic behavior of the form factors found in Ref. [83] and make the corresponding ansätze for $k \rightarrow \infty$,

$$\omega(k) = k \quad (3.58a)$$

$$\chi(k) \sim k/\sqrt{\ln(k/m_\chi)} \quad (3.58b)$$

$$d(k) \sim 1/\sqrt{\ln(k/m_d)} \quad (3.58c)$$

$$f(k) \sim 1/\sqrt{\ln(k/m_f)} \quad (3.58d)$$

extracting the coefficients as well as the different scale parameters m_χ , m_d , m_f using least-squares fitting. An ultraviolet behavior different from Eq. (3.58) will be proposed in chapter 4.

All numerical plots displayed in this section were calculated by D. Epple [86]. As seen from the left panel in Fig. 3.1, both $\omega(k)$ and $\chi(k)$ are enhanced like $1/k$ in the infrared, as predicted in

⁵We drop the bar on $\chi(k)$, still meaning $\bar{\chi}(k)$ in Eq. (3.36).

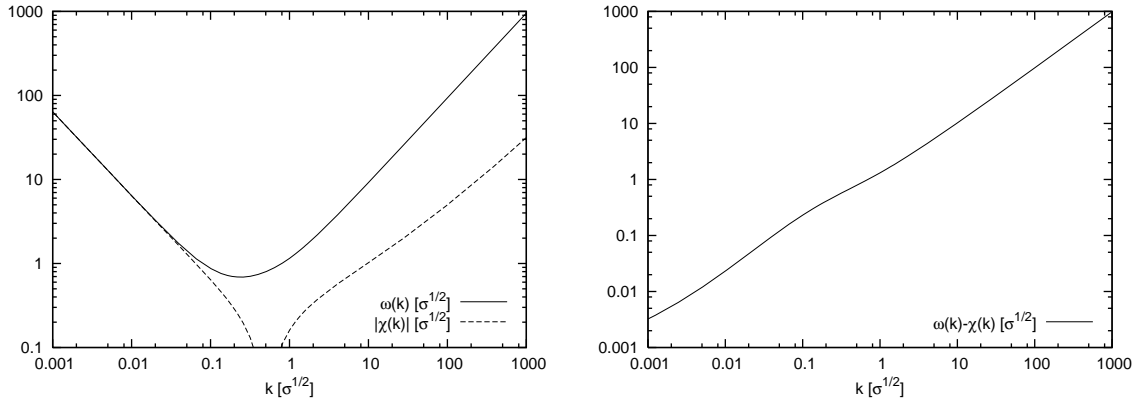


Figure 3.1: *Left: The gluon energy $\omega(k)$ and the modulus of the scalar curvature $\chi(k)$. Right: The difference $\omega(k) - \chi(k)$.*

the stochastic vacuum. The right panel of Fig. 3.1 shows the function $\omega(k) - \chi(k)$ vanishing for $k \rightarrow 0$, in accord with our choice of the renormalization condition $c = 0$. Fig. 3.2 (left panel) shows the infrared enhanced ghost form factor $d(k)$. Thus, the functions $d(k)$, $\omega(k)$ and $\chi(k)$ are all enhanced as $1/k$ in the infrared. On the right panel of Figure 3.2, the heavy quark Coulomb potential $V_C(r)$, as given by Eq. (2.74), is shown. An exactly linearly rising behavior (within an estimated error of less than one percent) is found, again in agreement with the infrared analysis of chapter 2. The linearly rising potential allows us to fit our scale from the string tension. Lattice calculations [127, 75, 128] show, however, that the Coulomb string tension σ_C is about a factor of 1.5...3 larger than the string tension σ_W extracted from the Wilson loop, in agreement with the analytic result [111] that the Coulomb string tension is an upper bound to the Wilson loop string tension. Setting $\sigma_C = \sigma_W$ therefore yields a small quantitative error. However, the *qualitative* features of the results shown in Figs. 3.1 and 3.2 are reliable on the one hand, and they successfully describe the physical nonperturbative phenomenon of confinement on the other. Quarks are confined by a linearly rising potential $V_C(r)$, and gluons are confined since the dispersion relation $\omega(k)$ diverges for $k \rightarrow 0$, prohibiting the propagation of gluons over large distances.

The numerical confirmation of the infrared behavior predicted by the analytical calculations in the stochastic vacuum, see chapter 2, deserves the following two comments. Firstly, among the full structure of the gap equation (3.54), the infrared leading contributions were obviously already accounted for by the stochastic vacuum. Fig. 3.1 clearly shows that the curvature $\chi(k)$, by which the gluon propagator in the stochastic vacuum is expressed over the entire momentum range, is the infrared asymptotic function of the (inverse) gluon propagator $\omega(k)$. In retrospect, these findings may be understood as a confirmation of the Gribov–Zwanziger scenario. The second comment is more a mathematical one. Given the full structure of the DSEs, how can an asymptotic solution be obtained analytically? We make power law ansätze for the infrared behavior and, knowing that in the UV they are not valid, we use them for integrating the propagators over the entire momentum range. This method was first used in

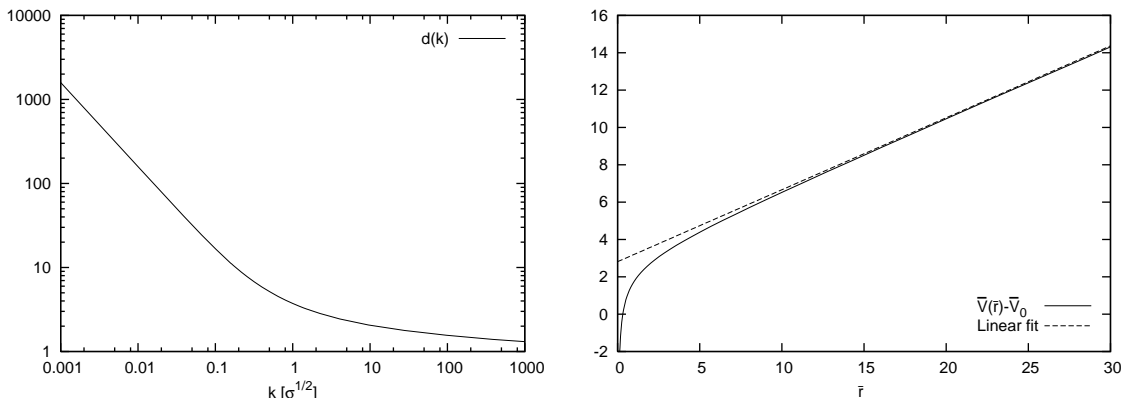


Figure 3.2: *Left: The ghost form factor $d(k)$. Right: The heavy quark Coulomb potential $V_C(r)$.*

Landau gauge DSE studies in Ref. [107] and later led to the now accepted infrared exponents by the calculations in Refs. [97, 102]. From the experience with the numerical evaluation of integrals, this procedure seems acceptable, but a justification would be desirable. In Ref. [54] some arguments are given why infrared asymptotics may be computed in the way mentioned above. A sketch of a proof was given in the context of the “infrared integral approximation” in Ref. [103]. It is also worth mentioning the useful reference [129] in the context of asymptotic expansions. Here, we give a short and rather obvious explanation why the method is correct. It follows from the Riemann-Lebesgue lemma that convolution integrals $C(k)$ of the type

$$\begin{aligned} C(k) &= \int dq D_1(q) D_2(q-k) = \int dq \int dx \int dy \tilde{D}_1(x) \tilde{D}_2(y) e^{-iqx - i(q-k)y} \\ &= \int dx \tilde{D}_1(x) \tilde{D}_2(-x) e^{-ikx} \end{aligned} \quad (3.59)$$

asymptotically approach the function $C^{as}(k)$ obtained by replacing in the integrand the infrared asymptotic functions $D_i^{as}(k) = \lim_{k \rightarrow 0} D_i(k)$ and $\tilde{D}_i^{as}(x) = \lim_{x \rightarrow \infty} \tilde{D}_i(x)$ ($i = 1, 2$),

$$\begin{aligned} C^{as}(k) &= \lim_{k \rightarrow 0} C(k) = \int dx \tilde{D}_1^{as}(x) \tilde{D}_2^{as}(-x) e^{-ikx} \\ &= \int dq D_1^{as}(q) D_2^{as}(q-k). \end{aligned} \quad (3.60)$$

This argument can be applied to the (renormalized) DSEs. Replacing the scalar products from the Lorentz structure by identities such as $2\ell \cdot k = k^2 + \ell^2 - (\ell - k)^2$, all (one-loop) DSEs turn into a sum of convolution integrals of the type $C(k)$ given in Eq. (3.59).

Recently, there have been investigations of Coulomb gauge Green functions on the lattice [131, 128, 70]. In Fig. 3.3, the lattice data for the ghost propagator and the inverse gluon propagator are shown in comparison to the continuum solutions. The qualitative infrared enhancement of the ghost propagator is reproduced by the lattice calculations. At the same time, the gluon form factor $\omega(k)$ seems to be infrared enhanced as well. It is difficult to extract

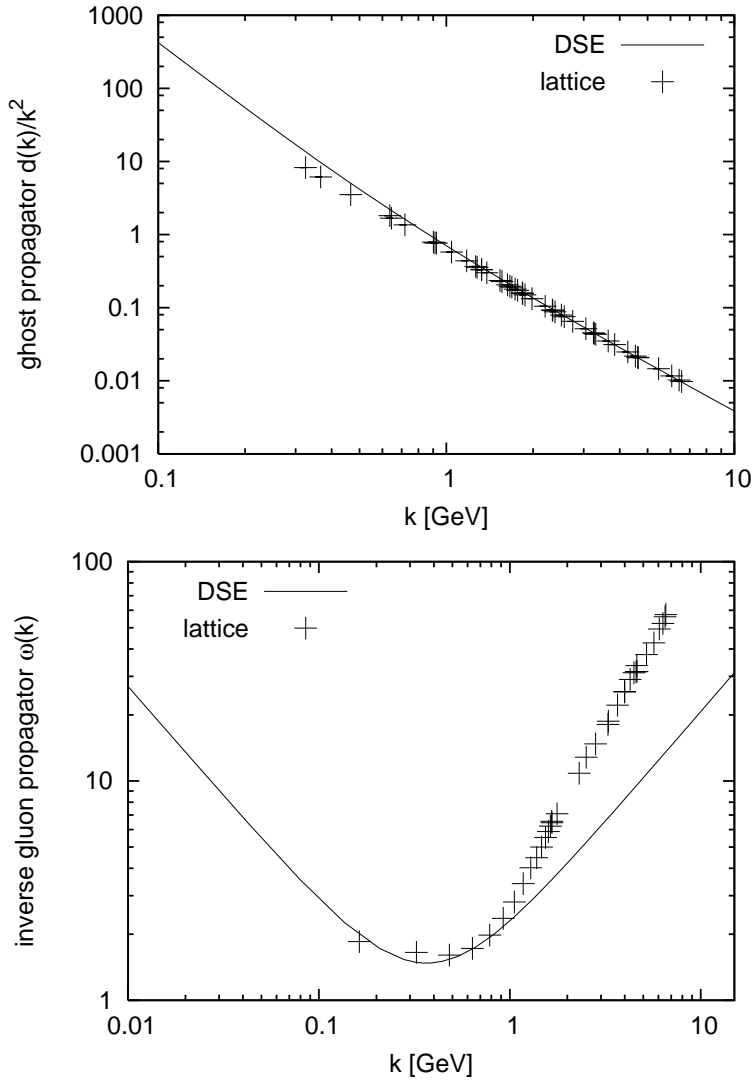


Figure 3.3: Ghost propagator [130] and inverse gluon propagator [70] from lattice calculations, in comparison to the continuum results in the Hamiltonian approach.

reliable data for the infrared sector on the lattice. Yet, the lattice data for the Coulomb gauge gluon propagator of Ref. [131] gives $\kappa \approx 0.49$, in agreement with the continuum result. In the ultraviolet the striking feature of Fig. 3.3 is that the lattice data for the function $\omega(k)$ rise stronger than linearly. This might actually be an indication that the ultraviolet properties of the continuum solutions need to be improved. We will come back to that in section 4.3.

Finally, let us mention that in $2 + 1$ dimensional Coulomb gauge YM theory, numerical continuum results from the Coulomb gauge Hamiltonian approach were recently obtained in Ref. [132]. Similarly to the $d = 3$ case, it is found that all form factors are infrared enhanced, with infrared exponents that approximately agree with $\kappa = \frac{1}{5}$, the value given in Table 2.1 for $d = 2$.

3.5 Vertices

The energy density that was minimized in the previous section to give rise to the vacuum Green functions was shown to be rather insensitive to the choice of the wave functional, according to the discussion in section 3.1. The three-gluon vertex we are turning to in this section will show a strong dependence on the wave functional, in particular on the exponent λ of the Faddeev–Popov determinant. Knowing the infrared behavior of the three-gluon vertex, it will be possible to further investigate the ghost-gluon vertex in the infrared.

Three-gluon vertex

As pointed out above, it is only the Faddeev–Popov determinant that influences the infrared behavior of Yang–Mills theory. The solution obtained for the infrared exponents of the propagators was found to be independent of the three-gluon vertex, in particular, since it contributes to neither the ghost self-energy term nor the ghost loop contribution to the gluon self-energy. In the Coulomb gauge, we have seen that any of the vacua $\Psi_\lambda[A]$ given by Eq. (3.1) minimizes the energy w.r.t. λ , evaluated to one-loop order in the DSE (two-loop order in the diagrams for the energy). The question is how the three-gluon vertex changes in the infrared for different values of λ without resorting to the one-loop approximation.

The full three-gluon vertex is defined as

$$(\Gamma_{\text{full}})_{ijk}^{abc}(x, y, z) = \left\langle A_i^a(x) A_j^b(y) A_k^c(z) \right\rangle . \quad (3.61)$$

In the particular case of $\lambda = 1/2$ it is found that

$$\int \mathcal{D}A A_i A_j A_k e^{-\int A \omega A} = 0 \quad (3.62)$$

in a symmetric integration domain. Leaving aside a discussion whether the Gribov region Ω is symmetric about $A = 0$, we here extend the integration domain to the whole gauge-fixed configuration space, for practical purposes. Hence, the three-gluon vertex vanishes for $\psi_{1/2}$

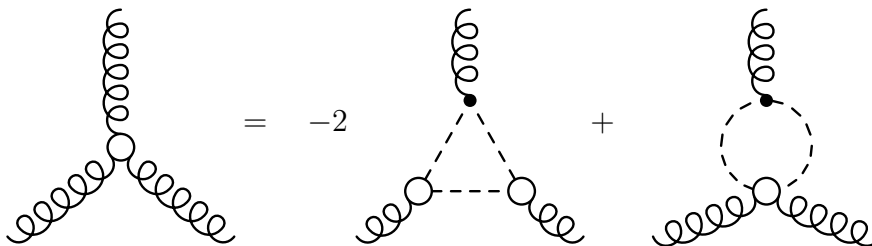


Figure 3.4: The (complete) DSE for the three-gluon vertex derived from the generating functional given in Eq. (3.2).

[83]. Now consider the case $\lambda \neq 1/2$. To one-loop order in the gap equation we may employ the form (3.14) for the generating functional $Z_\lambda[j]$. The three-gluon vertex then vanishes for any λ since the weighting of path integration remains in a Gaussian form.

On the other hand, without the use of the one-loop approximation, $\lambda \neq 1/2$ will give a non-zero three-gluon vertex, in contrast to Eq. (3.62), as will be shown. Thus, the three-gluon vertex shows great sensitivity to the choice of the vacuum wave functional ψ_λ , a behavior not exhibited to one-loop order. Making the choice $\lambda = 0$ permits the standard representation of the Faddeev–Popov determinant by ghosts. One can then derive [103] the Dyson–Schwinger equation for the Coulomb gauge three-gluon vertex. It is depicted diagrammatically in Fig. 3.4. Its complete form comprises a diagram with the unknown two-ghost-two-gluon vertex which is truncated here. For the following calculation, the ghost-gluon vertex is used at tree-level. The DSE for the proper three-gluon vertex then reads [103]

$$\Gamma_{ijk}(k_1, k_2, k_3) = N_c \int \bar{d}^d \ell D_G(\ell) D_G(\ell + k_1) D_G(\ell - k_2) \Gamma_i^0(\ell) \Gamma_j^0(\ell - k_2) \Gamma_k^0(\ell + k_1), \quad (3.63)$$

where the outgoing momenta k_i obey the conservation law

$$k_1 + k_2 + k_3 = 0. \quad (3.64)$$

The vertex given by Eq. (3.63) is projected onto the tensor subspace spanned by the tensor components of the tree-level vertex. Due to Bose symmetry, the coefficient functions of these six components are all the same, but their signs alternate as the vertex without the color structure is antisymmetric under gluon exchange. One finds

$$\begin{aligned} \Gamma_{ijk}(k_1, k_2, k_3) = & -i(k_2)_i \delta_{jk} F(k_2^2, k_1^2, k_3^2) + i(k_3)_i \delta_{jk} F(k_3^2, k_1^2, k_2^2) \\ & + i(k_1)_j \delta_{ik} F(k_1^2, k_2^2, k_3^2) - i(k_3)_j \delta_{ik} F(k_3^2, k_2^2, k_1^2) \\ & - i(k_1)_k \delta_{ij} F(k_1^2, k_3^2, k_2^2) + i(k_2)_k \delta_{ij} F(k_2^2, k_3^2, k_1^2). \end{aligned} \quad (3.65)$$

Equating Eq. (3.63) with (3.65) and contracting with these six tensors, yields a set of six linear equations for F , the solution of which reads

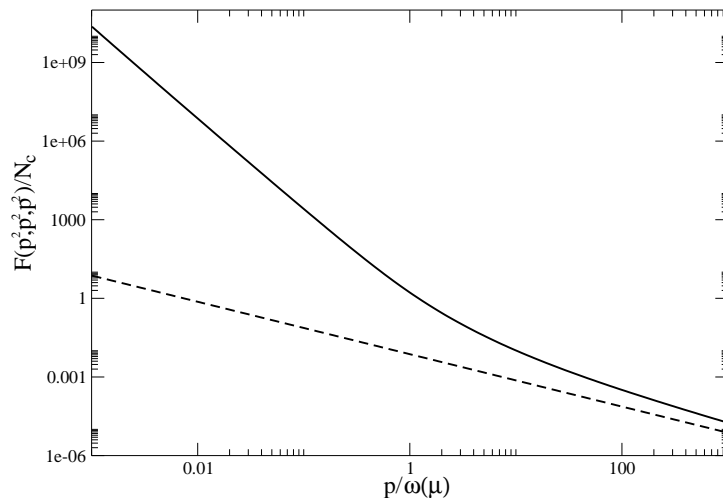


Figure 3.5: Calculation by M. Leder, published in [103]. Dressing function of the Coulomb gauge proper three-gluon vertex at the symmetric point. The dashed curve shows in contrast the perturbative case where the propagators in the loop are tree-level, i.e. $\kappa = 0$.

$$F(k_1^2, k_2^2, k_3^2) = \frac{-N_c}{10(k_1^2 k_2^2 - (k_1 \cdot k_2)^2)} \int d^d \ell D_G(\ell) D_G(k_3 + \ell) D_G(\ell - k_2) \\ ((k_1^2 + k_1 \cdot k_2)(-2J_2 - J_4 + 3J_5) + (k_2^2 + k_1 \cdot k_2)(2J_1 - 3J_3 + J_6)) \quad (3.66)$$

where

$$\begin{aligned} J_1 &:= (k_1 \cdot \ell) \ell^2 & J_2 &:= (k_2 \cdot \ell) \ell^2 & J_3 &:= (k_2 \cdot \ell)(k_1 \cdot \ell) \\ J_4 &:= k_2^2 \ell^2 & J_5 &:= (k_2 \cdot \ell)^2 & J_6 &:= (k_1 \cdot k_2) \ell^2. \end{aligned} \quad (3.67)$$

The integral (3.66) depends only on the ghost propagator in this truncation, and despite the infrared enhancement of the latter it is convergent. The numerical calculation of the form factor F at the symmetric point, where $k_1^2 = k_2^2 = k_3^2 =: k^2$, shows a strong infrared enhancement, see Fig. 3.5. For the ghost propagator we used the numerical results of Ref. [83] where $\kappa = 0.425$. A fit to the data in Fig. 3.5 yields an infrared power law, $F(k^2) \sim (k^2)^{-1.77}$. It is clear from the discussion on page 72 that this asymptotic power law can be obtained analytically. Replacing the integrand in Eq. (3.66) by its infrared behavior and shifting $\ell \rightarrow \lambda \ell$, one finds from the homogeneity that $F(k^2) \sim (k^2)^{d/2-2-3\kappa}$. Plugging in the value $\kappa = 0.425$ gives an infrared exponent of -1.775 which agrees (within errors) with the numerical result in Fig. 3.5. At large momenta the vertex vanishes which complies with asymptotic freedom since in the Gaussian vacuum there is no tree-level vertex.

The above results for the infrared behavior of the Coulomb gauge three-gluon vertex can be generalized to any value of κ and any dimension d . Therefore, we can also make statements

d	κ	$F(k^2)$
3	0.398	$\frac{1}{(k^2)^{1.775}}$
3	$\frac{1}{2}$	$\frac{1}{(k^2)^2}$
4	0.595	$\frac{1}{(k^2)^{1.785}}$

 Table 3.1: Infrared power laws of the function $F(k^2)$.

about the Landau gauge where d represents the dimension of Euclidean spacetime. Noting that $d/2 - 2 - 3\kappa = \alpha_A - \alpha_G$, see Eq. (2.54), we find

$$F(k^2) \sim \frac{1}{(k^2)^{\alpha_G - \alpha_A}}. \quad (3.68)$$

With the analytical results for κ in Coulomb ($d = 3$) as well as in Landau ($d = 4$) gauge, the exponents in Eq. (3.68) have the numerical values shown in Table 3.1. The Landau gauge result agrees exactly with Ref. [133].

Another interesting kinematic point is where one of the gluon momenta, say k_1 , is set to zero while the others remain finite. A technical remark: we switch here to the off-shell gauge condition. Thus, no ambiguities are found when trying to evaluate transverse projectors at zero momentum. Another technical problem is the following. Trying to calculate the vertex with one momentum vanishing from Eq. (3.65) by setting $k_1 = 0$, the projections onto the tensor components fail because the determinant of the coefficient matrix that defines the tensor expansion vanishes in this case.⁶ It is advisory to impose $k_1 = 0$ in the DSE (3.63),

$$\Gamma_{ijk}(0, k, -k) = -ig^3 N_c \int \bar{d}^d \ell \ell_i (\ell - k)_j \ell_k D_G^2(\ell) D_G(\ell - k). \quad (3.69)$$

One can then realize that this integral exists. It can be expanded into a tensor basis constructed by the only scale k and Lorentz invariant tensors, i.e. $\{k_i \delta_{jk}, k_j \delta_{ki}, k_k \delta_{ij}\}$. However, the only component that survives the transverse projections of the gluon legs of Γ_{ijk} with finite momenta, is obviously $k_i \delta_{jk}$. Thus, we can write

$$\Gamma_{ijk}(0, k, -k) = -ig^3 N_c k_i \delta_{jk} \frac{1}{(d-1)k^2} k_m t_{np}(k) \int \bar{d}^d \ell \ell_m \ell_n \ell_k D_G^2(\ell) D_G(\ell - k) + \dots \quad (3.70)$$

⁶In this context, one might note that the infrared limit of any tensor integral is non-trivial. Given an integral

$$I_{\mu_1 \mu_2 \dots \mu_M}(\{k^{(i)}\}) = \int \bar{d}^d \ell \ell_{\mu_1} \ell_{\mu_2} \dots \ell_{\mu_M} f(\ell, \{k^{(i)}\})$$

we can construct a tensor basis from the external scales $\{k^{(i)}\}$ and Lorentz invariant tensors. According to the Passarino–Veltman formalism [112], the above integral can then be expanded in this basis, which is nothing but solving a set of linear equations for the expansion coefficients in this basis. If one sets up a tensor expansion for finite $\{k^{(i)}\}$ and then tries to perform the infrared limit of a single external momentum, say $k^{(k)} \rightarrow 0$, the coefficient matrix becomes singular, and the tensor expansion is not well-defined. Instead, one can set $k^{(k)} = 0$ from the beginning (if the integral exists here) and construct the tensor basis spanning a vector space which is of a lower dimension than beforehand. The expansion coefficients are then well-defined.

where the ellipsis represents irrelevant tensor components which shall be discarded henceforth. In the asymptotic infrared, we use the power laws (2.50) for the propagators and obtain from Eq. (3.70)

$$\Gamma_{ijk}(0, k, -k) = -ig^3 B^3 N_c k_i \delta_{jk} \frac{I_3}{(k^2)^{\alpha_G - \alpha_A}}, \quad k \rightarrow 0 \quad (3.71)$$

with

$$\begin{aligned} I_3 &= \frac{(k^2)^{\alpha_G - \alpha_A}}{d-1} (\Xi_1(1+2\kappa, 1+\kappa) - \Xi_3(2+2\kappa, 1+\kappa)/k^2) \\ &= \frac{1}{2(4\pi)^{d/2}(d-1)} \frac{\Gamma(\frac{d}{2} - 2\kappa)\Gamma(\frac{d}{2} - \kappa)\Gamma(2 - \frac{d}{2} + 3\kappa)}{\Gamma(d-3\kappa)\Gamma(1+\kappa)\Gamma(2+2\kappa)}. \end{aligned} \quad (3.72)$$

In view of the strong infrared divergence of the three-gluon vertex, one has to check the ghost dominance in the propagator DSEs. The infrared power law of the three-gluon vertex (3.68), expresses that the vertex dressing replaces the infrared exponent of a gluon by that of a ghost propagator, for any dimension d . The infrared hierarchy of terms in the gluon DSE remains untouched, since even with the dressing of the three-gluon vertex, terms involving it remain subleading to the ghost-loop in the infrared. E.g., the gluon loop, which has an infrared exponent of $d/2 - 2 - 2\alpha_A$ with a tree-level three-gluon vertex, attains an infrared power law with the exponent $d/2 - 2 - \alpha_A - \alpha_G$ if the vertex is dressed. Clearly, this term is still subleading w.r.t. the ghost loop which bears an infrared exponent of $d/2 - 2 - 2\alpha_G$. In the Landau gauge, the infrared hierarchy was checked systematically by a skeleton expansion in Ref. [133].

Ghost-gluon vertex

The ghost-gluon vertex is investigated here with focus on the (off-shell) Landau gauge. The reason is that in this gauge the corresponding DSE is available from Ref. [93]. In the Coulomb gauge, with the choice $\lambda = 0$ for the wave functional $\Psi_\lambda[A]$, the derivation of the DSE should be straightforward, albeit tedious, and technically equivalent to the three-gluon vertex.

Since neither the DSE studies [93] nor the lattice calculations [98, 99, 100] show any infrared divergences, the dressing function of the ghost-gluon vertex must be some finite function. To investigate the consequences of a finite dressing function of the ghost-gluon vertex, let us assume, for simplicity, that it is given by a finite constant,

$$\Gamma_\mu(k; q, p) = C_0 \Gamma_\mu^0(q), \quad (3.73)$$

The constant C_0 can be determined by self-consistently solving the DSE for the ghost-gluon vertex in the infrared gluon limit, see section 2.6, where $\Gamma_\mu^0(q) = igq_\mu$ is the tree-level ghost-gluon vertex. Then, the infrared analysis of the propagators can be performed in the same way as above. The ghost self-energy and the ghost loop are both multiplied by the constant C_0 . After evaluation of the integrals, this constant appears on both sides of the equation

$C_0 I_G = C_0 I_A$, cf. Eq. (2.61), and thus trivially cancels. Therefore, a constant dressing of the ghost-gluon vertex is completely irrelevant for the infrared behavior of the propagators.

The question that arises is if a non-constant dressing of the ghost-gluon vertex might result in a change for the determining equation (2.61) of κ . The investigations in Ref. [93] showed that after one iteration step of the ghost-gluon vertex DSE, the vertex remains approximately tree-level over the whole momentum range, i.e. $C_0 \approx 1$. Also, the results in Ref. [93] confirmed that for vanishing incoming ghost momentum p , the ghost-vertex becomes tree-level in the Landau gauge⁷, see Eq. (2.41). Recalling the discussion in section 2.5, this is expected to hold true in the Coulomb gauge. If we discard the irrelevant component of the vertex along the gluon momentum k , $\Gamma_\mu(k; q, p)$ also becomes tree-level for vanishing outgoing ghost momentum q [97, 134], i.e.

$$\lim_{p \rightarrow 0} \Gamma_\mu(k; q, p) = \lim_{q \rightarrow 0} \Gamma_\mu(k; q, p) = \Gamma_\mu^0(q). \quad (3.74)$$

However, the infrared limits of the ghost and gluon momenta are generally not interchangeable. In particular, zero gluon momentum yields a dressing that is different from unity, although quite close to it, as we will see. The following relation shall define C ,

$$C \Gamma_\mu^0(q) \equiv \lim_{p \rightarrow 0} \left(\lim_{k \rightarrow 0} \Gamma_\mu(k; q, p) \right) \neq \lim_{k \rightarrow 0} \left(\lim_{p \rightarrow 0} \Gamma_\mu(k; q, p) \right) = \Gamma_\mu^0(q), \quad q \rightarrow 0. \quad (3.75)$$

Does $C \neq 1$ or a non-constant C affect the value for the infrared exponent κ ? To see this, it is not necessary to get involved in a numerical calculation but we can argue qualitatively instead. Consider any loop integral that involves the ghost-gluon vertex. Wherever it may appear in the loop diagram, the ghost-gluon vertex is always attached to ghost propagators. The integrand will be strongly enhanced for those loop momenta where the ghost propagator diverges, i.e. for $p \rightarrow 0$. Since the gluon propagator, on the other hand, is finite for all momenta, any infrared singularities in the integrand of the loop integral can actually be due to the ghost propagator only. The ghost-gluon vertex does not introduce any additional singularities, since its dressing function is finite. For the value of the integral, the singularities in the integrand will give the dominant contribution. The only value of the dressing function of the ghost-gluon vertex that is relevant to the integral, is then the one where any of the ghost momenta vanish. According to Eq. (3.74), the vertex is tree-level in these limits. We can therefore infer that in any loop integral the tree-level ghost-gluon vertex will yield the correct result. This circumstance can thus be traced back to the horizon condition and the transversality of the gluon propagator. In Ref. [97], infrared divergent dressing functions of the ghost-gluon vertex were employed and it was shown that κ does not vary much.

Nevertheless, the constant C , defined by Eq. (3.75) is not entirely meaningless since the introduction of a running coupling, see chapter 4 below, makes use of it. One can actually analytically calculate C by means of the DSE for the ghost-gluon vertex [93], see Fig. 3.6,

⁷This agrees with the corresponding Slavnov–Taylor identity in the Landau gauge.

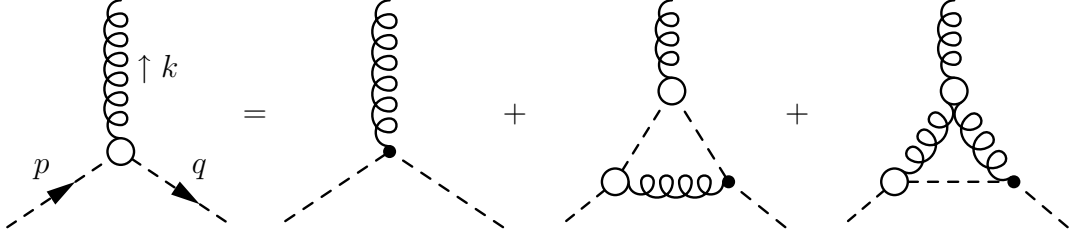


Figure 3.6: *The (truncated) Dyson–Schwinger equation for the ghost-gluon vertex.*

$$\Gamma_\mu(k; q, p) = \Gamma_\mu^0(q) + \Gamma_\mu^{(GGA)}(k; q, p) + \Gamma_\mu^{(GAA)}(k; q, p) . \quad (3.76)$$

Here, $\Gamma_\mu^{(GGA)}$ is a graph with two full ghost and one full gluon propagator in the loop,

$$\begin{aligned} \Gamma_\mu^{(GGA)}(k; q, p) = & -\frac{N_c}{2} \int \bar{d}^d \ell \Gamma_\alpha^0(-\ell) D_{\alpha\beta}(\ell - q) \Gamma_\beta(q - \ell; -p, -\ell - k) \\ & D_G(\ell + k) \Gamma_\mu(k; \ell, \ell + k) D_G(\ell) q_\alpha t_{\alpha\beta}(\ell - q) (\ell + k)_\beta \ell_\mu , \end{aligned} \quad (3.77)$$

and $\Gamma_\mu^{(GAA)}$ has two gluon and one ghost propagator in the loop, but involves a proper reduced three-gluon vertex $\Gamma_{\mu\nu\rho}$,

$$\begin{aligned} \Gamma_\mu^{(GAA)}(k; q, p) = & -\frac{N_c}{2} \int \bar{d}^d \ell \Gamma_\alpha^0(q) D_G(\ell - q) \Gamma_\beta(\ell + k; q - \ell, p) \\ & D_{\beta\rho}(\ell + k) \Gamma_{\mu\nu\rho}(k; \ell, -\ell - k) D_{\nu\alpha}(\ell) . \end{aligned} \quad (3.78)$$

Comparing Eq. (3.76) and Eq. (2.39), the four-point function $\Gamma_{\mu\nu}(k, \ell; q, p)$ used in section 2.5 can be expanded to yield the two graphs $\Gamma_\mu^{(GGA)}$ and $\Gamma_\mu^{(GAA)}$, as well as a proper four-point function omitted here. For further details, see Ref. [93].

Since $\Gamma_\mu(k; q, p)$ exists in the limit $k \rightarrow 0$ [93, 98, 99], we set $k = 0$ in the integrands which greatly simplifies the tensor structure of Eqs. (3.77) and (3.78). Furthermore, the proper ghost-gluon vertices that appear in the loop integrals are rendered tree-level, as discussed above. We then get

$$\Gamma_\mu^{(GGA)}(0; q, q) = ig^3 C \frac{N_c}{2} \int \bar{d}^d \ell \ell_\alpha D_{\alpha\beta}(\ell - q) q_\beta \ell_\mu D_G^2(\ell) , \quad (3.79)$$

and

$$\Gamma_\mu^{(GAA)}(0; q, q) = g^2 \frac{N_c}{2} \int \bar{d}^d \ell q_\alpha q_\beta D_{\alpha\nu}(\ell) D_{\beta\rho}(\ell) D_G(\ell - q) \Gamma_{\mu\nu\rho}(0; \ell, -\ell) . \quad (3.80)$$

Naively, we would expect from ghost dominance in the infrared that the contribution (3.80) is subdominant since it incorporates only one and not two ghost propagators, like (3.79). Using a

d	κ	C
3	0.398	1.089
3	$\frac{1}{2}$	1
4	0.595	1.108

 Table 3.2: Solution for the infrared dressing C of the ghost-gluon vertex.

tree-level three-gluon vertex, we can calculate both integrals for $q \rightarrow 0$ in the infrared integral approximation and indeed find that the graph (3.80) becomes negligible. If the dressed three-gluon vertex (3.71) is included, the graph (3.80) has a substantial contribution to this limit of the ghost-gluon vertex. The calculation is then somewhat more involved and deferred to appendix C, but one can extract from it the value of C solving the infrared limit of the DSE (3.76) self-consistently. For the various solutions of κ found in chapter 2.6, the numerical values of C are shown in Table 3.2.⁸

It is quite remarkable that in the Coulomb gauge with the solution $\kappa = \frac{1}{2}$, the two non-trivial graphs that appear in the DSE for the ghost-gluon vertex show an exact mutual cancellation in the infrared gluon limit,

$$\lim_{q \rightarrow 0} \lim_{k \rightarrow 0} \left(\text{Diagram 1} + \text{Diagram 2} \right) = 0 \quad , \quad (3.81)$$

so that the corrections to tree-level vanish and $C = 1$. Therefore, the interchangeability of limits is recovered in this case only and the ghost-gluon vertex becomes tree-level in all infrared limits.⁹ For other values of κ and d , the ghost-gluon vertex is not regular in the infrared. It must be granted that the omission of the four-point function in the vertex DSE spoils the argument. A skeleton expansion of the omitted object would be an interesting project. The original derivation of the Landau gauge solution for κ in Ref. [97] relied on the regularity of the ghost-gluon vertex in the infrared. Their result $\kappa = 0.595$ for $d = 4$ does not produce a regular ghost-gluon vertex though, the infrared limits are not interchangeable. As long as the omitted four-point function has no effect, this would contradict the working hypothesis of Ref. [97].

⁸Note that the results (3.2) are independent of N_c . The color trace that occurs in the loop diagrams of Eq. (3.76) yields a factor of $N_c/2$, see Eqs. (3.77) and (3.78), but it cancels with the propagator coefficient term $g^2 AB^2 = 1/(I_G N_c)$.

⁹An extension to ghost-antighost symmetric Landau gauge is straightforward and is seen not to alter the results for C .

3.6 Coulomb form factor

The success of finding a linear heavy quark potential $V_C(r \rightarrow \infty) \sim r$ in the Coulomb gauge Hamiltonian approach relies on the approximation made for the expectation value $\langle F \rangle$, see section 2.7. The Coulomb form factor $f(k)$ was defined by Eq. (3.24),

$$f(k) = \frac{\langle F \rangle(k)}{k^2 D_G^2(k)}, \quad (3.82)$$

and here we try and assess the factorization $\langle F \rangle = k^2 D_G^2(k)$, i.e. $f(k) = 1$. To this end, we employ the operator identity

$$F = \frac{\partial}{\partial g}(gG) \quad (3.83)$$

which follows easily from $g\partial G^{-1}/\partial g = G^{-1} - G_0^{-1}$. We refer to the interesting relation (3.83), first written down in Ref. [135], as the *Marrero-Swift relation*. Taking the expectation value of (3.83) in the Gaussian vacuum and neglecting contributions of $\frac{\partial \omega}{\partial g}$,

$$f(k) = -\frac{g^2}{k^2} \frac{\partial}{\partial g} \frac{1}{gD_G(k)}. \quad (3.84)$$

Plugging the ghost DSE (2.48) into Eq. (3.84), an integral equation for $f(k)$ is derived,

$$f(k) = -\frac{g^2}{k^2} \frac{\partial}{\partial g} \left(\frac{k^2}{g} - N_c k^2 \int \bar{d}^d \ell \left(1 - (\hat{\ell} \cdot \hat{k})^2 \right) D_A(\ell) (gD_G(\ell - k)) \right) \quad (3.85)$$

$$= 1 + g^2 N_c \int \bar{d}^3 \ell \left(1 - (\hat{\ell} \cdot \hat{k})^2 \right) D_A(\ell) D_G^2(\ell - k) f(\ell - k) (\ell - k)^2 \quad (3.86)$$

which agrees with the DSE (3.30) for $f(k)$ displayed above. With a power law ansatz for $f(k)$ in the infrared,

$$f(k) = \frac{C_f}{(k^2)^{\alpha_f}}, \quad k \rightarrow 0, \quad \alpha_f > 0, \quad (3.87)$$

we now aim at a solution of the Coulomb form factor DSE (3.86). For $k \rightarrow 0$, one finds

$$(k^2)^{-\alpha_f} = (k^2)^{-\alpha_f} g^2 AB^2 N_c I_f(\kappa, \alpha_f) \quad (3.88)$$

where

$$I_f(\kappa, \alpha_f) = \frac{(d-1)\kappa}{(4\pi)^{d/2}} \frac{\Gamma(\alpha_f) \Gamma(2\kappa) \Gamma(d/2 - 2\kappa - 2\alpha_f)}{\Gamma(d/2 - 2\kappa) \Gamma(d/2 - \alpha_f + 1) \Gamma(\alpha_f + 2\kappa + 1)}. \quad (3.89)$$

From Eq. (3.88) we can see that

$$g^2 AB^2 N_c I_f(\kappa, \alpha_f) = 1 \quad (3.90)$$

has to be fulfilled. The above relation from the Coulomb form factor DSE can now be plugged into the coefficient rule (2.60) from the ghost DSE to find

$$I_G(\kappa) = I_f(\kappa, \alpha_F). \quad (3.91)$$

We now specify the spatial dimension d . For $d = 3$, Eq. (3.91) yields

$$1 = \frac{(-1 + 2\kappa) \cos(\pi(\alpha_f + 2\kappa)) \Gamma(4 - 2\alpha_f) \Gamma(-2\kappa) \Gamma(1 + 2\alpha_f + 4\kappa) \sin(\pi\alpha_f)}{\pi(-1 + \alpha_f)(3 + 2\kappa)(-1 + 2\alpha_f + 4\kappa) \Gamma(2 + 2\kappa)}. \quad (3.92)$$

The numerical solution to this equation gives κ as a function of α_f , as shown in Fig. 3.7. One can see immediately that for any value of α_f , the ghost exponent κ yields

$$\kappa < \frac{1}{4}. \quad (3.93)$$

Therefore, recalling the results for κ in Table 2.1, there exists no value of α_f for which all three DSEs are satisfied.

It is instructive to focus on the case where

$$\alpha_f + 2\kappa = 1 \quad (3.94)$$

since this leads directly to a linearly rising potential for static quarks. Plugging this constraint into Eq. (3.92), we find

$$1 = \frac{-2\kappa(3 + 2\kappa) \cos(2\pi\kappa) \Gamma(-1 - 4\kappa) \Gamma(1 + 2\kappa)}{(-1 + 2\kappa) \Gamma(-1 - 2\kappa)} \quad (3.95)$$

which has the numerical solution $\kappa = 0.245227$. Surprisingly, this result is exactly agreed upon by lattice calculations [128], where $\kappa = 0.245(5)$ was found. However, one should notice that the lattice calculations carried out so far in Coulomb gauge and also in Landau gauge use too small lattices to give reliable results in the infrared.

In $2 + 1$ dimensional Coulomb gauge, the calculations are equivalent. From a simultaneous treatment of the ghost DSE and the gluon DSE we find from the stochastic vacuum results in section 2.6 a unique solution for the ghost exponent [102],

$$\kappa = \frac{1}{5}. \quad (3.96)$$

Note that with angular approximation the result is $\kappa = 1/4$. In a recent publication [132], the value (3.96) for κ was confirmed numerically. On the other hand, if we consider only the ghost DSE and the equation for the Coulomb form factor for $d = 2$, one gets by enforcement of the condition Eq. (3.91):

$$\frac{\Gamma(\alpha_f) \Gamma(1 - \alpha_f - 2\kappa) \Gamma(\kappa) \Gamma(2 + \kappa)}{\Gamma(2 - \alpha_f) \Gamma(-\kappa)^2 \Gamma(1 + \alpha_f + 2\kappa)} = 1. \quad (3.97)$$

The numerical solution is shown in Fig. 3.8. If we require the potential to be linearly rising, the solution has to obey $\alpha_f + 2\kappa = \frac{1}{2}$. Eq. (3.97) then leads to the numerical value of $\kappa = 0.138$. Lattice results do not agree with this value [136], although they do for $3 + 1$ dimensions.

It is interesting to note that, leaving the DSE for ω aside, a restriction on the infrared exponents (3.93) arises from self-consistency of the equations for d and f only. This restriction also

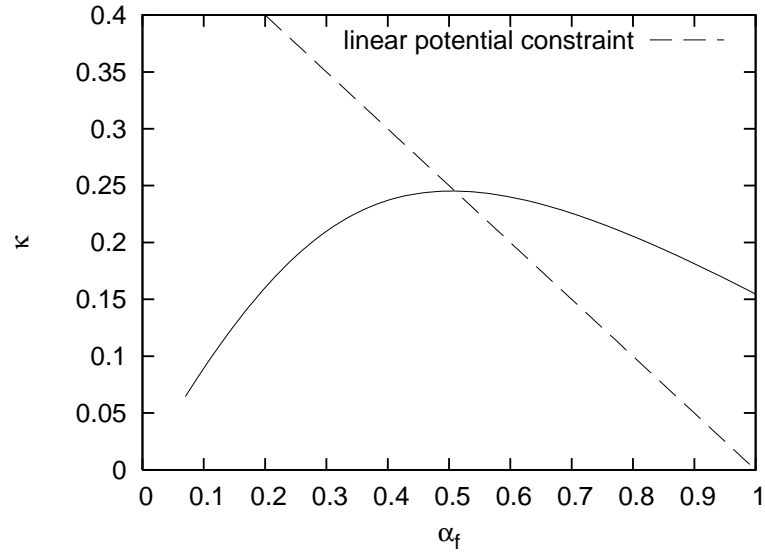


Figure 3.7: The ghost exponent κ as a function of α_f is shown by a solid line for 3 + 1 dimensions. A dashed line indicates the values for which a linear potential will arise.

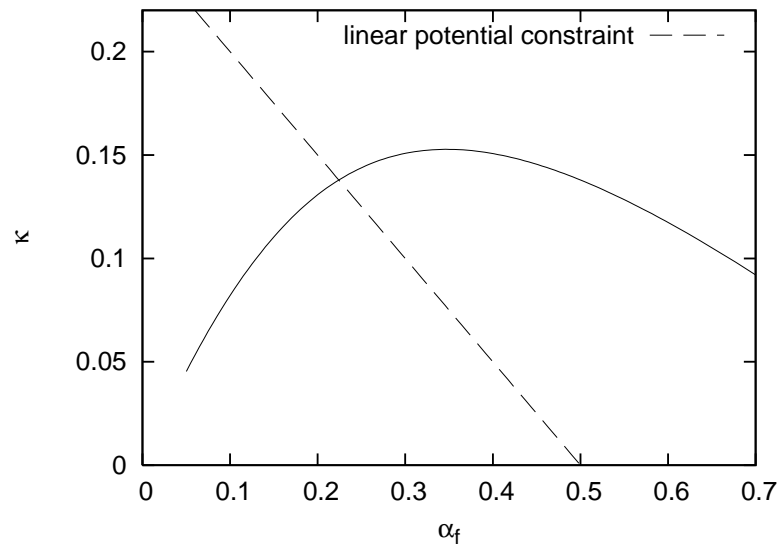


Figure 3.8: Same as Fig. 3.7, here in 2 + 1 dimensions.

concerns the infrared behavior of ω via the sum rule (2.54). Consider a fixed wave functional with a kernel ω that yields $\kappa > \frac{1}{4}$ by its infrared behavior. In principle, it should be possible to calculate d and f for such a wave functional. However, due to the restriction (3.93), no solution can be found. We therefore conclude that the Eq. (3.93) must be due to the approximations made in the DSEs for d and f . The relaxation of the horizon condition allows for a self-consistent solution of all DSEs where $\omega(k)$, $\chi(k)$, $f(k)$ and $d(k)$ are infrared finite. This will be shown in section 3.7. However, we consider the infrared enhancement, of $d(k)$ in particular, as the driving mechanism in the Gribov–Zwanziger confinement scenario. Therefore, we infer from the above discussion that the DSE for $f(k)$, as it stands in Eq. (3.86), along with the resulting restriction (3.93) on κ , must be ignored.

Let us reconsider the Marrero-Swift relation (3.83) with focus on the neglect of $\frac{\partial\omega}{\partial g}$. In the infrared limit, the ghost propagator becomes independent of the gauge coupling g , as seen in the stochastic vacuum,

$$\begin{aligned} \frac{\partial}{\partial g} \langle G \rangle &= \frac{\partial}{\partial g} \frac{\int \mathcal{D}A G[gA] \text{Det } G^{-1}[gA]}{\int \mathcal{D}A \text{Det } G^{-1}[gA]} \\ &= \frac{\partial}{\partial g} \frac{\int \mathcal{D}A' G[A'] \text{Det } G^{-1}[A']}{\int \mathcal{D}A' \text{Det } G^{-1}[A']} = 0, \end{aligned} \quad (3.98)$$

where in Eq. (3.98) the notation reads $G^{-1}[gA] = -\partial^2 - g\hat{A}\partial$. Using the above relation and taking a derivative $\partial/\partial g$ of the ghost DSE (2.48) yields

$$0 = -N_c k^2 \int \vec{d}^3\ell \left(1 - (\hat{\ell} \cdot \hat{k})^2\right) D_G(\ell - k) \frac{\partial}{\partial g} (g^2 D_A(\ell)) \neq 0. \quad (3.99)$$

Neglecting $\frac{\partial D_A}{\partial g}$, one must run into contradictions. In the expectation value of the Marrero-Swift relation (3.83), the neglected terms can be carried along for the stochastic vacuum to give

$$\begin{aligned} \frac{\partial}{\partial g} \langle gG \rangle &= \frac{\partial}{\partial g} \frac{\int \mathcal{D}A gG[A] \mathcal{J}[A]}{\int \mathcal{D}A \mathcal{J}[A]} \\ &= \frac{\int \mathcal{D}A \mathcal{J}[A] \frac{\partial}{\partial g} (gG)}{\int \mathcal{D}A \mathcal{J}[A]} + \frac{\int \mathcal{D}A \mathcal{J}[A] \frac{\partial \ln \mathcal{J}}{\partial g} gG}{\int \mathcal{D}A \mathcal{J}[A]} - \frac{\int \mathcal{D}A \mathcal{J}[A] gG}{\int \mathcal{D}A \mathcal{J}[A]} \frac{\int \mathcal{D}A \mathcal{J}[A] \frac{\partial \ln \mathcal{J}}{\partial g}}{\int \mathcal{D}A \mathcal{J}[A]} \\ &= \langle F \rangle + \left\langle gG \frac{\partial \ln \mathcal{J}}{\partial g} \right\rangle - \langle gG \rangle \left\langle \frac{\partial \ln \mathcal{J}}{\partial g} \right\rangle. \end{aligned} \quad (3.100)$$

There are two extra terms that were omitted in Eq. (3.84), having the mathematical structure of a *covariance*. This covariance also occurs in the Gaussian vacuum. Since with Eq. (3.98) we have $\frac{\partial}{\partial g} \langle gG \rangle = \langle G \rangle$, the covariance cancels the Coulomb propagator $\langle F \rangle$ on the r.h.s. of Eq. (3.100) in favor of a ghost propagator $\langle G \rangle$,

$$\langle F \rangle + \left\langle \frac{\partial \ln \mathcal{J}}{\partial g} gG \right\rangle - \langle gG \rangle \left\langle \frac{\partial \ln \mathcal{J}}{\partial g} \right\rangle = \langle G \rangle. \quad (3.101)$$

The derivation of the Coulomb form factor DSE (3.86) would therefore fail if the approximation $\frac{\partial\omega}{\partial g} \approx 0$ was relaxed. This does not mean that the DSE (3.86) is wrong within the chosen

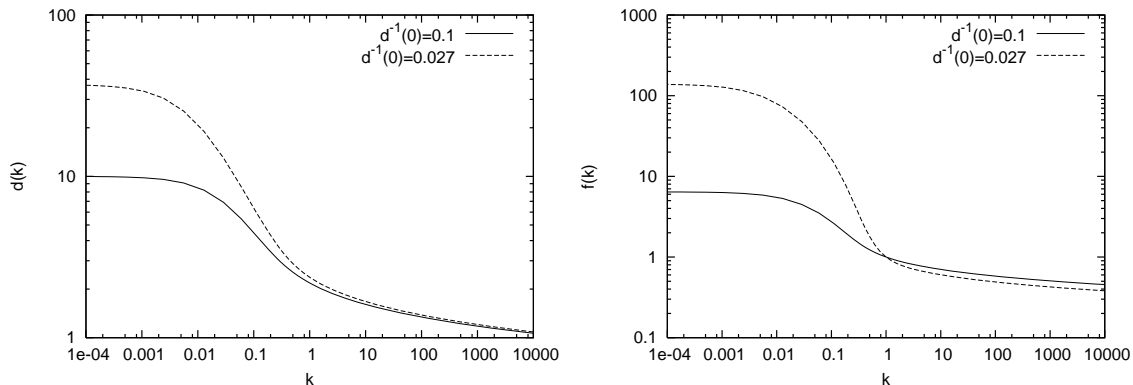


Figure 3.9: *Left: The subcritical ghost form factor $d(k)$. Right: The Coulomb form factor $f(k)$. Calculated by D. Epple in Ref. [120].*

approximation scheme. Applying Wick's theorem to derive an integral equation for $f(k)$ in the one-loop approximation also leads to Eq. (3.86). However, the above considerations do show that, for the asymptotic infrared, the DSE (3.86) for $f(k)$ describes a higher-order effect. On the level of approximations used, we find from Eqs. (3.84) and (3.98) that

$$f(k) = \frac{1}{k^2 D_G^2(k)} \frac{\partial}{\partial g} (g D_G) \xrightarrow{k \rightarrow 0} \frac{1}{k^2 D_G(k)} \equiv \frac{1}{d(k)}. \quad (3.102)$$

Plugging this into the Coulomb form factor DSE (3.30) yields

$$d^{-1}(k) = 1 + g^2 \frac{N_c}{2} \int \bar{d}^3 \ell \left(1 - (\hat{\ell} \cdot \hat{k})^2 \right) \frac{d(\ell - k)}{(\ell - k)^2 \omega(\ell)}, \quad k \rightarrow 0 \quad (3.103)$$

which explicitly contradicts the ghost DSE (3.29), note the plus sign. This contradiction is the analogon of Eq. (3.99) for $\frac{\partial D_A}{\partial g} = 0$.

In conclusion, the quality of the approximation scheme must be improved in order to satisfy the DSE for the Coulomb form factor. Vertex corrections, which effectively increment the loop order, would be an interesting starting point in that direction.

3.7 Subcritical solutions

Although it was argued above that in the chosen approximation scheme, the DSE (3.86) for the Coulomb form factor $f(k)$ should be ignored, we here relax the horizon condition to still find a solution to all DSEs. The renormalization parameter $d_0^{-1} := d^{-1}(\mu_d = 0)$ distinguishes the subcritical solutions for $d_0^{-1} > 0$ and the critical ones for $d_0^{-1} = 0$. The subcritical form factors $d(k)$ and $f(k)$, the gap function $\omega(k)$, and the curvature $\chi(k)$ are all infrared finite functions, as the numerical calculation shows [120]. In Fig. 3.9, the functions $d(k)$ and $f(k)$ are shown for $d_0^{-1} = 0.1$ and $d_0^{-1} = 0.027$. The functions $\omega(k)$ and $\chi(k)$ are shown in a common plot in Fig. 3.10, for several values of d_0^{-1} . These functions solve their respective DSEs self-consistently.

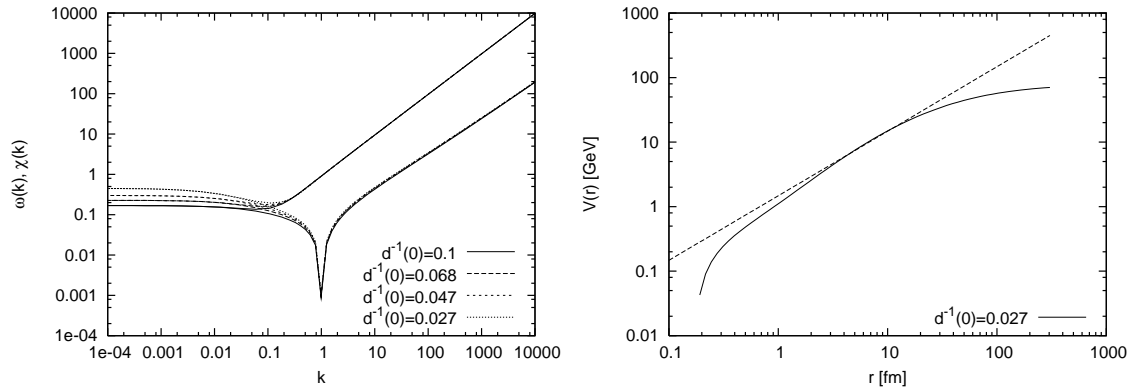


Figure 3.10: *Left: The gluon energy $\omega(k)$ and the modulus of the scalar curvature, $|\chi(k)|$, in the subcritical case. Note that $\chi(k)$ changes sign at $k = 1$. Internal units are used. Right: The heavy quark potential $V_C(r)$ for the subcritical solutions and a linear fit for the intermediate regime. Calculated by D. Epple in Ref. [120].*

The DSE (3.86) for $f(k)$ is solved as well for subcritical d_0^{-1} . Lowering the value of d_0^{-1} , the solutions are seen to break down. The smallest possible value for which all DSEs are solved self-consistently with positive $d(k)$ and $f(k)$ was found to be $d_0^{-1} \approx 0.02$. In the numerical calculations, the other renormalization parameters were chosen such that $\chi(\mu = 1) = 0$ and $f(\mu = 1) = 1$. With the subcritical solutions so obtained, one may calculate the heavy quark potential $V_C(r)$, as shown in Fig. 3.10. For intermediate quark separation r , the potential $V_C(r)$ is approximately linear; fitting the slope to the lattice string tension, r is found to be in the range of hadronic phenomenology. However, for $r \rightarrow \infty$, the heavy quark potential becomes questionable since permanent confinement is lost for the subcritical solutions. In addition, the running coupling $\alpha(k)$ *vanishes* in the infrared, as seen in the forthcoming chapter. Altogether, the implications of the subcritical solutions for the infrared physics are not compatible with Coulomb confinement. This indicates that the horizon condition must not be abandoned. Despite the inconsistency in the DSE for $f(k)$, which is due to higher-order effects, we favor the solutions with critical $d_0^{-1} = 0$, i.e. with the horizon condition implemented where the functions $\omega(k)$, $\chi(k)$ and $d(k)$ are infrared enhanced.

4 Running coupling and ultraviolet behavior

A quantitatively correct treatment of QCD, with the possibility to describe phenomenological effects, needs to take into account accurately its scale Λ_{QCD} . In the absence of flavor charges, $N_f = 0$, this is the only scale of the theory. The value of Λ_{QCD} can be related to the perturbative expansion of the (Gell–Mann–Low) beta function,

$$\beta(g) = \frac{\partial g(\mu)}{\partial \ln \mu} = -\beta_0 g^3 - \beta_1 g^5 - \beta_2 g^7 + \mathcal{O}(g^9) \quad (4.1)$$

that describes the dependence of the renormalized gauge coupling g on the renormalization scale μ . Solving the differential equation (4.1) with neglect of $\mathcal{O}(g^5)$, the gauge coupling is seen to diverge at the scale

$$\Lambda_{QCD} = \mu \exp\left(-\frac{1}{2\beta_0 g^2(\mu)}\right). \quad (4.2)$$

This breakdown of perturbation theory occurs at a finite Λ_{QCD} , if $g^2(\mu) > 0$, giving rise to dimensional transmutation of the dimensionless gauge coupling to the dimensionful energy scale Λ_{QCD} . The $\mathcal{O}(g^3)$ coefficient of the beta function (4.1), β_0 , is a gauge invariant quantity that is calculated in perturbation theory to be

$$\beta_0 = \frac{1}{(4\pi)^2} \frac{11N_c}{3}. \quad (4.3)$$

Higher order coefficients of the beta function were obtained in cumbersome calculations [137, 138] and serve for an improved matching of Λ_{QCD} to experiment.

High-energy experiments are able to provide us with the scale Λ_{QCD} immanent in QCD.¹ A physical process that involves measurable quantities, e.g. the mass of the Z boson, needs to be described by theoretical calculations which are then compared to the experimental data. The corresponding scattering matrix is computed by means of perturbative QCD, preferably in a covariant gauge, in a certain chosen renormalization scheme. As a result, the running coupling

$$\alpha(k) = \frac{g^2(k)}{4\pi} \quad (4.4)$$

can be extracted for the momentum k of the given process. For the mass $M_Z = 91.19 \text{ GeV}$ of the Z boson, it is found that $\alpha(M_Z) = 0.1187$ in the \overline{MS} scheme and by the extrapolation of the perturbative $\alpha(k)$ into the infrared,²

$$\alpha(\mu) = \frac{4\pi}{\bar{\beta}_0 \ln(\mu^2/\Lambda_{QCD}^2)} \left[1 - \frac{2\bar{\beta}_1}{\bar{\beta}_0^2} \frac{\ln[\ln(\mu^2/\Lambda_{QCD}^2)]}{\ln(\mu^2/\Lambda_{QCD}^2)} + \frac{4\bar{\beta}_1^2}{\bar{\beta}_0^4 \ln^2(\mu^2/\Lambda_{QCD}^2)} \right. \\ \left. \times \left(\left(\ln[\ln(\mu^2/\Lambda_{QCD}^2)] - \frac{1}{2} \right)^2 + \frac{\bar{\beta}_0 \bar{\beta}_2}{8\bar{\beta}_1^2} - \frac{5}{4} \right) \right], \quad (4.5)$$

¹Estimates can also be obtained directly by lattice simulations [139].

²Various conventions exist for the definition of the β function and its coefficients of the perturbative expansion. The barred symbols in Eq. (4.5) are related to those of Eq. (4.1) by $\beta_0 = \frac{\bar{\beta}_0}{(4\pi)^2}$, $\beta_1 = \frac{2\bar{\beta}_1}{(4\pi)^4}$ and $\beta_2 = \frac{\bar{\beta}_2}{2(4\pi)^6}$.

one finds $\Lambda_{\overline{MS}} = 217 \text{ MeV}$ [140]. They do, however, depend on the renormalization prescription, hence the subscript on $\Lambda_{\overline{MS}}$, as an artefact of perturbation theory. A change in the renormalization prescription can in fact be compensated for by a finite renormalization group transformation. It is the truncation of the perturbative series that makes the running coupling scheme dependent [141].

The variational solutions presented in the previous chapter only loosely account for the ultraviolet properties of the theory and it will be shown that the β function turns out to be slightly incorrect. The first few coefficients of the beta function, in particular β_0 , record inaccuracies of the solutions and any observable is immensely sensitive to such errors, as can be seen directly in Eq. (4.2). If the nonperturbative variational solutions are to give quantitatively sensible results, they have to reproduce β_0 with high accuracy. In this chapter, we first recall the crucial properties of the YM coupling constant and then define a nonperturbative running coupling to come by some information on how the Green functions are to behave in the ultraviolet.

4.1 Anti-screening of color charges

An effect specific to the non-abelian nature of YM theory is the *anti-screening* of color charges. The interaction of two color charges on a short distance can be treated by perturbation theory. The perturbative corrections increase the magnitude of the (renormalized) color charges, i.e. the potential is “anti-screened”, contrary to the abelian theory. Anti-screening is a crucial property of YM theory and intimately connected to asymptotic freedom.

One may find the potential between two color charges by setting up a basis of states $\{|n\rangle\}$ in the absence of external charges, then turning on ρ_{ext} , that is $\rho = \rho_{\text{dyn}} \rightarrow \rho_{\text{dyn}} + \rho_{\text{ext}}$, and calculating the correction to the potential energy E_C to second order in ρ_{ext} ,³

$$\begin{aligned}
 E_C = & \overbrace{\frac{g_B^2}{2} \int d^3[xy] \langle 0 | \rho_{\text{ext}}^a(x) F^{ab}(x, y) \rho_{\text{ext}}^b(y) | 0 \rangle}^{=: E_C^{(+)}} + \\
 & \underbrace{-\frac{g_B^2}{2} \int d^3[xy] \sum_n \frac{|\langle 0 | \rho_{\text{ext}}^a(x) F^{ab}(x, y) \rho_{\text{dyn}}^b(y) | n \rangle|^2}{E_n}}_{=: E_C^{(-)}}. \quad (4.6)
 \end{aligned}$$

The screening vacuum polarization is of course still present as the manifestly negative contribution $E_C^{(-)}$ in (4.6). Its calculation in a perturbative expansion in the bare gauge coupling g_B to order $\mathcal{O}(g_B^4)$ is familiar from the vacuum polarization in the abelian theory [2]. To let two point-like charges, $\rho_{\text{ext}}^a(x)$ as in (2.72), approach each other from an infinite separation to r , the energy $E_C|_{\infty} - E_C|r = \int \bar{d}^3 k V_C(k) e^{ik \cdot r}$ is needed. The momentum space potential

³The Faddeev-Popov determinants \mathcal{J} are omitted since they do not contribute in the lowest-order perturbation in g_B .

$$V_C(k) = \left| \text{---} \right| + \left| \text{---} \overset{\text{loop}}{\curvearrowright} \text{---} \right| - \left| \text{---} \text{loop} \text{---} \right|$$

Figure 4.1: *Perturbative screening and anti-screening contributions to the color Coulomb potential. The first graph represents the usual Coulomb interaction, the second graph shows the genuinely nonabelian anti-screening contribution and the last graph corresponds to the usual screening term. These graphs are not Feynman diagrams.*

$V_C(k) = V_C^{(+)}(k) + V_C^{(-)}(k)$ comprises the screening contribution

$$V_C^{(-)}(k) \approx \frac{g_B^2}{k^2} \left(-\frac{g_B^2}{(4\pi)^2} \frac{C_2}{3} \ln \frac{\Lambda^2}{k^2} \right), \quad (4.7)$$

where the cut-off Λ regularizes the UV divergence and the quadratic Casimir yields here for $SU(N_c)$ the value $C_2 = N_c$. The screening effect is, however, over-compensated by the contribution $V_C^{(+)}(k)$. To see that, expand the non-abelian Coulomb operator around its abelian part,

$$F^{ab}(x, y) = \left(G_0 + 2 G_0 g_B \hat{A} \partial G_0 + 3 G_0 g_B \hat{A} \partial G_0 g_B \hat{A} \partial G_0 + \mathcal{O}(g_B^3) \right)^{ab} (x, y), \quad (4.8)$$

and then take the expectation value, see e.g. Ref. [142], where the third term in (4.8) strengthens the potential,

$$V_C^{(+)}(k) = \frac{g_B^2}{k^2} \left(1 + \frac{g_B^2}{(4\pi)^2} \frac{12C_2}{3} \ln \frac{\Lambda^2}{k^2} \right). \quad (4.9)$$

Note that in the abelian theory only the first term in the perturbative expansion (4.8) exists, and thus $V_C^{(+)}(k) = g_B^2/k^2$. The anti-screening correction in Eq. (4.9) is genuinely non-abelian. In Fig. 4.1, the neatly separated screening and anti-screening contributions are shown diagrammatically. The net effect of the $\mathcal{O}(g^4)$ contributions increases the potential between static $SU(N_c)$ color charges,

$$V_C(k) = \frac{g_B^2}{k^2} \left(1 + \frac{g_B^2}{(4\pi)^2} \frac{11N_c}{3} \ln \frac{\Lambda^2}{k^2} \right) \quad (4.10)$$

as first demonstrated by Khriplovich for $N_c = 2$ [58]. The net anti-screening correction to the static quark potential can be used to define the renormalized coupling $g(\mu)$, with the ambiguity in subtracting the divergence inherent in the renormalization scale μ . From the so-defined $g(\mu)$, the β function may be calculated via Eq. (4.1), reproducing its Nobel-prize awarded perturbative expansion (with the interpretation of asymptotic freedom [143, 144]), as shown in Refs. [62, 145].

If we wish to extract correctly from the color Coulomb potential the β function for the variational solutions of chapter 3, the form factors are to behave appropriately in the ultraviolet.

What exactly “appropriately” means will become clear in the course of this chapter. For starters, consider the Coulomb potential

$$V_C^{(var)}(k) = \frac{g_B^2}{k^2} d^2(k) f(k) \quad (4.11)$$

as the part of the energy in the variational state that depends on the separation of the charges, see Eq. (2.74). The self-energies, which only regulate infrared divergences, are omitted. To lowest order in the bare gauge coupling g_B , $d(k) = f(k) = 1$. The $\mathcal{O}(g_B^4)$ term of Eq. (4.11) can be found by expanding the DSEs for d (3.29) and for f (3.30) up to $\mathcal{O}(g_B^2)$, using the lowest-order expression $\omega(k) = k$,

$$d(k) = 1 + g_B^2 \frac{N_c}{2} \int \bar{d}^3 \ell \left(1 - (\hat{\ell} \cdot \hat{k})^2 \right) \frac{1}{\ell(\ell - k)^2} \quad (4.12)$$

$$f(k) = 1 + g_B^2 \frac{N_c}{2} \int \bar{d}^3 \ell \left(1 - (\hat{\ell} \cdot \hat{k})^2 \right) \frac{1}{\ell(\ell - k)^2} \quad (4.13)$$

Note that $d(k)$ and $f(k)$ have the identical perturbative $\mathcal{O}(g_B^2)$ expansion. Plugging these into Eq. (4.11), yields three times the same $\mathcal{O}(g_B^4)$ term,

$$V_C^{(var)}(k) = \frac{g_B^2}{k^2} \left(1 + 3 \cdot g_B^2 \frac{N_c}{2} \int \bar{d}^3 \ell \left(1 - (\hat{\ell} \cdot \hat{k})^2 \right) \frac{1}{\ell(\ell - k)^2} \right) + \mathcal{O}(g_B^6), \quad (4.14)$$

cf. the factor of 3 in the expansion of the non-abelian Coulomb operator (4.8). Regularized by a UV cut-off Λ , the integral in Eq. (4.14) to $\mathcal{O}(g_B^4)$ gives

$$V_C^{(var)}(k) = \frac{g_B^2}{k^2} \left(1 + \frac{g_B^2}{(4\pi)^2} \frac{12N_c}{3} \ln \frac{\Lambda^2}{k^2} \right), \quad (4.15)$$

in agreement with Eq. (4.9). Note, however, that only the anti-screening contribution $V_C^{(+)}(k)$ is thus accounted for. Determining the state $|\Psi\rangle$ by the variational principle in the absence of color charges and deriving the color Coulomb potential $V_C(r)$ as a perturbation around the vacuum, necessitates that the screening contribution $V_C^{(-)}(k)$ is carried along in the full second-order perturbative expression as in Eq. (4.6).

The renormalized coupling g is defined so as to render the expression for $V_C(k)$ finite, order by order in perturbation theory. Decomposing an infinite quantity into a finite and an infinite part always leaves an ambiguity that is controlled by the renormalization scale μ . Using

$$g_B(\Lambda) = Z_g(\Lambda, \mu) g(\mu) \quad (4.16)$$

as the definition of the renormalized, μ -dependent $g(\mu)$, the expression $V_C^{(var)}(k)$ in Eq. (4.15) turns out finite up to $\mathcal{O}(g^4)$ if the renormalization constant is chosen as⁴

$$Z_g(\Lambda, \mu) = 1 - \frac{1}{2} \frac{g_B^2}{(4\pi)^2} \frac{12N_c}{3} \ln \frac{\Lambda^2}{\mu^2}. \quad (4.17)$$

⁴Swapping g_B for g does not matter to the order considered.

The β function, as defined by Eq. (4.1), can now be calculated from Eqs. (4.16) and (4.17) to lowest order,

$$\beta(g) = -\frac{g^3}{(4\pi)^2} \frac{12N_c}{3}. \quad (4.18)$$

This result does not agree with the canonical value of β_0 , see Eq. (4.3), but it is clear why: only the contributions of longitudinal gluons were considered to order $\mathcal{O}(g^4)$, the screening contribution from transversal gluons was omitted. For the same reason, the perturbative renormalization group calculation of the color Coulomb potential [146] relates $V_C(k)$ to the running coupling $g^2(k)$ by $k^2 V_C(k) = x_0 g^2(k)$ with $x_0 = \frac{12}{11}$. In the next sections, we aim to use a nonperturbative definition of the running coupling.

4.2 Nonperturbative running coupling

Since the variational Coulomb gauge solution from chapter 3 is nonperturbative, we seek here a nonperturbative definition of the running coupling in order to match $\alpha(M_Z) = 0.1187$ to our solutions. In the Coulomb gauge, there are two possibilities for its definition, either via the color Coulomb potential, or by means of the ghost-gluon vertex [101]. The nonrenormalization of the ghost-gluon vertex has proven above to be a useful common property of both the Coulomb and Landau gauge. Here, it is first discussed how the Landau gauge ghost-gluon vertex may define a nonperturbative running coupling and afterwards we turn to the Coulomb gauge.

Landau gauge running coupling from ghost-gluon vertex

The local off-shell formulation of Landau gauge YM theory allows for multiplicative renormalization of the fields by the introduction of renormalization constants $Z(\Lambda, \mu)$. Some of these are related to one another by the fact that Z_g , the renormalization constant of the gauge coupling, can be defined by any of the interaction terms in the YM Lagrangian, namely the ghost-gluon vertex, the quark-gluon vertex, the three- and the four-gluon vertex. The equality of the gauge coupling for all these interactions is expressed by the Slavnov–Taylor identity

$$\frac{Z_1}{Z_3} = \frac{\tilde{Z}_1}{\tilde{Z}_3} \quad (4.19)$$

where $Z_1 = Z_g Z_3^{3/2}$ is the renormalization constant of the three-gluon vertex, $\tilde{Z}_1 = Z_g \tilde{Z}_3 Z_3^{1/2}$ the one of the ghost-gluon vertex, while Z_3 and \tilde{Z}_3 renormalize gluon and ghost fields,

$$A_B = Z_3^{1/2} A, \quad c_B = \tilde{Z}_3^{1/2} c, \quad \bar{c}_B = \tilde{Z}_3^{1/2} \bar{c}. \quad (4.20)$$

An unambiguous definition of the Z 's requires renormalization prescriptions. We define the theory at the scale μ by setting

$$D_A(k = \mu; \mu) = \frac{C_A}{k^2}, \quad D_G(k = \mu; \mu) = \frac{C_G}{k^2}. \quad (4.21)$$

The nonrenormalization of the ghost-gluon vertex in Landau gauge infers that \tilde{Z}_1 is a finite number, independent of μ . Therefore the quantity

$$g_B^2(\Lambda)D_{A,B}(k;\Lambda)D_{G,B}^2(k;\Lambda) = \tilde{Z}_1^2 g^2(\mu)D_A(k;\mu)D_G^2(k;\mu) \quad (4.22)$$

is finite, due to $\tilde{Z}_1 < \infty$, and μ -independent, since the l.h.s. is μ -independent. One may set $\tilde{Z}_1 = 1$ but any other finite number will also do in an appropriate renormalization prescription, recall section 2.5. It is left arbitrary here. In the perturbative momentum subtraction scheme, the values $C_A = C_G = 1$ define the renormalized quantities on the r.h.s. of Eq. (4.22). Nonperturbative Green functions might not allow for such a simple subtraction scheme. We therefore generalize it [53] by setting

$$C_A C_G^2 = 1. \quad (4.23)$$

Other schemes can be accomplished by performing a finite renormalization, see below.

In Eq. (4.22), one may choose μ freely. Leaving μ once unspecified and setting it once to $\mu = k$ leads with (4.21) to a nonperturbative definition of the running coupling [53],

$$g^2(k) = k^6 g^2(\mu)D_A(k;\mu)D_G^2(k;\mu). \quad (4.24)$$

While the factors on the r.h.s. are μ -dependent, the running coupling $g^2(k)$ on the l.h.s. is renormalization scale- and scheme independent. Note that the finite value \tilde{Z}_1 drops out. Applying a finite renormalization such as $A \rightarrow z_3^{1/2}A$, $c \rightarrow \tilde{z}_3^{1/2}c$ in order to discuss the case $C_A C_G^2 \neq 1$, the running coupling can be expressed by the transformed quantities,

$$g^2(k) = \tilde{Z}_1^2 k^6 g^2(\mu)D_A(k;\mu)D_G^2(k;\mu). \quad (4.25)$$

where we have set $\tilde{Z}_1^2 z_3 \tilde{z}_3^2 \rightarrow \tilde{Z}_1^2$. Note that these simple scalings are not renormalization group transformations in the usual sense since they do not depend on the scale μ . It will be shown explicitly below that the (asymptotic) behavior of the running coupling is ignorant to such scalings.

A different point of view is frequently found in the literature, see e.g. Ref. [124]. One may always absorb finite transformations by a transformation in g such that $\tilde{Z}_1^2 = Z_g^2 Z_3 \tilde{Z}_3^2$ is left unchanged (usually chosen to be unity). The running coupling (4.24) then stays form-invariant. Here, we prefer to leave g unchanged and allow for a change in \tilde{Z}_1 and use Eq. (4.25) as the running coupling.

Coulomb gauge running coupling from ghost-gluon vertex

A running coupling in Coulomb gauge may be defined in analogy to the Landau gauge from the ghost-gluon vertex. The multiplicative renormalization, however, is not as well-understood in the Coulomb gauge. From within a class of interpolating gauges where multiplicative renormalization was discussed in Ref. [147], the Coulomb gauge limit may be taken, breaking the

path for a definition similar to Eq. (4.25) in the Landau gauge [101]. We adopt this definition here.

Using the notation $d(k)$ for the ghost form factor (3.23) and $\omega(k)$ for the equal-time gluon propagator (3.5), both renormalized multiplicatively,

$$d_B(k; \Lambda) = \tilde{Z}_3(\Lambda, \mu) d(k; \mu), \quad \omega_B(k, \Lambda) = Z_3(\Lambda, \mu) \omega(k; \mu) \quad (4.26)$$

$$d(k = \mu; \mu) = C_d, \quad \omega(k = \mu; \mu) = C_\omega k, \quad (4.27)$$

with $C_\omega^{-1} C_d^2 = 1$, we find from the ghost-gluon vertex analogously to Eq. (4.22),

$$g_B^2(\Lambda) d_B^2(k; \Lambda) \frac{1}{2} \omega_B^{-1}(k; \Lambda) = \tilde{Z}_1^2 g^2(\mu) d^2(k; \mu) \frac{1}{2} \omega^{-1}(k; \mu). \quad (4.28)$$

Allowing for a change in the renormalization prescription, $C_\omega^{-1} C_d^2 \neq 1$, one may either absorb it by a change in g , or (as above) redefine \tilde{Z}_1 . Accordingly to (4.25), the latter choice leads directly to the running coupling

$$g^2(k) = \tilde{Z}_1^2 k g^2(\mu) d^2(k, \mu) \omega^{-1}(k, \mu) \quad (4.29)$$

Note that k is here $k = |\mathbf{k}|$ and all interactions are instantaneous.⁵ The running coupling (4.29) was given in Ref. [101] with a prefactor of $\frac{8}{3}$, chosen as to recover the Landau gauge infrared limit from within the interpolating gauge. According to the discussion above, this factor needs to be interpreted as $\tilde{Z}_1^2 = \frac{8}{3}$.

Coulomb gauge running coupling from the color Coulomb potential

Another renormalization group invariant that qualifies to define a nonperturbative running coupling is the instantaneous color Coulomb potential $V_C(k)$. It was shown in Ref. [72] that the product gA_0 is a renormalization group invariant and in Ref. [146] how the quantity $\langle g^2 A_0 A_0 \rangle$ actually relates to $V_C(k)$. We may accordingly define the running coupling in Coulomb gauge also by

$$g^2(k) = \frac{11}{12} g^2(\mu) k^2 V_C(k; \mu), \quad k = |\mathbf{k}|. \quad (4.30)$$

The factor of $\frac{11}{12}$ accounts for the fact that $V_C(k)$ only comprises the anti-screening contribution and over-emphasizes this effect. While in the ultraviolet the definition (4.30) is expected to agree with the definition (4.29) of the running coupling from the ghost-gluon vertex, the infrared behavior turns out to disagree drastically. In view of the confining long-range part of $V_C(k)$, the running coupling in Eq. (4.30) diverges for $k \rightarrow 0$, a clear instance of infrared slavery. On the other hand, the definition (4.29) will yield a running coupling that freezes in the infrared, see below.

⁵For equal times, the tree-level gluon propagator is $D_A^0(k) = \frac{1}{2k}$, see Eq. (3.31). Therefore, the definition (4.29) is larger than in Landau gauge (4.25) by a factor of 2.

4.3 Ultraviolet behavior of Green functions

Given relations that express the running coupling in terms of the Green functions nonperturbatively, one may extract information on these Green functions in the UV domain, where the running coupling is known from perturbation theory. Solving the $\mathcal{O}(g^3)$ expansion of the β function (4.1) as a differential equation for $g^2(k)$ yields for large $k^2 = k_\mu k^\mu$

$$g^2(k) = \frac{1}{\beta_0 \ln \frac{k^2}{\Lambda_{QCD}^2}}. \quad (4.31)$$

The ultraviolet behavior of the nonperturbative propagators has to be such that the nonperturbative running couplings defined in section 4.2 approach the function (4.31). Further information can be extracted by solving the ghost Dyson–Schwinger equation self-consistently with an ansatz for the ultraviolet behavior. This ansatz requires an educated guess.

Despite asymptotic freedom, the Green functions do not asymptotically become tree-level in the ultraviolet. Weinberg’s theorem states that there can be logarithmic corrections [148], and an ansatz for the gluon and ghost propagators for $k \gg \mu$ might therefore read

$$D_A(k) \sim \frac{1}{k^2 \ln^\gamma \left(\frac{k^2}{\mu^2} \right)} \quad (4.32a)$$

$$D_G(k) \sim \frac{1}{k^2 \ln^\delta \left(\frac{k^2}{\mu^2} \right)} \quad (4.32b)$$

The exponents of the logarithms are specified by the renormalization group in relation to the anomalous dimensions of the gluon and the ghost field [143],

$$\gamma_A(g) = \frac{\partial \ln Z_3}{\partial \ln \mu^2} = \gamma_A^0 g^2 + \mathcal{O}(g^4) \quad (4.33a)$$

$$\gamma_G(g) = \frac{\partial \ln \tilde{Z}_3}{\partial \ln \mu^2} = \gamma_G^0 g^2 + \mathcal{O}(g^4) \quad (4.33b)$$

In the Landau gauge, this relation is given by [143]

$$\gamma = \frac{\gamma_A^0}{\beta_0} = \frac{13}{22} \quad (4.34a)$$

$$\delta = \frac{\gamma_G^0}{\beta_0} = \frac{9}{44} \quad (4.34b)$$

Oftentimes, the logarithmic exponents γ and δ in (4.32) are referred to as anomalous dimensions of the gluon and the ghost, although strictly speaking they are only the lowest order coefficients of the anomalous dimensions γ_A and γ_G defined in Eq. (4.33) and divided by β_0 .

We now try to reproduce the well-established results (4.34) from our nonperturbative study of Dyson–Schwinger equations in Landau gauge. In the same procedure, we may then go on to determine the UV behavior of Coulomb gauge propagators.

Landau gauge anomalous dimensions

Consider the ($d = 4$) Landau gauge ghost DSE multiplicatively renormalized in the scheme (4.21), where $\mu^2 D_A(\mu) = C_A$, $\mu^2 D_G(\mu) = C_G$ and the ghost-gluon vertex is evaluated at some momentum configuration to define a value of \tilde{Z}_1 ,

$$D_G^{-1}(k) = k^2 \tilde{Z}_3 - g^2 N_c \tilde{Z}_1^2 k^2 \int \tilde{d}^4 \ell \left(1 - (\hat{\ell} \cdot \hat{k})^2\right) D_A(\ell) D_G(\ell - k). \quad (4.35)$$

A renormalization prescription that does not agree with (4.23) is accounted for by a change in \tilde{Z}_1^2 . In order to study the ghost DSE (4.35) in the asymptotic ultraviolet limit, the following ansätze are made:

$$D_A(k) = \frac{C_A}{k^2 \left(1 + \frac{C_A}{A} \ln^\gamma \left(\frac{k^2}{\mu^2}\right)\right)} \xrightarrow{k \rightarrow \infty} \frac{A}{k^2 \ln^\gamma \left(\frac{k^2}{\mu^2}\right)} \quad (4.36a)$$

$$D_G(k) = \frac{C_G}{k^2 \left(1 + \frac{C_G}{B} \ln^\delta \left(\frac{k^2}{\mu^2}\right)\right)} \xrightarrow{k \rightarrow \infty} \frac{B}{k^2 \ln^\delta \left(\frac{k^2}{\mu^2}\right)} \quad (4.36b)$$

These satisfy the renormalization prescriptions (4.21) for $k = \mu$ and behave like the proposed ultraviolet behavior (4.32) for $k \rightarrow \infty$, with coefficients A and B . Rewrite the ghost DSE (4.35) by

$$\frac{1}{k^2 D_G(k)} = \tilde{Z}_3 - g^2 N_c \tilde{Z}_1^2 A B \mathcal{I}_G(k), \quad (4.37)$$

where the integral $\mathcal{I}_G(k)$ can then be asymptotically evaluated for $k \gg \mu$ with a dimensionally regularized UV divergence,⁶

$$\begin{aligned} \mathcal{I}_G(k \rightarrow \infty) &= \int \tilde{d}^{4-2\epsilon} \ell \frac{1 - (\hat{\ell} \cdot \hat{k})^2}{\ell^2 (\ell - k)^2 \ln^\gamma \left(\frac{\ell^2}{\mu^2}\right) \ln^\delta \left(\frac{(\ell - k)^2}{\mu^2}\right)} = \int_{\ell > k} \tilde{d}^{4-2\epsilon} \ell \frac{1 - (\hat{\ell} \cdot \hat{k})^2}{\ell^4 \ln^{\gamma+\delta} \left(\frac{\ell^2}{\mu^2}\right)} \\ &= \frac{2}{(2\pi)^3} \int_0^\pi d\eta \sin^4 \eta (1 + \mathcal{O}(\epsilon)) \int_k^\infty \frac{d\ell}{\ell} \frac{1}{(\ell^2)^\epsilon \ln^{\gamma+\delta} \left(\frac{\ell^2}{\mu^2}\right)}, \quad x := \epsilon \ln \left(\frac{\ell^2}{\mu^2}\right) \\ &= \frac{3}{32\pi^2} (1 + \mathcal{O}(\epsilon)) (\mu^2)^{-\epsilon} \frac{1}{\epsilon^{1-\gamma-\delta}} \frac{1}{2} \int_{\epsilon \ln \left(\frac{k^2}{\mu^2}\right)}^\infty dx x^{-\gamma-\delta} e^{-x} \\ &= \frac{3}{64\pi^2} (1 + \mathcal{O}(\epsilon)) \left(\frac{\Gamma(1-\gamma-\delta)}{\epsilon^{1-\gamma-\delta}} - \frac{1}{1-\gamma-\delta} \ln^{1-\gamma-\delta} \left(\frac{k^2}{\mu^2}\right) + \mathcal{O}(\epsilon) \right) \\ &= \frac{1}{(4\pi)^2} \frac{3\Gamma(1-\gamma-\delta)}{4\epsilon^{1-\gamma-\delta}} - \frac{1}{(4\pi)^2} \frac{3}{4(1-\gamma-\delta)} \ln^{1-\gamma-\delta} \left(\frac{k^2}{\mu^2}\right). \end{aligned} \quad (4.38)$$

⁶One can integrate for $\ell < k$ and $\ell > k$ and expand in ℓ/k and k/ℓ , respectively. Only one term is dominant which turns out to be the one found by the ‘‘angular approximation’’. We restrict the calculation to $0 < 1 - \gamma - \delta < 1$. Furthermore, the expansion of the incomplete gamma function

$$\int_\tau^\infty dx x^{z-1} e^{-x} = \Gamma(z) - \sum_{n=0}^\infty \frac{(-1)^n \tau^{z+n}}{n!(z+n)}$$

is used.

Terms that vanish for $\epsilon \rightarrow 0$ were discarded. Matching this result to the l.h.s. of the ghost DSE (4.37) leads to a sum rule of the anomalous dimensions,

$$\gamma + 2\delta = 1, \quad (4.39)$$

as well as the relation

$$g^2 N_c \tilde{Z}_1^2 AB^2 \frac{1}{(4\pi)^2} \frac{3}{4\delta} = 1. \quad (4.40)$$

The infinite part of the renormalization constant \tilde{Z}_3 is identified by

$$\tilde{Z}_3 = \frac{\Gamma(\delta + 1)}{B} \frac{1}{\epsilon^\delta} + \text{finite} \quad (4.41)$$

where setting the finite part to zero puts QCD into a nonperturbative phase.⁷

We may now plug the asymptotic forms (4.36) into the running coupling (4.25) to obtain with Eq. (4.40)

$$g^2(k \rightarrow \infty) = \tilde{Z}_1^2 g^2 \frac{AB^2}{\ln\left(\frac{k^2}{\mu^2}\right)} = \frac{1}{\frac{1}{(4\pi)^2} \frac{3N_c}{4\delta} \ln\left(\frac{k^2}{\mu^2}\right)} \quad (4.42)$$

Note that the finite value of \tilde{Z}_1 specific to the renormalization scheme drops out. The above UV limit expression for the nonperturbative $g^2(k)$ can be compared to the perturbative expression (4.31) to yield

$$\delta = \frac{1}{(4\pi)^2} \frac{3N_c}{4\beta_0} = \frac{9}{44}, \quad (4.43)$$

in agreement with the perturbative result for δ in Eq. (4.34).

Coulomb gauge anomalous dimensions

Since the above UV analysis of the nonperturbative ghost Dyson–Schwinger equation successfully yielded the correct anomalous dimensions for the Landau gauge, we use the same method to extract the anomalous dimensions for the gluon and ghost fields in the Coulomb gauge.

The multiplicatively renormalized ghost DSE reads in terms of $d(k)$ and $\omega(k)$,

$$d^{-1}(k) = \tilde{Z}_3 - g^2 N_c \tilde{Z}_1^2 \int \tilde{d}^3 \ell \left(1 - (\hat{\ell} \cdot \hat{k})^2\right) \frac{d(\ell - k)}{2\omega(\ell)(\ell - k)^2}, \quad (4.44)$$

and the ansätze

$$\omega^{-1}(k) = \frac{C_\omega^{-1}}{k \left[1 + \frac{C_\omega^{-1}}{A} \ln^\gamma\left(\frac{k^2}{\mu^2}\right)\right]}, \quad d(k) = \frac{C_d}{1 + \frac{C_d}{B} \ln^\delta\left(\frac{k^2}{\mu^2}\right)} \quad (4.45)$$

⁷It was discussed in Ref. [78] that the horizon condition does not allow $\tilde{Z}_3 \rightarrow 1$ for $g \rightarrow 0$ and hence contradicts perturbation theory.

give for $k = \mu$ the values C_ω^{-1} and C_d , resp., whereas the $k \rightarrow \infty$ behavior is determined by the coefficients A and B and the exponents γ, δ , similarly to the Landau gauge. Setting the renormalization constant \tilde{Z}_3 to

$$\tilde{Z}_3 = \frac{\Gamma(\delta + 1)}{B} \frac{1}{\epsilon^\delta}, \quad (4.46)$$

enforces the horizon condition (cf. Eq. 4.41), and one may calculate the integral in Eq. (4.45) for $k \rightarrow \infty$ by

$$\begin{aligned} B^{-1} \ln^\delta \left(\frac{k^2}{\mu^2} \right) &= \tilde{Z}_3 - g^2 N_c \tilde{Z}_1^2 \int_{\ell \geq k} d^{3-2\epsilon} \ell \left(1 - (\hat{\ell} \cdot \hat{k})^2 \right) \frac{AB}{2\ell^3 \ln^{\gamma+\delta} \left(\frac{\ell^2}{\mu^2} \right)} \\ &= \tilde{Z}_3 - g^2 N_c \tilde{Z}_1^2 AB \frac{1}{2} \frac{4}{(2\pi)^2} \frac{1}{2} \frac{1}{\epsilon^\delta} \int_{\epsilon \ln \left(\frac{k^2}{\mu^2} \right)}^{\infty} dx x^{\delta-1} e^{-x} \\ &= \tilde{Z}_3 - g^2 N_c \tilde{Z}_1^2 AB \frac{1}{(4\pi)^2} \left(\frac{4\Gamma(\delta)}{3} \frac{1}{\epsilon^\delta} - \frac{4}{3\delta} \ln^\delta \left(\frac{k^2}{\mu^2} \right) \right) \\ &= g^2 N_c \tilde{Z}_1^2 AB \frac{1}{(4\pi)^2} \frac{4}{3\delta} \ln^\delta \left(\frac{k^2}{\mu^2} \right) \end{aligned} \quad (4.47)$$

where we have matched the exponents by means of the sum rule

$$\gamma + 2\delta = 1, \quad (4.48)$$

and the coefficients are found to obey

$$g^2 N_c \tilde{Z}_1^2 AB^2 \frac{1}{(4\pi)^2} \frac{4}{3\delta} = 1. \quad (4.49)$$

With these results, the Coulomb gauge running coupling (4.29) gives for the ultraviolet limit

$$g^2(k \rightarrow \infty) = \tilde{Z}_1^2 g^2 \frac{AB^2}{\ln \left(\frac{k^2}{\mu^2} \right)} = \frac{1}{\frac{1}{(4\pi)^2} \frac{4N_c}{3\delta} \ln \left(\frac{k^2}{\mu^2} \right)} \quad (4.50)$$

and in comparison to its known gauge invariant behavior (4.31) this yields

$$\delta = \frac{1}{(4\pi)^2} \frac{4N_c}{3\beta_0}. \quad (4.51)$$

With the canonical value (4.3) for β_0 and by virtue of the sum rule (4.48), the logarithmic exponents of ghost and gluon propagators can thus be found to yield

$$\gamma = \frac{3}{11}, \quad \delta = \frac{4}{11}. \quad (4.52)$$

The lowest order anomalous dimensions (cf. Eq. 4.34) $\gamma_A^0 = \beta_0 \gamma = N_c$ and $\gamma_G^0 = \beta_0 \delta = \frac{4N_c}{3}$ agree with the purely perturbative calculation [56, 149, 72]. Therefore, a full numerical nonperturbative solution is expected to yield the ultraviolet behavior specified by (4.45) with the logarithmic exponents (4.52).

Recalling the numerical solution from chapter 3, the values for γ and δ , see Eq. (3.58), were

$$\gamma_{\text{num}} = 0, \quad \delta_{\text{num}} = \frac{1}{2}. \quad (4.53)$$

Note that the sum rule (4.48) is satisfied by the above values. In the calculation that led to (4.52), we required β_0 to be the canonical value. We may turn the argument around, assume the numerical solutions (4.53) and calculate β_0 from the UV behavior of the resulting running coupling, cf. Eq. (4.51). This procedure yields

$$\beta_0^{\text{num}} = \frac{1}{(4\pi)^2} \frac{4N_c}{3\delta_{\text{num}}} = \frac{1}{(4\pi)^2} \frac{8N_c}{3}. \quad (4.54)$$

The disagreement of β_0^{num} with β_0 is small, but in view of the exponential dependence of the QCD scale on β_0 , a slightly erroneous result for β_0 will make a sensible assignment of Λ_{QCD} hopeless. The failure to find the correct β_0 is clearly due to the approximations made. The Gaussian wave functionals used eliminate the gluon loop in the gap equation since there exists no tree-level three-gluon vertex. From purely perturbative calculations it is known that the gluon loop is essential for the gluon self-energy to preserve gauge invariance and produce the correct β_0 . A nonperturbative calculation therefore requires a truncation that involves the gluon loop as well. However, DSE studies in Landau gauge showed that the dressing of the three-gluon vertex in the gluon loop must be highly non-trivial [53, 124], and to achieve results with the canonical β_0 value a momentum dependent renormalization constant Z_1 is proposed [51]. In the Hamiltonian approach with a wave functional, the extraction of the right β_0 was pursued from the Coulomb interaction using perturbative UV tails for the form factors [150, 151]. It is not clear at present how to manipulate the wave functional such that the nonperturbative UV behavior (4.45) with correct values for δ and γ is reproduced from analyzing the gap equation in the Coulomb gauge Hamiltonian approach.

The agreement of the result (4.54) with Refs. [152, 83] is coincidental. There, after factoring out g_B from the ghost form factor, the β function was defined as the (logarithmic) derivative of the tree-level term in the ghost equation, being $g_B^{-1}(\Lambda)$. However, this term is actually \tilde{Z}_3 , see Eq. (4.44). What was proposed as the β function was actually

$$\bar{\beta} = \frac{\partial}{\partial \ln \mu} \ln \tilde{Z}_3 = 2\gamma_d \quad (4.55)$$

i.e. twice the anomalous dimension of the ghost form factor. With the specific value of $\delta = 1/2$, these objects are indeed identical, since $\delta = \frac{\gamma_d^0}{\beta_0}$.

An alternative way to calculate the β function from the nonperturbative variational solutions in the Coulomb gauge is to extract information from the heavy quark potential $V_C(k)$. Since the nonperturbative running coupling can also be defined via $V_C(k)$, see Eq. (4.30), the Coulomb form factor $f(k)$ must yield

$$V_C(k) = \frac{d^2(k)f(k)}{k^2} \sim \frac{1}{\ln \frac{k^2}{\mu^2}}. \quad (4.56)$$

Making an ansatz for the Coulomb form factor $f(k)$ in the ultraviolet,

$$f(k) = \frac{C}{\ln^\varphi \frac{k^2}{\mu^2}}, \quad (4.57)$$

therefore provides a sum rule for the logarithmic exponents δ and φ ,

$$2\delta + \varphi = 1. \quad (4.58)$$

Furthermore, the UV ansatz (4.57) for the form factor $f(k)$ can be plugged into its DSE (3.30) to yield after UV analysis⁸

$$g^2 N_c \tilde{Z}_1^2 AB^2 \frac{1}{(4\pi)^2} \frac{4}{3\varphi} = 1. \quad (4.59)$$

By comparison of the above relation to the identity (4.49) from the UV analysis of the ghost DSE, we infer that $\varphi = \delta$ and with the sum rules (4.58) and (4.48) this yields

$$\delta = \varphi = \gamma = \frac{1}{3}. \quad (4.60)$$

One may now use Eq. (4.51) from the ghost-gluon vertex to calculate β_0 as a function of δ ,

$$\beta_0^{\text{anti}} = \frac{1}{(4\pi)^2} \frac{4N_c}{3\delta_{\text{anti}}} = \frac{1}{(4\pi)^2} \frac{12N_c}{3}. \quad (4.61)$$

The occurrence of the anti-screening contribution $\frac{12N_c}{3}$ is familiar from the consideration of the instantaneous potential, see section 4.1. Apparently, the non-instantaneous part needs to be taken into account, possibly in the manner proposed in Ref. [146].

Apart from the technical difficulties to arrive at the correct value for β_0 automatically, the above considerations showed that it is possible to extract a certain ultraviolet behavior of the Coulomb gauge Green functions, having *imposed* the known value for β_0 . It may therefore be expected that, once approximations can be relaxed, the ultraviolet behavior according to Eqs. (4.45) and (4.52), i.e.

$$\omega(k) \sim k \ln^{3/11} k, \quad d(k) \sim \frac{1}{\ln^{4/11} k}, \quad (4.62)$$

will be found numerically. Lattice calculations [128] claimed a counter-intuitive UV power law $\omega \sim k^{3/2}$. The data displayed in Fig. 3.3 also indicate an UV enhancement of $\omega(k)$. However, a stronger than linear rising of $\omega(k)$ might as well be an indication of the logarithmic correction in (4.62). The lattice calculations in [70] agree with such a statement. This should be investigated further.

4.4 Infrared fixed point

In this section we investigate the infrared behavior of the Coulomb gauge running coupling as defined by Eq. (4.29). Due to the nonrenormalization property of the ghost-gluon vertex, the

⁸In the same manner as for the infrared analysis in section 3.6, the asymptotic evaluation of the DSE for $f(k)$ gives no additional condition on the (power or logarithmic) exponents. This is due to the fact the product $\frac{d^2(k)}{k^2 \omega(k)}$ behaves like $\frac{1}{k}$ in the infrared and like $\frac{1}{k \ln k}$ in the ultraviolet, as a consequence of the ghost-gluon vertex' nonrenormalization.

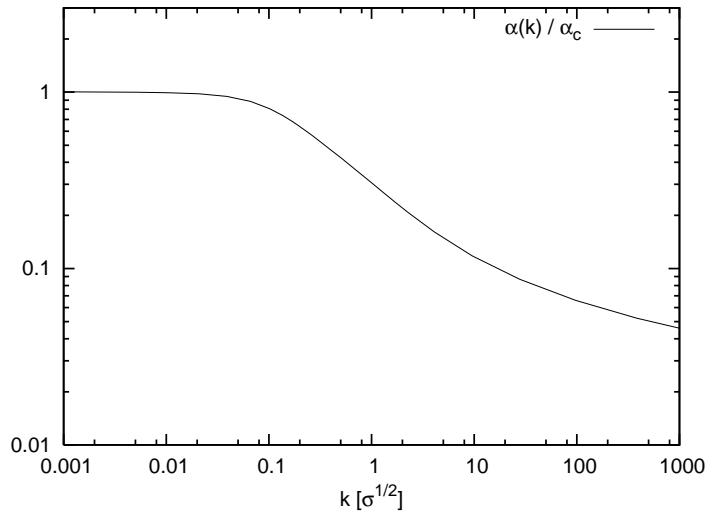


Figure 4.2: *The running coupling $\alpha(k)$ as defined by Eq. (4.29) with the variational solutions presented in chapter 3.*

running coupling attains a finite value in the infrared. The corresponding β function then has a fixed point in the infrared. This can be readily seen by noting that the sum rule (2.54) for infrared exponents yields

$$1 - 2(2\alpha_G + 1 + \alpha_A) = 0 \quad (4.63)$$

in the Coulomb gauge where $d = 3$. Hence, with the infrared power laws (2.50) with coefficients $2A$ for $\omega^{-1}(k)$ and B for $d(k)$, we find for the infrared limit of the (equal-time) running coupling $\alpha(k) = \frac{g^2(k)}{4\pi}$ in Eq. (4.29)

$$\alpha_c := \lim_{k \rightarrow 0} \alpha(k) = \tilde{Z}_1^2 g^2 \frac{2AB^2}{4\pi} = \frac{1}{2\pi N_c I_G(\kappa)}, \quad (4.64)$$

where we have made use of Eq. (2.60) which relates the infrared coefficients A and B to the function $I_G(\kappa)$ defined by Eq. (2.59b).⁹ For the preferred solution with $\kappa = \frac{1}{2}$, we evaluate $I_G(\kappa)$ to find

$$\alpha_c \Big|_{d=3}^{\kappa=\frac{1}{2}} = \frac{2\pi}{N_c}. \quad (4.65)$$

In Fig. 4.2, the running coupling as given in Eq. (4.29) is shown with the full numerical solutions for $d(k)$ and $\omega(k)$ given in chapter 3. The numerical value of α_c is in excellent agreement with Eq. (4.65).¹⁰

⁹A factor of \tilde{Z}_1^2 needs to be reintroduced here, it was set to unity in the infrared analysis of chapter 2.

¹⁰In Ref. [86], the definition of the running coupling from Ref. [101] with a factor of $\frac{8}{3}$ in Eq. (4.29) was used without adjustment of \tilde{Z}_1 . Therefore, the value of α_c was found to be higher by that factor, i.e. $16\pi/(3N_c)$.

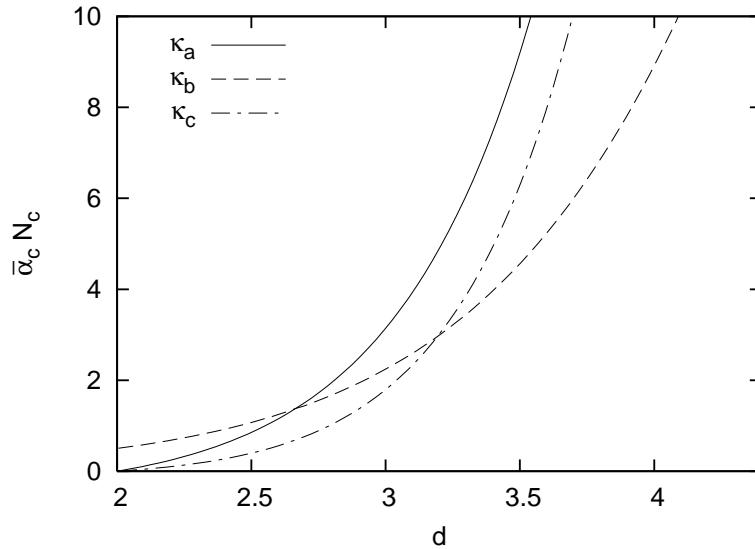


Figure 4.3: Infrared limit $\bar{\alpha}_c$ of the running coupling as function of d . The three solutions κ_a , κ_b and κ_c from Fig. 2.5 are shown.

The other critical solutions for various spatial dimensions d and the respective solutions for $\kappa(d)$ yield different values for the infrared limit of the running coupling. To study the dependence on the dimension d , we use here the Landau gauge running coupling $\bar{\alpha}(k) := \frac{g^2(k)}{4\pi}$ with $g^2(k)$ defined in Eq. (4.25). The infrared limit yields

$$\bar{\alpha}_c := \lim_{k \rightarrow 0} \bar{\alpha}(k) = \frac{1}{4\pi N_c I_G(\kappa)}, \quad (4.66)$$

cf. Eq. (4.64). For the three solution branches $\kappa_a(d)$, $\kappa_b(d)$ and $\kappa_c(d)$ shown in Fig. 2.5, the value of $\bar{\alpha}_c$ is shown in Fig. 4.3 as a function of the dimension d . It is seen that for large d , $\bar{\alpha}_c(d)$ rises exponentially. For $d \rightarrow 2$, which corresponds to the Landau gauge 1+1 dimensional YM theory, the solutions $\kappa_a(d)$ and $\kappa_c(d)$ yield $\bar{\alpha}_c(d=2) = 0$ whereas for $\kappa_b(d)$ the infrared limit $\bar{\alpha}_c$ approaches a finite value

$$\bar{\alpha}_c|_{d=2}^{\kappa=\frac{1}{5}} \cdot N_c = \frac{2^{8/5} \Gamma^2(\frac{6}{5}) \Gamma(\frac{13}{10})}{\sqrt{\pi} \Gamma(\frac{2}{5}) \Gamma(\frac{4}{5})} N_c \approx 0.501 N_c \quad (4.67)$$

The root $\kappa_b(d)$ does not show any qualitative change for $d = 2$ where all Landau gauge degrees of freedom are frozen. The solutions $\kappa_a(d)$ and $\kappa_c(d)$, on the other hand, do show a qualitative change at $d = 2$. Granted the approximations made, the latter solutions with $\bar{\alpha}_c = 0$ for $d = 2$ indicate what one may expect: the 1 + 1 dimensional Landau gauge calls for a separate treatment.

Returning to the $d = 3$ Coulomb gauge, it is reassuring to see that the running coupling in Fig. 4.2 is a monotonic function. Otherwise the β function would have spurious zeros (a problem that occurs in the Landau gauge [106]). The infrared finite value of the running coupling infers

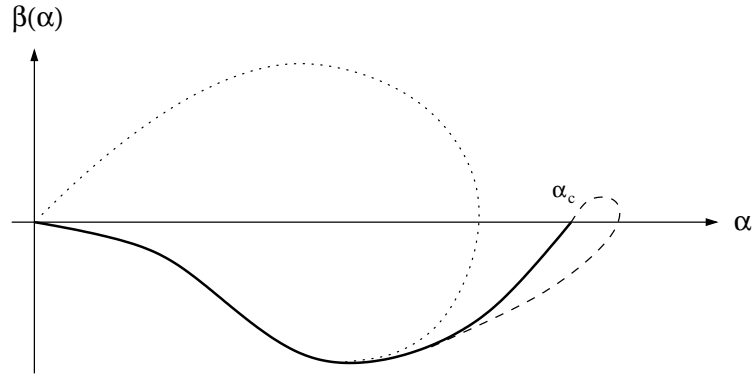


Figure 4.4: *Sketch of the β function. The solid line qualitatively describes the behavior of the running coupling as shown in Fig. 4.2. The dashed line shows the case where there is a small bump in the running coupling. With a dotted line, the β function is shown for the subcritical solution.*

that the β function has an infrared fixed point for $\frac{g^2}{4\pi} = \alpha_c$.¹¹ In Fig. 4.4, several cases of the β function are sketched. The subcritical solutions (section 3.7), as opposed to the critical solutions, do not have a sum rule of infrared exponents since all form factors are infrared finite. The running coupling $\alpha(k)$ should have an ultraviolet behavior similar to the one shown in Fig. 4.2 since the form factor are qualitatively the same in the UV. However, in the infrared one finds

$$\alpha(k \rightarrow 0) \sim k, \quad (4.68)$$

that is the running coupling from the ghost-gluon vertex *vanishes* in the infrared for the subcritical solution. This behavior is unacceptable for a theory that is strongly coupled in the infrared. In contrary to the $1 + 1$ dimensional theory, the $3 + 1$ dimensional case requires a non-vanishing coupling strength for the infrared degrees of freedom. Moreover, if we hold onto asymptotic freedom, the additional requirement (4.68) yields a multi-valued β function. The interpretation of $\alpha(k)$ as a running coupling is then questionable since the zeros of the β function are not necessarily fixed points [153].¹² Aside from the discussion in section 3.7, this indicates that the subcritical solutions are unphysical.

Vertex corrections

There exists the possibility of nonperturbative corrections to the running coupling. This might be interesting even for the extraction of Λ_{QCD} by comparison to experiment [140]. It was suggested in Ref. [98] to multiply the running coupling with a contraction of the ghost-gluon

¹¹The infrared divergent running coupling (4.30) from the heavy quark potential would not exhibit this infrared fixed point.

¹²The running coupling (4.30) extracted from the Coulomb potential would yield an infrared finite limit for the subcritical solution and might serve as a more sensible definition in this case.

vertex in a certain momentum configuration. The infrared limit of the thus corrected running coupling is denoted by

$$\alpha_c^{(C)} = \lim_{k \rightarrow 0} \alpha(k) C^2 . \quad (4.69)$$

The value C , defined by Eq. (3.75), describes the dressing of the vertex in the infrared limit where first the gluon momentum is approached to zero and afterwards the ghost momentum is taken to be zero. With the help of the result obtained in table 3.2 for the number C , the corrections to α_c can be specified. They are shown in table 4.1 for the various solutions of $\kappa(d)$ in question, in comparison to the uncorrected values α_c . Note that the solution $\kappa = \frac{1}{2}$ for $d = 3$ is particular in the sense that it is not corrected by the vertex contribution since $C = 1$.

d	κ	$\bar{\alpha}_c^{(-)} N_c$	$\bar{\alpha}_c^{(-)(C)} N_C$
3	0.398	4.488	5.32
3	$\frac{1}{2}$	2π	2π
4	0.595	8.915	10.94

Table 4.1: *Infrared finite values of the running coupling for the various infrared solutions, with and without vertex corrections. For $d = 3$, we used the definition α_c in Eq. (4.64) whereas for $d = 4$, $\bar{\alpha}_c$ from Eq. (4.66) is used and reproduces the result in Ref. [97] without vertex correction.*

In concluding this chapter, we give a brief outlook on future investigations with the nonperturbative running coupling in the Coulomb gauge. With an improved ultraviolet behavior of the Green functions, see section 4.3, it will be possible to adjust the scale in the Hamiltonian approach to YM theory. This may be pursued by comparison to experimental scattering amplitudes from deep inelastic scattering. The nonperturbative feature of the variational solutions makes it then possible to quantify other interesting objects numerically, such as, e.g., the Coulomb string tension, or correlators of the high-temperature phase of QCD.

5 Inclusion of external charges

In the Coulomb gauge, the Green functions were investigated in the infrared limit in chapter 2 and for the entire momentum range with variational methods in chapter 3. These vacuum calculations include only the interaction of gluons and ghosts, the coupling to the quark sector is suppressed by setting $\rho_{\text{ext}}^a(x) = 0$. The translationally invariant Green functions so obtained were discussed in the previous chapters, and it was shown that the heavy quark potential is obtained by a perturbation in $\rho_{\text{ext}}^a(x)$. Although the crucial feature of linear confinement is already given by the Green functions of the pure glue theory, the back-reaction of the external charges on the wave functional is lacking. One may expect that by extending the ansatz for the wave functional in the presence of a quark-antiquark pair, for instance, the energy can be lowered further by the formation of a flux tube connecting these external charges. In this section, various approaches are discussed by which the back-reaction of the external charges on the gauge field sector can be studied.

5.1 Gluons in a quasi-particle representation

The vacuum wave functional used in chapter 3 is of Gaussian type. In analogy to the quantum harmonic oscillator where the Gaussian ground state is annihilated by a linear combination of the coordinate and momentum operators, the variational YM vacuum state $|0\rangle$ suggests the introduction of an annihilation operator that yields $a_k^a(x)|0\rangle = 0$. Its hermitian conjugate $a_k^a(x)^\dagger$ may then be considered the creation operator of a gluonic excitation at point x . By means of these gluonic excitations, an orthonormal basis of particle excitations can be constructed [154]. In a normal order expansion of the Yang–Mills Hamiltonian, the term $\omega a^\dagger a$ occurs so that $\omega(k)$ represents part of the energy of a gluonic excitation with momentum k . Since in the infrared, the dispersion relation departs substantially from the behavior $\omega(k) = k$ of a free particle, these particle excitations are regarded as quasi-particles, incorporating non-perturbative effects.

Before we define the quasi-particle basis, recall that the choice $\lambda = \frac{1}{2}$ for the wave functional in Eq. (3.1),

$$\Psi[A] = \langle A|0\rangle = \mathcal{N} \frac{1}{\sqrt{\mathcal{J}[A]}} \exp\left[-\frac{1}{2} \int d^3[xy] A_i^a(x) \omega(x, y) A_i^a(y)\right], \quad (5.1)$$

formally eliminates the Faddeev–Popov determinant \mathcal{J} from expectation values. The Coulomb gauge scalar product $\langle | \rangle$ that comprises \mathcal{J} after gauge fixing can be related to a scalar product $\langle | \rangle_{\text{flat}}$ with a flat measure,

$$\begin{aligned} \langle 0| \mathcal{O}[A, \Pi] |0\rangle &= \int \mathcal{D}A \mathcal{J}[A] \Psi^*[A] \mathcal{O}[A, \Pi] \Psi[A] \\ &= \int \mathcal{D}A \tilde{\Psi}^*[A] \tilde{\mathcal{O}}[A, \Pi] \tilde{\Psi}[A] =: \langle \tilde{0} | \tilde{\mathcal{O}}[A, \Pi] | \tilde{0} \rangle_{\text{flat}} \end{aligned} \quad (5.2)$$

if we identify

$$\tilde{\Psi}[A] = \langle A | \tilde{0} \rangle = \sqrt{\mathcal{J}[A]} \Psi[A], \quad \tilde{\mathcal{O}}[A, \Pi] = \sqrt{\mathcal{J}[A]} \mathcal{O}[A, \Pi] \frac{1}{\sqrt{\mathcal{J}[A]}}. \quad (5.3)$$

With these manipulations, expectation values can be calculated straightforwardly by means of Wick's theorem. Note that the expectation values considered are not taken in the auxiliary Gaussian state $\tilde{\Psi}[A]$ but actually in the state (5.1). The Gaussian $\tilde{\Psi}[A]$ is suitable to define an annihilation operator

$$a_k^a(x) = \frac{1}{\sqrt{2}} \int d^3y (\alpha_{km}^{-1}(x, y) A_m^a(y) + i\alpha_{km}(x, y) \Pi_m^a(y)) \quad (5.4)$$

that yields¹

$$a_k^a(x) |\tilde{0}\rangle = 0. \quad (5.5)$$

Above, the function $\alpha_{ij}(x, y)$ is defined as the inverse square root of the variational kernel ω ,

$$\alpha_{ij}(x, y) = t_{ij}(x) \alpha(x, y), \quad \int d^3y \alpha(x, y) \alpha(y, z) = \omega^{-1}(x, z), \quad (5.6)$$

and has the same dimension as the field operator A . Adopting the canonical commutation relations²

$$[A_i^{a\perp}(x), \Pi_j^{b\perp}(y)] = it_{ij}^{ab}(x, y), \quad (5.7)$$

the hermitian conjugate of Eq. (5.4) obeys

$$[a_i^a(x), a_j^b(y)^\dagger] = t_{ij}^{ab}(x, y), \quad (5.8)$$

and creates gluonic excitations by acting on the vacuum,

$$|\{x^{(k)}, a_k, i_k\}\rangle = \mathcal{N}_n \prod_{k=1}^n a_{i_k}^{a_k}(x^{(k)})^\dagger |\tilde{0}\rangle \quad (5.9)$$

which can be shown to be orthogonal. Normalization of the states (5.9) by an appropriate choice of \mathcal{N}_n may be issued, if needed, in a finite volume $V = \int d^3x$.

5.2 Coherent states

With the set of gluonic excitations formulated in the previous section, we have a basis of the Hilbert space at our disposal in which a state can be constructed taking the presence of external

¹Strictly speaking, only the auxiliary vacuum $|\tilde{0}\rangle$ and not the true vacuum $|0\rangle$ is annihilated by the operator a . Employing the replacement $\ln \mathcal{J} = -\int A \chi A$ in the one-loop approximation, see Eq. (3.13), a definition of the operator a by means of Ω that annihilates $|0\rangle$ could be pursued.

²Here, we write the \perp explicitly in order to emphasize that all fields are transverse. The commutation relations (1.89) that involve the field dependent operator T_{ij} are not considered here.

color charges into account. This state, $|Z\rangle$, is here chosen as a coherent superposition of the excited states (5.9), where a localized function controls the excitation of gluons in between the external color charges. This function, $Z_k^a(x)$, may be determined by the variational principle, minimizing the expectation value of $H' = H + H_{\text{ext}}$ with the external charges ρ_{ext} contained in H_{ext} .

Coherent states were first introduced by Schrödinger [155] in 1926 and further established by Glauber [156] in 1963 who laid the keystone for developments in quantum optics and thus gained the 2005 physics Nobel prize (along with Hall and Häntsch). It will be instructive here to briefly discuss the simple case of the three-dimensional harmonic oscillator and thus expose the main features of the coherent state. The Hamiltonian reads

$$H = \frac{p^2}{2m} + \frac{1}{2}m\omega^2 x^2 = \omega a_k^\dagger a_k + E_0, \quad (5.10)$$

where

$$a_k = \frac{1}{\sqrt{2}} \left(\frac{x_k}{\sigma} + i\sigma p_k \right) \quad \text{and} \quad a_k^\dagger = \frac{1}{\sqrt{2}} \left(\frac{x_k}{\sigma} - i\sigma p_k \right) \quad (5.11)$$

are linear combinations of x_k and p_k that diagonalize H for $\sigma^{-1} = \sqrt{m\omega}$. Due to $[x_i, p_j] = i\delta_{ij}$, we have $[a_i, a_j^\dagger] = \delta_{ij}$ and the orthonormal states $|n\rangle = \prod_k (n_k!)^{-1/2} (a_k^\dagger)^{n_k} |0\rangle$ can be shown to yield the equidistant spectrum $H|n\rangle = E_n|n\rangle$ with $E_n = \omega(n_x + n_y + n_z + \frac{3}{2})$. The vacuum state $|0\rangle$ for $n = \mathbf{0}$ has minimal energy $E_0 = \frac{3}{2}$ and is annihilated by (5.11), $a|0\rangle = 0$. The solution to the latter differential equation yields the vacuum wave function in coordinate space,

$$\psi_0(x) := \langle x|0\rangle = \frac{1}{(\pi\sigma^2)^{3/4}} e^{-\frac{1}{2}x^2/\sigma^2}. \quad (5.12)$$

We now define the coherent state $|z\rangle$ by acting with a unitary operator U on the vacuum state $|0\rangle$,

$$|z\rangle = U(z)|0\rangle, \quad U(z) = e^{z_k a_k^\dagger - z_k^* a_k}, \quad z_k \in \mathbb{C}. \quad (5.13)$$

The coherent states so defined are normalized if $|0\rangle$ is, but they are not orthogonal. The continuous index z makes the set of coherent states over-complete in the given Hilbert space with a countable basis. Further properties of the coherent state are listed below:

a) eigenstate of annihilation operator

$$a_k |z\rangle = z_k |z\rangle \quad (5.14a)$$

b) closure relation³

$$1 = \frac{1}{\pi^3} \int d^2z |z\rangle \langle z| \quad (5.14b)$$

³The integral is taken over the complex planes of all components of z . By inserting the closure relation into $1 = \langle 0|0\rangle$, the factor $\frac{1}{\pi^3}$ is cancelled by the integration of the polar angles in the complex planes.

c) minimal uncertainty

$$(\Delta x_k)(\Delta p_k) = \frac{1}{4} \quad (\text{no sum}) \quad (5.14c)$$

d) Poissonian distribution

$$|\langle n|z\rangle|^2 = \prod_k \frac{|z_k|^2}{n_k!} e^{-|z_k|^2} \quad (5.14d)$$

e) shifted vacuum wave function

$$\langle x|z\rangle \sim \langle x - \sqrt{2}\sigma \operatorname{Re} z|0\rangle \quad (5.14e)$$

To see the property e) first note that the operator $U(z)$ in Eq. (5.13) can be expressed by coordinate and momentum operators x and p using Eq. (5.11),

$$U(z) = e^{z_k a_k^\dagger - z_k^* a_k} = e^{iI_k x_k - iR_k p_k}, \quad (5.15)$$

having abbreviated

$$I_k := \sqrt{2}\sigma^{-1} \operatorname{Im}(z_k), \quad R_k := \sqrt{2}\sigma \operatorname{Re}(z_k). \quad (5.16)$$

The well-known Campbell-Baker-Hausdorff formula

$$\ln(e^X e^Y) = X + Y + \frac{1}{2}[X, Y] + \frac{1}{12}[X, [X, Y]] - \frac{1}{12}[Y, [X, Y]] + \dots \quad (5.17)$$

which infers $e^{A+B} = e^A e^B e^{-\frac{1}{2}[A, B]}$ for $[A, B]$ a c -number, helps to rewrite the coherent state (5.13) and interpret it by a shifted vacuum wave function,

$$\begin{aligned} \psi_z(x) &= \langle x|z\rangle = e^{-\frac{1}{2}iI_k R_k} e^{iI_k x_k} e^{-R_k \partial_k^x} \psi_0(x) \\ &= e^{-\frac{1}{2}iI_k R_k} e^{iI_k x_k} \psi_0(x - R). \end{aligned} \quad (5.18)$$

Here, we have used $\langle x|ip_k|y\rangle = \partial_k^x \delta^{(3)}(x - y)$ and assumed analyticity of $\psi_0(x)$. That is, the wave function of the coherent state is, up to a x -dependent phase, the vacuum wave function, evaluated at $x - R$. This proves Eq. (5.14e). Equivalently, using $\langle p|ix_k|q\rangle = -\partial_k^p \delta^{(3)}(p - q)$, we find for the momentum space wave function

$$\psi_z(p) = \langle p|z\rangle = e^{\frac{1}{2}iI_k R_k} e^{-iR_k p_k} \psi_0(p - I). \quad (5.19)$$

Expectation values in the coherent state can thus be easily related to vacuum expectation values,

$$\begin{aligned} \langle z|\mathcal{O}(x)|z\rangle &= \int d^3x \psi_0^*(x - R) \mathcal{O}(x) \psi_0(x - R) \\ &= \int d^3x \psi_0^*(x) \mathcal{O}(x + R) \psi_0(x) \\ &= \langle 0|\mathcal{O}(x + R)|0\rangle \end{aligned} \quad (5.20)$$

For an operator $\mathcal{O}(x, p)$ that depends on both x and p , an equivalent relation is derived. The most general form shall be referred to as the *shift rule*:

$$\begin{aligned} \langle z | \mathcal{O}(x, p) | z \rangle &= \langle 0 | e^{-iI_k x_k} \mathcal{O}(x + R, p) e^{iI_k x_k} | 0 \rangle \\ &= \langle 0 | \mathcal{O}(x + R, p + I) | 0 \rangle \end{aligned} \quad (5.21)$$

The utility of the above identities can be presented in a simple example. Consider the three-dimensional harmonic oscillator (5.10) and construct coherent states as defined above, Eq. (5.13). Now think of the particles as charged and an external electric field \mathcal{E} being switched on, $H \rightarrow H' = H - q\mathcal{E} \cdot x$. A prime in this chapter shall always indicate that external fields are present. Let $x = x_{\parallel} + x_{\perp}$ be split into a vector x_{\parallel} parallel to \mathcal{E} and one perpendicular to it (accordingly for R). The energy $E'(z)$ in the coherent state is readily calculated using the shift rule (5.21),

$$\begin{aligned} E'(z) &= \langle z | H' | z \rangle = E_0 + \omega |z|^2 - q\mathcal{E} \cdot \langle 0 | x + R | 0 \rangle \\ &= E_0 + \frac{1}{2}\omega\sigma^2 I^2 + \frac{1}{2}\frac{\omega}{\sigma^2} R_{\perp}^2 + \frac{1}{2}\frac{\omega}{\sigma^2} \left(R_{\parallel} - \frac{q\mathcal{E}}{m\omega^2} \right)^2 - \frac{q^2 \mathcal{E}^2}{2m\omega^2}. \end{aligned} \quad (5.22)$$

Minimizing $E'(z)$ clearly gives $I = R_{\perp} = 0$ and $R_{\parallel} = \frac{q\mathcal{E}}{m\omega^2}$. The wave function $\psi_0(x)$ is therefore shifted to $\psi_z(x) = \psi_0(x - \frac{q\mathcal{E}}{m\omega^2})$. This happens to be the exact vacuum wave function of H' , as seen directly by quadratic completion,

$$H' = \frac{p^2}{2m} + \frac{1}{2}m\omega^2 x_{\perp}^2 + \frac{1}{2}m\omega^2 \left(x_{\parallel} - \frac{q\mathcal{E}}{m\omega^2} \right)^2 - \frac{q^2 \mathcal{E}^2}{2m\omega^2} \quad (5.23)$$

The ground state energy (actually the entire spectrum) is shifted to $E'_0 = E_0 - \frac{q^2 \mathcal{E}^2}{2m\omega^2}$.

In Yang–Mills theory, a less trivial situation is encountered. The Hamiltonian H is not diagonalized exactly, but by means of the variational principle a quasi-particle basis can be set up. A coherent state constructed in this basis is used to calculate the expectation value of H' , and minimize the latter. We now discuss a comparable quantum mechanic example. Let the anharmonic oscillator be defined by

$$H_{\text{anh.}} = \frac{p^2}{2m} + \frac{1}{2}m\omega^2 x^2 + \lambda m^2 \omega^3 x^4, \quad \lambda \in \mathbb{R}^+ \quad (5.24)$$

may be a helpful quantum mechanic example. We also fail to diagonalize this Hamiltonian, but a Gaussian ansatz as in Eq. (5.12) with σ as a variational parameter aids to find an approximate ground state. Its width σ can be shown to yield for

$$\sigma^2 = \frac{1}{30\lambda m\omega} \left(C^{1/3} + C^{-1/3} - 1 \right), \quad C = 1350\lambda^2 + 30\sqrt{2025\lambda^4 - 3\lambda^2} - 1 \quad (5.25)$$

the minimal energy⁴

$$E_0 = \frac{3}{4m\sigma^2} + \frac{3}{4}m\omega^2\sigma^2 + \frac{15}{4}\lambda m^2 \omega^3 \sigma^4. \quad (5.26)$$

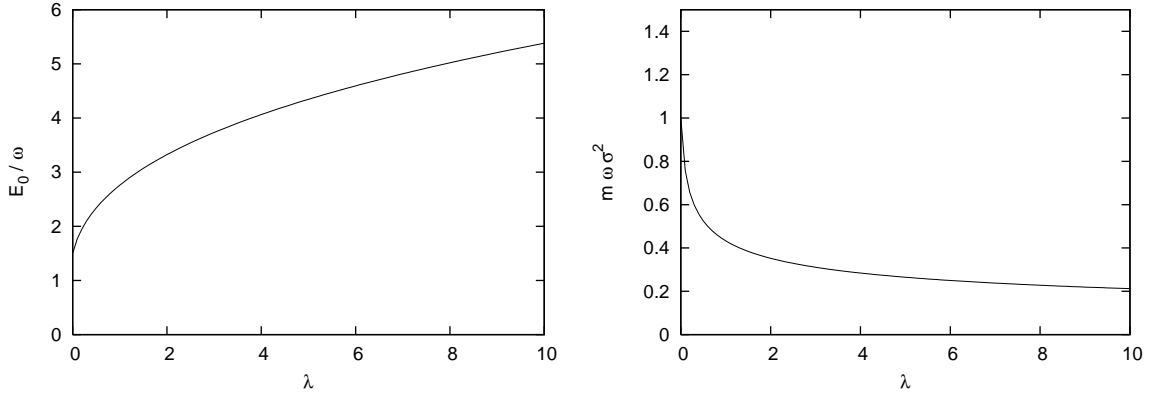


Figure 5.1: Variational solution for the ground state of the anharmonic oscillator. Left: Energy E_0 as a function of the parameter λ of the quartic potential. Right: Width σ of the Gaussian ground state, as a function of λ .

As can be seen in Fig. 5.1, the Gaussian ground state wave functional becomes narrower for increasing the coefficient λ of the quartic potential, while the energy increases. Note that for $\lambda \rightarrow 0$, the results for the harmonic oscillator are recovered. For a comparison to field theory, we discuss the variational solution to the ϕ^4 theory in the Hamiltonian approach in appendix D.

Similarly to the variational approach to YM theory, we have found an approximate Gaussian ground state and can create quanta by the creation operator in Eq. (5.11) with the Gaussian width σ given by Eq. (5.25). Now switch on an external electric field,

$$H'_{\text{anh.}} = H_{\text{anh.}} - q\mathcal{E} \cdot x \quad (5.27)$$

and calculate the energy in the coherent state. The result gives the ground state energy E_0 , see Eq. (5.26), and a correction dependent on z ,

$$\begin{aligned} E'(z) &= \langle z | H'_{\text{anh.}} | z \rangle \\ &= E_0 + \frac{I^2}{2m} + \lambda m^2 \omega^3 \sigma^4 R^4 + \frac{1}{2} m \omega^2 (1 + 18 \lambda m \omega \sigma^2) R^2 - q\mathcal{E} \cdot R \end{aligned} \quad (5.28)$$

For $z = 0$, the energy $E'(z)$ is equal to E_0 , as expected. Minimizing $E'(z)$ w.r.t. z yields some value z^{min} . The result will depend on the parameter λ of the quartic potential and the electric force $F = -q\mathcal{E}$. Without giving the result explicitly, we can see from Eq. (5.28) that for all values of $\lambda > 0$ and $F \neq 0$ there exists a $z^{\text{min}} = R_{\parallel}^{\text{min}} \neq 0$ such that $E'(R_{\parallel}^{\text{min}}) < E_0$, i.e. the energy is lowered in the coherent state.

We now turn back to the original task, writing down a coherent state in the quasi-particle basis of Yang–Mills theory. The over-complete set of states, here given by Eq. (5.9), incorporates

⁴A lowest-order expansion for small λ agrees with Ref. [157] for the one-dimensional case. Particular care is required concerning the Riemann sheets when taking the $\lambda \rightarrow 0$ limit.

already the nontrivial effects of the Hamiltonian H (1.107) without external charges, similar to the treatment of the quartic quantum mechanic potential above. Using these states, the coherent state for Yang–Mills theory is introduced here by

$$|\tilde{Z}\rangle = \tilde{U}|\tilde{0}\rangle \quad (5.29)$$

with

$$\tilde{U} = \exp \left\{ \int d^3x \left(Z_k^a(x) a_k^a(x)^\dagger - Z_k^a(x)^* a_k^a(x) \right) \right\}, \quad (5.30)$$

where the field $Z_k^a(x)$ controls the excitations of gluons. By means of Eq. (5.4), one can rewrite U in terms of field operators,

$$\tilde{U} = \exp \left\{ \int d^3x \left(iI_k^a(x) A_k^a(x) - iR_k^a(x) \Pi_k^a(x) \right) \right\}, \quad (5.31)$$

where the abbreviations

$$R_j^a(x) = \sqrt{2} \int d^3x' \alpha_{jk}(x, x') \operatorname{Re} (Z_k^a(x')) \quad (5.32a)$$

$$I_j^a(x) = \sqrt{2} \int d^3x' \alpha_{jk}^{-1}(x, x') \operatorname{Im} (Z_k^a(x')) \quad (5.32b)$$

were used. The expectation value of the Hamiltonian with charges, $H' = H + H_{\text{ext}}$, in the state (5.29) will be calculated in the next section. Optimistically, we may hope that in analogy to the quantum mechanical example, a nontrivial solution for a coherent state exists that lowers the energy.

We provide here the definition of the coherent state energy,

$$E[Z] := \langle \tilde{Z} | \tilde{H} | \tilde{Z} \rangle_{\text{flat}} = \int \mathcal{D}A \left(\tilde{U} \tilde{\Psi} \right)^* \tilde{H} \left(\tilde{U} \tilde{\Psi} \right). \quad (5.33)$$

It is important to clarify which state it refers to as a Coulomb gauge expectation value of H (not \tilde{H}). Carefully treating operator ordering, the energy (5.33) can be rewritten as a Coulomb gauge expectation value,

$$\begin{aligned} E[Z] &= \int \mathcal{D}A \tilde{\Psi}^* \tilde{U}^\dagger \tilde{H} \tilde{U} \tilde{\Psi} \\ &= \int \mathcal{D}A \left(\sqrt{\mathcal{J}} \Psi^* \right) \left(\frac{1}{\sqrt{\mathcal{J}}} U^\dagger \sqrt{\mathcal{J}} \right) \left(\sqrt{\mathcal{J}} H \frac{1}{\sqrt{\mathcal{J}}} \right) \left(\sqrt{\mathcal{J}} U \frac{1}{\sqrt{\mathcal{J}}} \right) \left(\sqrt{\mathcal{J}} \Psi \right) \\ &= \int \mathcal{D}A \mathcal{J} \Psi^* \left(\frac{1}{\mathcal{J}} U^\dagger \mathcal{J} \right) H U \Psi \\ &= \int \mathcal{D}A \mathcal{J} (U \Psi)^* H (U \Psi) \\ &\equiv \langle U \Psi | H | U \Psi \rangle \end{aligned} \quad (5.34)$$

It is seen that by calculating $E[Z]$ via the auxiliary expectation value (5.33) with a flat measure, the Coulomb gauge expectation value of the Hamiltonian H is taken in the state

$$|Z\rangle = U |0\rangle, \quad (5.35)$$

cf. Eq. (5.29). The corresponding wave functional is obtained by acting with U on the vacuum wave functional $\Psi[A]$. With \tilde{U} given by Eq. (5.30), a Campbell-Baker-Hausdorff formula is needed to find $U = \mathcal{J}^{-1/2} \tilde{U} \mathcal{J}^{1/2}$. From Eq. (5.17), it can be derived that for $[X, [X, Y]]$ and $[Y, [X, Y]]$ c -numbers,

$$e^Y e^X e^{-Y} = e^{X - [X, Y] - \frac{1}{2}[Y, [X, Y]]} . \quad (5.36)$$

Using this relation, and the one-loop Gaussian approximation for the Faddeev–Popov determinant (3.13), we find after some algebra

$$U = e^{-\frac{1}{2} \int R_X R + \int A_X R} \tilde{U} . \quad (5.37)$$

5.3 Energy of Yang–Mills theory in the coherent state

In this section, the calculation of the energy $E'[Z]$ in the coherent state is presented. First of all, let us clarify how this energy is defined. The coherent state (5.35) is used to calculate the expectation value of the Yang–Mills Hamiltonian (1.107) in the presence of external charges $\rho_{\text{ext}}^a(x)$. Without external charges, the Hamiltonian reads

$$H = H_k + H_p + H_C^{(0)} \quad (5.38)$$

with the definitions of the kinetic part,

$$H_k = \frac{1}{2} \int d^d x \frac{1}{\mathcal{J}[A]} \Pi_k^a(x) \mathcal{J}[A] \Pi_k^a(x) \quad (5.39)$$

the magnetic potential part,

$$H_p = \frac{1}{4} \int d^d x F_{ij}^a(x) F_{ij}^a(x) \quad (5.40)$$

and the Coulomb part H_C of the Hamiltonian which involves a contribution coming from dynamical gluonic charges,

$$H_C^{(0)} = \frac{g^2}{2} \int d^d [xy] \frac{1}{\mathcal{J}[A]} \rho_{\text{dyn}}^a(x) \mathcal{J}[A] F^{ab}(x, y) \rho_{\text{dyn}}^b(y) . \quad (5.41)$$

In the presence of external charges, the total charge distribution $\rho^a(x) = \rho_{\text{dyn}}^a(x) + \rho_{\text{ext}}^a(x)$ adds extra terms to the Coulomb part H_C , so that the Hamiltonian under consideration reads

$$H' = H + H_C^{(1)} + H_C^{(2)} \quad (5.42)$$

with

$$H_C^{(1)} = \frac{g^2}{2} \int d^d [xy] \left(\frac{1}{\mathcal{J}[A]} \rho_{\text{dyn}}^a(x) \mathcal{J}[A] F^{ab}(x, y) \rho_{\text{ext}}^b(y) + \rho_{\text{ext}}^a(x) F^{ab}(x, y) \rho_{\text{dyn}}^b(y) \right) \quad (5.43)$$

and

$$H_C^{(2)} = \frac{g^2}{2} \int d^d [xy] \rho_{\text{ext}}^a(x) F^{ab}(x, y) \rho_{\text{ext}}^b(y) . \quad (5.44)$$

The energy in the presence of external charges in the coherent state $|Z\rangle$ is defined by

$$E'[Z] = \langle Z | H' | Z \rangle , \quad (5.45)$$

where this expectation value involves after Coulomb gauge fixing the Faddeev–Popov determinant \mathcal{J} . For the calculation of $E'[Z]$, it will be extremely helpful to employ the shift rule as it was written down in Eq. (5.21) for the quantum mechanic oscillator. Here, we can find the equivalent “shifting effect” of the operator \tilde{U} , given in Eq. (5.30), on the operator \tilde{H}' (the use of the tilde was explained in Eq. (5.3)),

$$\begin{aligned} E'[Z] &= \langle \tilde{Z} | \tilde{H}'[A, \Pi] | \tilde{Z} \rangle_{\text{flat}} \\ &= \langle \tilde{0} | \tilde{H}'[A + R, \Pi + I] | \tilde{0} \rangle_{\text{flat}} \end{aligned} \quad (5.46)$$

In the calculations below, we always use the transformations (5.3), ending up with the flat scalar product $\langle | \rangle_{\text{flat}}$. For brevity, the notation

$$\langle \tilde{\mathcal{O}} \rangle_{\omega} = \langle \tilde{0} | \tilde{\mathcal{O}} | \tilde{0} \rangle_{\text{flat}} , \quad \langle \tilde{\mathcal{O}} \rangle_Z = \langle \tilde{Z} | \tilde{\mathcal{O}} | \tilde{Z} \rangle_{\text{flat}} \quad (5.47)$$

is used. Furthermore, recall the matrix notation in coordinate space from chapter 1. It will sometimes be convenient in this chapter as well. The spatial dimension d is left unspecified.

The energy $E'[Z]$ can be expressed by the results from chapter 3 if we set $Z = 0$,

$$E'[0] = E + V_C . \quad (5.48)$$

Here, E is the vacuum energy displayed below Eq. (3.19) and V_C is the Coulomb potential (2.73) in the vacuum state. In Eq. (5.48), there are no contributions coming from $H_C^{(1)}$,

$$\begin{aligned} E_C^{(1)}[0] &= \langle \tilde{H}_C^{(1)} \rangle_{\omega} \\ &= \frac{1}{2} \langle \tilde{\rho}_{\text{dyn}}^{\dagger} F \rho_{\text{ext}} + \rho_{\text{ext}} F \tilde{\rho}_{\text{dyn}} \rangle_{\omega} \\ &= \frac{g^2}{2} \left\langle \left((i\hat{A}Q)^* F \rho_{\text{ext}} + \rho_{\text{ext}} F (i\hat{A}Q) \right) \right\rangle_{\omega} \\ &= 0 \end{aligned} \quad (5.49)$$

We will see that in the coherent state the mixed term $H_C^{(1)}$ does have a contribution to the energy. Let us emphasize that it is instructive to stick to the coordinate space representation of the Green functions. The transformation to momentum space is helpful in the vacuum where thus an overall infinite factor $(2\pi)^d \delta^d(0)$ can be extracted from the energy, due to translational invariance. The coherent state, on the other hand, accounts for localized external color charges and translational invariance is lost. Therefore, an overall volume factor cannot be expected and the Fourier transformation provides no simplification whatsoever.

Let us turn to the calculation of the kinetic energy in the coherent state. The kinetic part \tilde{H}_k in Eq. (5.39) comprises the operator

$$\tilde{\Pi}_k^a(x)[A, \Pi] = \Pi_k^a(x) - \frac{1}{2i} \frac{\delta \ln \mathcal{J}[A]}{\delta A_k^a(x)} \quad (5.50)$$

that may be understood as a function of A and Π . Applying the shift rule (5.46), we obtain

$$\begin{aligned} E_k[Z] &= \left\langle H_k[A, \tilde{\Pi}[A, \Pi]] \right\rangle_Z = \left\langle H_k[A + R, \tilde{\Pi}[A + R, \Pi + I]] \right\rangle_\omega \\ &= \frac{1}{2} \int d^d x \int \mathcal{D}A \left| \tilde{\Pi}_i^a(x)[A + R, \Pi + I] \tilde{\Psi}[A] \right|^2. \end{aligned} \quad (5.51)$$

With the explicit form (5.3) of the Gaussian vacuum wave functional $\tilde{\Psi}[A] = \langle A | \tilde{0} \rangle$, we use

$$\tilde{\Pi}_k[A + R, \Pi] \tilde{\Psi}[A] = iQ_k[A; R] \tilde{\Psi}[A] \quad (5.52)$$

to define

$$Q_k^a(x)[A; R] = \int d^d x' \omega_{kj}^{ab}(x, x') A_j^b(x') + \frac{1}{2} \frac{\delta \ln \mathcal{J}[A + R]}{\delta A_k^a(x)} \quad (5.53)$$

with the obvious notation $\omega_{ij}^{ab}(x, y) = \delta^{ab} t_{ij}(x) \omega(x, y)$. The kinetic energy in the coherent state thus yields schematically

$$E_k[Z] = \frac{1}{2} \text{Tr} \left(\omega \langle AA \rangle \omega + \omega \left\langle A \frac{\delta \ln \mathcal{J}}{\delta A} \right\rangle + \frac{1}{4} \left\langle \frac{\delta \ln \mathcal{J}}{\delta A} \frac{\delta \ln \mathcal{J}}{\delta A} \right\rangle \right) + \frac{1}{2} \int d^d x I^2(x) \quad (5.54)$$

which we calculate, following Ref. [83], with a quadratic completion. To this end, define the curvature χ_Z by

$$\begin{aligned} (\chi_Z)_{ij}^{ab}(x, y) &:= -\frac{1}{2} \left\langle \frac{\delta^2 \mathcal{J}[A + R]}{\delta A_i^a(x) \delta A_j^b(y)} \right\rangle_\omega \\ &= +\frac{1}{2} \text{Tr} \left\langle G[A + R] \Gamma_i^{0,a}(x) G[A + R] \Gamma_j^{0,b}(y) \right\rangle_\omega \end{aligned} \quad (5.55)$$

With the definition of the ghost propagator D_G^Z with a coherent background field,

$$D_G^{Z,ab}(x, y) = \langle G[A] \rangle_Z^{ab}(x, y), \quad (5.56)$$

the curvature (5.55) can be expressed by

$$(\chi_Z)_{ij}^{ab}(x, y) = \frac{1}{2} \text{Tr} D_G^Z \Gamma_i^{Z,a}(x) D_G^Z \Gamma_j^{0,b}(y). \quad (5.57)$$

This implicitly establishes a definition of the proper ghost-gluon vertex $\Gamma_i^{Z,a}(x)$ in the coherent state; the latter will in actual calculations be rendered tree-level, as before. Now, the second term in Eq. (5.54) can be written using a partial integration as

$$\begin{aligned} \left\langle A_i^a(x) \frac{\delta \ln \mathcal{J}[A + R]}{\delta A_j^b(y)} \right\rangle_\omega &= \frac{1}{2} \int d^d z (\omega^{-1})_{ik}^{ac}(x, z) \left\langle \frac{\delta^2 \mathcal{J}[A + R]}{\delta A_k^c(z) \delta A_j^b(y)} \right\rangle_\omega \\ &= - \int d^d z (\omega^{-1})_{ik}^{ac}(x, z) (\chi_Z)_{kj}^{cb}(z, y) \end{aligned} \quad (5.58)$$

In the one-loop approximation, one can realize by expansion of the Faddeev–Popov operators that the third term in Eq. (5.54), $\left\langle \frac{\delta \ln \mathcal{J}}{\delta A} \frac{\delta \ln \mathcal{J}}{\delta A} \right\rangle$, is simply obtained by writing the first two terms as a modulo square. With $Q = Q[A; R]$ as in Eq. (5.53), one thus finds

$$\left\langle Q_i^a(x) Q_j^b(y) \right\rangle_\omega = \frac{1}{2} \int d^d [uv] [\omega - \chi_Z]_{ik}^{ac}(x, u) \omega^{-1}(u, v) [\omega - \chi_Z]_{kj}^{cb}(v, y) \quad (5.59)$$

and is ready to write down the result for the kinetic energy,

$$E_k[Z] = \frac{1}{4} \int d^d[xyz][\omega - \chi_Z]_{ij}^{ab}(x, y) \omega^{-1}(y, z)[\omega - \chi_Z]_{ji}^{ba}(z, x) + \frac{1}{2} \int d^d x I_k^a(x) I_k^a(x). \quad (5.60)$$

By setting the coherent field to zero, $Z = 0$, the vacuum result (3.20) is recovered.

We now proceed to the Coulomb part H_C of the Hamiltonian where Eq. (5.41) amounts to the Coulomb interaction of gluonic charges,

$$\tilde{\rho}_{\text{dyn}}^a(x)[A, \Pi] = \hat{A}_k^{ab}(x) \tilde{\Pi}_k^b(x)[A, \Pi] \quad (5.61)$$

Taking the expectation value of such operators, relation (5.52) can be used. Noting that $E_C^{(0)}[Z] = \langle \tilde{H}_C^{(0)}[A, \Pi] \rangle_Z$ is a modulo square, the imaginary terms can be explicitly eliminated to find

$$\begin{aligned} E_C^{(0)}[Z] &= \frac{g^2}{2} \int d^d[xy] \left\langle (\hat{A} + \hat{R})_k^{ab}(x) I_k^b(x) F^{ac}(x, y) [A + R] (\hat{A} + \hat{R})_j^{cd}(y) I_j^d(y) \right\rangle_\omega \\ &+ \frac{g^2}{2} \int d^d[xy] \left\langle (\hat{A} + \hat{R})_k^{ab}(x) Q_k^b(x) F^{ac}(x, y) [A + R] (\hat{A} + \hat{R})_j^{cd}(y) Q_j^d(y) \right\rangle_\omega \end{aligned} \quad (5.62)$$

with $Q = Q[A; R]$ as given in Eq. (5.53). To 2-loop order in the energy, there are no contractions with the operator F . On the assumption that D_G^Z is symmetric in color and coordinate space separately (just like D_G), we have

$$\langle Q_k(x)[A; R] \rangle_\omega = \frac{1}{2} \text{Tr} D_G^Z \Gamma_k^0(x) = 0. \quad (5.63)$$

The non-vanishing contractions in Eq. (5.62) then are

$$\left\{ \langle \overline{AQFAQ} \rangle, \langle \overline{AQFAQ} \rangle, RI \langle F \rangle RI, \langle \overline{AIFAI} \rangle, \langle \overline{RQFRQ} \rangle \right\}.$$

A careful treatment of all indices gives⁵

$$\begin{aligned} E_C^{(0)}[Z] &= -\frac{g^2}{8} \int d^d[xy] (\hat{T}^g)^{bb'} F_Z^{b'd'}(x, y) (\hat{T}^h)^{d'd} \\ &\left\{ (\omega^{-1})_{ij}^{gh}(x, y) \int d^d[uv] [\omega - \chi_Z]_{ik}^{be}(x, u) \omega^{-1}(u, v) [\omega - \chi_Z]_{kj}^{ed}(v, y) \right. \\ &+ \left(t_{ij}^{gd}(x) \delta^d(x, y) - \int d^d w \omega^{-1}(x, w) (\chi_Z)_{ij}^{gd}(w, y) \right) \\ &\left. \left(t_{ij}^{bh}(x) \delta^d(x, y) - \int d^d w \omega^{-1}(x, w) (\chi_Z)_{ij}^{bh}(w, y) \right) \right\} \\ &+ \frac{g^2}{2} \int d^d[xy] \hat{R}_k^{ab}(x) I_k^b(x) F_Z^{ac}(x, y) \hat{R}_j^{cd}(y) I_j^d(y) \\ &- \frac{g^2}{4} \int d^d[xy] \omega_{ij}^{-1}(x, y) \text{tr} \left(\hat{I}_i(x) F_Z(x, y) \hat{I}_j(y) \right) \\ &- \frac{g^2}{4} \int d^d[xyuv] [\omega - \chi_Z]_{ik}^{ac}(x, u) \omega^{-1}(u, v) [\omega - \chi_Z]_{kj}^{cb}(v, y) \hat{R}_i^{ad}(x) F_Z^{de}(x, y) \hat{R}_j^{eb}(y) \end{aligned} \quad (5.64)$$

⁵The vacuum result (3.22) can be recovered for $Z = 0$ by using $\text{tr}(\hat{T}^a \hat{T}^a) = -N_c(N_c^2 - 1)$.

where we assigned

$$F_Z^{ab}(x, y) := \langle F^{ab}(x, y)[A] \rangle_Z. \quad (5.65)$$

The expectation value of the dynamical charge $\rho_{\text{dyn}} = -\hat{\mathbf{A}} \cdot \mathbf{\Pi}$ in the coherent state is in view of Eq. (5.63)

$$\langle \tilde{\rho}_{\text{dyn}}^a(x)[A, \mathbf{\Pi}] \rangle_Z = -\hat{R}_k^{ab}(x) I_k^b(x). \quad (5.66)$$

Hence, the mixed terms $\sim \rho_{\text{dyn}} F \rho_{\text{ext}}$ in the Coulomb energy yield without contractions of the Coulomb operator F

$$E_C^{(1)}[Z] = -g^2 \int d^d[xy] \hat{R}_k^{ab}(x) I_k^b(x) F_Z^{ac}(x, y) \rho_{\text{ext}}^c(y). \quad (5.67)$$

The Coulomb energy of solely external charges obviously yields

$$E_C^{(2)}[Z] = \frac{g^2}{2} \int d^d[xy] \rho_{\text{ext}}^a(x) F_Z^{ab}(x, y) \rho_{\text{ext}}^b(y). \quad (5.68)$$

The magnetic potential energy in the coherent state is yet to be calculated. With the Hamiltonian given by Eq. (5.40), we find that the vacuum energy $E_p[0]$ as given in Eq. (3.21) is found in addition to terms involving the coherent field,

$$\begin{aligned} E_p[Z] &= E_p[0] \\ &+ \frac{1}{4} g^2 \int d^d x f^{eab} f^{ecd} R_i^a(x) R_j^b(x) R_i^c(x) R_j^d(x) \\ &+ g \int d^d x f^{abc} (\partial_i R_j^a(x)) R_i^b(x) R_j^c(x) \\ &+ \frac{1}{2} \int d^d x R_i^a(x) (-\partial^2) R_i^a(x) \\ &+ \frac{1}{4} g^2 N_c \frac{(d-1)^2}{d} \omega^{-1}(0, 0) \int d^d x (R_k^a(x))^2 \end{aligned} \quad (5.69)$$

All but the last term, call it $E_p^{\text{div}}[Z]$, are quite trivially obtained using the shift rule (5.47). Since it is divergent, let us look at it more carefully. It comes from the quartic part of H_p after applying the shift rule and contracting two gauge fields A , leaving two coherent fields R ,

$$\begin{aligned} E_p^{\text{div}}[Z] &= \frac{1}{4} g^2 \int d^d x \left\{ \langle A_i(x) \hat{R}_j(x) \hat{R}_i(x) A_j(x) \rangle_\omega + \langle R_i(x) \hat{A}_j(x) \hat{A}_i(x) R_j(x) \rangle_\omega \right. \\ &+ \langle A_i(x) \hat{R}_j(x) \hat{A}_i(x) R_j(x) \rangle_\omega + \langle R_i(x) \hat{A}_j(x) \hat{R}_i(x) A_j(x) \rangle_\omega \\ &\left. + \langle A_i(x) \hat{A}_j(x) \hat{R}_i(x) R_j(x) \rangle_\omega + \langle R_i(x) \hat{R}_j(x) \hat{A}_i(x) A_j(x) \rangle_\omega \right\} \end{aligned} \quad (5.70)$$

Using the symmetry of the vacuum gluon propagator, we get

$$\begin{aligned} E_p^{\text{div}}[Z] &= \frac{1}{4} g^2 \int d^d x \left\{ 2 \langle A_i(x) \hat{R}_j(x) \hat{R}_i(x) A_j(x) \rangle_\omega - 2 \langle A_i(x) \hat{R}_j(x) \hat{R}_j(x) A_j(x) \rangle_\omega \right\} \\ &= \frac{1}{4} g^2 \int d^d x \left\{ (t_{ij}(x) \omega^{-1}(x, y))|_{y=x} \text{tr} \hat{R}_j(x) \hat{R}_i(x) \right. \\ &\quad \left. - (t_{ii}(x) \omega^{-1}(x, y))|_{y=x} \text{tr} \hat{R}_j(x) \hat{R}_j(x) \right\}. \end{aligned} \quad (5.71)$$

Using a Fourier transform for $\omega^{-1}(x, y)$ and $\text{tr}(\hat{T}^a \hat{T}^b) = -N_c \delta^{ab}$, we recover the proposed expression in the last line of Eq. (5.69):

$$\begin{aligned}
 E_p^{\text{div}}[Z] &= \frac{1}{4} g^2 \text{tr}(\hat{T}^a \hat{T}^b) \\
 &\int d^d x \left\{ \left(\int \bar{d}^d p t_{ij}(p) \omega^{-1}(p) \right) R_j^a(x) \hat{R}_i^b(x) - \left(\int \bar{d}^d p t_{ii}(p) \omega^{-1}(p) \right) R_j^a(x) \hat{R}_j^b(x) \right\} \\
 &= \frac{1}{4} g^2 N_c \int \bar{d}^d p \omega^{-1}(p) \int d^d x R_i^a(x) \left(\delta_{ij}(d-1) - \delta_{ij} \frac{d-1}{d} \right) R_i^a(x) \\
 &= \frac{1}{4} g^2 N_c \frac{(d-1)^2}{d} \omega^{-1}(0, 0) \int d^d x (R_k^a(x))^2, \tag{5.72}
 \end{aligned}$$

where the identity

$$\int d^d p f(p^2) t_{ij}(p) = \delta_{ij} \frac{d-1}{d} \int d^d p f(p^2) \tag{5.73}$$

has been employed. We note here, however, that $\omega^{-1}(0, 0) = \int \bar{d}^d p \omega^{-1}(p)$ is not necessarily a well-defined quantity. Actually, if we consider that the gluon will essentially behave like a free particle for high momentum, $\tilde{\omega}(p) \rightarrow p$, there is an ultraviolet divergence of degree $d-1$, i.e. quadratic for $d=3$. We therefore have an undefined expression in the coherent state magnetic potential (5.69) which calls for renormalization.

Renormalization

The renormalization of the vacuum Green functions as discussed in chapter 3, suffices to render the shift $\Delta E'[Z] := E'[Z] - E'[0]$ of the coherent state energy from the vacuum energy finite, as will be shown now. The ultraviolet divergence in the magnetic potential energy (5.69) comes as no surprise, for the magnetic potential operator (5.40) is a highly local object. We now try to single out the divergent object from the magnetic energy (5.69). To this end, we first realize that it is contained in the quadratic term in the (terminating) Taylor series of $E_p[Z]$ about $Z=0$,

$$\begin{aligned}
 E_p[Z] &= \langle H_p[A+R] \rangle_\omega \\
 &= \langle H_p[A] \rangle_\omega + \left\langle \frac{\delta H_p[A]}{\delta A_i} \right\rangle_\omega R_i + \frac{1}{2!} \left\langle \frac{\delta^2 H_p[A]}{\delta A_i A_j} \right\rangle_\omega R_i R_j \\
 &\quad + \frac{1}{3!} \left\langle \frac{\delta^3 H_p[A]}{\delta A_i A_j A_k} \right\rangle_\omega R_i R_j R_k + \frac{1}{4!} \left\langle \frac{\delta^4 H_p[A]}{\delta A_i A_j A_k A_m} \right\rangle_\omega R_i R_j R_k R_m \tag{5.74}
 \end{aligned}$$

Such a term with a second derivative inside a Gaussian expectation value can be rewritten as, see Eq. (E.6) in the appendix,

$$\begin{aligned}
 E_p^{(R^2)}[Z] &= \frac{1}{2} \int d^d[xy] R_i^a(x) \left\langle \frac{\delta^2 H_p}{\delta A_i^a(x) \delta A_j^b(y)} \right\rangle_\omega R_j^b(y) \\
 &= -2 \int d^d[xyuv] R_i^a(x) \omega_{im}^{ac}(x, u) \frac{\delta \langle H_p \rangle_\omega}{\delta \omega_{mn}^{cd}(u, v)} \omega_{nj}^{db}(v, y) R_j^b(y) \tag{5.75}
 \end{aligned}$$

Note that $E_p^{(R^2)}[Z]$ is not given by only $E_p^{\text{div}}[Z]$ in Eq. (5.72) but also includes the other term in Eq. (5.69) that is quadratic in R .

In view of the gap equation, we know that ω was chosen to minimize the vacuum energy, $\delta\langle\tilde{H}\rangle_\omega/\delta\omega = 0$. Therefore, the divergent expression $\delta\langle H_p\rangle_\omega/\delta\omega$ in Eq. (5.75) can be expressed in terms of the kinetic vacuum energy $\langle\tilde{H}_k\rangle_\omega$ and the Coulomb vacuum energy $\langle\tilde{H}_C^{(0)}\rangle_\omega$,

$$E_p^{(R^2)}[Z] = +2 \int d^d[xyuv] R_i^a(x) \omega_{im}^{ac}(x, u) \frac{\delta\langle H_k + H_C^{(0)}\rangle_\omega}{\delta\omega_{mn}^{cd}(u, v)} \omega_{nj}^{db}(v, y) R_j^b(y). \quad (5.76)$$

The above expression is now finite if we replace the bare form factors by the renormalized ones.

To arrive at the finite expression for $E_p^{(R^2)}[Z]$, one needs to evaluate

$$\frac{\delta\langle A_m^c(u) A_n^d(v)\rangle_\omega}{\delta\omega_{ij}^{ab}(x, y)} = -\frac{1}{2}(\omega^{-1})_{im}^{ac}(x, u)(\omega^{-1})_{nj}^{db}(v, y) \quad (5.77a)$$

$$\frac{\delta\langle A_m^c(u) Q_n^d(v)\rangle_\omega}{\delta\omega_{ij}^{ab}(x, y)} = \frac{1}{2}(\omega^{-1})_{im}^{ac}(x, u) \int d^d z (\omega^{-1})_{jk}^{bg}(y, z) \chi_{kn}^{gd}(z, v) \quad (5.77b)$$

$$\begin{aligned} \frac{\delta\langle Q_m^c(u) Q_n^d(v)\rangle_\omega}{\delta\omega_{ij}^{ab}(x, y)} &= \frac{1}{2} t_{im}^{ac}(x, u) t_{jn}^{bd}(y, v) \\ &\quad - \frac{1}{2} \int d^d x' (\omega^{-1})_{ii'}^{aa'}(x, x') \chi_{i'm}^{a'c}(x', u) \int d^d y' (\omega^{-1})_{jj'}^{bb'}(y, y') \chi_{j'n}^{b'd}(y', v) \end{aligned} \quad (5.77c)$$

The implicit ω dependence of the form factors $\chi(k)$ and of the vacuum Coulomb propagator,

$$F_\omega^{ab}(x, y) := \langle F[A]\rangle_\omega^{ab}(x, y), \quad (5.78)$$

is omitted in the computation of Eq. (5.76); it would bring about two-loop terms in the equations of motion. With the relations (5.77), Eq. (5.76) can be shown to give

$$\begin{aligned} E_p^{(R^2)}[Z] &= \frac{1}{2} \int d^d[xyz] R_i^a(x) (\omega(x, y)\omega(y, z) - \chi(x, y)\chi(y, z)) R_i^a(z) \\ &\quad + \frac{g^2}{4} N_c \int d^d[xy] F_\omega(x, y) \\ &\quad \times \left\{ - \int d^d[uv] R_i^a(x) [\omega(x, u) - \chi(x, u)] t_{ij}(u) \omega^{-1}(u, v) [\omega(v, y) - \chi(v, y)] R_j^a(y) \right. \\ &\quad \quad + (t_{ij}(x) \omega^{-1}(x, y)) \int d^d[uv] R_i^a(u) [\omega(u, x)\omega(y, v) - \chi(u, x)\chi(y, v)] R_j^a(v) \\ &\quad \quad \left. - 2 \int d^d u R_i^a(x) \chi(y, u) R_j^a(u) t_{ji}(y) \left(\delta^d(y, x) - \int d^d v \omega^{-1}(y, v) \chi(v, x) \right) \right\} \end{aligned} \quad (5.79)$$

The magnetic potential energy in the coherent state thus finally yields

$$\begin{aligned} E_p[Z] - E_p[0] &= \frac{1}{4} g^2 \int d^d x f^{cab} f^{ecd} R_i^a(x) R_j^b(x) R_i^c(x) R_j^d(x) \\ &\quad + g \int d^d x f^{abc} (\partial_i R_j^a(x)) R_i^b(x) R_j^c(x) + E_p^{(R^2)}[Z] \end{aligned} \quad (5.80)$$

where $E_p[0]$ is given by Eq. (3.21) and $E_p^{(R^2)}[Z]$ by Eq. (5.79). The shift $\Delta E_p = E_p[Z] - E_p[0]$ is indeed finite for the variational solution of the coherent field (any divergence will be suppressed, for $Z = 0$ is an option).

Solution for the imaginary part of the coherent field

The energy $E'[Z]$ in the coherent state sums up the magnetic energy (5.80), the kinetic energy (5.60), and the Coulomb energy contributions (5.65), (5.67) and (5.68). The real and imaginary parts of the coherent field $Z_k^a(x)$ are to be determined by the variational principle,

$$\frac{\delta E'[Z]}{\delta R_k^a(x)} = 0, \quad \frac{\delta E'[Z]}{\delta I_k^a(x)} = 0. \quad (5.81)$$

Since the Yang–Mills Hamiltonian has cubic and quartic terms in the fields, we cannot algebraically solve these equations. However, the energy expression is quadratic in the imaginary part of Z . The relevant terms can be written in matrix notation as

$$E^{(I)} = \frac{1}{2}IMI - bI. \quad (5.82)$$

This defines the matrix M as well as b by

$$M_{ij}^{ab}(x, y) = t_{ij}^{ab}(x, y) - g^2 \hat{R}_i^{ad}(x) F_Z^{dc}(x, y) \hat{R}_j^{cb}(y) - \frac{g^2}{2} (\hat{T}^a)^{cd} \omega_{ij}^{-1}(x, y) F_Z^{de}(x, y) (\hat{T}^b)^{ec} \quad (5.83)$$

$$b_k^a(x) = g^2 \int d^d y \rho_{\text{ext}}^c(y) F_Z^{cb}(y, x) \hat{R}_k^{ba}(x) \quad (5.84)$$

The quadratic form (5.82) attains its minimal value $E^{(I)} = -\frac{1}{2}bA^{-1}b$ for

$$I_k^a(x) = \int d^d y (M^{-1})_{kj}^{ab}(x, y) b_j^b(y). \quad (5.85)$$

In order to write down the coherent state energy $E'[Z]$ minimal for the imaginary part of the coherent field, replace the fields $I_k^a(x)$ by the expression (5.85). This yields the complete energy expression

$$\begin{aligned} E'[Z] = & \frac{1}{4} \int d^d [xyz] [\omega - \chi_Z]_{ij}^{ab}(x, y) \omega^{-1}(y, z) [\omega - \chi_Z]_{ji}^{ba}(z, x) \\ & - \frac{g^2}{8} \int d^d [xy] (\hat{T}^g)^{bb'} F_Z^{b'd'}(x, y) (\hat{T}^h)^{d'd} \\ & \left\{ (\omega^{-1})_{ij}^{gh}(x, y) \int d^d [uvw] [\omega - \chi_Z]_{ik}^{be}(x, u) \omega^{-1}(u, v) [\omega - \chi_Z]_{kj}^{ed}(v, y) \right. \\ & + \left(t_{ij}^{gd}(x) \delta^d(x, y) - \int d^d w \omega^{-1}(x, w) (\chi_Z)_{ij}^{gd}(w, y) \right) \\ & \left. \left(t_{ij}^{bh}(x) \delta^d(x, y) - \int d^d w \omega^{-1}(x, w) (\chi_Z)_{ij}^{bh}(w, y) \right) \right\} \end{aligned}$$

$$\begin{aligned}
 & - \frac{g^2}{4} \int d^d[xyuv] [\omega - \chi_z]_{ik}^{ac}(x, u) \omega^{-1}(u, v) [\omega - \chi_z]_{kj}^{cb}(v, y) \left(\hat{R}_i(x) F_Z(x, y) \hat{R}_j(y) \right)^{ab} \\
 & + \frac{g^2}{2} \int d^d[xy] \rho_{\text{ext}}^a(x) F_Z^{ab}(x, y) \rho_{\text{ext}}^b(y) \\
 & + g^4 \int d^d[xyuv] \rho_{\text{ext}}^a(x) F_Z^{ab}(x, u) \hat{R}_i^{bc}(u) (M^{-1})_{ij}^{cc'}(u, v) \hat{R}_j^{c'd}(v) F_Z^{de}(v, y) \rho_{\text{ext}}^e(y) \\
 & + E_p[0] \\
 & + \frac{1}{4} g^2 \int d^d x f^{eab} f^{ecd} R_i^a(x) R_j^b(x) R_i^c(x) R_j^d(x) \\
 & + g \int d^d x f^{abc} (\partial_i R_j^a(x)) R_i^b(x) R_j^c(x) \\
 & + \frac{1}{2} \int d^d[xyz] R_i^a(x) (\omega(x, y) \omega(y, z) - \chi(x, y) \chi(y, z)) R_i^a(z) \\
 & + \frac{g^2}{4} N_c \int d^d[xy] F_\omega(x, y) \\
 & \times \left\{ - \int d^d[uv] R_i^a(x) [\omega(x, u) - \chi(x, u)] t_{ij}(u) \omega^{-1}(u, v) [\omega(v, y) - \chi(v, y)] R_j^a(y) \right. \\
 & \quad + (t_{ij}(x) \omega^{-1}(x, y)) \int d^d[uv] R_i^a(u) [\omega(u, x) \omega(y, v) - \chi(u, x) \chi(y, v)] R_j^a(v) \\
 & \quad \left. - 2 \int d^d u R_i^a(x) \chi(y, u) R_j^a(u) t_{ji}(y) \left(\delta^d(y, x) - \int d^d v \omega^{-1}(y, v) \chi(v, x) \right) \right\}
 \end{aligned} \tag{5.86}$$

with the abbreviation $(M^{-1})_{ij}^{bc}(u, v)$ given as the inverse of the matrix M in Eq. (5.83).

Estimate for translationally invariant form factors

The expression (5.86) for the energy in the coherent state is quite large and it might be useful to make crude approximations to get an idea about its main characteristics. In Eq. (5.86), the kernel $\omega(x, y)$ is fixed by the variational calculation in the absence of external charges, see chapter 3. The other Green functions, $(D_G^Z)^{ab}(x, y)$, $F_Z^{ab}(x, y)$ and $(\chi_z)_{ij}^{ab}(x, y)$, are dependent on the location of the charges and thus have lost their translational invariance. Moreover, neither the Lorentz nor the color structure can be expected to be trivial. Therefore, a minimization of the energy $E'[Z]$ is a very costly calculation, not even vaguely comparable to the challenge in solving the integral equations in the vacuum.

A possible simplification is achieved by rendering the Green functions insensitive to the presence of quarks. Setting $D_G^Z = D_G$, $\chi_z = \chi$ and $F_Z = F_\omega$, we can simplify the expression (5.86) for $E'[Z]$ quite significantly,

$$\begin{aligned}
 E'[Z] &= E_k[0] + E_C^{(0)}[0] + E_C^{(2)}[0] + E_p[R] \\
 &+ N_c \frac{g^2}{4} \int d^d[xyuv] F_\omega(x, y) R_i^a(x) [\omega - \chi](x, u) \omega_{ij}^{-1}(u, v) [\omega - \chi](v, y) R_j^a(y) \\
 &+ g^4 \int d^d[xyuv] \rho_{\text{ext}}^a(x) F_\omega(x, u) \hat{R}_i^{ab}(u) (M^{-1})_{ij}^{bc}(u, v) \hat{R}_j^{cd}(v) F_\omega(v, y) \rho_{\text{ext}}^d(y). \tag{5.87}
 \end{aligned}$$

The imaginary part of Z is already chosen so that $E'[Z]$ is minimal, this gives the last term quadratic in F_ω . The term in the second line of Eq. (5.87) is exactly cancelled by the term in $E_p[R]$ that came from the expectation value $\langle \hat{R}QF\hat{R}Q \rangle_\omega$, so that the energy shift $\Delta E' = E'[Z] - E'[0]$ yields

$$\begin{aligned}
 \Delta E'[Z] = & \frac{1}{4}g^2 \int d^d x f^{eab} f^{ecd} R_i^a(x) R_j^b(x) R_i^c(x) R_j^d(x) \\
 & + g \int d^d x f^{abc} (\partial_i R_j^a(x)) R_i^b(x) R_j^c(x) \\
 & + \frac{1}{2} \int d^d [xyz] R_i^a(x) (\omega(x, y)\omega(y, z) - \chi(x, y)\chi(y, z)) R_i^a(z) \\
 & + \frac{g^2}{4} N_c \int d^d [xyuv] F_\omega(x, y) \omega_{ij}^{-1}(x, y) R_i^a(u) [\omega(u, x)\omega(y, v) - \chi(u, x)\chi(y, v)] R_j^a(v) \\
 & - \frac{g^2}{2} N_c \int d^d [xyuv] F_\omega(x, y) R_i^a(x) \chi(y, u) R_j^a(u) t_{ji}(y) \\
 & \quad \left(\delta^d(y, x) - \int d^d v \omega^{-1}(y, v) \chi(v, x) \right) \\
 & + g^4 \int d^d [xyuv] \rho_{\text{ext}}^a(x) F_\omega(x, u) \hat{R}_i^{ab}(u) (M^{-1})_{ij}^{bc}(u, v) \hat{R}_j^{cd}(v) F_\omega(v, y) \rho_{\text{ext}}^d(y). \quad (5.88)
 \end{aligned}$$

The prominent terms are the very first and the very last ones, resembling the energy of the anharmonic oscillator (5.28) in an external electric field.⁶ Approximating $M \approx \mathbb{1}$,

$$\begin{aligned}
 \Delta E'[Z] = & -\frac{g^2}{4} \int d^d x R_j^a(x) \hat{R}_k^{ab}(x) \hat{R}_k^{bc}(x) R_j^c(x) \\
 & + g^4 \int d^d [xyu] \rho_{\text{ext}}^a(x) F_\omega(x, u) \hat{R}_k^{ab}(u) \hat{R}_k^{bc}(u) F_\omega(u, y) \rho_{\text{ext}}^c(y), \quad (5.89)
 \end{aligned}$$

and furthermore replacing the matrix $\hat{R}_k \hat{R}_k$ by its mean diagonal elements,

$$\hat{R}_k(x) \hat{R}_k(x) \approx \mathbb{1} \frac{\text{tr} \hat{R}_k(x) \hat{R}_k(x)}{\text{tr} \mathbb{1}} = -\mathbb{1} \frac{N_c}{N_c^2 - 1} \phi(x), \quad \phi(x) := R_k^a(x) R_k^a(x), \quad (5.90)$$

we get

$$\Delta E'[Z] = +\frac{g^2 N_c}{4(N_c^2 - 1)} \int d^d x \phi^2(x) - \frac{g^4 N_c}{N_c^2 - 1} \int d^d x \phi(x) \left(\int d^d y F_\omega(x, y) \rho_{\text{ext}}^a(y) \right)^2. \quad (5.91)$$

The expression (5.91) attains for $\phi(x) = 2g^2 \left(\int d^d y F_\omega(x, y) \rho_{\text{ext}}^a(y) \right)^2$ its minimal value

$$\Delta E'[Z] = -\frac{g^6 N_c}{N_c^2 - 1} \int d^d x \left(\left(\int d^d y F_\omega(x, y) \rho_{\text{ext}}^a(y) \right)^2 \right)^2. \quad (5.92)$$

By dimensional analysis we find in the infrared limit of quark separation r , noting that $F_\omega \sim \sigma_C r^{4\kappa+2-d}$ with Coulomb string tension σ_C , we get in general dimensions $\Delta E'[Z] \sim -\sigma_C^4 r^{16\kappa+11-4d}$ and hence for $d = 3$ and $\kappa = \frac{1}{2}$

$$\Delta E'[Z] \sim -\sigma_C^4 r^7, \quad (5.93)$$

⁶Studying the infrared limit, the third, fourth and fifth terms can be neglected since $\omega(k) = \chi(k)$ for $k \rightarrow 0$.

a completely senseless result. First of all, confinement is lost since Eq. (5.93) overwhelms the confining potential for large r . But even worse, the energy $E'[Z]$ is negative which contradicts the positive definiteness of the YM Hamiltonian.

What has been done wrong? With various ansätze, such as for $SU(2)$

$$R_k^a(x) = f^{akm} \partial_m \varphi(x), \quad (5.94)$$

the energy in the form (5.87) was minimized and the erroneous large r behavior (5.93) was confirmed. Therefore, the approximations done after Eq. (5.87) cannot be blamed, the awkward result (5.93) must come from the use of vacuum Green functions. In a sensible approach, the Green functions must take into account the presence of external charges.

The proper way to go about this has to involve solving a set of Dyson–Schwinger equations without translational invariance. One of these equations follows from the variational principle, $\delta E'[Z]/\delta Z_k^a(x) = 0$. The ghost propagator D_G^Z can be determined by the DSE

$$(D_G^Z)^{-1} = G^{-1}[R] - \Sigma_Z \quad (5.95)$$

where the self-energy Σ_Z is obtained by using the propagator D_G^Z in the definition of Σ in Eq. (2.31). A relation for the inverse ghost propagator, such as Eq. (5.95), might not be so useful. Instead, the equation

$$D_G^Z = D_G + \int d^d x \left\langle G[A] \Gamma_k^{0,a}(x) R_k^a(x) G[A+R] \right\rangle_\omega \quad (5.96)$$

seems more applicable for solving the set of integral equations.

It was not attempted to solve the DSEs in the variational coherent state. Immense computer power would be necessary and such a project is at best problematical. In the upcoming section, the effect of the coherent field on the confining property of the heavy quark potential will be discussed with alternative methods.

5.4 The gluon chain

Having learned from first approximations that the Green function need to be sensitive to the presence of external charges in order to arrive at a sensible result, we try to make estimates for such Green functions in this section. The quest for the correct wave functional has been long-standing. After Dirac’s description of the abelian case [158], the generalization to YM theories proved to be difficult [159]. There have been various attempts of formulating flux tube models (see e.g. Ref. [160]), calculations in the Hamiltonian approach to QCD [161], and also lattice calculations [162] that elaborate on the subject of the ground state in the presence of heavy quarks. One of the most intuitive notions might be the gluon chain model [163, 164, 165], and we will come back to it below.

An advantage of the variational approach is that any ansatz for the wave functional will do. A too wild guess will be rejected if it leads to a rise in the energy. If the ansatz is somewhat

sensible, however, and a decrease in the energy can be detected, this wave functional is to be favored over the vacuum wave functional. A description of the back reaction of the presence of external charges on the vacuum wave functional is then found. With this reasoning, we here try to find a coherent field $Z_k^a(x)$ that leads to a lowering of the infrared Coulomb propagator. At very high quark separation, the Coulomb energy $E_C^{(2)}[Z]$ can be expected to give a dominant contribution. We will now focus on the calculation of the respective expectation value in the coherent field.

Note that the Coulomb propagator F_Z corresponds to the vacuum counterpart F_ω with the coherent field R as a background field,

$$F_Z = \langle F[A + R] \rangle_\omega = \int \mathcal{D}A |\tilde{\Psi}[A]|^2 \exp \left[\int d^3x R_k^a(x) \frac{\delta}{\delta A_k^a(x)} \right] F[A]. \quad (5.97)$$

We find a series in the coherent field where each term is treated using the identity

$$\frac{\delta G[A]}{\delta A_k^a(x)} = G[A] \Gamma_k^{0,a}(x) G[A]. \quad (5.98)$$

Acting on the Coulomb operator $F = G G_0^{-1} G$, the variational derivative generates a sum of terms,

$$\frac{\delta F[A]}{\delta A_k^a(x)} = F[A] \Gamma_k^{0,a}(x) G[A] + G[A] \Gamma_k^{0,a}(x) F[A]. \quad (5.99)$$

One can check that the combinatorial factors cancel the $1/n!$ from the expansion of the exponential function in Eq. (5.97), and one obtains⁷

$$\begin{aligned} F_Z &= \langle F + FMG + GMF + FMGMG + GMFMG + GMGMF + \dots \rangle_\omega \\ &= \langle (\mathbb{1} + GM + GMGM + \dots) F (\mathbb{1} + MG + MGMG + \dots) \rangle_\omega \\ &\approx \sum_m \sum_n (D_G M)^m F_\omega (M D_G)^n \end{aligned} \quad (5.100)$$

with the abbreviation

$$M^{ab}(x, y) = \int d^3z R_k^c(z) (\Gamma_k^{0,c}(z))^{ab}(x, y), \quad (5.101)$$

where the tree-level ghost-gluon vertex $\Gamma_k^{0,a}(x)$ was defined in Eq. (2.20). In the last line of Eq. (5.100), the approximation of factorizing the Coulomb expectation value was employed (for a discussion, see section 3.6). We have thus expressed the Coulomb propagator F_Z in the coherent field by vacuum expectation values, i.e. the vacuum ghost propagator D_G and the vacuum Coulomb propagator F_ω (5.78), and the coherent field itself via M in Eq. (5.101).

The Coulomb potential $V_C^Z(r)$ in the coherent field is defined for a given charge distribution $\rho_{\text{ext}}^a(x)$ by

$$V_C^Z(r) := \frac{g^2}{2} \int d^3[xy] \rho_{\text{ext}}^a(x) F_Z^{ab}(x, y) \rho_{\text{ext}}^b(y), \quad (5.102)$$

⁷A proof is given by showing $(R_k \frac{\delta}{\delta A_k})^n G = n! (GM)^n G$ by induction, which is trivial, and plugging it into $G[A + R] = \sum_n \frac{1}{n!} (R_k \frac{\delta}{\delta A_k})^n G[A]$ which leads with $F = G G_0^{-1} G$ directly to the second line in Eq. (5.100).

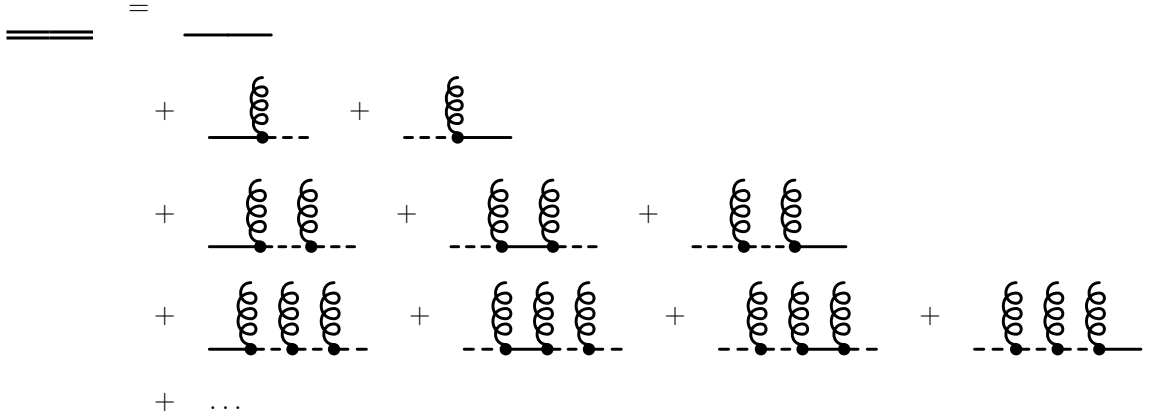


Figure 5.2: The Coulomb propagator in the coherent field, denoted by the double line on the l.h.s., and its expansion (5.100). The solid lines represent vacuum Coulomb propagators, the dashed lines vacuum ghost propagators, the dots are tree-level ghost-gluon vertices, and the wiggly lines indicate that gluons are excited by the coherent field.

cf. the vacuum Coulomb potential V_C in Eq. (2.73). With two point-like heavy charges located at the origin and at r ,

$$\rho_{\text{ext}}^a(x) = \delta^{a3} (\delta^3(x) - \delta^3(x - r)) , \quad (5.103)$$

one may think of the expectation value in Eq. (5.102) as shown in Fig. 5.2. As the charges are separated by a large distance r , it can be energetically more favorable to excite a gluon in between the charges. This notion basically corresponds to the gluon chain model proposed in Refs. [163, 164, 165]. These gluons possibly screen the potential and thus account for a lowering of the Coulomb string tension σ_C to the string tension σ_W from the gauge invariant Wilson loop. Moreover, with excited gluons along the flux tube, the thickness of the string (lacking for the one-gluon exchange) may be generated. The coherent state is suitable to check whether this mechanism is realized in the framework of the variational approach.

The guiding properties for choosing an ansatz for the coherent field are *transversality* and *symmetry*. Firstly, let us exploit transversality. The coherent field $Z_k^a(x)$, here the real part $R_k^a(x)$, is always projected transversally, i.e. it occurs only in the form $t_{jk}(x)R_k^a(x)$. Without loss of generality, we can therefore set

$$R_k^a(x) = \epsilon_{kij} \partial_i h_j^a(x) \quad (5.104)$$

and determine the field $h_k^a(x)$ instead.

Secondly, we can assume that the symmetry of the charge distribution is mirrored in the field $R_k^a(x)$. While in the absence of charges, the Green functions are translationally invariant, a charge distribution $\rho_{\text{ext}}^a(x)$ will remove this invariance, yet leaving us with some weaker

symmetry. Assume for instance, one of the charges is located at the origin of our coordinate system, and the second charge is smeared on the surface of a concentric sphere with radius r ,⁸

$$\rho_{\text{ext}}^a(\mathbf{x}) = \delta^{a3} \delta^3(\mathbf{x}) - \delta^{a3} \frac{1}{4\pi \mathbf{x}^2} \delta(|\mathbf{x}| - r) \quad (5.105)$$

The exchange energy is the same as for the charge distribution Eq. (5.103), and the choice (5.105) may therefore equally be used for the purpose of these investigations. We refer to the setting (5.105) as the *sphere picture* and Eq. (5.103) as the *string picture*. For the charge contribution of the sphere picture (5.105), the coherent field $Z_k^a(x)$ can be expected to be point symmetric,

$$\mathbf{Z}^a(D\mathbf{x}) = D\mathbf{Z}^a(\mathbf{x}), \quad (5.106)$$

that is, for any rotation $D \in SO(3)$ about an axis that contains the origin $\mathbf{x} = 0$, it behaves according to Eq. (5.106). Expanding $\mathbf{Z}^a(\mathbf{x})$ in spherical coordinates, this means that the coefficients merely depend on the distance $|\mathbf{x}|$ from the origin, The field $\mathbf{h}^a(x)$ defined in Eq. (5.104) inherits this property from $Z_k^a(x)$ via Eq. (5.32) and suggests an expansion into spherical coordinates. On the other hand, if we use the string picture, see Eq. (5.103), only a cylindrical symmetry may be expected, i.e. the rotations D are restricted to those about the symmetry axis along \mathbf{r}_0 . It is then useful to decompose $\mathbf{h}^a(\mathbf{x})$ in the cylindrical basis $\mathfrak{B}_{\mathbf{x}} = \{\mathbf{e}_\rho(\mathbf{x}), \mathbf{e}_\varphi(\mathbf{x}), \mathbf{e}_z\}$ with $\mathbf{e}_z \parallel \mathbf{r}_0$,

$$\mathbf{h}^a(\mathbf{x}) = h_\rho^a(\rho, z)\mathbf{e}_\rho(\mathbf{x}) + h_\varphi^a(\rho, z)\mathbf{e}_\varphi(\mathbf{x}) + h_z^a(\rho, z)\mathbf{e}_z. \quad (5.107)$$

Now consider the gluon chain integral (5.100).⁹ Plugging in the definition of the field $h_k^a(x)$ into the matrices M , any integral involving $h_k^a(x)$ is of the form¹⁰

$$[D_G M D_G](\mathbf{z}, \mathbf{y}) = g\epsilon_{ijk} \int d^3x \partial_i^z D_G(\mathbf{z}, \mathbf{x}) \hat{h}_j(\mathbf{x}) \partial_k^{\mathbf{x}} D_G(\mathbf{x}, \mathbf{y}) = \text{---} \overset{\text{ghost}}{\text{---}} \quad (5.108)$$

The above object corresponds to one "chain link" and the entire gluon chain is a convolution of chain links we intend to re-sum.

We may choose the first integrations as the one where the charge sitting at the origin is attached to the ghost line. This corresponds to setting $\mathbf{z} = 0$ in Eq. (5.108). The distance r between the charges being considered very large, the infrared asymptotic forms of the vacuum ghost propagator may be used. From the momentum space expression (see table 2.1), we find the dimensionally regularized ($d = 3 + 2\epsilon$) coordinate space ghost propagator

$$D_G(\mathbf{x}, \mathbf{y}) = \int \bar{d}^d k \frac{B}{(\mathbf{k}^2)^{1+\kappa}} e^{i\mathbf{k}\cdot(\mathbf{x}-\mathbf{y})} = \frac{B}{(4\pi)^{d/2}} \frac{\Gamma(\frac{d}{2} - (1 + \kappa))}{\Gamma(1 + \kappa)} \left(\frac{(\mathbf{x} - \mathbf{y})^2}{4} \right)^{(1+\kappa) - \frac{d}{2}}, \quad (5.109)$$

⁸The bold type notation for vectors is reinstated for the remainder of this chapter.

⁹A transformation to momentum space would be, on the one hand, convenient since the infrared asymptotic vacuum Green functions from chapter 2 can be used. However, a subtlety is accompanied by the Fourier transformation. The real part of the coherent field in coordinate space, $\frac{1}{2}(Z(x) + Z(x)^*)$, transfers to $\frac{1}{2}(Z(k) + Z(-k)^*)$ and only by knowledge of the parity properties of $Z(x)$ can we tell whether the above momentum space quantity is real, purely imaginary, or complex.

¹⁰Recall that a caret denotes an object in the adjoint representation. Here: $\hat{h}_j(\mathbf{x}) = \hat{T}^a h_j^a(\mathbf{x})$.

and taking the derivative as in Eq. (5.108) gives for $\kappa = \frac{1}{2}$ and $d = 3$,

$$\partial_k^{\mathbf{x}} D_G(\mathbf{x}, \mathbf{y}) = \frac{B}{4\pi^2} \partial_k^{\mathbf{x}} \Gamma(\epsilon) e^{-\epsilon \ln \frac{(\mathbf{x}-\mathbf{y})^2}{4}} \Big|_{\epsilon \rightarrow 0} = -\frac{B}{2\pi^2} \frac{x_k - y_k}{(\mathbf{x} - \mathbf{y})^2}. \quad (5.110)$$

Plugging this into the chain link (5.108), we get

$$[D_G M D_G](\mathbf{0}, \mathbf{y}) = -g \frac{B^2}{4\pi} \int d^3 x \frac{\hat{\mathbf{h}}(\mathbf{x}) \cdot (\mathbf{x} \times \mathbf{y})}{\mathbf{x}^2 (\mathbf{x} - \mathbf{y})^2} \quad (5.111)$$

The vector $\mathbf{h}(\mathbf{x})$ is expanded in the cylindrical basis $\mathfrak{B}_{\mathbf{x}}$, see Eq. (5.107), and we expand $\mathbf{x} = \rho_x \mathbf{e}_\rho(\mathbf{x}) + z_x \mathbf{e}_z$ and $\mathbf{y} = \rho_y \cos \varphi \mathbf{e}_\rho(\mathbf{x}) - \rho_y \sin \varphi \mathbf{e}_\varphi(\mathbf{x}) + z_y \mathbf{e}_z$ accordingly. The outer product in Eq. (5.111) then reads

$$\mathbf{x} \times \mathbf{y} = \begin{pmatrix} \rho_y z_x \sin \varphi \\ \rho_y z_x \cos \varphi - \rho_x z_y \\ -\rho_x \rho_y \sin \varphi \end{pmatrix}_{\mathfrak{B}_{\mathbf{x}}}. \quad (5.112)$$

The φ -integration eliminates both the ρ - and the z -component of $\mathbf{h}^a(\mathbf{x})$ in Eq. (5.111). To prove this, note that both $\hat{h}_k = \hat{h}_k(\rho, z) \forall k$ and the product $\mathbf{x} \cdot \mathbf{y} = \rho_x \rho_y \cos \varphi + z_x z_y$ that occurs in the denominator are even functions in φ . The components \hat{h}_ρ and \hat{h}_φ contribute with the outer product (5.112) a factor of $\sin \varphi$, odd in φ , and hence must vanish. We are left with $\hat{h}_\varphi(\rho, z)$, the only function that will contribute to the corrections to the Coulomb propagator.

In order to estimate the effect of the infrared ($|\mathbf{x}| \rightarrow \infty$) behavior of $\mathbf{h}^a(\mathbf{x})$, we switch to the sphere picture. This is achieved by letting $\mathbf{y} \parallel \mathbf{e}_z$ which infers $\rho_y = 0$, $\rho_y \equiv y$, and $\cos \varphi = 1$. On the assumption that a non-vanishing \hat{h}_φ component can be realized in the sphere picture, use the ansatz

$$\hat{h}_\varphi(\mathbf{x}) \sim \frac{1}{|\mathbf{x}|^{\alpha_h}}. \quad (5.113)$$

By virtue of the homogeneity of the functions in the chain link integral (5.111), one can show that for $\alpha_h < 1$, the infrared strength of the Coulomb propagation is weakened by each chain link in the series in Fig. 5.2. This means that for $r \rightarrow \infty$, the only linearly rising term would be the very first one of the expansion, the vacuum Coulomb propagator F_ω . On the other hand, if $\alpha_h > 1$, the infrared strength is enhanced by each chain link integral, meaning that for some minimal number of chain links, the integral would be divergent. Such a choice will be avoided by the variational principle. If (and only if) $\alpha_h = 1$, each chain link produces a constant factor and all terms of the expansion contribute to a linearly rising potential. The numerical value of this factor can be computed by means of the two-point integral (B.26) in the appendix which applies to Eq. (5.111) by

$$\int d^3 x \frac{|\mathbf{x} \times \mathbf{y}|}{|\mathbf{x}|^3 (\mathbf{x} - \mathbf{y})^2} = 2\pi^2. \quad (5.114)$$

The string picture will require a more involved calculation but the statement aimed at here is only on a qualitative level. It shall only be noted that with the choice $\alpha_h = 1$, the chain link

The series converges if

$$\mathbf{L}^2 < 1, \quad (5.120)$$

and the elements of C are found in view of Eq. (5.117),¹³

$$C^{ab} = \frac{1}{1 + \mathbf{L}^2} \left(\delta^{ab} + L^a L^b + \hat{L}^{ab} \right). \quad (5.121)$$

The Coulomb potential in the coherent field $V_C^Z(r)$, see Eq. (5.116), depends on the matrix element $(CC)^{33}$. Defining a string tension σ_Z by the infrared limit of the Coulomb potential $V_C^Z(r)$ in the coherent field,

$$V_C^Z(r \rightarrow \infty) = (CC)^{33} \sigma_C r =: \sigma_Z r, \quad (5.122)$$

we get from Eq. (5.121) that¹⁴

$$\sigma_Z = \frac{1 - \mathbf{L}^2 + (3 + \mathbf{L}^2) (L^3)^2}{(1 + \mathbf{L}^2)^2} \sigma_C. \quad (5.123)$$

The variables \mathbf{L}^2 and L^3 are entangled by the convergence condition (5.120). With spherical coordinates in color space, $\xi := |\mathbf{L}|$ and $L^3 =: |\mathbf{L}| \cos \eta$, Eq. (5.123) can be expressed in terms of independent variables $0 < \xi < 1$ and $0 < \eta < \pi$,

$$\sigma_Z = \left(1 - \sin^2 \eta \frac{(3 + \xi^2) \xi^2}{(1 + \xi^2)^2} \right) \sigma_C. \quad (5.124)$$

It is thus seen that

$$0 < \sigma_Z < \sigma_C, \quad (5.125)$$

i.e. the Coulomb string tension is indeed lowered by the excitation of gluons. This very notion was proposed in the gluon chain model and it follows here from an ansatz for the wave functional of $SU(2)$ YM theory with heavy quarks. The upper bound, $\sigma_Z = \sigma_C$ is reached only if $\eta = 0$, i.e. $|\mathbf{L}| = L^3$.

Depending on the coherent field $Z_k^a(\mathbf{x})$, the string tension σ_Z could in principle be lowered just above zero. In this case, \mathbf{L} has no component along the color vector $\boldsymbol{\rho}_{\text{ext}}(\mathbf{x})$, i.e. $\eta = \frac{\pi}{2}$, and its length is maximal, i.e. $|\mathbf{L}| \nearrow 1$. Thus, we find $\sigma_Z \searrow 0$. However, one may expect that this leads to a rise in the magnetic potential energy. Adding more and more gluons into the Coulomb interaction must increase this part of the energy since it is ultralocal in the coherent field, see Eq. (5.80). At a given mean number of excited gluons (the peak of the Poisson distribution), a saturation of the energy must occur. Realizing this effect computationally may be difficult, though. If the magnetic potential energy indeed saturated the number of gluons for large separations r , it would have to also rise linearly in r , otherwise it would be negligible in the asymptotic infrared.

¹³This matrix is the inverse to $\mathbb{1} - \hat{L}$, as one may expect.

¹⁴This result is sensitive to the approximations made above. At this stage, only qualitative statements can be made.

5.5 Squeezed states

Although the estimate of the Coulomb propagator in the coherent state in the previous section indicated a lowering of the string tension, it is not clear whether a full self-consistent solution will exhibit the same feature. A possible alternative description of the back reaction of the gluonic sector on the external charges may be motivated, again, from the quantum mechanic harmonic oscillator. In three dimensions, the charged oscillator can be studied in an external uniform magnetic field $\mathbf{B} = B\mathbf{e}_{\parallel}$ which couples to the angular momentum. To this end, the Hamiltonian (5.10) is supplemented by the substitution

$$p_k \rightarrow p_k - qA_k, \quad \mathbf{A} = -\frac{1}{2}\mathbf{x} \times \mathbf{B}. \quad (5.126)$$

The new Hamiltonian $H' = H + H_P + H_D$ contains the Larmor frequency $\omega_L = -\frac{qB}{2m}$ linearly in the paramagnetic term

$$H_P = \omega_L L_{\parallel}, \quad (5.127)$$

and quadratically in the diamagnetic term

$$H_D = \frac{1}{2}m\omega_L^2 \mathbf{x}_{\perp}^2. \quad (5.128)$$

The coupling of the angular momentum operator $\mathbf{L} = \mathbf{x} \times \mathbf{p}$ to the external magnetic field \mathbf{B} in H_P (5.127) is reminiscent of the coupling of the dynamical charge $\rho_{\text{dyn}}^a(x)$ of YM theory to the external charge $\rho_{\text{ext}}^a(x)$ in the Coulomb interaction $\rho_{\text{dyn}} F \rho_{\text{ext}}$. This similarity is acknowledged by noting that $\rho_{\text{dyn}}^a = -\hat{\mathbf{A}}^{ab} \cdot \mathbf{\Pi}^b$ is an outer product of coordinate and momentum operators, albeit in color space, just like the angular momentum \mathbf{L} . For the calculation of the energy in the coherent state, this has important consequences, as will be seen.

Before we focus on the coherent state, let us give the exact ground state solution of the rather simple Hamiltonian H' . The primed quantities always include the effect of the external field. Thus, we can interpret

$$H + H_D = \frac{1}{2}\omega \left(\sigma^2 \mathbf{p}_{\parallel}^2 + \sigma^{-2} \mathbf{x}_{\parallel}^2 \right) + \frac{1}{2}\omega' \left(\sigma'^2 \mathbf{p}_{\perp}^2 + \sigma'^{-2} \mathbf{x}_{\perp}^2 \right) \quad (5.129)$$

as one harmonic oscillator of frequency ω (and width $\sigma^2 = \frac{1}{m\omega}$) in the \mathbf{e}_{\parallel} -direction, and two oscillators perpendicular to it with frequency $\omega' = (\omega^2 + \omega_L^2)^{1/2}$ (and width $\sigma'^2 = \frac{1}{m\omega'}$). Using the annihilation operators

$$a_{\parallel} = \frac{1}{\sqrt{2}} \left(\sigma^{-1} x_{\parallel} + i\sigma p_{\parallel} \right), \quad a_k = \frac{1}{\sqrt{2}} \left(\sigma'^{-1} x_k + i\sigma' p_k \right), \quad k = x, y, \quad (5.130)$$

where $\mathbf{a}_{\perp} = a_x \mathbf{e}_x + a_y \mathbf{e}_y$, the Hamiltonian H' can be re-expressed, but the paramagnetic part H_P is still not diagonal. By means of a Bogoliubov transformation,

$$a_{\pm} = \frac{1}{\sqrt{2}} (a_x \pm ia_y), \quad (5.131)$$

the complete Hamiltonian is diagonal,

$$H' = \omega \left(a_z^\dagger a_z + \frac{1}{2} \right) + \omega' \left(a_+^\dagger a_+ + a_-^\dagger a_- + 1 \right) - \omega_L \left(a_+^\dagger a_+ - a_-^\dagger a_- + 1 \right), \quad (5.132)$$

in the orthogonal basis of the states $(a_+^\dagger)^{n_+} (a_-^\dagger)^{n_-} (a_z^\dagger)^{n_z} |0\rangle$. The exact ground state of H' therefore has the energy

$$E'_0 = \frac{1}{2}\omega + \sqrt{\omega^2 + \omega_L^2} > \frac{3}{2}\omega = E_0, \quad (5.133)$$

i.e. it is higher than without the external field ($\omega_L = 0$). The interesting part is that the exact ground state $\psi'_0(\mathbf{x}) = \psi'_{0,\parallel}(\mathbf{x})\psi'_{0,\perp}(\mathbf{x})$ is Gaussian,

$$\psi'_{0,\parallel}(\mathbf{x}) = \frac{1}{(\pi\sigma^2)^{1/4}} e^{-\frac{1}{2}\mathbf{x}_\parallel^2/\sigma^2}, \quad (5.134)$$

$$\psi'_{0,\perp}(\mathbf{x}) = \frac{1}{(\pi\sigma'^2)^{1/2}} e^{-\frac{1}{2}\mathbf{x}_\perp^2/\sigma'^2}, \quad (5.135)$$

but the width σ' in the directions perpendicular to the external field \mathbf{B} is changed, as compared to the width σ of the Gaussian in the direction parallel to \mathbf{B} . By switching on the external field \mathbf{B} , the ground state wave function is squeezed by a factor smaller than 1,

$$\sigma' = \sqrt{\frac{1}{1 + \frac{\omega_L^2}{\omega^2}}} \sigma, \quad (5.136)$$

in perpendicular directions.

The effect of squeezing cannot be expected from a coherent state which merely shifts the vacuum wave functional. We now construct a coherent state in the eigenbasis of H , and determine the parameters z_k by minimizing $E'(\mathbf{z}) := \langle \mathbf{z} | H' | \mathbf{z} \rangle$. This is equivalent to the approach in YM theory, see section 5.3. The minimal value $E'(\mathbf{z})$ can then be compared to E'_0 in Eq. (5.133).

Define the coherent state by

$$|\mathbf{z}\rangle = e^{\mathbf{z}\cdot\mathbf{a}^\dagger - \mathbf{z}^*\cdot\mathbf{a}} |0\rangle, \quad \mathbf{a} = \frac{1}{\sqrt{2}} (\sigma^{-1}\mathbf{x} + i\sigma\mathbf{p}) \quad (5.137)$$

and calculate the coherent state energy $E'(\mathbf{z}) = E(\mathbf{z}) + E_P(\mathbf{z}) + E_D(\mathbf{z})$,

$$E(\mathbf{z}) = \omega \left((\text{Im } \mathbf{z})^2 + (\text{Re } \mathbf{z})^2 + \frac{3}{2} \right) \quad (5.138a)$$

$$E_P(\mathbf{z}) = 2\omega_L (\text{Re } \mathbf{z}_\perp \times \text{Im } \mathbf{z}_\perp) \cdot \mathbf{e}_\parallel \quad (5.138b)$$

$$E_D(\mathbf{z}) = \frac{1}{2}m\omega_L^2 (\sigma^2 + 2\sigma^2(\text{Re } \mathbf{z}_\perp)^2) \quad (5.138c)$$

Note that the coupling of the angular momentum to the magnetic field brings about a term $E_P(z)$ linear in $\text{Im } \mathbf{z}_\perp$. This also occurs in the energy expression (5.86) of YM theory where

the coupling of ρ_{dyn} to ρ_{ext} is responsible for such a term. By quadratic completion, it is easily found that for $\text{Im } \mathbf{z} = \frac{\omega_L}{\omega} \text{Re } \mathbf{z} \times \mathbf{e}_{\parallel}$ the energy $E'(\mathbf{z})$ is minimal. In this case,

$$\begin{aligned} E'(\mathbf{z}) &= E_0 + \omega \left(1 - \frac{\omega_L^2}{\omega^2} \right) (\text{Re } \mathbf{z}_{\perp})^2 + \omega (\text{Re } \mathbf{z}_{\parallel})^2 + E_D(z) \\ &= \frac{3}{2}\omega + \frac{1}{2}\frac{\omega_L^2}{\omega} + \omega(\text{Re } \mathbf{z})^2 . \end{aligned} \quad (5.139)$$

Minimizing this expression w.r.t. $\text{Re } \mathbf{z}$, one finds that $\text{Re } \mathbf{z} = 0$ and thus $\text{Im } \mathbf{z} = 0$. Therefore, the trivial solution $|\mathbf{z}\rangle = |\mathbf{0}\rangle$ is energetically most favorable. In the first line of Eq. (5.139) one might hope for a non-trivial solution due to the minus sign. Such a situation occurs also in YM theory. However, this negative term is exactly cancelled by the diamagnetic energy (5.138c) with $\sigma^2 = \frac{1}{m\omega}$. Since the coherent state with $\mathbf{Z} = \mathbf{0}$ still gives a higher energy than the exact ground state energy (5.133),

$$E'(\mathbf{0}) - E'_0 = \omega \left(1 + \frac{1}{2}\frac{\omega_L^2}{\omega^2} - \sqrt{1 + \frac{\omega_L^2}{\omega^2}} \right) > 0 , \quad (5.140)$$

it must be inferred that the coherent state cannot mimic the squeezing of a Gaussian wave function.

Of course, the comparison of the coherent state to the quantum mechanical harmonic oscillator and the Yang–Mills theory is by no means supposed to indicate a complete analogy. For instance, quartic and cubic terms may allow for a nontrivial shifted ground state—the coherent state—to be energetically more favorable. Also, the coupling of the "outer product" ρ_{dyn} to the external field in YM theory is mediated by the Coulomb operator $F[A]$ which is dependent on the field operator A itself. Such a situation is not encountered for the harmonic oscillator and we have seen in the previous section that the expectation value of $F[A]$ in the coherent state may alone provide part of the desired effect. Despite these differences of the oscillator coupled to a magnetic field on the one hand and the gluonic vacuum with external charges on the other, it might be a useful idea to consider squeezed states as an alternative to coherent states. This is a possible future investigation. An introduction to squeezed states can be found in the literature on quantum optics [166].

Summary and outlook

The gauge principle, which is the main ingredient in the very definition of the gauge field sector, recurs in all aspects of Yang–Mills theory. Starting with the quantization procedure, discussed in chapter 1, gauge invariance requires a careful treatment which is particularly difficult for nonabelian gauge groups. The generator of (time-independent) gauge transformations is the Gauss law operator. In the canonical quantization approach, it is not possible to promote the Gauss law to an operator identity. We have shown that by means of fixing the gauge completely on the classical level and imposing quantization conditions within the Dirac bracket formalism, the Gauss law does hold on the quantum level. The gauge-fixed Hamiltonian operator thus derived determines an unambiguous time evolution of the quantum system. It agrees with the Christ-Lee Hamiltonian [24] where a projection on gauge invariant states is employed. This agreement is notably reassuring in the sense that there is no ambiguity in the choice of the quantization procedure. For Yang–Mills theory in the temporal Coulomb gauge, it makes no difference whether Dirac quantization (*first quantize, then constrain*) or constrained quantization (*first constrain, then quantize*) is used. In the light of the gravitational force, the method of quantization is to date a controversial issue.

In the temporal Coulomb gauge-fixed configuration space of Yang–Mills theory, the uniqueness of the gauge fixing condition demands the restriction to a compact region, the fundamental modular region. In the Gribov–Zwanziger scenario, this infers the enhancement of boundary effects in that region. We have investigated in chapter 2 the consequences for the Green functions in the temporal Coulomb gauge in d spatial dimensions of $(d+1)$ -dimensional Minkowski spacetime. The Landau gauge results for $(d+1)$ -dimensional Euclidean spacetime can be obtained by shifting $d \rightarrow d+1$. In the temporal Coulomb gauge, the stochastic vacuum ($\Psi[A] = 1$) is sufficient to account for the infrared asymptotics of the theory. The horizon condition, which enhances the ghost propagator in the infrared, is along with the nonrenormalization of the ghost-gluon vertex the most important feature for the infrared behavior of propagators in the temporal Coulomb or the Landau gauge. Using power law ansätze for these propagators, the set of Dyson–Schwinger equations was solved with a tree-level ghost-gluon vertex. A single infrared exponent κ can be extracted to specify the infrared power laws of both the ghost and gluon propagators, for a given dimension d . In the $3+1$ dimensional Coulomb gauge, the result $\kappa = \frac{1}{2}$ is shown to yield a heavy quark potential which rises linearly. Quark confinement is thus, qualitatively speaking, a consequence of the horizon condition. It was argued that this result, is not necessarily unique. First of all, there is one further solution for $d = 3$, $\kappa \approx 0.398$, which leads to a Coulomb potential $V_C(r)$ that rises less than linearly [83]. With the Coulomb potential being an upper bound to the gauge invariant quark potential $V_W(r)$, the latter solution would indicate that $V_W(r)$ also rises less than linearly, contradicting the lattice results. In this sense, it is more likely that the solution $\kappa = \frac{1}{2}$ is realized. Moreover, the off-shell gauge condition introduces an additional parameter ζ into the infrared analysis, on which the solution for κ generally depends, due to the approximation of the ghost-gluon vertex. It was found that all solutions but the one for $d = 3$ and $\kappa = \frac{1}{2}$ depend on the value of ζ . This infers that the latter solution is less sensitive to the approximations made. Its corre-

sponding continuous branch of solutions $\kappa_a(d) = \frac{d}{2} - 1$ as a function of the dimension d exists for all d , even for very high dimensions where the other solutions cease to exist (see Fig. 2.6). The infrared power laws were furthermore extended by an ansatz that incorporates powers of logarithms in the infrared. It was found that values for these exponents exist for which the set of integral equations is also solved in the asymptotic infrared. The power law exponents, however, remain unchanged. Hence, there is a degeneracy in the asymptotic power law solutions, also for $d = 3$ and $\kappa = \frac{1}{2}$. Qualitatively, the logarithmic corrections do not change the power law behavior and thus also not the confining property of the Coulomb potential.

A full solution for the propagators of Yang–Mills theory in the temporal Coulomb gauge is expected to show both, the infrared behavior that infers confinement and the ultraviolet behavior that agrees with perturbation theory. The variational solution to the Yang–Mills Schrödinger equation, discussed in chapter 3, provides such a solution approximatively. The Gaussian types of wave functionals were shown to reproduce exactly the infrared behavior ($\kappa = \frac{1}{2}$) anticipated in the previous chapter. Thus, numerical results with a linearly confining potential were obtained [86]. While the propagators are insensitive to the details of the wave functional, it was found that the three-gluon vertex is extremely dependent on it. For one wave functional considered, it is equally zero, whereas for another it shows a strong infrared enhancement. However, in the Dyson–Schwinger equations of the propagators the dressing of the three-gluon vertex was found to have no effect in the infrared [103]. The ghost-gluon vertex was studied in the infrared gluon limit from its corresponding Dyson–Schwinger equation. It was shown that generally the infrared limits of the vertex’ momenta are not interchangeable, except for the solution $d = 3$ and $\kappa = \frac{1}{2}$. Again, the regularity of the vertex indicates that this solution may be favored. Chapter 3 is furthermore concerned with the assessment of the approximation of the Coulomb form factor. It was shown that the horizon condition needs to be relaxed in order to arrive at a solution that satisfies the Coulomb form factor DSE. The infrared analysis of the ghost DSE and the Coulomb form factor DSE proves that a simultaneous solution with infrared divergent form factors is impossible. The so-called ”subcritical solution” [120] where the form factors are infrared finite solves all DSEs but does not provide the expected infrared behavior of the quark potential. If a critical solution exists, then the Coulomb form factor DSE, as it stands, will be violated. Higher-order effects must then be included. An approach that includes higher-order effects may be to calculate the gap equation in the form of Eq. (E.14) up to two loops (avoiding a three-loop expression for the energy density). This may be tedious but possible.

The ultraviolet tails of the variational solutions for the Coulomb gauge Green functions have the correct power law behavior but the anomalous dimensions, related to the powers of logarithms, turn out incorrect. This might be an effect of the simple Gaussian shape of the wave functional. In chapter 4, the ultraviolet gluon energy $\omega(k) \sim k \ln^{3/11} k$ and ghost form factor $d(k) \sim 1/\ln^{4/11} k$ were motivated. This followed from a nonperturbative definition of the running coupling by the ghost-gluon vertex. In a calculation carried out in both Landau and Coulomb gauge, the ghost DSE was analyzed in the asymptotic ultraviolet using appropriate ansätze. From the requirement that the nonperturbative running coupling coincide with the ultraviolet limit of perturbation theory, it can be deduced what the anomalous dimensions are to leading

order. The way to reproduce these anomalous dimensions must be to extend the Gaussian wave functional. At the very least, the gluon loop must be included. A non-trivial dressing of the three-gluon vertex, similar to Landau gauge studies, is most probably necessary. This is a possible future investigation.

Moreover, chapter 4 dealt with the infrared limit of the running coupling which can be calculated analytically. In all gauges that interpolate between the Landau and the Coulomb gauge, this value is the same, but changes discontinuously in the Coulomb gauge limit [103]. Vertex corrections to the infrared limit of the running coupling were also calculated, showing that the only solution that has no vertex correction is the one where $d = 3$ and $\kappa = \frac{1}{2}$.

The final chapter 5 uses a quasi-particle representation of gluonic excitations to incorporate the back reaction of the presence of external charges on the gluon sector. To this end, coherent states are motivated from quantum mechanical examples. The calculation of the Yang-Mills energy in the coherent state produces a vast expression that depends on a localized background field. It was possible to remove divergences from this expression by usage of the gap equation. Even after the explicit variational solution for the imaginary part of the background field, the energy expression requires some approximation to be processed further. A first approximation, rendering the Green function insensitive to the presence of external charges, yielded senseless results. Subsequently, the Coulomb potential was estimated in the asymptotic infrared by an ad hoc ansatz for the background field. It was possible to expand, calculate, and resum this expectation value and indeed show that the string tension can be lowered by such an ansatz. The determination of the exact factor by which the string tension is lowered, requires further investigation. Another quantum mechanical example was put forward to motivate that squeezed states may serve equally well for the incorporation of external charges.

A Conventions and notation

A.1 Units, metric and group conventions

Throughout this thesis, natural units are used,

$$\hbar = c = 1. \quad (\text{A.1})$$

Since $\hbar c \approx 200 \text{ MeV fm}^{-1}$, Eq. (A.1) infers that 1 fm corresponds to 200 MeV. The Minkowski metric is here defined by the metric tensor

$$(g_{\mu\nu}) = \begin{pmatrix} 1 & 0 & 0 & 0 \\ 0 & -1 & 0 & 0 \\ 0 & 0 & -1 & 0 \\ 0 & 0 & 0 & -1 \end{pmatrix} \quad (\text{A.2})$$

Antihermitian generators of group transformation in $SU(N_c)$ are normalized as follows. For the fundamental representation, we choose

$$\text{tr} \left(T^a T^b \right) = -\frac{1}{2} \delta^{ab} \quad (\text{A.3})$$

and for the adjoint representation

$$\text{tr} \left(\hat{T}^a \hat{T}^b \right) = -f^{acd} f^{bcd} = -N_c \delta^{ab}. \quad (\text{A.4})$$

It follows that

$$\text{tr} \left(\hat{T}^a \hat{T}^b \hat{T}^c \right) = -f^{ade} f^{beg} f^{cgd} = -\frac{N_c}{2} f^{abc}. \quad (\text{A.5})$$

A.2 Notation

In momentum space integration, the phase space factor 2π is absorbed by the definition

$$\bar{d}^d k := \frac{d^d k}{(2\pi)^d}, \quad (\text{A.6})$$

in analogy to \hbar . In the case of multiple integrations, the abbreviation

$$d[xyz] = dx dy dz \quad (\text{A.7})$$

is frequently used.

Matrices in coordinate and intrinsic space, for instance G , have the components $G^{ab}(x, y)$. The functional trace “Tr” is then defined by

$$\text{Tr} G = \int d^d[xy] \delta^d(x, y) \delta^{ab} G^{ab}(x, y) \quad (\text{A.8})$$

Functional determinants can be related to the functional traces (A.8) by the identity $\text{Det } G = \exp \text{Tr} \ln G$.

The Fourier transformation of a function $\mathcal{O}(x)$, operating on spacetime, defines by

$$\mathcal{O}(x) = \int \bar{d}^d p \tilde{\mathcal{O}}(p) e^{ip \cdot x} \quad (\text{A.9})$$

the function $\tilde{\mathcal{O}}(p)$ operating on momentum space. Although these are different functions, the tilde is often omitted. For a function of two variables, we may define a Fourier transform by

$$\mathcal{O}(x, y) = \int \bar{d}^d [pq] e^{ip \cdot x} \tilde{\mathcal{O}}(p, q) e^{-iq \cdot y} . \quad (\text{A.10})$$

In translationally invariant systems, $\mathcal{O}(x, y) = \mathcal{O}(x - y)$, and

$$\begin{aligned} \tilde{\mathcal{O}}(p, q) &= \int d^d [xy] e^{-ip \cdot x} \mathcal{O}(x, y) e^{iq \cdot y} \\ &= \int d^d y e^{i(q-p) \cdot y} \left\{ \int d^d x e^{-ip(x-y)} \mathcal{O}(x - y) \right\} \\ &= (2\pi)^d \delta^d(p - q) \tilde{\mathcal{O}}(p) , \end{aligned} \quad (\text{A.11})$$

such that the propagator-like object $\mathcal{O}(x - y)$ is directly related to $\tilde{\mathcal{O}}(p)$ via Eq. (A.9). Whereas in coordinate space, a matrix in coordinate and intrinsic space is denoted by a single symbol, for instance G , the Fourier transformed object is usually a function of a single momentum scale and has no color structure, cf. Eq. (2.11).

Higher n -point functions are defined equivalently. A vertex function with translational invariance, $\mathcal{O}(x, y, z) = \mathcal{O}(x - y, x - z)$, leads to

$$\begin{aligned} \tilde{\mathcal{O}}(k, q, p) &= \int d^d [xyz] e^{-ik \cdot x} \mathcal{O}(x, y, z) e^{-iq \cdot y} e^{-ip \cdot z} \\ &= \int d^d z e^{-i(p+q+k) \cdot z} \left\{ \int d^d [xy] e^{-ik \cdot (x-z)} \mathcal{O}(x - y, x - z) e^{-iq \cdot (y-z)} \right\} \\ &= (2\pi)^d \delta^d(p + q + k) \tilde{\mathcal{O}}(k, q) \end{aligned} \quad (\text{A.12})$$

and momentum is conserved by the delta function. Choosing the momentum routing sets the signs in the exponent of the definition of the Fourier transform.

Functional derivatives can be shown to yield

$$\frac{\delta}{\delta \mathcal{O}(x)} = \int \bar{d}^d p e^{-ip \cdot x} \frac{\delta}{\delta \tilde{\mathcal{O}}(p)} . \quad (\text{A.13})$$

Note that the sign in the exponent is opposite of that in Eq. (A.9).

B Two-point integrals

Here we sketch the evaluation of nonperturbative Euclidean loop integrals in asymptotic limits. According to the discussion on page 72, we can replace the integrands by their asymptotic forms and encounter the two-point integrals

$$\Xi_m(\alpha, \beta) := \int \bar{d}^d \ell \frac{(\ell \cdot k)^m}{(\ell^2)^\alpha ((\ell - k)^2)^\beta}, \quad \alpha, \beta \in \mathbb{R}, \quad m \in \mathbb{N}. \quad (\text{B.1})$$

These can be shown to be homogeneous functions of the momentum k . By a scaling of the integration variable, $\ell \rightarrow \lambda \ell$, one readily finds that since the two-point integral can only depend on the scale, it should obey $\Xi_m(\alpha, \beta) \sim (k^2)^\kappa$ and the exponent of the power law can be determined to be $\kappa = d/2 - \alpha - \beta + m$. After applying the usual trick of introducing Feynman parameters,

$$\frac{1}{C_1^\alpha C_2^\beta} = \int_0^1 dx \int_0^1 dy \delta(x + y - 1) \frac{x^{\alpha-1} y^{\beta-1}}{(xC_1 + yC_2)^{\alpha+\beta}} \frac{1}{B(\alpha, \beta)}, \quad (\text{B.2})$$

where $B(\alpha, \beta)$ is the Euler beta function, we can shift the integration variable, $\ell \rightarrow \ell - yk$. The integrand then depends on ℓ^2 only and we can integrate it out. For $m = 0, 1, 2, 3$ we need the following standard integrals [2]:

$$\int \frac{\bar{d}^d \ell}{(\ell^2 + \Delta)^n} = \frac{1}{(4\pi)^{d/2}} \frac{\Gamma(n - d/2)}{\Gamma(n)} \left(\frac{1}{\Delta}\right)^{n-d/2} \quad (\text{B.3})$$

$$\int \frac{\bar{d}^d \ell \ell_i \ell_j}{(\ell^2 + \Delta)^n} = \frac{1}{2} \delta_{ij} \frac{1}{(4\pi)^{d/2}} \frac{\Gamma(n - d/2 - 1)}{\Gamma(n)} \left(\frac{1}{\Delta}\right)^{n-d/2-1} \quad (\text{B.4})$$

Integrals with an odd number of vectors ℓ in the numerator vanish by symmetry. For our purposes, we have $\Delta = xyk^2$. The two-point integrals can be straightforwardly computed using the identity

$$\int_0^1 dx \int_0^1 dy \delta(x + y - 1) x^{\alpha-1} y^{\beta-1} = B(\alpha, \beta) = \frac{\Gamma(\alpha)\Gamma(\beta)}{\Gamma(\alpha + \beta)} \quad (\text{B.5})$$

for the Euler beta function. One then finds the results

$$\Xi_0(\alpha, \beta) = \frac{1}{(4\pi)^{d/2}} \frac{\Gamma(d/2 - \alpha)\Gamma(d/2 - \beta)\Gamma(\alpha + \beta - d/2)}{\Gamma(\alpha)\Gamma(\beta)\Gamma(d - \alpha - \beta)} (k^2)^{d/2 - \alpha - \beta} \quad (\text{B.6a})$$

$$\Xi_1(\alpha, \beta) = \frac{1}{(4\pi)^{d/2}} \frac{\Gamma(d/2 - \alpha + 1)\Gamma(d/2 - \beta)\Gamma(\alpha + \beta - d/2)}{\Gamma(\alpha)\Gamma(\beta)\Gamma(d - \alpha - \beta + 1)} (k^2)^{d/2 - \alpha - \beta + 1} \quad (\text{B.6b})$$

$$\begin{aligned} \Xi_2(\alpha, \beta) &= \frac{1}{(4\pi)^{d/2}} \frac{\Gamma(d/2 - \alpha + 2)\Gamma(d/2 - \beta)\Gamma(\alpha + \beta - d/2)}{\Gamma(\alpha)\Gamma(\beta)\Gamma(d - \alpha - \beta + 2)} (k^2)^{d/2 - \alpha - \beta + 2} \\ &+ \frac{1}{2} \frac{1}{(4\pi)^{d/2}} \frac{\Gamma(d/2 - \alpha + 1)\Gamma(d/2 - \beta + 1)\Gamma(\alpha + \beta - d/2 - 1)}{\Gamma(\alpha)\Gamma(\beta)\Gamma(d - \alpha - \beta + 2)} (k^2)^{d/2 - \alpha - \beta + 2} \end{aligned} \quad (\text{B.6c})$$

$$\begin{aligned} \Xi_3(\alpha, \beta) &= \frac{1}{(4\pi)^{d/2}} \frac{\Gamma(d/2 - \alpha + 3)\Gamma(d/2 - \beta)\Gamma(\alpha + \beta - d/2)}{\Gamma(\alpha)\Gamma(\beta)\Gamma(d - \alpha - \beta + 3)} (k^2)^{d/2 - \alpha - \beta + 3} \\ &+ \frac{3}{2} \frac{1}{(4\pi)^{d/2}} \frac{\Gamma(d/2 - \alpha + 2)\Gamma(d/2 - \beta + 1)\Gamma(\alpha + \beta - d/2 - 1)}{\Gamma(\alpha)\Gamma(\beta)\Gamma(d - \alpha - \beta + 2)} (k^2)^{d/2 - \alpha - \beta + 3} \end{aligned} \quad (\text{B.6d})$$

The above formulae are valid for those values of α , β , m only for which the integrals converge. At $\ell = k$, a pole is integrable as long as $\beta < d/2$. On the other hand, the infrared convergence at $\ell = 0$ depends on m :

$$\alpha < \begin{cases} d/2 + m/2 & \text{for even } m \\ d/2 + m/2 + 1/2 & \text{for odd } m \end{cases}. \quad (\text{B.7})$$

One can relate this inequality to the requirement that the arguments of the first gamma functions in the numerators of Eqs. (B.6) be positive. The ultraviolet convergence is contained in the third gamma function of the numerators. For convergence, the relation

$$\alpha + \beta > \begin{cases} d/2 + m/2 & \text{for even } m \\ d/2 + m/2 - 1/2 & \text{for odd } m \end{cases} \quad (\text{B.8})$$

has to be satisfied. Obviously, odd values of m , compared to even values, work “in favor” of convergence both in the infrared and in the ultraviolet, due to the angular integration. In sums of UV divergent two-point integrals, the angular integration eliminates the divergence in some cases. For instance, the Brown-Pennington projection of the gluon propagator in Landau gauge [167],

$$R_{\mu\nu}^{\zeta=d}(k) D_{\mu\nu}(k) \sim \ln \Lambda \quad (\text{B.9})$$

eliminates the unphysical quadratic divergences proportional to the metric tensor, by virtue of $R_{\mu\nu}^d(k)$ in Eq. (2.82). We demonstrate that this elimination can be due to the angular integration for the Brown-Pennington projection of the off-shell ghost loop (2.81a) for $d = 3$ and the ultraviolet ghost propagator (3.58c),

$$\begin{aligned} \chi^\zeta(k) &= g^2 \frac{N_c}{4} \int \bar{d}^3 \ell \left[1 - \zeta (\hat{\ell} \cdot \hat{k})^2 + (\zeta - 1) \frac{\ell \cdot k}{\ell^2} \right] \frac{d(\ell) d(\ell - k)}{(\ell - k)^2} \\ &= \frac{g^2 N_c}{16\pi^2} \int^\Lambda d\ell \frac{\ell^2}{\sqrt{\ln(\ell^2)}} \int_{-1}^1 dx \left[1 - \zeta x^2 + (\zeta - 1) \frac{kx}{\ell} \right] \\ &\quad \frac{1}{(\ell^2 + k^2 - 2\ell kx) \sqrt{\ln(\ell^2 + k^2 - 2\ell kx)}} \\ &= \frac{g^2 N_c}{16\pi^2} \int^\Lambda d\ell \frac{1}{\ln(\ell^2)} \left(\frac{2}{3} (3 - \zeta) + \mathcal{O}\left(\frac{k^2}{\ell^2}\right) \right) \\ &= (3 - \zeta) \mathcal{O}\left(\frac{\Lambda}{\ln(\Lambda^2)}\right) + \text{finite} \end{aligned} \quad (\text{B.10})$$

For $\zeta = d = 3$, the linear divergence of the ghost loop vanishes.

Another cancellation of UV divergences is encountered when implementing the horizon condition in the ghost DSE (2.49). The proposition claimed in section 2.6 is that although the ghost self-energy Σ is UV divergent, the naive usage of the formulae (B.6) yields the correct result for the finite difference $d^{-1}(k) - d^{-1}(0)$. The proof is here restricted to two-point integrals

$I(k) = \Xi_0(\alpha, \beta)$ with $n := \alpha + \beta$ such that $I(k)$ does not converge in the UV. Let $\frac{d}{2} > n > \frac{d}{2} - 1$. With the Feynman parameter trick (B.2), we get

$$\begin{aligned} I(k) &= \frac{1}{B(\alpha, \beta)} \int_0^1 dx \int_0^1 dy \delta(x + y - 1) x^{\alpha-1} y^{\beta-1} \int d^d \ell \frac{1}{(x\ell - y(\ell - k))^n} \\ &= \frac{\Omega_d}{(2\pi)^d B(\alpha, \beta)} \int_0^1 dx \int_0^1 dy \delta(x + y - 1) x^{\alpha-1} y^{\beta-1} J(x, y; k) \end{aligned} \quad (\text{B.11})$$

where $\Omega_d = 2\pi^{d/2}/\Gamma(d/2)$ and the function

$$J(x, y; k) = \frac{1}{2} \int_0^{\Lambda^2} d\ell^2 \frac{(\ell^2)^{\frac{d}{2}-1}}{(\ell^2 + \Delta)^n} \quad (\text{B.12})$$

with $\Delta = xyk^2$ is regulated by the UV cut-off Λ . Employ the mean-value theorem,

$$\frac{1}{(\ell^2 + \Delta)^n} = \frac{1}{(\ell^2)^n} - \frac{n\Delta}{(\ell^2 + \xi\Delta)^{n+1}}, \quad 0 < \xi < 1, \quad (\text{B.13})$$

to realize that J can be written as $J = J_{\text{reg}} + J_{\infty}$ with

$$J_{\infty} = \frac{1}{2} \frac{1}{\frac{d}{2} - n} (\Lambda^2)^{\frac{d}{2} - n} \xrightarrow{\Lambda \rightarrow \infty} \infty \quad (\text{B.14})$$

$$J_{\text{reg}}(k) = -\frac{n\Delta}{2} \int_0^{\Lambda^2} d\ell^2 \frac{(\ell^2)^{\frac{d}{2}-1}}{(\ell^2 + \xi\Delta)^{n+1}} \xrightarrow{\Lambda \rightarrow \infty} < \infty \quad (\text{B.15})$$

for the values $\frac{d}{2} > n > \frac{d}{2} - 1$ of the exponent $n = \alpha + \beta$. In order to determine $J_{\text{reg}} = J - J_{\infty}$ explicitly, write

$$\begin{aligned} J_{\text{reg}}(k) &= \frac{1}{2} \int_0^{\Lambda^2} d\ell^2 (\ell^2)^{\frac{d}{2}-1} \left[\frac{1}{(\ell^2 + \Delta)^n} - \frac{1}{(\ell^2)^n} \right] \\ &= \frac{1}{2} \int_0^{\Lambda^2} d\ell^2 (\ell^2)^{\frac{d}{2}-1} \frac{1}{\Gamma(n)} \int_0^{\infty} dt t^{n-1} \left[e^{-(\ell^2 + \Delta)t} - e^{-\ell^2 t} \right] \end{aligned} \quad (\text{B.16})$$

With help of the identity

$$e^{-at} - e^{-bt} = e^{-bt} (b - a)t \int_0^1 ds e^{-(a-b)ts} \quad (\text{B.17})$$

we can now compute J_{reg} :

$$\begin{aligned}
 J_{\text{reg}}(k) &= \frac{1}{2} \int_0^{\Lambda^2} d\ell^2 (\ell^2)^{\frac{d}{2}-1} \frac{1}{\Gamma(n)} \int_0^\infty dt t^{n-1} e^{-\ell^2 t} \int_0^1 ds e^{-st\Delta} (-t\Delta) \\
 &= -\frac{1}{2} \frac{\Delta}{\Gamma(n)} \Gamma\left(\frac{d}{2}\right) \int_0^1 ds \int_0^\infty dt t^{n-\frac{d}{2}} e^{-st\Delta}, \quad n+1 > \frac{d}{2} \\
 &= -\frac{1}{2} \Delta \frac{\Gamma\left(\frac{d}{2}\right) \Gamma\left(n - \frac{d}{2} + 1\right)}{\Gamma(n)} \int_0^1 ds \frac{1}{(s\Delta)^{n-\frac{d}{2}+1}}, \quad n < \frac{d}{2} \\
 &= +\frac{1}{2} \Delta^{\frac{d}{2}-n} \frac{\Gamma\left(\frac{d}{2}\right) \Gamma\left(n - \frac{d}{2}\right)}{\Gamma(n)}
 \end{aligned} \tag{B.18}$$

Plugging this result back into the definition of $I(k)$ in Eq. (B.11), one finds

$$I(k) = I_\infty + I_{\text{reg}}(k) \tag{B.19}$$

$$I_\infty = \frac{1}{(4\pi)^{\frac{d}{2}} \Gamma\left(\frac{d}{2}\right) \left(\frac{d}{2} - n\right)} (\Lambda^2)^{\frac{d}{2}-n} \tag{B.20}$$

$$\begin{aligned}
 I_{\text{reg}}(k) &= \frac{2\pi^{\frac{d}{2}}}{(2\pi)^d \Gamma\left(\frac{d}{2}\right)} \frac{\Gamma\left(\frac{d}{2}\right) \Gamma\left(n - \frac{d}{2}\right)}{B(\alpha, \beta) \Gamma(n)} \frac{1}{2} B\left(\frac{d}{2} - \alpha, \frac{d}{2} - \beta\right) (k^2)^{\frac{d}{2}-n} \\
 &= \frac{1}{(4\pi)^{d/2}} \frac{\Gamma(d/2 - \alpha) \Gamma(d/2 - \beta) \Gamma(\alpha + \beta - d/2)}{\Gamma(\alpha) \Gamma(\beta) \Gamma(d - \alpha - \beta)} (k^2)^{d/2 - \alpha - \beta}.
 \end{aligned} \tag{B.21}$$

The regular part of $I(k)$ would have been found correctly by direct usage of Eq. (B.6a), despite the UV divergence.

Finally, another result of a two-point sort of integral is provided that comes into play in the gluon chain in chapter 5.4. It reads

$$X(\alpha, \beta) := \int d^d \ell \frac{|\ell \times k|}{(\ell^2)^\alpha ((\ell - k)^2)^\beta}, \tag{B.22}$$

where in d dimensions $|\ell \times k|$ can be understood as the projection of ℓ to the hypersurface perpendicular to k . The Feynman trick (B.2) yields after the shift $\ell \rightarrow \ell - yk$ (which does not affect the numerator in Eq. (B.22))

$$X(\alpha, \beta) = \frac{1}{B(\alpha, \beta)} \int_0^1 dx \int_0^1 dy \delta(x + y - 1) x^{\alpha-1} y^{\beta-1} \int d^d \ell \frac{|\ell \times k|}{(\ell^2 + \Delta)^{\alpha+\beta}}. \tag{B.23}$$

If θ is the enclosed angle of ℓ and k , $|\ell \times k| = \ell k \sin \theta$, its integration gives

$$\int_0^\pi d\theta \sin^{d-1} \theta = B\left(\frac{d}{2}, \frac{1}{2}\right), \tag{B.24}$$

whereas the remnant angular integrals simple yield surface of the unit sphere with $d \rightarrow d - 1$,

$$\Omega_{d-1} = \frac{2\sqrt{\pi}^{d-1}}{\Gamma(\frac{d}{2} - \frac{1}{2})}. \quad (\text{B.25})$$

Thus, Eq. (B.23) is calculated by

$$\begin{aligned} X(\alpha, \beta) &= \frac{1}{(2\pi)^d} \frac{B(\frac{d}{2}, \frac{1}{2})\Omega_{d-1}}{B(\alpha, \beta)} \int_0^1 dy \delta(x+y-1) x^{\alpha-1} y^{\beta-1} \frac{1}{2} \int_0^\infty d\ell^2 \frac{k\ell^{\frac{d}{2}-\frac{1}{2}}}{(\ell^2 + \Delta)^{\alpha+\beta}} \\ &= \frac{1}{(4\pi)^{d/2}} \frac{\Gamma(\frac{d}{2} + \frac{1}{2} - \alpha)\Gamma(\frac{d}{2} + \frac{1}{2} - \beta)\Gamma(\frac{d}{2})\Gamma(\alpha + \beta - \frac{d}{2} - \frac{1}{2})}{\Gamma(\alpha)\Gamma(\beta)\Gamma(\frac{d}{2} - \frac{1}{2})\Gamma(d + 1 - \alpha - \beta)} (k^2)^{\frac{d}{2}+1-\alpha-\beta} \end{aligned} \quad (\text{B.26})$$

C Infrared limit of the ghost-gluon vertex

The rather technical project of determining the infrared limit of the ghost-gluon vertex to yield the solution shown in Table 3.2, is presented here. We use the truncated vertex DSE as shown in Fig. 3.6. To illustrate how to keep track of color group and vertex factors, first note that the triangle diagrams comprise a trace of generators, $\text{tr}(\hat{T}^a \hat{T}^b \hat{T}^c)$, as well as three vertex factors of ig , i.e.

$$\begin{array}{c} \text{a} \\ | \\ \bullet \\ / \quad \backslash \\ \bullet \quad \bullet \\ | \quad | \\ \text{b} \quad \text{c} \end{array} = (ig)^3 \text{tr}(\hat{T}^a \hat{T}^b \hat{T}^c) = g^2 \frac{N_c}{2} \begin{array}{c} \text{a} \\ | \\ \bullet \\ / \quad \backslash \\ \text{b} \quad \text{c} \end{array} \quad (\text{C.1})$$

due to Eq. (A.5). We now consider the infrared gluon limit of the first loop diagram (3.79). With the identity

$$\ell_{\alpha\beta}(q)t_{\alpha\beta}(\ell - q) = \frac{\ell^2}{(\ell - q)^2} - \frac{(\ell \cdot q)^2}{q^2(\ell - q)^2} \quad (\text{C.2})$$

we can express this diagram in the infrared limit of the remnant ghost momentum q by two-point integrals,

$$\begin{aligned} \lim_{q \rightarrow 0} \Gamma_{\mu}^{(GGA)}(0; q, q) &= \Gamma_{\mu}^{(0)}(q) C g^2 \frac{N_c}{2} AB^2 \left(\Xi_1(1 + 2\kappa, \frac{d}{2} - 2\kappa) - \Xi_3(2 + 2\kappa, \frac{d}{2} - 2\kappa)/q^2 \right) \\ &= \Gamma_{\mu}^{(0)}(q) C \frac{1}{2} \frac{I_1}{I_A}, \end{aligned} \quad (\text{C.3})$$

where

$$I_1 = \frac{1}{(4\pi)^{d/2}} \frac{d-1}{d(1+2\kappa)\Gamma(d/2)}. \quad (\text{C.4})$$

and we have used Eq. (2.60). The factor of C appears in Eq. (C.3) since the infrared limit is taken as in Eq. (3.75). A factor of $\frac{1}{2}$ stemming from the color trace (C.1) is left explicit. Considering the second loop integral of the ghost-gluon vertex DSE, the result (3.71) for the three-gluon vertex in the infrared limit is plugged into the expression (3.78) to find that

$$\begin{aligned} \lim_{q \rightarrow 0} \Gamma_{\mu}^{(GAA)}(0; q, q) &= (-2)ig^5 A^2 B^4 I_3 q_{\mu} \frac{N_c^2}{4} \int d^d \ell \ell \cdot q \left(1 - (\hat{p} \cdot \hat{\ell})^2 \right) \\ &\quad D_Z^2(\ell) D_G(\ell - p) (\ell^2)^{-(\alpha_G - \alpha_Z)} \\ &= (-2)igq_{\mu} \frac{1}{4} \frac{I_3}{I_A^2} \left(\Xi_1(d/2 - \kappa, 1 + \kappa) - \Xi_3(d/2 - \kappa + 1, 1 + \kappa)/q^2 \right) \\ &= \Gamma_{\mu}^{(0)}(q) (-2) \frac{1}{4} \frac{I_2 I_3}{I_A^2} \end{aligned} \quad (\text{C.5})$$

where I_3 was defined in Eq. (3.72) and

$$I_2 = \frac{1}{(4\pi)^{d/2}} \frac{d-1}{(d-2\kappa)\Gamma(d/2+1)}. \quad (\text{C.6})$$

The factor of (-2) in Eq. (C.5) is the prefactor of the ghost triangle in the three-gluon vertex DSE, see Fig. 3.4. Altogether, the infrared gluon limit of the ghost-gluon vertex, defined by Eq. (3.75) yields,

$$C = 1 + \frac{1}{2}C \frac{I_1}{I_A} - \frac{1}{2} \frac{I_2 I_3}{I_A^2} \quad (\text{C.7})$$

and one can find C to obey

$$\begin{aligned} C = & 2 \left\{ 4^\kappa (d-1) d \left(\Gamma\left(1 + \frac{d}{2}\right) - \kappa \Gamma\left(\frac{d}{2}\right) \right) \Gamma(d-3\kappa) \Gamma\left(\frac{d}{2} - \kappa\right) \Gamma(-\kappa)^2 \Gamma\left(\frac{1}{2} + \kappa\right) \Gamma(1+2\kappa) \right. \\ & \left. \Gamma(2+2\kappa) - \sqrt{\pi} \Gamma\left(\frac{d}{2} - 2\kappa\right)^3 \Gamma\left(1 + \frac{d}{2} + \kappa\right)^2 \Gamma\left(2 - \frac{d}{2} + 3\kappa\right) \right\} / \\ & \left\{ (d-1) (d-2\kappa) \Gamma(d-3\kappa) \Gamma(-\kappa) \Gamma(1+2\kappa)^2 \right. \\ & \left. \left(4^{1+\kappa} \Gamma\left(1 + \frac{d}{2}\right) \Gamma\left(\frac{d}{2} - \kappa\right) \Gamma(-\kappa) \Gamma\left(\frac{3}{2} + \kappa\right) + \sqrt{\pi} \Gamma\left(\frac{d}{2} - 2\kappa\right) \Gamma\left(1 + \frac{d}{2} + \kappa\right) \right) \right\} \quad (\text{C.8}) \end{aligned}$$

As can be checked, this leads to the numerical values of C given by table 3.2 for the various solutions of κ . A cancellation of the two loop diagrams, see Eq. (3.81), must yield $C = 1$ in Eq. (C.7). In this case

$$1 = \frac{I_1 I_G}{I_2 I_3} = \frac{(d-1)(d-2\kappa)\Gamma(d-3\kappa)\Gamma(1-\kappa)\Gamma(2\kappa)\Gamma(2\kappa+2)}{\Gamma^2\left(\frac{d}{2} - 2\kappa\right)\Gamma\left(\frac{d}{2} + \kappa + 1\right)\Gamma\left(2 + 3\kappa - \frac{d}{2}\right)} \quad (\text{C.9})$$

and among the solution $\kappa_a(d)$ and $\kappa_b(d)$ that solve $I_G = I_A$, see Fig. 2.5, Eq. C.9 uniquely yields $\kappa = \frac{1}{2}$ with $d = 3$.

One might object that the Bose symmetry of the ghost triangle contribution to the three-gluon vertex is broken, for only the upper vertex is dressed while the others are at tree-level (see Fig. 3.4). In the derivation of the DSE, the channel to start the calculation in is an arbitrary choice. Therefore, one might as well find the upper vertex dressed. If we repeat the calculation, the DSE for the ghost-gluon vertex now reads

$$C = 1 + \frac{1}{2}C \frac{I_1}{I_A} - \frac{1}{2}C \frac{I_2 I_3}{I_A^2}, \quad (\text{C.10})$$

cf. Eq. (C.7), and the solution can be found to be

$$\begin{aligned}
C = & 4(d-1)(2\kappa+1)^2\Gamma^2\left(\frac{d}{2}+1\right)\Gamma(d-3\kappa)\Gamma\left(\frac{d}{2}-\kappa+1\right)\Gamma^2(-\kappa)\Gamma^3(2\kappa+1)/ \\
& \left\{ d(2\kappa+1)\Gamma\left(\frac{d}{2}\right)\Gamma(\kappa+1)\Gamma^2\left(\frac{d}{2}+\kappa+1\right)\Gamma\left(3\kappa+2-\frac{d}{2}\right)\Gamma^3\left(\frac{d}{2}-2\kappa\right) \right. \\
& + (d-1)(d-2\kappa)\Gamma\left(\frac{d}{2}+1\right)\Gamma(d-3\kappa)\Gamma(-\kappa)\Gamma(2\kappa+1)\Gamma(2\kappa+2) \\
& \left. \left(\Gamma\left(\frac{d}{2}-2\kappa\right)\Gamma(\kappa+1)\Gamma\left(\frac{d}{2}+\kappa+1\right) + 2\Gamma\left(\frac{d}{2}+1\right)\Gamma\left(\frac{d}{2}-\kappa\right)\Gamma(-\kappa)\Gamma(2\kappa+2) \right) \right\} \\
& \tag{C.11}
\end{aligned}$$

Again, the limit $d \rightarrow 3$ and $\kappa \rightarrow \frac{1}{2}$ yields the result $C = 1$. Apparently, it makes no difference which one of the vertices is at tree-level.

D Hamiltonian approach to ϕ^4 theory

The ϕ^4 theory is a popular toy model to illustrate some aspect of a physical field theory in a simpler context. Unfortunately, the ϕ^4 theory in $d = 4$ dimensions suffers from the *triviality problem* which states that after renormalization, the coupling parameter is equally zero and a free field theory is considered [168]. This problem can be circumvented by choosing a negative coupling parameter which is at the prize of losing the boundedness of the spectrum. In this appendix, we will use the ϕ^4 theory in order to show how the variational principle can be applied, in accordance to chapter 3.

With the classical Lagrangian density

$$\mathcal{L} = \frac{1}{2}(\partial_\mu\phi)\partial^\mu\phi - \frac{1}{2}m^2\phi^2 - \frac{\lambda}{4!}\phi^4 \quad (\text{D.1})$$

and the conjugate momenta

$$\pi = \frac{\delta\mathcal{L}}{\delta\partial_0\phi} = \partial^0\phi \quad (\text{D.2})$$

we can define the classical Hamiltonian

$$H = \int d^3x \left(\frac{1}{2}\pi^2 + \frac{1}{2}(\nabla\phi)^2 + \frac{1}{2}m^2\phi^2 + \frac{\lambda}{4!}\phi^4 \right). \quad (\text{D.3})$$

The equal-time canonical quantization relations, $[\phi(x, t), \pi(y, t)] = i\delta^3(x, y)$, lead to the representation

$$\pi(x) = \frac{\delta}{i\delta\phi(x)} \quad (\text{D.4})$$

of the momentum operator, where x is a 3-vector and the time is fixed in the Schrödinger picture. Thus, the quantum theory is defined by the Hamiltonian (D.3) in terms of the field operators.

The time-independent Schrödinger equation $H|\psi\rangle = E|\psi\rangle$, along with the semi-definiteness of H for $\lambda > 0$ infers that the vacuum wave functional $\psi[\phi] = \langle\phi|\psi\rangle$ can be determined by a variational principle

$$E_0 = \langle\psi| H |\psi\rangle \longrightarrow \min. \quad (\text{D.5})$$

As an ansatz, we choose a Gaussian wave functional

$$\psi[\phi] = \mathcal{N} \exp\left(-\frac{1}{2}\int d^3x \int d^3y \phi(x)\omega(x, y)\phi(y)\right) \equiv \mathcal{N} \exp\left(-\frac{1}{2}\phi_x\omega_{xy}\phi_y\right) \quad (\text{D.6})$$

where the short-hand notation keeps the coordinate dependence as an index and the integration is implicit by means of the sum convention. The kernel ω is determined by the variational principle (D.5).

Expectation values are computed by

$$\langle \mathcal{O}[\phi] \rangle = \langle \phi | \mathcal{O}[\phi] | \phi \rangle = \int \mathcal{D}\phi \psi^*[\phi] \mathcal{O}[\phi] \psi[\phi] = \mathcal{O} \left[\frac{\delta}{\delta\phi} \right] Z[j] \Big|_{j=0} \quad (\text{D.7})$$

where the generating functional $Z[j]$ is defined as

$$\begin{aligned} Z[j] &= \mathcal{N}^2 \int \mathcal{D}\phi \exp(-\phi_x \omega_{xy} \phi_y + j_x \phi_y) \\ &= \left\{ \mathcal{N}^2 \int \mathcal{D}\phi' \exp(-\phi'_x \omega_{xy} \phi'_y) \right\} \cdot \exp\left(\frac{1}{4} j_x \omega_{xy}^{-1} j_y\right) \\ &= \exp\left(\frac{1}{4} j_x \omega_{xy}^{-1} j_y\right) \end{aligned} \quad (\text{D.8})$$

Above, after a quadratic completion, the expression in the curly brackets is $\langle 1 \rangle = 1$ by virtue of the normalization of the wave functional via \mathcal{N} .

The vacuum energy E_0 is now calculated term by term, as a functional of ω . First of all, the mass term yields

$$\begin{aligned} \frac{m^2}{2} \langle \phi_x \phi_y \rangle &= \frac{m^2}{2} \frac{\delta}{\delta j_x} \frac{\delta}{\delta j_x} e^{\frac{1}{4} j_u \omega_{uv}^{-1} j_v} \Big|_{j=0} \\ &= \frac{m^2}{2} \frac{\delta}{\delta j_x} \frac{1}{2} \omega_{xx'}^{-1} j_{x'} e^{\frac{1}{4} j_u \omega_{uv}^{-1} j_v} \Big|_{j=0} \\ &= \frac{m^2}{4} \omega_{xx}^{-1} \end{aligned} \quad (\text{D.9})$$

The above term is basically the trace of the propagator

$$\langle \phi(x) \phi(y) \rangle = \frac{1}{2} \omega^{-1}(x, y). \quad (\text{D.10})$$

In order to understand better the meaning of the quantity ω_{xx}^{-1} , use the explicit notation and relate it to its Fourier transform,

$$\begin{aligned} \omega_{xx}^{-1} &= \int d^3[xy] \omega^{-1}(x, y) \delta^3(x, y) = \int d^3[xy] \int \bar{d}^3 k \omega^{-1}(k) e^{ik \cdot (x-y)} \delta^3(x, y) \\ &= V \int \bar{d}^3 k \omega^{-1}(k) \end{aligned} \quad (\text{D.11})$$

where $V = \int d^3 x$ is the volume of coordinate space. The first variational derivative in the calculation (D.9) brings down a source term $j_{x'}$ from the exponential so that the second variational derivative acts not only on the exponential but also on the latter source term $j_{x'}$. Setting sources to zero at the end of the calculation generally eliminates some terms. Some combinatorics is necessary to deal with the quartic term in the energy, we just write down the result:

$$\frac{\lambda}{4!} \int d^3 x \langle (\phi(x))^4 \rangle = \frac{\lambda}{8} V \int \bar{d}^3 \ell \omega^{-1}(\ell) \omega^{-1}(\ell - k) \quad (\text{D.12})$$

The kinetic energy is found to give

$$\begin{aligned} \frac{1}{2} \langle \pi_x \pi_x \rangle &= \frac{1}{2} \int \mathcal{D}\phi \left| \frac{\delta}{i\delta\phi_x} \psi[\phi] \right|^2 = \frac{1}{2} \omega_{xy} \omega_{xz} \langle \phi_y \phi_z \rangle = \frac{1}{4} \omega_{xx} \\ &= \frac{1}{4} V \int \bar{d}^3 k \omega(k) \end{aligned} \quad (\text{D.13})$$

where the propagator (D.10) was used.

Furthermore, the spatial derivative terms of the Hamiltonian (D.3) yield explicitly

$$\begin{aligned} \frac{1}{2} \int d^3 x \langle \phi(x) (-\partial_x^2) \phi(x) \rangle &= \int d^3 [xy] \delta^3(x, y) (-\partial_x^2) \langle \phi(y) \phi(x) \rangle \\ &= \int d^3 [xy] \delta^3(x, y) (-\partial_x^2) \int \bar{d}^3 k \frac{1}{2} \omega^{-1}(k) e^{ik \cdot (x-y)} \\ &= \frac{1}{2} V \int \bar{d}^3 k \omega^{-1}(k) k^2 \end{aligned} \quad (\text{D.14})$$

Summing up all contributions, the energy is found to be

$$E = V \int \bar{d}^3 k \left(\frac{1}{4} \omega^{-1}(k) (k^2 + m^2) + \frac{1}{4} \omega(k) + \frac{\lambda}{8} \int \bar{d}^3 \ell \omega^{-1}(k) \omega^{-1}(\ell - k) \right) \quad (\text{D.15})$$

and it is minimized w.r.t. the kernel ω ,

$$0 = \frac{\delta E/V}{\delta \omega^{-1}(k)} = \frac{1}{4} (k^2 + m^2) - \frac{1}{4} \omega^2(k) + \frac{\lambda}{4} \int \bar{d}^3 \ell \omega^{-1}(\ell) \quad (\text{D.16})$$

which leads to the "gap equation":

$$\omega^2(k) = k^2 + m^2 + \lambda \int \bar{d}^3 \ell \omega^{-1}(\ell) \quad (\text{D.17})$$

The term "gap equation" is sensible since even if the mass parameter m was zero to begin with, there would be a mass dynamically generated by the last term in Eq. (D.17). Hence, it describes the lowest allowed energy level of the spectrum, i.e. a mass gap. That term stems from the quartic term in the Hamiltonian and is also present in the YM Hamiltonian. It is a divergent constant subtracted in our approach. In the ϕ^4 theory, Eq. (D.17) must be solved iteratively and renormalization becomes necessary. For further reading, see e.g. Ref. [169]. If such a term is of any significance for YM theory, then it will have an effect only on the intermediate regime of $\omega(k)$. The infrared dominant curvature term from gauge fixing is of course absent in the ϕ^4 version (D.17) of the gap equation.

E Identities for Gaussian expectation values

The Gaussian expectation values

$$\langle \mathcal{O} \rangle_\omega = \int \mathcal{D}A \tilde{\Psi}^*[A] \mathcal{O} \tilde{\Psi}[A] \quad (\text{E.1})$$

with the normalized wave functional,

$$1 = \int \mathcal{D}A \left| \tilde{\Psi}[A] \right|^2 = \mathcal{N}^2 \int \mathcal{D}A e^{-\int d^d[xy] A_i^a(x) \omega_{ij}^{ab}(x,y) A_j^b(y)}, \quad (\text{E.2})$$

can be shown to yield some useful identities. Take a variational derivative of Eq. (E.2) w.r.t. $\omega_{ij}^{ab}(x,y) = t_{ij}(x) \omega(x,y) \delta^{ab}$,

$$0 = \frac{\delta \ln \mathcal{N}^2}{\delta \omega_{ij}^{ab}(x,y)} - \left\langle A_i^a(x) A_j^b(y) \right\rangle_\omega, \quad (\text{E.3})$$

to find

$$\frac{\delta \ln \mathcal{N}^2}{\delta \omega_{ij}^{ab}(x,y)} = \frac{1}{2} (\omega^{-1})_{ij}^{ab}(x,y). \quad (\text{E.4})$$

For expectation values (E.1) of operators $\mathcal{O} = \mathcal{O}[A]$, a variational derivative thus gives

$$\frac{\delta \langle \mathcal{O} \rangle_\omega}{\delta \omega_{ij}^{ab}(x,y)} = \left\langle A_i^a(x) A_j^b(y) \right\rangle_\omega \langle \mathcal{O} \rangle_\omega - \left\langle A_i^a(x) A_j^b(y) \mathcal{O} \right\rangle_\omega, \quad (\text{E.5})$$

i.e. a covariance. Using Wick's theorem, a few manipulations yield the identity

$$\left\langle \frac{\delta^2 \mathcal{O}}{\delta A_i^a(x) \delta A_j^b(y)} \right\rangle_\omega = -4 \int d^d[uv] \omega_{im}^{ac}(x,u) \frac{\delta \langle \mathcal{O} \rangle_\omega}{\delta \omega_{mn}^{cd}(u,v)} \omega_{nj}^{db}(v,y). \quad (\text{E.6})$$

For $\mathcal{O} = H_p[A]$, this leads directly to Eq. (5.75).

A little more effort is required for expectation values of operators $\mathcal{O} = \tilde{H}[A, \Pi]$ that involve the momentum operator Π . The equivalent of Eq. (E.5) is then

$$\frac{\delta \langle \tilde{H} \rangle_\omega}{\delta \omega_{ij}^{ab}(x,y)} = \left\langle A_i^a(x) A_j^b(y) \right\rangle_\omega \langle \tilde{H} \rangle_\omega - \frac{1}{2} \left\langle [A_i^a(x) A_j^b(y), \tilde{H}]_\mp \right\rangle_\omega, \quad (\text{E.7})$$

whereby $[\ ,]_\mp$ denotes the anticommutator (+), or the commutator (-), respectively. The anticommutator in Eq. (E.7) can be rewritten as

$$[A_i^a(x) A_j^b(y), \tilde{H}]_+ = -\frac{\delta^2 \tilde{H}}{\delta \Pi_i^a(x) \delta \Pi_j^b(y)} + A_i^a(x) \tilde{H} A_j^b(y) + A_j^b(y) \tilde{H} A_i^a(x) \quad (\text{E.8})$$

using $[A_i, [A_j, \tilde{H}]_-]_- = -\frac{\delta^2 \tilde{H}}{\delta \Pi_i \delta \Pi_j}$ with $A_k^a(x) = i\delta / \delta \Pi_k^a(x)$. With knowledge of the wave functional,

$$A_k^a(x) \tilde{\Psi}[A] = - \int d^d y (\omega^{-1})_{kj}^{ab}(x,y) \frac{\delta}{\delta A_j^b(y)} \tilde{\Psi}[A], \quad (\text{E.9})$$

the last two terms in Eq. (E.8) result in

$$\begin{aligned}
 & \langle A_i^a(x) \tilde{H} A_j^b(y) + A_j^b(y) \tilde{H} A_i^a(x) \rangle_\omega \\
 &= \int d^d u (\omega^{-1})_{im}^{ac}(x, u) \left\langle \frac{\delta}{\delta A_m^c(u)} \tilde{H} A_j^b(y) - A_j^b(y) \tilde{H} \frac{\delta}{\delta A_m^c(u)} \right\rangle_\omega \\
 &= \int d^d u (\omega^{-1})_{im}^{ac}(x, u) \left\{ \left\langle \frac{\delta \tilde{H}}{\delta A_m^c(u)} A_j^b(y) \right\rangle_\omega + \langle \tilde{H} \rangle_\omega t_{mj}^{cb}(u, y) \right. \\
 &\quad \left. - \int d^d v \langle \tilde{H} A_j^b(y) A_n^d(v) \rangle_\omega \omega_{mn}^{cd}(u, v) - \int d^d v \langle A_j^b(y) A_n^d(v) \tilde{H} \rangle_\omega \omega_{mn}^{cd}(u, v) \right. \\
 &\quad \left. + \left\langle A_j^b(y) \frac{\delta \tilde{H}}{\delta A_m^c(u)} \right\rangle_\omega + \langle \tilde{H} \rangle_\omega t_{mj}^{cb}(u, y) \right\} \\
 &= - \left\langle [A_i^a(x) A_j^b(y), \tilde{H}]_+ \right\rangle_\omega + 2(\omega^{-1})_{ij}^{ab}(x, y) \langle \tilde{H} \rangle_\omega \\
 &\quad + \int d^d u (\omega^{-1})_{im}^{ac}(x, u) \left\langle \left[\frac{\delta \tilde{H}}{\delta A_m^c(u)}, A_j^b(y) \right]_+ \right\rangle_\omega \quad (E.10)
 \end{aligned}$$

The anticommutator in the last line can be rewritten as a commutator, according to the following identity,

$$\langle [A, \mathcal{O}]_\pm \rangle_\omega = i \omega^{-1} \langle [\Pi, \mathcal{O}]_\mp \rangle_\omega \quad (E.11)$$

which holds for Gaussian expectation values, such as (E.1).

Proof: Inside the expectation value, the field operator A can be expressed by a momentum operator Π , see Eq. E.9. Thus,

$$\begin{aligned}
 \langle [A_k^a(x), \mathcal{O}]_\pm \rangle_\omega &= \int d^d y (\omega^{-1})_{kj}^{ab}(x, y) \left\langle \frac{\delta}{\delta A_j^b(y)} \mathcal{O} \mp \mathcal{O} \frac{\delta}{\delta A_j^b(y)} \right\rangle_\omega \\
 &= i \int d^d y (\omega^{-1})_{kj}^{ab}(x, y) \langle [\Pi, \mathcal{O}]_\mp \rangle_\omega \quad \square \quad (E.12)
 \end{aligned}$$

Therefore,

$$\left\langle \left[\frac{\delta \tilde{H}}{\delta A_m^c(u)}, A_j^b(y) \right]_+ \right\rangle_\omega = \int d^d v (\omega^{-1})_{jn}^{bd}(y, v) \left\langle \frac{\delta^2 \tilde{H}}{\delta A_m^c(u) \delta A_n^d(v)} \right\rangle_\omega. \quad (E.13)$$

Plugging Eq. (E.13) into the expression (E.10) and the latter with (E.8) into Eq. (E.7), some cancellations occur and we end up with

$$\begin{aligned}
 \frac{\delta \langle \tilde{H} \rangle_\omega}{\delta \omega_{ij}^{ab}(x, y)} &= \frac{1}{4} \left\langle \frac{\delta^2 \tilde{H}}{\delta \Pi_i^a(x) \delta \Pi_j^b(y)} \right\rangle_\omega \\
 &\quad - \frac{1}{4} \int d^d [uv] (\omega^{-1})_{im}^{ac}(x, u) \left\langle \frac{\delta^2 \tilde{H}}{\delta A_m^c(u) \delta A_n^d(v)} \right\rangle_\omega (\omega^{-1})_{nj}^{db}(v, y). \quad (E.14)
 \end{aligned}$$

Such an identity was also derived in Ref. [154].

Bibliography

- [1] H. Weyl, "Elektron und Gravitation," *Z. Phys.* **56** (1929) 330–352.
- [2] M. E. Peskin and D. V. Schroeder, "An Introduction To Quantum Field Theory," *Westview* (1995).
- [3] O. Klein, "On the Theory of Charged Fields.," in *New Theories in Physics. Paris: International Institute of Intellectual Cooperation*, pp. 77–93. 1939. See also D. Gross, hep-th/9411233.
- [4] C. Yang and R. L. Mills, "Conservation of isotopic spin and isotopic gauge invariance," *Phys. Rev.* **96** (1954) 191–195.
- [5] R. Jackiw, "Introduction to the Yang-Mills Quantum Theory," *Rev. Mod. Phys.* **52** (1980) 661.
- [6] C. Itzykson and J. B. Zuber, "Quantum field theory," *New York: McGraw-Hill, International Series In Pure and Applied Physics* (1980).
- [7] B. S. DeWitt, "Quantum theory of gravity. II. The manifestly covariant theory," *Phys. Rev.* **162** (1967) 1195–1239.
- [8] G. S. Bali, "QCD forces and heavy quark bound states," *Phys. Rept.* **343** (2001) 1–136, hep-ph/0001312.
- [9] C. S. Fischer, P. Watson, and W. Cassing, "Probing unquenching effects in the gluon polarisation in light mesons," *Phys. Rev.* **D72** (2005) 094025, hep-ph/0509213.
- [10] C. T. H. Davies *et al.*, "High-precision lattice QCD confronts experiment," *Phys. Rev. Lett.* **92** (2004) 022001, hep-lat/0304004.
- [11] I. H. Duru and H. Kleinert, "Solution of path integral for H atom," *Phys. Lett.* **B84** (1979) 185.
- [12] O. Brill and B. Goodman, "Causality in Coulomb gauge," *Am. J. Phys.* **35** (Sept, 1967) 832–837.
- [13] J. S. Schwinger, "Non-Abelian gauge fields. Relativistic invariance," *Phys. Rev.* **127** (1962) 324–330.
- [14] P. A. M. Dirac, "Generalized Hamiltonian dynamics," *Can. J. Math.* **2** (1950) 129–148.
- [15] P. A. M. Dirac, "Generalized Hamiltonian dynamics," *Proc. Roy. Soc. Lond.* **A246** (1958) 326–332.
- [16] P. A. M. Dirac, "Lectures on quantum mechanics," *Belfer Graduate School of Science, Yeshiva Univ. Press, New York* (1964).

- [17] S. Carlip, “Quantum gravity: A progress report,” *Rept. Prog. Phys.* **64** (2001) 885, gr-qc/0108040.
- [18] M. Henneaux and C. Teitelboim, “Quantization of gauge systems,” *Princeton Univ. Pr.* (1992).
- [19] K. Sundermeyer, “Constrained dynamics with applications to Yang-Mills theory, general relativity, classical spin, dual string model,” *Lect. Notes Phys.* **169** (1982) 1–318.
- [20] A. Hanson, T. Regge, and C. Teitelboim, “Constrained Hamiltonian systems,” *Accademia Nazionale dei Lincei* (1976).
- [21] P. Senjanovic, “Path Integral Quantization of Field Theories with Second Class Constraints,” *Ann. Phys.* **100** (1976) 227–261.
- [22] R. Cawley, “Determination of the Hamiltonian in the Presence of Constraints,” *Phys. Rev. Lett.* **42** (1979), no. 7, 413–416.
- [23] L. D. Faddeev, “Feynman integral for singular Lagrangians,” *Theor. Math. Phys.* **1** (1969) 1–13.
- [24] N. H. Christ and T. D. Lee, “Operator ordering and Feynman rules in gauge theories,” *Phys. Rev.* **D22** (1980) 939.
- [25] P. Bergmann, “Quantisierung Allgemein-kovarianter Feldtheorien,” *Helv. Phys. Acta Suppl.* **4** (1956) 79.
- [26] M. Creutz, I. J. Muzinich, and T. N. Tudron, “Gauge fixing and canonical quantization,” *Phys. Rev.* **D19** (1979) 531.
- [27] J.-L. Gervais and B. Sakita, “Gauge degrees of freedom, external charges, and quark confinement criterion in the $A_0 = 0$ canonical formalism,” *Phys. Rev.* **D18** (1978) 453.
- [28] H. Cheng and E. Tsai, “Canonical quantization of nonabelian gauge field theories and Feynman rules,” *Chin. J. Phys.* **25** (1987), no. 1, 95–128.
- [29] P. Landshoff, “Physical and Nonstandard Gauges,” *Lect. Notes Phys.* **361** (1989) 74–86. *Vienna 1989, Proceedings, Physical and nonstandard gauges*, Eds. P. Gaigg, W. Kummer, M. Schweda.
- [30] J. D. Bjorken, “Elements of Quantum Chromodynamics,” *Presented at the SLAC Summer Institute on Particle Physics, Stanford, Calif.* (1979) 219–289.
- [31] H. Reinhardt, “Resolution of Gauss’ law in Yang-Mills theory by gauge- invariant projection: Topology and magnetic monopoles,” *Nucl. Phys.* **B503** (1997) 505–529, hep-th/9702049.
- [32] G. C. Rossi and M. Testa, “Canonical commutation relations and Gauss’ law in the temporal gauge,” *Phys. Rev.* **D29** (1984) 2997.

- [33] L. D. Faddeev and S. L. Shatashvili, “Realization of the Schwinger Term in the Gauss Law and the Possibility of Correct Quantization of a Theory with Anomalies,” *Phys. Lett.* **B167** (1986) 225–228.
- [34] L. D. Faddeev and A. A. Slavnov, “Gauge fields,” *Front. Phys.* **83** (1991) 1–217.
- [35] S. Caracciolo, G. Curci, and P. Menotti, “The Propagator in the $A_0 = 0$ Gauge,” *Phys. Lett.* **B113** (1982) 311.
- [36] J. P. Leroy, J. Micheli, and G. C. Rossi, “A quasitemporal gauge,” *Z. Phys.* **C36** (1987) 305.
- [37] H. O. Girotti and K. D. Rothe, “Quantization of QCD and QCD in a fully fixed temporal gauge,” *Z. Phys.* **C27** (1985) 559.
- [38] T. Kugo, “Eichtheorie,” *Springer* (1997).
- [39] K. Haller and H.-C. Ren, “Gauge equivalence in QCD: The Weyl and Coulomb gauges,” *Phys. Rev.* **D68** (2003) 085002.
- [40] T. N. Tudron, “Gauge fixing and operator ordering,” *Phys. Rev.* **D21** (1980) 2348.
- [41] H. O. Girotti and K. D. Rothe, “Quantization of nonabelian gauge theories in the Dirac bracket formalism,” *Nuovo Cim.* **A72** (1982) 265.
- [42] L. D. Faddeev and V. N. Popov, “Feynman diagrams for the Yang-Mills field,” *Phys. Lett.* **B25** (1967) 29–30.
- [43] M. Nakahara, “Geometry, topology and physics,”. Bristol, UK: Hilger (1990) 505 p. (Graduate student series in physics).
- [44] K. V. Kuchar, “Covariant factor ordering of gauge systems,” *Phys. Rev.* **D34** (1986) 3044–3057.
- [45] J. D. Romano and R. S. Tate, “Dirac versus reduced space quantization of simple constrained systems,” *Class. Quant. Grav.* **6** (1989) 1487.
- [46] K. Schleich, “Is reduced phase space quantization equivalent to Dirac quantization?,” *Class. Quant. Grav.* **7** (1990) 1529–1538.
- [47] R. Loll, “Noncommutativity of constraining and quantizing: A $U(1)$ gauge model,” *Phys. Rev.* **D41** (1990) 3785–3791.
- [48] S. V. Shabanov, “Geometry of the physical phase space in quantum gauge systems,” *Phys. Rept.* **326** (2000) 1–163, [hep-th/0002043](#).
- [49] J. Greensite, “The confinement problem in lattice gauge theory,” *Prog. Part. Nucl. Phys.* **51** (2003) 1, [hep-lat/0301023](#).

- [50] C. S. Fischer, A. Maas, J. M. Pawłowski, and L. von Smekal, “Large volume behaviour of Yang-Mills propagators,” *Annals Phys.* **322** (2007) 2916–2944, [hep-ph/0701050](#).
- [51] C. S. Fischer, R. Alkofer, and H. Reinhardt, “The elusiveness of infrared critical exponents in Landau gauge Yang-Mills theories,” *Phys. Rev.* **D65** (2002) 094008, [hep-ph/0202195](#).
- [52] L. von Smekal, R. Alkofer, and A. Hauck, “The infrared behavior of gluon and ghost propagators in Landau gauge QCD,” *Phys. Rev. Lett.* **79** (1997) 3591–3594, [hep-ph/9705242](#).
- [53] Smekal, Lorenz von and Hauck, Andreas and Alkofer, Reinhard , “A solution to coupled Dyson-Schwinger equations for gluons and ghosts in Landau gauge,” *Ann. Phys.* **267** (1998) 1, [hep-ph/9707327](#).
- [54] C. S. Fischer, “Infrared properties of QCD from Dyson-Schwinger equations,” *J. Phys.* **G32** (2006) R253–R291, [hep-ph/0605173](#).
- [55] P. Watson and H. Reinhardt, “Propagator Dyson-Schwinger equations of Coulomb gauge Yang-Mills theory within the first order formalism,” *Phys. Rev.* **D75** (2007) 045021, [hep-th/0612114](#).
- [56] P. Watson and H. Reinhardt, “Perturbation Theory of Coulomb Gauge Yang-Mills Theory Within the First Order Formalism,” *Phys. Rev.* **D76** (2007) 125016, [arXiv:0709.0140 \[hep-th\]](#).
- [57] P. Watson and H. Reinhardt, “Two-Point Functions of Coulomb Gauge Yang-Mills Theory,” *Phys. Rev.* **D77** (2008) 025030, [arXiv:0709.3963 \[hep-th\]](#).
- [58] I. B. Khriplovich, “Green’s functions in theories with non-abelian gauge group,” *Yad. Fiz.* **10** (1969) 409–424.
- [59] V. N. Gribov, “Quantization of non-Abelian gauge theories,” *Nucl. Phys.* **B139** (1978) 1.
- [60] D. Zwanziger, “Lattice Coulomb Hamiltonian and static color-Coulomb field,” *Nucl. Phys.* **B485** (1997) 185–240, [hep-th/9603203](#).
- [61] I. M. Singer, “Some Remarks on the Gribov Ambiguity,” *Commun. Math. Phys.* **60** (1978) 7–12.
- [62] V. N. Gribov, “Instability of non-Abelian gauge theories and impossibility of choice of Coulomb gauge,” *SLAC-TRANS-0176* (1977).
- [63] J. E. Mandula and M. Ogilvie, “The Gluon Is Massive: A Lattice Calculation of the Gluon Propagator in the Landau Gauge,” *Phys. Lett.* **B185** (1987) 127–132.
- [64] R. Jackiw, I. Muzinich, and C. Rebbi, “Coulomb gauge description of large yang-mills fields,” *Phys. Rev.* **D17** (1978) 1576.

- [65] F. S. Henyey, “Gribov ambiguity without topological charge,” *Phys. Rev.* **D20** (1979) 1460.
- [66] M. Semenov-Tyan-Shanskii and V. Franke, “A variational principle for the Lorentz condition and restriction of the domain of path integration in non-abelian gauge theory,” *Zapiski Nauchnykh Seminarov Leningradskogo Otdeleniya Matematicheskogo Instituta im. V.A. Steklov AN SSSR* **120** (1982) 159. *J. Sov. Math.* **34**, Plenum, New York (1986), p. 1999.
- [67] G. Dell’Antonio and D. Zwanziger, “Every gauge orbit passes inside the Gribov horizon,” *Commun. Math. Phys.* **138** (1991) 291–299.
- [68] J. E. Mandula and M. C. Ogilvie, “A possible resolution of the lattice gribov ambiguity,” *Phys. Rev.* **D41** (1990) 2586.
- [69] P. Marenzoni and P. Rossi, “Gribov copies in lattice QCD,” *Phys. Lett.* **B311** (1993) 219–222, [hep-lat/9306010](#).
- [70] M. Quandt, G. Burgio, S. Chimchinda, and H. Reinhardt, “Coulomb gauge Green functions and Gribov copies in SU(2) lattice gauge theory,” *PoS LAT2007* (2007) 325, [arXiv:0710.0549 \[hep-lat\]](#).
- [71] P. van Baal, “More (thoughts on) Gribov copies,” *Nucl. Phys.* **B369** (1992) 259–275.
- [72] D. Zwanziger, “Renormalization in the Coulomb gauge and order parameter for confinement in QCD,” *Nucl. Phys.* **B518** (1998) 237–272.
- [73] D. Zwanziger, “Non-perturbative Faddeev-Popov formula and infrared limit of QCD,” *Phys. Rev.* **D69** (2004) 016002, [hep-ph/0303028](#).
- [74] D. Zwanziger, “Fundamental modular region, Boltzmann factor and area law in lattice gauge theory,” *Nucl. Phys.* **B412** (1994) 657–730.
- [75] J. Greensite and S. Olejnik, “Coulomb energy, vortices, and confinement,” *Phys. Rev.* **D67** (2003) 094503, [hep-lat/0302018](#).
- [76] J. Gattnar, K. Langfeld, and H. Reinhardt, “Signals of confinement in Green functions of SU(2) Yang- Mills theory,” *Phys. Rev. Lett.* **93** (2004) 061601, [hep-lat/0403011](#).
- [77] G. Dell’Antonio and D. Zwanziger, “Ellipsoidal bound on the gribov horizon contradicts the perturbative renormalization group,” *Nucl. Phys.* **B326** (1989) 333–350.
- [78] D. Zwanziger, “Analytic calculation of color-Coulomb potential and color confinement,” *Phys. Rev.* **D70** (2004) 094034, [hep-ph/0312254](#).
- [79] D. Zwanziger, “Critical limit of lattice gauge theory,” *Nucl. Phys.* **B378** (1992) 525–590.
- [80] J. Greensite, S. Olejnik, and D. Zwanziger, “Center vortices and the Gribov horizon,” *JHEP* **05** (2005) 070, [hep-lat/0407032](#).

- [81] S. G. Rajeev, “Yang-Mills theory on a cylinder,” *Phys. Lett.* **B212** (1988) 203.
- [82] J. E. Hetrick and Y. Hosotani, “Yang-Mills theory on a circle,” *Phys. Lett.* **B230** (1989) 88.
- [83] C. Feuchter and H. Reinhardt, “Variational solution of the Yang-Mills Schroedinger equation in Coulomb gauge,” *Phys. Rev.* **D70** (2004) 105021, [hep-th/0408236](#).
- [84] C. Feuchter and H. Reinhardt, “Quark and gluon confinement in Coulomb gauge,” [hep-th/0402106](#).
- [85] H. Reinhardt and C. Feuchter, “On the Yang-Mills wave functional in Coulomb gauge,” *Phys. Rev.* **D71** (2005) 105002, [hep-th/0408237](#).
- [86] D. Epple, H. Reinhardt, and W. Schleifenbaum, “Confining Solution of the Dyson-Schwinger Equations in Coulomb Gauge,” *Phys. Rev.* **D75** (2007) 045011, [hep-th/0612241](#).
- [87] V. A. Smirnov, “Evaluating Feynman integrals,” *Springer Tracts Mod. Phys.* **211** (2004) 1–244.
- [88] F. J. Yndurain, “The theory of quark and gluon interactions,”. Berlin, Germany: Springer (1999) 413 p.
- [89] T. Kugo and I. Ojima, “Local Covariant Operator Formalism of Nonabelian Gauge Theories and Quark Confinement Problem,” *Prog. Theor. Phys. Suppl.* **66** (1979) 1.
- [90] T. Kugo, “The universal renormalization factors $Z(1) / Z(3)$ and color confinement condition in non-Abelian gauge theory,” [hep-th/9511033](#).
- [91] Slavnov, A. A., “Ward identities in gauge theories,” *Theor. Math. Phys.* **10** (1972) 99–107.
- [92] R. Alkofer and L. von Smekal, “The infrared behavior of QCD Green’s functions: Confinement, dynamical symmetry breaking, and hadrons as relativistic bound states,” *Phys. Rept.* **353** (2001) 281, [hep-ph/0007355](#).
- [93] W. Schleifenbaum, A. Maas, J. Wambach, and R. Alkofer, “Infrared behaviour of the ghost gluon vertex in Landau gauge Yang-Mills theory,” *Phys. Rev.* **D72** (2005) 014017, [hep-ph/0411052](#).
- [94] Taylor, J. C., “Ward identities and charge renormalization of the Yang-Mills field,” *Nucl. Phys.* **B33** (1971) 436–444.
- [95] A. I. Davydychev, P. Osland, and O. V. Tarasov, “Three-gluon vertex in arbitrary gauge and dimension,” *Phys. Rev.* **D54** (1996) 4087–4113, [hep-ph/9605348](#).
- [96] Marciano, William J. and Pagels, Heinz, “Quantum Chromodynamics,” *Phys. Rept.* **36** (1978) 137.

-
- [97] C. Lerche and L. Smekal, “On the infrared exponent for gluon and ghost propagation in Landau gauge QCD,” *Phys. Rev.* **D65** (2002) 125006, [hep-ph/0202194](#).
- [98] A. Cucchieri, T. Mendes, and A. Mihara, “Numerical study of the ghost-gluon vertex in Landau gauge,” *JHEP* **12** (2004) 012, [hep-lat/0408034](#).
- [99] A. Sternbeck, E. M. Ilgenfritz, M. Muller-Preussker, and A. Schiller, “Studying the infrared region in Landau gauge QCD,” *PoS LAT2005* (2006) 333, [hep-lat/0509090](#).
- [100] A. Maas, “Two- and three-point Green’s functions in two-dimensional Landau-gauge Yang-Mills theory,” *Phys. Rev.* **D75** (2007) 116004, [arXiv:0704.0722 \[hep-lat\]](#).
- [101] C. S. Fischer and D. Zwanziger, “Infrared behaviour and running couplings in interpolating gauges in QCD,” *Phys. Rev.* **D72** (2005) 054005, [hep-ph/0504244](#).
- [102] D. Zwanziger, “Non-perturbative Landau gauge and infrared critical exponents in QCD,” *Phys. Rev.* **D65** (2002) 094039, [hep-th/0109224](#).
- [103] W. Schleifenbaum, M. Leder, and H. Reinhardt, “Infrared analysis of propagators and vertices of Yang-Mills theory in Landau and Coulomb gauge,” *Phys. Rev.* **D73** (2006) 125019, [hep-th/0605115](#).
- [104] P. Watson and R. Alkofer, “Verifying the Kugo-Ojima confinement criterion in Landau gauge QCD,” *Phys. Rev. Lett.* **86** (2001) 5239, [hep-ph/0102332](#).
- [105] M. Q. Huber, R. Alkofer, C. S. Fischer, and K. Schwenzer, “The infrared behavior of Landau gauge Yang-Mills theory in d=2, 3 and 4 dimensions,” *Phys. Lett.* **B659** (2008) 434–440, [arXiv:0705.3809 \[hep-ph\]](#).
- [106] C. S. Fischer and R. Alkofer, “Infrared exponents and running coupling of SU(N) Yang-Mills theories,” *Phys. Lett.* **B536** (2002) 177–184, [hep-ph/0202202](#).
- [107] D. Atkinson and J. C. R. Bloch, “QCD in the infrared with exact angular integrations,” *Mod. Phys. Lett.* **A13** (1998) 1055–1062, [hep-ph/9802239](#).
- [108] I. S. Gradshteyn and I. Ryzhik, *Table of Integrals, Series, and Products*. Academic Press, New York, 5th edition ed., 1994.
- [109] E. Seiler, “Upper bound on the color confining potential,” *Phys. Rev.* **D18** (1978) 482–483.
- [110] C. Bachas, “Convexity of the quarkonium potential,” *Phys. Rev.* **D33** (1986) 2723.
- [111] D. Zwanziger, “No confinement without Coulomb confinement,” *Phys. Rev. Lett.* **90** (2003) 102001, [hep-lat/0209105](#).
- [112] G. Passarino and M. J. G. Veltman, “One loop corrections for e+ e- annihilation into mu+ mu- in the Weinberg model,” *Nucl. Phys.* **B160** (1979) 151.
-

- [113] A. Maas, J. Wambach, B. Gruter, and R. Alkofer, “High-temperature limit of Landau-gauge Yang-Mills theory,” *Eur. Phys. J.* **C37** (2004) 335–357, [hep-ph/0408074](#).
- [114] J. T. A.A. Kilbas, H.M. Srivastava, *Fractional Integrals and Derivatives*. Yverdon, Switzerland: Gordon and Breach, 1993.
- [115] K.-I. Kondo, “Infrared and ultraviolet asymptotic solutions to gluon and ghost propagators in Yang-Mills theory,” *Phys. Lett.* **B551** (2003) 324–336, [hep-th/0209236](#).
- [116] L. I. Schiff, “Application of the Variation Method to Field Quantization,” *Phys. Rev.* **130** (Apr, 1963) 458–464.
- [117] L. Polley and D. E. L. Pottinger, “Variational calculations in quantum field theory. proceedings, international workshop, Wangerooge, Germany,” *Singapore, Singapore: World Scientific (1988) 293 p. (Proceedings of the international workshops on the physics of small systems, 2) (1987)*.
- [118] J. Zinn-Justin, “Quantum field theory and critical phenomena,” *Int. Ser. Monogr. Phys.* **85** (1993) 1–996.
- [119] J. C. Collins, “Renormalization. An introduction to renormalization, the renormalization group, and the operator product expansion,”. Cambridge, Uk: Univ. Pr. (1984) 380p.
- [120] D. Epple, H. Reinhardt, W. Schleifenbaum, and A. P. Szczepaniak, “Subcritical solution of the Yang-Mills Schroedinger equation in the Coulomb gauge,” *Phys. Rev.* **D77** (2008) 085007, 0712.3694.
- [121] H. Reinhardt and D. Epple, “The ’t Hooft loop in the Hamiltonian approach to Yang-Mills theory in Coulomb gauge,” *Phys. Rev.* **D76** (2007) 065015, [arXiv:0706.0175 \[hep-th\]](#).
- [122] H. Reinhardt, “On ’t Hooft’s loop operator,” *Phys. Lett.* **B557** (2003) 317–323, [hep-th/0212264](#).
- [123] H. Reinhardt, D. Epple, and W. Schleifenbaum, “Hamiltonian approach to Yang-Mills theory in Coulomb gauge,” *AIP Conf. Proc.* **892** (2007) 93–99, [hep-th/0610324](#).
- [124] D. Atkinson and J. C. R. Bloch, “Running coupling in non-perturbative QCD. I: Bare vertices and y -max approximation,” *Phys. Rev.* **D58** (1998) 094036, [hep-ph/9712459](#).
- [125] J. C. R. Bloch, “Numerical investigation of fermion mass generation in QED,” [hep-ph/0208074](#). PhD thesis, Durham.
- [126] A. Maas, “Solving a set of truncated Dyson-Schwinger equations with a globally converging method,” *Comput. Phys. Commun.* **175** (2006) 167–179, [hep-ph/0504110](#).
- [127] A. Cucchieri and D. Zwanziger, “Gluon propagator and confinement scenario in Coulomb gauge,” *Nucl. Phys. Proc. Suppl.* **119** (2003) 727–729, [hep-lat/0209068](#).

-
- [128] K. Langfeld and L. Moyaerts, “Propagators in Coulomb gauge from SU(2) lattice gauge theory,” *Phys. Rev.* **D70** (2004) 074507, [hep-lat/0406024](#).
- [129] A. Erdélyi, *Asymptotic Expansions*. Dover, 1956.
- [130] G. Burgio, “private communication,” 2008.
- [131] A. Cucchieri and D. Zwanziger, “Numerical study of gluon propagator and confinement scenario in minimal Coulomb gauge,” *Phys. Rev.* **D65** (2002) 014001, [hep-lat/0008026](#).
- [132] C. Feuchter and H. Reinhardt, “The Yang-Mills Vacuum in Coulomb Gauge in D=2+1 Dimensions,” [arXiv:0711.2452 \[hep-th\]](#).
- [133] R. Alkofer, C. S. Fischer, and F. J. Llanes-Estrada, “Vertex functions and infrared fixed point in Landau gauge SU(N) Yang-Mills theory,” *Phys. Lett.* **B611** (2005) 279–288, [hep-th/0412330](#).
- [134] W. Schleifenbaum, “The ghost-gluon vertex of Landau gauge Yang-Mills theory in four and three dimensions,” *diploma thesis, TU Darmstadt, Germany* (2004).
- [135] J. L. Rodriguez Marrero and A. R. Swift, “Color confinement and the quantum chromodynamic vacuum. 2. Gluon propagation and the Coulomb interaction,” *Phys. Rev.* **D31** (1985) 917.
- [136] L. Moyaerts, *A numerical study of quantum forces*. PhD thesis, Univ. of Tübingen, Germany, 2004.
- [137] O. V. Tarasov, A. A. Vladimirov, and A. Y. Zharkov, “The Gell-Mann-Low Function of QCD in the Three Loop Approximation,” *Phys. Lett.* **B93** (1980) 429–432.
- [138] T. van Ritbergen, J. A. M. Vermaseren, and S. A. Larin, “The four-loop beta function in quantum chromodynamics,” *Phys. Lett.* **B400** (1997) 379–384, [hep-ph/9701390](#).
- [139] G. M. Prosperi, M. Raciti, and C. Simolo, “On the running coupling constant in QCD,” *Prog. Part. Nucl. Phys.* **58** (2007) 387–438, [hep-ph/0607209](#).
- [140] S. Eidelman *et al.*, “Review of particle physics,” *Phys. Lett.* **B592** (2004) 1.
- [141] W. Celmaster and R. J. Gonsalves, “The Renormalization Prescription Dependence of the QCD Coupling Constant,” *Phys. Rev.* **D20** (1979) 1420.
- [142] T. D. Lee, “Particle physics and introduction to field theory,” *Contemp. Concepts Phys.* **1** (1981) 1–865.
- [143] Gross, D. J. and Wilczek, Frank, “Ultraviolet behavior of non-abelian gauge theories,” *Phys. Rev. Lett.* **30** (1973) 1343–1346. Nobel prize 2004.
- [144] Politzer, H. David, “Reliable perturbative results for strong interactions?,” *Phys. Rev. Lett.* **30** (1973) 1346–1349. Nobel prize 2004.
-

- [145] S. D. Drell, “Asymptotic freedom,” *SLAC-PUB-2694* (1981).
- [146] A. Cucchieri and D. Zwanziger, “Renormalization group calculation of color Coulomb potential,” *Phys. Rev.* **D65** (2002) 014002, [hep-th/0008248](#).
- [147] L. Baulieu and D. Zwanziger, “Renormalizable non-covariant gauges and Coulomb gauge limit,” *Nucl. Phys.* **B548** (1999) 527–562, [hep-th/9807024](#).
- [148] S. Weinberg, “High-energy behavior in quantum field theory,” *Phys. Rev.* **118** (1960) 838–849.
- [149] A. Weber, “private communication,” 2007.
- [150] W. E. Brown, “Equivalence of the beta-function of the variational approach to that of QCD,” *Int. J. Mod. Phys.* **A13** (1998) 5219–5244, [hep-th/9711189](#).
- [151] W. E. Brown and I. I. Kogan, “A variational approach to the QCD wave functional: Calculation of the QCD beta-function,” *Int. J. Mod. Phys.* **A14** (1999) 799, [hep-th/9705136](#).
- [152] A. P. Szczepaniak and E. S. Swanson, “Coulomb gauge QCD, confinement, and the constituent representation,” *Phys. Rev.* **D65** (2001) 025012, [hep-ph/0107078](#).
- [153] L. von Smekal, “private communication,” 2008.
- [154] H. Reinhardt, “Quasi-particle basis for the Yang–Mills Hamiltonian in Coulomb gauge,” *unpublished notes* (2007).
- [155] E. Schrödinger, “Der stetige Übergang von der Mikro- zur Makromechanik,” *Naturwissenschaften* **14** (1926), no. 28,.
- [156] R. J. Glauber, “Coherent and incoherent states of the radiation field,” *Phys. Rev.* **131** (1963) 2766–2788.
- [157] C. M. Bender and T. T. Wu, “Anharmonic oscillator,” *Phys. Rev.* **184** (1969) 1231–1260.
- [158] P. A. M. Dirac, “Gauge invariant formulation of quantum electrodynamics,” *Can. J. Phys.* **33** (1955) 650.
- [159] P. E. Haagensen and K. Johnson, “On the wavefunctional for two heavy color sources in Yang- Mills theory,” [hep-th/9702204](#).
- [160] N. Isgur and J. E. Paton, “A Flux Tube Model for Hadrons in QCD,” *Phys. Rev.* **D31** (1985) 2910.
- [161] A. P. Szczepaniak and P. Krupinski, “Coulomb energy and gluon distribution in the presence of static sources,” *Phys. Rev.* **D73** (2006) 034022, [hep-ph/0511083](#).

- [162] T. Heinzl *et al.*, “Probing the ground state in gauge theories,” *Phys. Rev.* **D77** (2008) 054501, [arXiv:0709.3486](#) [hep-lat].
- [163] C. B. Thorn, “Quark Confinement in the Infinite Momentum Frame,” *Phys. Rev.* **D19** (1979) 639.
- [164] J. Greensite and C. B. Thorn, “Gluon chain model of the confining force,” *JHEP* **02** (2002) 014, [hep-ph/0112326](#).
- [165] J. Greensite, “The gluon chain model revisited,” [hep-lat/0204026](#).
- [166] C. C. Gerry and P. Knight, “Introductory Quantum Optics,” *Cambridge University Press* (2005).
- [167] N. Brown and M. R. Pennington, “Studies of confinement: How quarks and gluons propagate,” *Phys. Rev. D* **38** (Oct, 1988) 2266–2276.
- [168] Fröhlich, J., “On the triviality of $\lambda\varphi_d^4$ theories and the approach to the critical point in $D \geq 4$ dimensions,” *Nucl. Phys.* **B200** (1982) 281–296.
- [169] S. Paban and R. Tarrach, “On the effective action and field renormalization for variational $\lambda\phi^4$,” *Phys. Lett.* **B213** (1988) 48–53.

Acknowledgments

First of all, I would like to thank my supervisor Prof. Dr. Hugo Reinhardt. He supported me throughout my PhD thesis unconditionally and I was always glad to have his experienced advice. His continuous interest in my work and the brilliant ideas coming from his side were the driving mechanisms for this thesis to be completed. Moreover, I was glad to come along with him to the Trento workshop in 2007.

It is a pleasure to recall the great inspiration I received from numerous people in my undergraduate years that made a way around the fascinating topic of quantum field theory barely avoidable. I would like to mention Prof. Dr. Samson Shatashvili from my Erasmus year in Dublin as well as Prof. Dr. Jochen Wambach, Prof. Dr. Reinhard Alkofer and Dr. Axel Maas from the collaborations during my diploma thesis in Darmstadt.

During my PhD studies, I profited from discussions with Prof. Dr. Adam Szczepaniak, Prof. Dr. Axel Weber, Prof. Dr. Jeff Greensite, Prof. Dr. Daniel Zwanziger and Prof. Dr. Christian Fischer. I highly appreciated the opportunity to embrace topics directly related to my thesis.

In the institute of theoretical physics in Tübingen, the company of Dr. habil. Markus Quandt, Dr. Claus Feuchter, Dr. Peter Watson, Dr. Giuseppe Burgio, Dr. Diana Nicmorus, Davide Campagnari, Markus Leder, Dominik Epple, Burghard Grüter, Hakan Turan, Carina Popovici and Wolfgang Lutz was very helpful not only for the understanding of physics issues but also for getting through all this.

For a careful and critical reading of the manuscript, I am indebted to Davide Campagnari and Dr. Peter Watson.

The European Graduate School Basel–Graz–Tübingen (EUROGRAD) supported this thesis both financially and educationally with graduate days and workshops. The efforts of the Tübingen speakers Prof. Dr. Dr. h.c. mult. Amand Fäßler and Prof. Dr. Josef Jochum in particular are very much appreciated.

My wife, my family and my friends did a great job backing me up, challenging me, and giving me all I needed, and I will not forget any of it.

Finally, I want to emphasize that without the help and support of my parents, beginning from the first years of my life up till now, I would have most probably never accomplished this doctoral thesis, and I am most thankful for that.

Publications

- I. S.J. Cox, S. Neethling, W.R. Rossen, W. Schleifenbaum, P. Schmidt-Wellenburg, and J.J. Cilliers, “A theory of the effective yield stress of foam in porous media: the motion of a soap film traversing a three-dimensional pore”, *Colloids and Surfaces A* **245** (2004) 143–151,
<http://dx.doi.org/10.1016/j.colsurfa.2004.07.004>.
- II. W. Schleifenbaum, A. Maas, J. Wambach, and R. Alkofer, “Infrared behaviour of the ghost-gluon vertex in Landau gauge Yang-Mills theory”, *Phys. Rev.* **D72** (2005) 014017,
<http://dx.doi.org/10.1103/PhysRevD.72.014017>,
<http://arXiv.org/abs/hep-ph/0411052v2>.
- III. W. Schleifenbaum, A. Maas, J. Wambach, and R. Alkofer, “The ghost-gluon vertex in Landau gauge Yang-Mills theory”, *Proceedings of the 42nd International School of Sub-nuclear Physics in Erice, Italy* (2004),
<http://arXiv.org/abs/hep-ph/0411060v1>.
- IV. W. Schleifenbaum, M. Leder, and H. Reinhardt, “Infrared analysis of propagators and vertices of Yang-Mills theory in Landau and Coulomb gauge”, *Phys. Rev.* **D73** (2006) 125019,
<http://dx.doi.org/10.1103/PhysRevD.73.125019>,
<http://arXiv.org/abs/hep-th/0605115v2>.
- V. H. Reinhardt, D. Epple, and W. Schleifenbaum, “Hamiltonian approach to Yang-Mills theory in Coulomb gauge”, *AIP Conf. Proc.* **892** (2007) 93–99,
<http://arXiv.org/abs/hep-th/0610324v1>.
- VI. D. Epple, H. Reinhardt, and W. Schleifenbaum, “Confining Solution of the Dyson-Schwinger Equations in Coulomb Gauge”, *Phys. Rev.* **D75** (2007) 045011,
<http://dx.doi.org/10.1103/PhysRevD.75.045011>,
<http://arXiv.org/abs/hep-th/0612241v2>.
- VII. H. Reinhardt, W. Schleifenbaum, D. Epple, and C. Feuchter, “Hamiltonian approach to Coulomb gauge Yang-Mills Theory”, *PoS LAT2007* (2007),
<http://arxiv.org/abs/0710.0316v1>.
- VIII. D. Epple, H. Reinhardt, W. Schleifenbaum, and A. P. Szczepaniak, “Subcritical solution of the Yang-Mills Schroedinger equation in the Coulomb gauge”, *Phys. Rev.* **D77** (2008) 085007,
<http://dx.doi.org/10.1103/PhysRevD.77.085007>,
<http://arxiv.org/abs/0712.3694v1>.